University of Nottingham
UK | CHINA | MALAYSIA

Brain Imaging Biomarkers in Multiple Sclerosis

Thesis submitted in partial satisfaction of the requirements of the University of Nottingham for the degree of Doctor of Philosophy

Amjad Ibrahim AlTokhis
Mental Health and Clinical Neurosciences
School of Medicine

Supervisors
Dr Nikos Evangelou
Prof Cris Constantinescu

Nottingham, United Kingdom
November 2022

To my parents

Ibrahim Abdulrahman AlTokhais

and

Sarah Abdulaziz AlZamil

Abstract

Background: Iron rim lesions (IRLs), white matter lesions (WMLs) accumulation and linear brain atrophy measurements have been suggested to be important imaging biomarkers in multiple sclerosis (MS). The extent to which these markers are related to MS diagnosis and predict disease prognosis remains unclear. Furthermore, research Magnetic Resonance Imaging (MRI) findings need validation in clinical settings before they can be incorporated into clinical practice.

Methods: I conducted two reviews one was a mapping review on IRLs and the other was a meta-analysis on WMLs in MS. I then tested the diagnostic and prognostic usefulness of the IRL in two studies: (1) a large, cross-sectional, multi-centre study of patients with MS and mimicking disorders using 3T MRI, (2) a retrospective single-centre study of patients with first presentation of a clinically isolated syndrome (CIS) or at the early stage of the disease using 7T MRI. I also explored the utility of routine, non-standardised MRI scans measuring WMLs number, volume and linear measures of atrophy at the early stage of the disease and examined their role in predicting long-term disability.

Results: The IRLs achieved high specificity (up to 99%) in diagnosing MS compared to MS-mimics but low sensitivity of 24%. All patients with IRLs showing a central vein sign (CVS) had MS or CIS, giving a diagnostic specificity of 100% but equally low sensitivity of 21%. Moreover, the presence of IRLs was also a predictor of long-term disability, especially in patients with ≥4 IRLs. IRLs had a greater impact on disability compared to the WMLs number and volume. Linear brain atrophy of Inter-Caudate Distance (ICD) and Third Ventricle Width (TVW) had a significant impact in predicting disability after 10 years.

Conclusions: The perilesional IRLs may reduce diagnostic uncertainty in MS by being a highly specific imaging diagnostic biomarker, especially when used in conjunction with the CVS. Also, the presence and number of IRLs hold prognostic value for long-term physical disability in MS. Simple and reliable assessment of brain atrophy remains challenging in clinical practice.

Declaration

I hereby confirm that the present thesis

Brain Imaging Biomarkers in Multiple Sclerosis

Is the result of my independent scholarly work, and that in all cases material from the work of others (in books, articles, essays, dissertations, and on the internet) is acknowledged, and quotations and paraphrases are clearly indicated. No material other than that listed has been used. I have read and understood the Institute's regulations and procedures concerning plagiarism.

Acknowledgements

Appreciation and deepest gratitude for the help and support to the following people for their professional and personal support during my PhD.

First and foremost, I would like to thank my supervisors, Dr Nikos Evangelou and Professor Cris Constantinescu, for their guidance and support throughout this journey. Thank you for making this experience as enjoyable as it could be, for your knowledge and good humour throughout!

Special thanks to Dr Chris Tench for all the support and input I received from him. Dr Tench assessed me with the statistical analyses, methodology and thesis feedback. His insights, sense of humour and smart ideas helped me to tackle many challenges I faced during this journey.

I would like also to thank Dr Radu Tanasescu, Dr Rasha Abdel-Fahim Dr Olivier Mougin and Paul Morgan for their help with various aspects

of this work and invaluable input regarding the practical implications of the findings reported in this thesis.

I was fortunate enough to work alongside a fantastic group of colleagues in the department of Clinical Neurology, Dr Afagh Garjani, Abdulmajeed Alotaibi, Aimee Hibbert, Nanci Frakich and Dr Christopher Allen. I am grateful for their warmth, encouragement support and friendship.

Thanks to Rebecca Stevenson, and Alison Ashmore for their help in searching the database for the systematic reviews. Thanks to Dr Andrea Venn and Paul Bassett for their statistical assistance in chapter 8. Great appreciation to Dr Abdullah Almohaizeie, Dr Adam Spencer and Samar Altokhais for their feedback and their professional advice in different aspects throughout this thesis.

This work would not have been possible without those patients with MS who agreed to share their data for medical research.

I wish to express my appreciation to my parents, and family, especially my nephew Abdulelah Altokhais, who was with me from the start of

this journey and moved with me to the UK. Many thanks to my friends Raya AlMaamari and Sarah Marair, who celebrated all the ups and were with me through all the lows during this PhD.

Lastly, special thanks go to the Ministry of higher education in Saudi Arabia, which financially funded my PhD scholarship.

Table of Contents

List of Tables

List of Figures

Abbreviations

ABN	Association of British Neurologists
ACTRIMS	American Committee for Treatment and Research in Multiple Sclerosis
AUC	Area Under the Curve
ARMSS	Age-Related Multiple Sclerosis Severity Score
BBB	Blood-Brain Barrier
CAL	Chronic Active lesion
CCI	Corpus Callosum Index
CDMS	Clinically Defined Multiple Sclerosis
CI	Confidence Interval
CIS	Clinically Isolated Syndrome
CNR	Contrast to Noise Ratio
CNS	Central Nervous System
CSF	Cerebrospinal Fluid
CVS	Central Vein Sign
DGM	Deep Grey Matter
DIS	Dissemination in Space
DIT	Dissemination in Time
DMT	Disease-Modifying Therapy
ECTRIMS	European Committee for Treatment and Research in Multiple
EDSS	Expanded Disability Status Scale
EMA	European Medicines Agency
EPI	Echo Planner Imaging
FDA	Food and Drug Administration
FID	Free Induction Decay
FLAIR	Fluid Attenuation Recovery
GM	Grey Matter
ICD	Inter Caudate Distance
IR	Iron Rim
IRLs	Iron Rim Lesions
MAGNIMS	Magnetic Resonance Imaging in Multiple Sclerosis
MEDW	Medulla Width
MPRAGE	Magnetisation-Prepared Rapid Gradient-Echo
MRI	Magnetic Resonance Imaging
MRS	Magnetic Resonance Spectroscopy
MS	Multiple Sclerosis

MTR	Magnetization Transfer Rate
NAIMS	North American Imaging in Multiple Sclerosis Cooperative
NAWM	Normal-appearing White Matter
NEDA	No Evidence of Disease Activity
NMOSD	Neuromyelitis Optica spectrum disorders
NMR	Nuclear Magnetic Resonance
OCB	Oligoclonal Band
PD	Proton Density
PPMS	Primary Progressive Multiple Sclerosis
PPV	Positive Predictive Value
PRL	Paramagnetic Rim Lesions
PSIR	Phase-Sensitive Inversion Recovery
RF	Radiofrequency
RRMS	Relapsing-Remitting Multiple Sclerosis
RIS	Radiologically Isolated Syndrome
ROC	Receiver Operating Characteristic
SAR	Specific Absorption Rate
SD	Standard Deviation
SE	Spin Echo
SEL	Slowly Expanding Lesions
SLE	Systemic Lupus Erythematosus
SNR	Signal to Noise Ratio
SPMS	Secondary Progressive Multiple Sclerosis
SWI	Susceptibility Weighted Imaging
T	Tesla
T_1W	T_1-Weighted Image
T_2W	T_2-weighted Image
TE	Echo Time
TI	Inversion Time
TVW	Third Ventricle Width
TR	Repetition Time
UHF	Ultra-High Field
UVR	Ultraviolet Radiation
WMLs	White Matter Lesions

Chapter 1 . Introduction

1.1 Thesis Overview

This PhD thesis aims to assess the ever-challenging role of Magnetic Resonance Imaging (MRI) in Multiple Sclerosis (MS) to establish an accurate diagnosis and predict prognosis at an early stage of the disease. This is a thesis by publication and the research papers describing the five projects detailed in this thesis have been published [1–5].

The author will first lay the foundations of the thesis by reviewing the clinical manifestation of MS and the role MRI currently plays in the diagnosis and prognosis. Then, describe three different retrospective studies and two different systematic reviews related to the use of clinical MRI in MS.

The second and third chapters summarise the literature on MS, the MRI basic physics concepts and their use in MS. ***The fourth, fifth and sixth chapters*** focus on Iron Rim Lesions (IRL) in MS as a diagnostic and prognostic imaging biomarker. ***The seventh*** *and* ***eighth chapters*** will cover White Matter Lesions (WMLs) load and volume as imaging biomarkers in predicting long-term disability in MS. ***The concluding chapter*** of the thesis is a summary of the main findings and a description of potential future directions for the use of MRI in MS research and clinical practice.

1.2 Motivation

MS is one of the leading causes of disability in young adults. Clinically, some patients with MS experience a relatively benign course in which they develop limited disabilities after many years, can perform everyday activities independently, and can have a fulfilling life whilst they are not on any treatment. Others have multiple disabling attacks and develop severe progressive disability, which requires special care or assisted living [6].

Slowing, stopping, or reversing the development of disability is the top priority of MS clinicians, patients, and carers [7]. To achieve this goal, clinicians after diagnosis of MS, need to decide if and what type of treatment is needed to reduce long-term disability [8,9]. Hence, ideally soon after diagnosis, identification of the patients who have a higher risk of developing a disability is a crucial step [10].

Different clinical factors have been shown to have prognostic significance, but their usefulness is affected by the method of reporting. Motor manifestation seen with initial relapse is considered a prognostic factor for faster disease progression [11], but is it the same if patients have dense hemiplegia versus fatigability of muscles? Quantifying those factors can be challenging.

The use of MRI has facilitated objective quantification of the visible pathology, which can be used in prognostic modelling. MRI white matter lesions are used in the diagnosis and prognosis of MS as their appearance suggests acute inflammation (Gadolinium-enhancing, T_2 lesions), demyelination (T_2 lesions, iron rim "appear as a dark circle at the lesion's edge"), or permanent tissue destruction (T_1 black holes).

One can quantify the numbers and/or volume of WMLs that have been used as outcome measures in clinical trials. This quantification is used as one of the components of the "No Evidence of Disease Activity" (NEDA) designation, a treatment goal in MS characterised by no new or enlarging T_2 or Gadolinium-enhancing lesions, no relapses, and no disability as measured by the Expanded Disability Status Scale (EDSS)[12].

Aside from WMLs, accelerated brain atrophy (loss of brain tissue) is also a common feature of MS patients' brains. Clinicians have known of brain atrophy since the earliest descriptions of MS [13,14] but only recently has the amount of atrophy been quantified in vivo using modern imaging. Atrophy has been found to be a useful biomarker of future disability[15], cognitive decline [16,17] and disease progression (i.e., transition from the relapsing form of MS

to a progressive form of the disease termed secondary progressive MS) [18] suggesting it could be used to predict the future course of the disease. It has been also used to measure the outcomes of clinical trials that examine the utility of new therapeutic approaches to MS (e.g., Disease-Modifying Therapies (DMTs)) [19]. More recently, brain atrophy has been suggested as the most viable addition to incorporate into the future revisions of NEDA[20], which already includes information about WMLs in the assessment of patients. Despite these advances and extensive use of MRI, we still lack accurate prediction models to help individual MS patients plan their life and treatment.

This thesis explores the application of research and clinical brain MRI scans testing if reliably visualise a new MRI possibly biomarker the IRLs and assess WML together with quantifying brain atrophy in MS patients, to provide clinically relevant information that could be used in diagnosing and monitoring patients. Although post-mortem studies and Ultra-High Field (UHF) MRI (7T and higher) provide unparalleled visualisation of MS-related pathology, to be of clinical value, research findings need to be translated to the clinical level where 1.5 and/or 3T imaging are used by most "service" in radiology departments.

1.3 Thesis Aims

The research aims are to facilitate the translation of research findings into clinical practice and test if brain WML accumulation, IRL and brain atrophy could help better diagnose, monitor, and assess MS patients. The aims are:

1. Evaluate the sensitivity and specificity of IRL in differentiating MS from MS-mimics using clinical 3T MRI scanners.

2. Assess whether the presence and number of IRLs are associated with a long-term physical disability.

3. Evaluate the presence of IRL in different MS disease phenotypes

4. Explore the association between IRL number and WML count/volume in predicting long-term disability.

5. Evaluate a quick clinician-based assessment of the number and volume of WML on clinical MRI in predicting long-term disability.

6. Examine if linear measurements of brain atrophy on clinical MRI scans can be used clinically in predicting disease progression.

Based on the aims and literature, I hypothesised the following:

1. IRL could be a diagnostic imaging biomarker for MS.
2. IRL presence is associated with worse disease progression and disability in MS.
3. The number of IRL can be a prognostic imaging biomarker for MS.
4. WML count and volume detected in routine MRI images could predict long-term disability in MS.
5. Routine, clinical scans will be able to successfully estimate atrophy, and predict long-term disability.

1.4 Impact of Covid-19

Before passing the first-year viva of the proposed project (the upgrade to PhD), the government of the United Kingdom announced the first national lockdown due to the spread of the Covid-19 pandemic (March 2020). Consequently, the University of Nottingham announced the closure of all campuses including the venues where this PhD project was planned to be conducted (clinical neurology offices, nursing stations and Sir Peter Mansfield Imaging Centre (SPMIC)). Due to this impact, the proposed project was cancelled.

The plan of the project was to recall previous 7T MRI patients for scanning to evaluate the evolution of IRL longitudinally. The aims were to (1) estimate the incidence of IRL in different MS disease phenotypes using 7T MRI, (2) evaluate its evolution over different disease

courses, (3) investigate the correlation of IRL presence with lesion evolution and the association of rims with focal demyelination as measured by MTR, and (4) examine the associations between baseline IRL load and at 11-year intervals with the degree of physical disability. During the first year, I finalised the study protocol and drafted the University and RAIS ethics. My supervisors, Dr Evangelou, Professor Constantinescu and I decided to establish contingency plans and strategies to overcome the impact of Covid-19 on the research progress. Thus, two systematic reviews and three retrospective studies were conducted as an alternative plan.

1.5 Publications arising from this thesis

Amjad I. AlTokhis, Abdulmajeed M. Alotaibi, Ghadah A. Felmban, Cris S. Constantinescu and Nikos Evangelou. *Iron Rims as an Imaging Biomarker in MS: A Systematic Mapping Review. Diagnostics*. Accepted November 2020. doi: 10.3390/diagnostics10110968

Amjad I AlTokhis, Abrar AlAmrani, Abdulmajeed Alotaibi, Anna Podlasek and Cris S. Constantinescu. *Magnetic Resonance Imaging as a Prognostic Disability Marker in Clinically Isolated Syndrome and Multiple Sclerosis: A Systematic Review and Meta-Analysis*. Diagnostics. Accepted January 2022. doi: 10.3390/diagnostics12020270

Amjad I. AlTokhis*, Aimee Hibbert*, Christopher Allen, Olivier Mougin, Abdulmajeed Alotaibi, Su-Yin Lim, Cris S. Constantinescu, Rasha Abdel-Fahim, and Nikos Evangelou. *Longitudinal Clinical Study of Patients with White Matter Iron Rim Lesions in Multiple Sclerosis*. Multiple Sclerosis. Accepted June 2022. doi: 10.1177/13524585221114750

Isobel Meaton*, **Amjad AlTokhis*,** Christopher Martin Allen, Margareta A Clarke, Tim Sinnecker Dominik Meier, Christian Enzinger, Massimiliano Calabrese, Nicola De Stefano, Alain Pitiot, Antonio Giorgio, Menno M Schoonheim, Friedemann Paul, Mikolaj A Pawlak, Reinhold Schmidt, Cristina Granziera, Ludwig Kappos, Xavier Montalban, Alex Rovira, Jens Wuerfel*, and Nikos Evangelou*. *Paramagnetic rims are a promising diagnostic imaging biomarker in multiple sclerosis.* Multiple Sclerosis. Accepted July 2022. doi:10.1177/13524585221118677

Amjad I AlTokhis, Abdulmajeed Alotaibi, Paul Morgan, Radu Tanasescu and Nikos Evangelou. *Predictors of long-term disability in MS patients using routine MRI data: a 15-year retrospective study*. The Neuroradiology Journal. Accepted December 2022. doi: 10.1177/19714009221150853

1.6 Publications indirectly related to this thesis

Abdulmajeed M. Alotaibi, Christopher Tench, Rebecca Stevenson, Ghadah Felmban, **Amjad AlTokhis**, Ali Aldhebaib, Rob A. Dineen and Cris S. Constantinescu. *Investigating Brain Microstructural Alterations in Type 1 and Type 2 Diabetes Using Diffusion Tensor Imaging: A Systematic Review*. Brain Sciences. Accepted January 2021.doi: 10.3390/brainsci11020140

Alotaibi A, Podlasek **A, AlTokhis A,** Aldhebaib A, Dineen RA, Constantinescu CS**.** *Investigating Microstructural Changes in White Matter in Multiple Sclerosis: A Systematic Review and Meta-Analysis of Neurite Orientation Dispersion and Density Imaging*. Brain Sciences. Accepted August 2021.doi: 10.3390/brainsci11091151

Abdulmajeed Alotaibi, **Amjad AlTokhis,** Anna Podlasek, Chris Tench, Ali-Reza, Mohammadi-Nejad, Stamatios N. Sotiropoulos, Cris S. Constantinescu, Sieun Lee, Rob A. Dineen. *White Matter Microstructural Alteration in Type 2 Diabetes: A Combined UK Biobank Study of Diffusion Tensor Imaging and Neurite Orientation Dispersion and Density Imaging.* Human Brain Mapping (Preprint).

Abdulmajeed Alotaibi, Anna Podlasek, **Amjad AlTokhis,** Cris S. Constantinescu, Rob A. Dineen. *White Matter Abnormalities in Patients with Multiple Sclerosis: A Systematic Review and Network-Meta-Analysis of Diffusion Kurtosis Imaging Studies* (Under review).

1.7 Conference Presentations

Amjad I. AlTokhis, Abdulmajeed M. Alotaibi, Ghadah A. Felmban, Cris S. Constantinescu and Nikos Evangelou. *Iron Rims as an Imaging Biomarker in MS: A Systematic Mapping Review*. Presented at the Americas Committee for Treatment and Research in Multiple Sclerosis ACTRIMS, Online, February 2021. (Poster)

Amjad I. AlTokhis, A. Hibbert, C. Allen, O. Mougin, C. Constantinescu, R. Abdel-Fahim and N. Evangelou. *Clinical longitudinal study of iron rims in white matter MS lesions.* Presented at the European Committee for Treatment and Research in Multiple Sclerosis ECTRIMS, Online, October 2021. (Poster)

Amjad I. AlTokhis, Abdulmajeed Alotaibi and Anna Pedlasek. *Predictors of long-term disability in MS patients using routine MRI data: a 15-year retrospective study.* Presented at the Americas Committee for Treatment and Research in Multiple Sclerosis ACTRIMS, Online, Florida, USA, February 2022. (Poster)

Amjad I. AlTokhis, Aimee Hibbert, Chris Allen, Olivier Mougin, Abdulmajeed Alotaibi, Cris Constantinescu, Rasha Fahim and Nikos Evangelou. *Longitudinal Clinical Study of Patients with White Matter Iron Rims Lesions in Multiple Sclerosis.* Presented at the Americas Committee for Treatment and Research in Multiple Sclerosis ACTRIMS, Online, Florida, USA, February 2022. (Poster)

Amjad I. AlTokhis, Aimee Hibbert, Chris Allen, Olivier Mougin, Abdulmajeed Alotaibi, Cris Constantinescu, Rasha Fahim and Nikos Evangelou. *Longitudinal Clinical Study of Patients with White Matter Iron Rims Lesions in Multiple Sclerosis.* Presented at the Americas Committee for Treatment and Research in Multiple Sclerosis ACTRIMS/NAIMS, Online, Florida, USA, February 2022. (Oral presentation)

Amjad I. AlTokhis, Abrar AlAmrani, Abdulmajeed Alotaibi, Anna Pedlasek and Cris Constantinescu. *Magnetic resonance imaging as a prognostic disability marker in clinically isolated syndrome: A systematic review and Meta-Analysis*. Presented at the

Americas Committee for Treatment and Research in Multiple Sclerosis ACTRIMS, Online, Florida, USA, February 2022. (Poster)

Amjad I. AlTokhis, Aimee Hibbert, Chris Allen, Olivier Mougin, Abdulmajeed Alotaibi, Cris Constantinescu, Rasha Fahim and Nikos Evangelou. *Iron Rim Lesions in Multiple Sclerosis: Insights from 7T MRI cohort with longitudinal clinical follow-up.* Presented at the Association of British Neurologists ABN, Harrogate, UK, May 2022. (Oral presentation).

Amjad I. AlTokhis, Aimee Hibbert, Chris Allen, Olivier Mougin, Abdulmajeed Alotaibi, Cris Constantinescu, Rasha Fahim and Nikos Evangelou. *Longitudinal Clinical Study of Patients with White Matter Iron Rims Lesions in Multiple Sclerosis.* Presented at Multiple Sclerosis Frontiers, Swansea, UK, July 2022. (Oral presentation).

Amjad I. AlTokhis, Aimee Hibbert, Chris Allen, Olivier Mougin, Abdulmajeed Alotaibi, Cris Constantinescu, Rasha Fahim and Nikos Evangelou. *Iron Rim Lesions in Multiple Sclerosis: Insights from 7T MRI cohort with longitudinal clinical follow-up.* Presented at ECTRIMS, Amsterdam, Netherlands, October 2022. (Oral presentation).

Amjad I. AlTokhis, Abdulmajeed Alotaibi, Anna Pedlasek. *Predictors of long-term disability in MS patients using routine MRI data: a 15-year retrospective study.* Presented at the Americas Committee for Treatment and Research in Multiple Sclerosis ACTRIMS, Online, Florida, USA, February 2023. (Poster)

Abdulmajeed M. Alotaibi, Christopher Tench, Rebecca Stevenson, Ghadah Felmban, **Amjad I. AlTokhis**, Ali Aldhebaib, Rob Dineen and Cris S. Constantinescu. *Investigating Brain Microstructural Alteration in Diabetes: A Systematic Review of Diffusion Tensor Imaging.* Presented at American Society of Neuroimaging ASN, Online, January 2021. (Poster)

Chris. Allen, I. Meaton, **Amjad I. AlTokhis,** M. Clarke, T. Sinnecker, D. Meier, C. Enzinger, M. Calabrese, N. De Wuerfel and N. Evangelou. *Paramagnetic rims are a*

specific imaging biomarker in multiple sclerosis. Presented at the European Committee for Treatment and Research in Multiple Sclerosis ECTRIMS, Online, October 2021. (Poster)

Abdulmajeed M. Alotaibi, Anna Pedlasek, **Amjad I. AlTokhis**, Cris S. Constantinescu and Rob Dineen. *Investigating Microstructural Changes in White Matter in Multiple Sclerosis: A Systematic Review and Individual Participant Data Meta-analysis of Neurite Orientation Dispersion and Density Imaging*. Presented at the European Committee for Treatment and Research in Multiple Sclerosis ECTRIMS, Online, October 2021. (Poster)

Abdulmajeed Alotaibi, Anna Podlasek, **Amjad AlTokhis**, Chris R. Tench, Ali-Reza, Mohammadi-Nejad, Stamatios N. Sotiropoulos, Cris S. Constantinescu, Sieun Lee, Rob A. Dineen. *White Matter Microstructural Alteration in Type 2 Diabetes: A UK Biobank Study of Neurite Orientation Dispersion and Density Imaging. Neuroimaging.* Presented at the International Society Magnetic Resonance in Medicine ISMRM, London, May 2022. (Poster).

1.8 Awards/Press

- Educational Grant, from the Americas Committee for Treatment and Research in Multiple Sclerosis ACTRIMS, December 2020

- Educational Grant, from the Americas Committee for Treatment and Research in Multiple Sclerosis ACTRIMS, December 2021

- Poster Award Nominee at ACTRIMS, February 2022

- Sue Watson award winner, University of Nottingham, March 2022

- Medscape, February 2022 (https://www.medscape.com/viewarticle/969330#vp_1)

- The Video Journal of Neurology (VJN), February 2022
  1. (https://vjneurology.com/video/q-hrmmufx7a-iron-rim-lesions-linked-to-disease-worsening-in-ms/)
  2. (https://vjneurology.com/video/tbwaeucwqe-investigating-mri-predictors-of-long-term-disability-in-ms/).

- Tri campus award nominee, for the contribution to the research community, University of Nottingham, April 2022

- Educational Grant, from the European Committee for Treatment and Research in Multiple Sclerosis ECTRIMS, October 2022

1.9 Journal's Permission

- All the publications in this thesis were published as open-access publications,

  therefore, no journal permissions are required.

1.10 Thesis Outline

The thesis is divided into three parts and nine chapters. *Chapter one* is an overall introductory to the thesis. *Part one* includes two chapters covering the literature overview of MS (***chapter two***) looking at our current understanding knowledge on aetiology, clinical presentations, diagnosis, prognosis, pathogenesis and treatment. ***Chapter three***, a brief overview is added to cover the basic concepts and techniques of MRI physics and the use of MRI in MS clinically. Then, different potential MRI biomarkers were also briefly highlighted.

Part two focuses on IRL in MS, and involves three separate projects, ***chapters four, five*** and ***six***, exploring the role of IRL in MS diagnosis and prognosis. ***Chapter four*** is a systematic mapping review assessing the usefulness of IRL as an imaging biomarker in MS. ***Chapter five*** evaluates the images of an international, multi-centre study involving over 500 subjects with MS and MS-mimicking disorders to determine whether IRL can be reliably used to classify patients as MS and non-MS using variable, non-standardised, imaging protocols. ***Chapter six*** is a retrospective study including 91 MS patients to assess IRL as a prognostic imaging biomarker for long-term disability.

Part three focuses on WML count and volume together with linear measures of brain atrophy in MS and involves two separate projects. ***Chapter seven*** is a systematic and meta-analysis review that assesses WML count and volume and their role in predicting long-term disability. ***Chapter eight*** evaluates these MRI measures in a retrospective study from clinical scans of 82 MS patients to predict long-term disability.

The ***last chapter*** summarises the main findings from this PhD thesis, discusses their implications and provides recommendations for future study. Each chapter was written based on the journal's requirements.

PART 1

LITERATURE REVIEW

Chapter 2 . Multiple Sclerosis

2.1 Introduction

MS is an autoimmune, inflammatory, demyelinating and degenerative disease of the Central Nervous System (CNS), where autoreactive lymphocytes infiltrate across the Blood-Brain Barrier (BBB) and lead to myelin and axon damage [21]. The disease is associated with focal inflammatory demyelinating lesions in both white and grey matter [22]. It is the most common cause of non-traumatic disability in young adults, developing between the age of 20 and 50 with the peak age of onset around 30 years old [23]. In the UK, an estimated 105,800 people (2.8 million worldwide) were diagnosed with MS, and is two-to-three times more common in women compared to men [23,24]. The incidence of MS and the gender gap are continuously increasing based on epidemiological studies [25–27]. MS has a substantial impact on mobility, occupation, mental state and quality of life [28].

The precise aetiology of MS has yet to be fully determined. Nevertheless, MS could be considered a disorder caused by a combination of environmental and genetic risk factors. From the environmental perspective, smoking, obesity, gut microbiome, and virus (i.e., EBV) are the most convincing risk factors for MS at this time [29–33]. Additionally, it has been reported that the rates of MS are higher further from the equator, which might be linked to the lack of Ultraviolet Radiation (UVR)[34]. Historically, MS takes its name from the *Latin sclerosis multiplex* meaning “multiple scars”. It is a reference to the demyelinating lesions in the white matter (WM) of the CNS[35].

2.2 Clinical Course

MS is a heterogeneous disease in terms of clinical and radiological manifestations as well as immunological background. Clinically Isolated Syndrome (CIS), Relapsing-Remitting MS (RRMS), Secondary Progressive MS (SPMS), and Primary Progressive MS (PPMS) are the four commonly referred types of MS. RRMS is the most common clinical pattern in MS patients, in which individuals have disease-free periods followed by attacks [36]. A proportion of patients experience a steady decrease in neurological function with no (or few) attacks: this is known as progressive MS [37].

Before RRMS or other demyelinating disorders can be diagnosed, the first presentation of neurological symptoms is referred to as CIS. CIS is thought to belong to the MS spectrum, and it has been found in 85% of MS patients [38]. It begins with a rapid onset of clinical symptoms that continue for at least 24 hours, caused by acute inflammatory lesion(s) [39]. The recovery might be natural or aided by steroid-based medication treatment. The optic nerve, brainstem, and spinal cord are the most commonly affected areas. Optic neuritis, a unilateral inflammation of the optic nerve that causes symptoms ranging from minor visual blurring to full blindness, is the most frequent presentation of CIS [40]. CIS when it affects the spinal cord can produce the typical Lhermitte's sign (a sense of electric shocks running down one's back and spreading out to the limbs) [41] or transverse myelitis [42].

Previous research has shown that the three-year conversion rate from CIS to Clinically Definite MS (CDMS), which is defined by evidence of at least two different clinical episodes, is about 40%, and this rate rises to over 80% after seven years [43,44]. When compared to individuals with normal MRI, CIS patients with MRI abnormalities are more likely to transition to CDMS [45].

Fisniku and colleagues observed that 82% of CIS patients with T_2 lesions at MRI baseline scan transitioned to CDMS 20 years later, compared to just 21% of those with normal MRI baseline [46].

According to the International Advisory Committee on Clinical Trials of MS's most recent changes in 2013[38], after confirming MS diagnosis, the disease may be classed as either RRMS or PPMS. RRMS is characterized by disease-free periods followed by relapses and remissions, and it affects roughly 80-85% of the MS population [47]. PPMS, on the other hand, is characterized by a constant progression of impairment from the onset of the disease, usually with no clinical relapses.

The degree of the inflammatory component of the disease, which is more prevalent in the RR course, is thought to represent a pathological difference between the two subtypes. As the disease progress, so does the neurodegenerative component, and it is expected that over half of RR patients will reach the SP stage after 15 years of disease [48]. The progression of SPMS is marked by a progressive change in disease activity, with fewer or no relapses and a continuous buildup of neurological damage. Over 25 years, about nine out of 10 RRMS patients will accumulate disability and enter the SP course [49,50].

In 2013, Lublin et al. further classified the existing MS phenotypes based on disease activity and progression [22]. As such, CIS, RRMS and progressive patients can be classed as either active or inactive while progressive patients can additionally be classed in terms of their disease progression (disease worsening).

2.3 Diagnosis

Diagnosing MS is generally based on clinical relapses and the presence of WMLs on MRI in RRMS. The so-called 2017 McDonald criteria[51] are the updated diagnostic criteria for MS,

which are still based on lesion Dissemination in Space and Time (DIS and DIT, respectively), together with excluding any MS-mimicking disorders.

DIS is evidence of damage found in at least two parts of the CNS [51]. It can be demonstrated on MRI by identifying at least one T_2 hyperintense lesion in at least two out of four anatomical locations considered MS characteristic (periventricular, cortical or juxtacortical, infratentorial, spinal cord).

DIT is the damage that occurs at a different time point [51]. It is demonstrated by using a single MRI scan and identifying the presence of (1) gadolinium-enhancing and non-enhancing lesions or (2) new T_2 hyperintense and/or gadolinium-enhancing lesions on follow-up MRI compared to baseline, regardless of the time interval between the two scans.

The most recent updates to the McDonald criteria enable a positive lumbar puncture with Cerebrospinal Fluid (CSF)-specific bands to be used in place of DIT [52]. OCBs testing entails analyzing CSF; the immune system produces IgG antibodies, which are released into the CSF in response to CNS inflammation, resulting in many bands (two or more) when electrophoresis is used. Although OCB testing can be used to support an MS diagnosis, only about 80% of CDMS patients have positive OCBs [53], but can be found in other diseases such as Lyme disease [54], Neuromyelitis Optica Spectrum Disorders (NMOSD)[55], and Systemic Lupus Erythematosus (SLE)[56].

Unlike the 2010 McDonald criteria, the 2017 McDonald criteria do not differentiate between symptomatic and asymptomatic lesions, making the diagnosis procedure easier. Symptomatic lesions were previously not counted toward demonstrating DIT or DIS, but they may now be used to support a diagnosis in patients with WML in the brainstem or spine (but not in the optic nerve).

Although MRI is usually used to support the diagnosis of MS, if evidence of at least two typical clinical episodes, also known as relapses, exacerbations, and flare-ups, can be recorded, the diagnosis may be made solely on clinical grounds. A relapse is defined as a symptom onset or worsening that lasts at least 24 hours and occurs at least 30 days following the start of a prior episode. Also, there must be no alternative cause for the onset of symptoms, such as the presence of infection or a rise in body temperature that may explain the occurrence of symptoms. A relapse may be recognized either retrospectively, by looking at the patient's medical history, or at the time of the incident, by doing a neurological examination.

Patients are diagnosed with RRMS when all the above-mentioned criteria are met. Patients with PPMS must have at least one year of continuous disease progression (retrospectively or prospectively) without relapses, as well as two of the following: (1) established DIS in the brain (2) and/or spinal cord, and/or (3) positive OCBs in the CSF. SPMS, on the other hand, is often identified in RRMS patients 10 to 20 years after diagnosis, with the majority of MS patients beginning the conversion to the SP course closer to the 20-year mark [57,58]. SPMS is diagnosed based on a six- to 12-month retrospective evaluation of disease progression, which is marked by a considerable decrease or total cessation of relapses and the accumulation of neurological dysfunction.

Alternative diagnoses of other demyelinating diseases must be ruled out before a diagnosis of MS can be established, since the current criteria include the idea of "no better explanation" for the patient's symptoms. The McDonald criteria were also improved and validated in populations of individuals with typical demyelinating disease presentations indicative of MS [51]. As a result, they can only be used in individuals at high risk of having MS at the time of presentation. Clinical and imaging presentations of demyelination might also cause delays in diagnosis since more

clinical follow-up and testing are required to collect adequate evidence to accept or reject an MS diagnosis. In consequence, biomarkers that may reliably discriminate between MS and mimicking disorders are gaining research attention. NMOSD, for example, may cause clinical symptoms and MRI appearances that are similar to MS, and the finding of a link between serum aquaporin-4 immunoglobulin G antibodies (AQP4-IgG) and NMOSD has improved the differential diagnosis of NMOSD significantly [59]. Researchers are looking for MS-specific biomarkers that might help distinguish MS from other conditions that resemble it.

2.4 Prognosis

As previously stated, although the majority of RRMS patients (65%) convert to SPMS, the pace of progression varies greatly. Around the age of 40, SPMS can enter the progressive stage [60]. A number of promising prognostic factors have been identified for clinical disability in relapse onset MS from natural history studies (first presentation with ON, mono-focal presentation, or sensory symptoms, being female, younger age of disease onset, longer time between the first and next episode, low relapse rate on the first two years, minimal disability after 5 years)[49,58,61,62]. MRI is a very important prognostic factor and is discussed in detail in Chapters 3, 5, 6 and 7.

MS is associated with physical and cognitive disabilities. EDSS is a scale used in MS to estimate the level of disability and disease progression, which is widely used in clinics and research[63]. The EDSS scores assess ambulation together with eight different functional systems, including ocular, brainstem, pyramidal, cerebellar, sensory, bowel and bladder, and cerebral function. It is an ordinal scale, from 0 to 10, with 0 indicating no sign or symptom of disability and 10 indicating death due to MS. EDSS of four or more is assessed based on the ability to ambulate (*Appendix A.1*). The larger and most widely reported studies are relatively older studies

that followed untreated patients, whereas in contemporary cohorts, disability progression is influenced by current different DMTs. The reported time to EDSS 6 (requiring an assistant to walk) ranges from 15 years (Canadian and Swedish series) [57,64] to 23 years (French series) [65].

EDSS does not consider the role of disease duration, which is a key factor in the accumulation of both CNS damage over time and functional disability. To overcome this limitation, Roxburgh and his group, based on databases from 11 countries, have introduced the Multiple sclerosis Severity Score (MSSS) as a method for comparing disease progression in MS using a single assessment at a single point in time [66]. MSSS is obtained by normalising the EDSS score for disease duration and has been a valuable tool in cross-sectional studies. However, other investigators found that the Age-related Multiple Sclerosis Severity Score (ARMSS), which counts for age instead of disease duration is slightly superior to the MSSS in detecting small increases in EDSS. One benefit of ARMSS compared to MSSS is that it allows investigators to study patients for whom the time of disease onset is unknown. Since age is typically unbiased and readily obtained, and the ARMSS and MSSS were comparable, the ARMSS may provide a more versatile tool and could minimise study biases and loss of statistical power caused by inaccurate or missing onset dates[67].

The result of MS disability likely varies depending on where a patient lives [68] and the level of disability also varies between MS patients over time. In two-thirds of instances, death is due to MS, as well as increased risk and consequences of infections such as skin, lung, and urine infections. Thirty-five years is the median time from the MS diagnosis to death, and 73.9 is the median age to death [69].

2.5 Pathogenesis

Historically, MS used to be thought of as a disease characterized mostly by focal WM pathology [70]. Thanks to recent advances in MR technology and pathological studies, scientists have been able to uncover more subtle pathologies connected to MS, such as diffuse WM damage, often known as "Normal-appearing" WM (NAWM), and cortical lesions [71,72]. Furthermore, MS used to be considered a two-phase disease, with an inflammatory component in the early stages and irreversible neurodegeneration in the later stages. CNS tissue loss, on the other hand, is now widely accepted to be present at the start of the disease. The key pathological characteristics of MS, such as WML, brain and spinal cord atrophy, are summarized below, as well as their role in MS patients.

2.5.1 White Matter Lesions

- ***Classification and Formation***

In MS, myelin sheaths, which shield and protect neurons, are attacked by the immune system, resulting in their death. Oligodendrocytes, which support glial cells in the CNS that create myelin, are also destroyed. This causes a decrease in myelin content, and in some cases, a complete loss of myelin, which can damage the axons as they are left exposed. Consequently, MS is classified as a demyelinating disease marked by astrocytic scarring and axon sparing.

Shapes, locations, and sizes of MS lesions are variable, and they play a crucial role in supporting MS diagnosis. The size may vary from less than 1 mm to crossing extensive areas of the brain; these are known as confluent lesions. The most common anatomical locations of MS WML are optic nerve, corpus callosum, cerebellum, around the ventricles, in juxtacortical WM, and in the spinal cord [73–75]. Typically, inflammatory lesions in MS are around the veins; thus, MS lesions are often oval and oriented perpendicular to the axes of the ventricles [76]. When present

around ventricles, these lesions have the appearance of fingers, called "Dawson's fingers" [77] (*Figure 2.1*).

A well-defined nodular gadolinium enhancement usually occurs in small acute lesions. In contrast, a ring-like appearance may be present in large subacute lesions, which have a higher level of tissue destruction and, therefore, tend to resolve more slowly. In such cases, the diameters of the lesions are equal to or greater than 3 mm [78].

Different types of WML have been identified depending on the stage of the disease, all of which are characterized by inflammation, with higher levels of inflammation detected in the early stages of the disease [22]. Acute lesions, also known as active plaques/lesions, are the most common in the early stage of RRMS. While active lesions are characterized by the relative sparing of axons, the fate of oligodendrocytes is less apparent, with some studies showing that they are preferentially targeted in early lesions[79] and others reporting their relative sparing and indications of remyelination [80]. In early MS lesions, there is some indication of inter-patient pathological variation in terms of oligodendrocyte fate [81]. Acute lesions are also invaded by macrophages, which are present throughout the lesional region because demyelination occurs in all sections of the lesion at the same time [75,80,82]. Lymphocytes, most notably CD-8-positive T lymphocytes with some CD-4-positive T cells and B cells, are also present, as are hypertrophic astrocytes with large nuclei [83–85]. The inflammatory infiltrates may penetrate the CNS across the BBB, which enables these relatively young, active lesions to be seen on MRI.

Chronic lesions are increasingly prevalent in the progressive stage of the disease and could be further subdivided into chronic active and chronic inactive lesions. Chronic active lesions (CALs) are identified as loss of myelin with axonal preservation [75]. There is a significant change

in the lesion's neuroinflammatory profile, with overall less inflammation in chronic compared to the active lesions and seen mostly in the lesion's expanding borders [86].

When a lesion becomes inactive, there is a significant decrease in the expansion of inflammatory agents, macrophages, and oedema; instead, astrocytic scarring occurs [75,86]. Chronic inactive lesions are well-defined and characterized by up to 80% of axonal loss within the lesion centre[22]. T_1-hypointensity on MR images is a characteristic of many MS lesions that reflects tissue destruction within lesions; it is estimated that around 40% of T_1-hypointense plaques, also known as 'black holes,' will become chronic as a result of multiple demyelinating events or persistent chronic active inflammation [87].

Even though many axons are demyelinated, certain MS lesions show active remyelination. The existence of fresh myelin sheaths and oligodendrocyte precursor cells in previously demyelinated sites supports this theory [75]. Shadow plaques are lesions that have completely remyelinated and have a lower myelin density than NAWM. Remyelination is expected to occur in around 40% of lesions[88].

Many studies have assessed the sequence of events that lead to the formation of WML in MS over the years. Myelin sheaths are believed to be targets of immune attacks, which are thought to be the cause of MS pathogenesis. Inflammation, demyelination, and neurodegeneration are all clearly implicated, but the exact order of events in this complicated process is still being debated. Several studies using frequent MR (more than once a month) to investigate early lesion formation found gadolinium enhancement in all new lesions [89–91], implying that the breakdown of the BBB is an important step in the process. Other studies reported T_2, MR Spectroscopy (MRS), Magnetization Transfer Rate (MTR), diffusion, and perfusion changes before contrast enhancement [92–95], suggesting that the breakdown of the BBB could be a secondary event preceded

by a variety of changes in both cerebral tissue and blood [92]. The presence of (p)reactive lesions, also known as NAWM, has lately been proposed [96]. They are characterised by the presence of microglia and lymphocytes, but there is no evidence of myelin loss, indicating that inflammatory processes may precede demyelination. Many pre-active lesions have been found to resolve without becoming demyelinating lesions, so understanding their pathophysiology could help researchers to understand the cause of WML formation [97]. Recently, interest is growing in using WML as a tool for diagnosis, monitoring, and clinical trial outcome because WMLs are easily identified even at low field strengths.

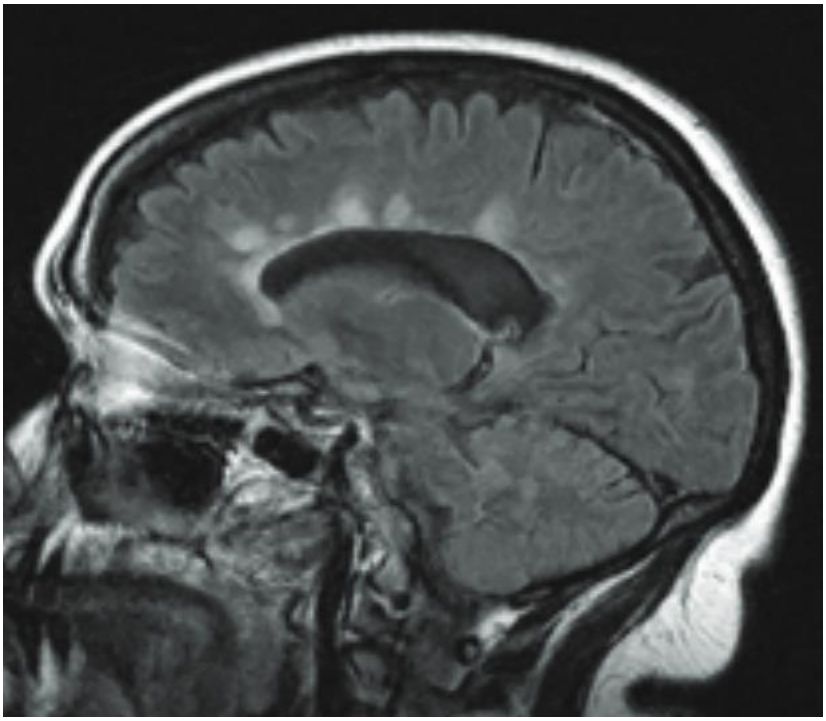

Figure 2.1. Dawson fingers lesions on a sagittal fluid-attenuation inversion recovery (FLAIR) MRI. Finger-like projections found perpendicularly to the lateral ventricles, are MS-specific [449].

2.5.2 Brain Atrophy

- ***Brain Atrophy in healthy ageing and MS***

Brain atrophy is the slow loss of brain tissue over the lifetime, and it is a feature of neurodegenerative diseases like Alzheimer's and MS. It causes a reduction in brain weight and volume, thinning of the gyri and expansion of the sulci and ventricles[98]. A meta-analysis of over 2,000 healthy individuals indicated that the human brain expands at a rate of around 1% per year until early adolescence, after which there is no noticeable yearly change in volume in young adults[99]. After the age of 35, a steady brain volume loss was reported of 0.2% per year [99]. The rate of atrophy rises with age; beyond the age of 40, the brain shrinks roughly 5% per decade, and after the age of 70, it decreases even more [99,100].

In MS, brain shrinkage is accelerated, and MS patients are estimated to lose 0.46 to 1.34% of their brain volume each year [101]. These reported atrophy ranges were pooled from 12 studies (n = 767 patients) which included untreated patients or patients treated with first-generation DMTs. They reported a cut-off point of -0.37% that could consistently distinguish healthy controls from those with MS, with 67% sensitivity and 80% specificity [102].

Previously, brain shrinkage in MS was thought to be a late-stage symptom of the disease, but more recent finding suggests that brain tissue loss begins from the first disease onset [103–105]. In MS, accelerated brain shrinkage is hypothesized to represent direct, permanent damage and death of the CNS's glial cells, axons, and neurons. Indirect pathological changes in the lesion and normal-appearing tissue have also been noted. Evidence suggests that early treatment with DMTs reduces the rate of atrophy, therefore brain atrophy is considered to be a treatment target [106].

- ***White and Grey Matter Atrophy***

The WM, GM, and CSF are one of the primary compartments of the brain. Physiological or disease-related changes in any of those tissues may lead to changes in total brain volume. Several studies have looked at the individual contributions of Grey and White matter as well as global brain volume to patient disability and progression in MS. The goal was to identify which brain tissue most accurately reflects MS-related damage and to determine whether it could be measured easily in a clinical setting.

The volume of WM changes throughout life, growing during childhood and early adolescence before beginning to diminish between the ages of 30 and 40 [107,108]. The exact mechanisms that cause WM atrophy are still being investigated. Several theories have been proposed, including (1) increased volume of WML with age [109], (2) vascular risk factors that cause a decrease in the amount of blood supplied to deep WM [110], and (3) age-related changes in the myelin structure [111].

Axonal transection and apoptosis certainly play a role in WM volume reductions in MS. However, in MS, even the NAWM has been reported to have up to 50% axonal loss and decreased axonal density, suggesting that considerable tissue loss occurs not just in regions with WML, such as black holes with permanent tissue loss, but also in non-lesional tissue [73]. However, different studies in MS have failed to discover substantial decreases in WM volume. This might suggest that tissue swelling and oedema associated with neuroinflammation might obscure the detection of WM tissue loss [112]. On the contrary, GM atrophy was shown consistently to be present from the beginning of the disease and proceeded at a rate of roughly 0.7% each year [113].

Finally, measures of whole brain volume could reflect all degenerative processes occurring in MS brains and might offer a global index of neurodegeneration. Maghzi et al. studied 43 patients

over 3 years and found that brain atrophy is a reliable marker of long-term disease progression in MS [114]. Early atrophy might be expected to correlate with cognitive dysfunction, which is neglected during clinical evaluation.

Caution is needed as global atrophy is a non-specific sign of damage that may be impacted by a variety of disease-related processes, as mentioned before such as oedema, as well as variations owing to physiological changes, such as the patient's hydration level [113]. As a consequence, at least six months of follow-up is recommended, and any atrophy measures should be taken with care [115].

2.5.3 Spinal Cord

Although this thesis focuses on the role of brain MRI in predicting disease progression in MS, it is important not to ignore and to briefly address the role of spinal cord in MS. Imaging of the spinal cord has been reported to be abnormal in three-quarters of MS patients [116]. Although spinal cord imaging is not always required at diagnosis (except when excluding other causes of cord pathology or looking for evidence of DIS), it is of considerable value in patients with suspected MS with few brain lesions or normal brain imaging [117]. It is also more specific than brain imaging as areas of the high signal are not seen in the spinal cord as a result of normal ageing [116].

Demyelinating plaques occur in the spinal cord with the cervical region affected more frequently than the thoracic or lumbar cord [118]. Considerable neuroaxonal loss within lesions, NAWM and GM have been reported resulting in spinal cord atrophy [119–121]. It has been demonstrated both in-vivo [122] and ex-vivo [120], that atrophy in the spinal cord occurs independently of focal lesions. There is no correlation between the rate of spinal cord atrophy and the rate of brain atrophy which raises the possibility of independent disease processes causing the atrophy in these two regions.

Spinal cord atrophy is seen in all MS stages, with volume loss most marked in the progressive forms [123–127]. It has even been detected in CIS patients, even in the absence of spinal cord symptoms [128].

Cord atrophy is independently related to disability in MS patients with long disease duration [123,129,130]. In a study of patients with optic neuritis with brain and spinal cord MRI at the time of CIS, spinal cord lesions were found to be the best predictor of disability after 6 years [131].

However, the structure and location of the spinal cord make it difficult to image. The spinal cord is a much smaller structure than the brain and MRI scanning is prone to artefacts due to patient motion, surrounding CSF and the effects of respiration and the cardiac cycle [130].

2.6 Management and Treatment

Despite the development of new DMTs recently, there is no cure for MS yet. Currently, there are over 20 approved DMTs for MS. Based on the broad categories recommended guidelines published by the Association of British Neurologists (ABN), some DMTs were classified as moderately effective (reduce relapses by 30%) while others were highly effective (reduce relapse by 70%). As a rule, the more effective DMTs appear to be associated with adverse events. The benefits of taking these treatments are their efficacy in reducing the relapse rate, disability progression, and fewer, smaller, or no new lesions.

In CIS patients with a high-risk to convert to CDMS, the use of DMTs in such cases has demonstrated that may be slowed, but not stopped the conversion [132–136]. One of the licensed DMTs for use in RRMS is interferons (INF), which could be injected either under the skin or into a muscle. It has a role in reducing the number of relapses and their severity by a third, but they have a smaller effect on disease progression [137,138]. Several new oral medicines have been used in MS,

for example, Fingolimod which works by integrating with the sphingosine-1-phosphate receptor to stop immune cells from migrating to the brain. It exhibited substantial reductions in relapses and disease progression when compared to placebo and superiority when compared to interferons[139].

Infusion (drip) DMTs are used for MS including Natalizumab [140,141] and Ocrelizumab[142], which are exclusively used in patients with relapsing that are extremely active. When compared to placebo, Natalizumab was demonstrated to lower relapse rates by two-thirds and the progression of persistent disability by 40% in RRMS patients [140,143]. For SPMS patients, Siponimod has been shown to have a good safety profile and reduced the risk of disability progression [144]. For PPMS patients, Ocrelizumab showed its effectiveness especially at the early stage of the disease when it is highly active[142].

Unfortunately, none of the DMTs are without side effects. While the -INF group of drugs cause flu-like syndromes and abnormal blood tests, the extremely serious side effect is the development of neutralizing antibodies (Nabs), and while the continuous debate, there is growing proof that their presence decreases DMTs efficacy. Natalizumab induces a life-threatening disease called progressive multifocal leukoencephalopathy (PML) in about 1/500-1/1000 people [145,146]. Fingolimod is associated with bradycardia, atrioventricular block (rare), and herpesvirus infections.

Developing tools and strategies to optimize the risk-benefit ratio of ever-increasing treatment options for RRMS patients is undoubtedly one of the most challenging issues for neurologists treating MS patients. Relevant to this thesis is the question of trying to identify early patients with MS that are likely to progress and have a significant disability, so trials can test which of the above medications are more valuable.

The remaining of MS therapy is symptomatic, focusing on symptoms such as stiffness, bladder problems, and exhaustion. High-dose, short-course corticosteroids might be an option in MS during acute relapses, when they may expedite recovery but have little effect on the eventual result[147]. In the treatment of MS patients, a multidisciplinary strategy that includes physiotherapy, occupational therapy, speech and language therapy, and neuro-rehabilitation is critical, particularly when they are developing considerable impairment [148,149].

Chapter 3 . Magnetic Resonance Imaging

3.1 Technical Background in MRI

Nuclear Magnetic Resonance (NMR) provide a basis for Magnetic Resonance Imaging (MRI). The negative connotations of the term “nuclear” led to its exclusion from the name of this imaging modality, which is now known as MRI rather than NMR. The magnetic resonance phenomenon was discovered separately in 1946 by Felix Bloch and Edward Purcell, both of whom were awarded the Nobel Prize in 1952, but it took several years for Lauterbur (1974) and Mansfield (1976) to independently refine the technology for medical imaging. The hydrogen nucleus ^{1}H is the particle of interest in this research, which is mainly found in the form of water or lipids. However, other nuclei with an unequal number of protons and neutrons, such as ^{19}F, ^{23}Na, and ^{31}P, may also be studied using MRI, but they are less common in biological tissues.

"MRI comprises three main components - a strong magnet to align the protons in the body, radiofrequency coils (RF) to excite and detect protons signals, and gradient coils for spatial localization. In principle, MRI mainly utilizes the natural properties of hydrogen protons which as part of water or lipids, make up 75–80% of the human body[150].

Protons have a positive charge, and when spinning creates a magnetic force, a vector with a direction and magnitude (*Figure 3.1*). In a normal state, protons move randomly and cancel each other out. However, when placed in an MRI scanner (B_0), the protons with the lower energy align with the main magnet slightly more in the parallel direction than the antiparallel, forming a net magnetization vector. To generate signals, a special frequency known as the Larmor frequency which matches the frequency of proton precession, is applied to excite the protons - known as resonance, which is the reason behind the term “magnetic resonance imaging”. After the excitation

pulse, the protons absorb energy and flip to transverse magnetization (represented by T_2) inducing a current in the receiver coil. When the RF pulse is removed the protons return to the longitudinal magnetization (described by T_1) and the signals start to fluctuate - known as free Induction Decay (FID)"[151]. T_1 is influenced by the rate of energy transfer back to the surroundings as protons return to their preferred low-energy state while T_2 is affected by the inhomogeneities of the local and external magnetic fields, which cause the protons to become out of phase (precess at different frequencies) [152]. Furthermore, protons in different tissues return to equilibrium at different rates, resulting in different signal strengths for various tissues. The energy released during the return to equilibrium determines how bright the image will be, thus providing contrast between tissues [152,153]. Much of the contrast seen in MRI sequences is based on T_1 and T_2 relaxation times, as well as Proton Density (PD), which is the concentration of protons in a specific tissue.

In the brain, MRI scans reflect those principles of physics. As CSF is largely composed of water in the brain, it has relatively long T_1 and T_2 values and, because the spins take longer to rephrase, CSF appears bright in T_2-weighted images with the appropriate detector settings [154]. WM has shorter T_1 and T_2 values because it is more highly organized (i.e., more solid-like in structure). GM contains more macromolecules than CSF, thus, its T_1 and T_2 relaxation times are intermediate. MS lesions may have a structural change that may be seen on MR imaging. Using multiple RF pulses time to repeat (TR) and modifying the time interval (TI) between them can result in different image contrasts that can be used to distinguish differences between various tissues in the brain, e.g. normal-appearing and WM lesions [155].

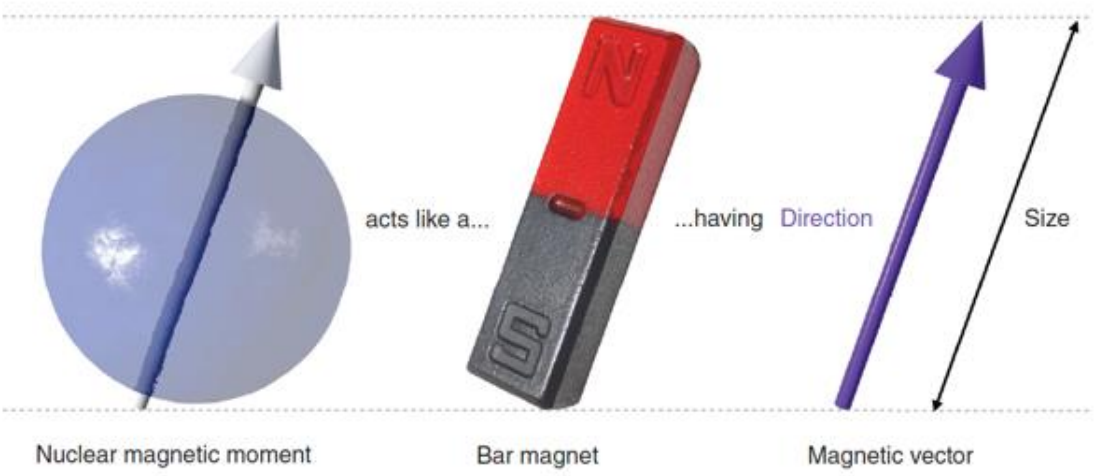

Figure 3.1. The magnetic moment of the hydrogen nucleus which is represented by a vector [156].

3.1.1 Imaging Sequences

- ***Spin Echo Sequence***

In MRI, the routinely used sequence is the so-called Spin-echo (SE) sequence. An initial excitatory 90° RF pulse is applied to generate a SE sequence, followed by a second 180° refocusing pulse. Applying the 90° pulse along the x-axis creates transverse magnetisation along the y-axis (T_2 relaxation time). Due to time-invariant local inhomogeneities, the transverse magnetization dephases (T_2 decay). The spins are flipped from the near y-axis to the –y-axis when a 180° pulse is applied at a different time from the 90° pulse along the x-axis. The spins continue to precess in the same direction and at the same rate as before the 180° was given, causing the transverse magnetization to rephase. The spins completely rephases along the x-axis, resulting in a detectable spin-echo signal (Echo Time TE). The Repetition Time (TR) is the time between two excitation 90° pulses.

The scan acquisition parameters TE and TR are important for the type of images produced. Images can be weighted depending on the T_1 and T_2 features of the substance imaged by changing these values. The appearance of a SE image is determined by these two parameters (TE and TR); various mixtures of TE and TR generate varying degrees of contrast (intensity difference) across tissues. Changing TR alters the contrast between tissues with various T_1 relaxation times, whereas altering TE alters the contrast between tissues with different T_2 relaxation times. TR is usually longer than TE and the signal is proportional to PD. PD-weighted image is generated with a short TE (avoids T_2-weighting) and a long TR (avoids T_1-weighting). Short TE and TR are used to provide a T_1-weighted image (T_1W) which the intensity contrast is mostly owing to the tissue's T_1 relaxation characteristics. A T_2-weighted image (T_2W) with a long TE and TR produces an intensity contrast that is mostly owing to the tissue's T_2 characteristics.

Fluid Attenuation Inversion Recovery (FLAIR) and Susceptibility weighted imaging (SWI) were the main sequences used in this thesis; these sequences are briefly described below.

FLAIR is a technique commonly used in brain imaging to suppress fluid signals as lesions frequently located near bright CSF. This is achieved by using an Inversion Recovery sequence and setting the inversion time (TI) to nullify the signal from fluid. A range of TIs is used, typically between 1800 and 2500 ms depending on the magnet's field strength[152].

On the other hand, SWI is an MRI technique combining magnitude and phase information, offering an excellent contrast between tissues with different magnetic susceptibilities, allowing qualitative assessment of diamagnetic and paramagnetic features in the brain. Phase images provide information on the local susceptibility changes between tissues together with unwanted background field effects. The phase images must undergo further processing to reconstruct the susceptibility weighted images. After pre-processing, a phase mask is created to emphasise tissues

with different susceptibilities. The magnitude image is digitally multiplied by the phase mask several times until the desired mix of phase information is imparted [157–159]. In MS, SWI uses the magnetic susceptibility variations in the brain which show the distribution of iron and myelin in WML[160].

- ***Gradients and Image Formation***

Magnetic fields that shift from point to point, generally in a linear fashion, are known as gradients. While the magnetic field B_0 is always present throughout the acquisition, the gradient pulses are supplied in a controlled manner to generate an MR pulse sequence [152]. The MRI gradients are used for image formation. To provide 3D spatial encoding in the x, y, and z directions, three orthogonal gradient coils (slice-select, phase encoding, and frequency [read or readout] encoding gradient) are applied. The slice-selective gradient, which is activated during the RF pulse, permits stimulation of a slice of tissue matching the slice-selective RF pulse's bandwidth, activating those protons at the Larmor frequency pulse.

Performing this step-by-step with subsequent excitations selects specific slices to cover the tissue under investigation. Slice thickness is dependent on the RF pulse bandwidth and the amplitude of the slice-select gradient.

When the echo is received, the frequency-encoding gradient is applied following the slice-selective gradient. This results in distinct precession frequencies along the axis, resulting in a different frequency for each section of the sample. It is only applied while the signal is being measured, therefore, allowing the measurement of signal intensity at each frequency. The phase encoding gradient is used after the excitation RF pulse but before the frequency encoding gradient, to give spatial information about the orthogonal direction by generating a phase shift in the protons,

with protons at various places in the gradient processing at different frequencies. Except for single-shot approaches, the procedure is repeated with phase-encoding gradients of increasing amplitude and a distinct TR for each encoding stage. The number of frequencies encoded multiplied by the number of phases encoded is described by an image's matrix (most commonly 256 x 256).

The plane of imaging is determined by the vector of application of the three gradients (axial, sagittal, coronal, or oblique). The slice-select gradient solely defines the plane in two-dimensional (2D) imaging, whereas the other gradients determine the in-plane orientation. In two-dimensional (2D) imaging, frequency encoding is used in one direction and phase encoding in the other, but in three-dimensional (3D) imaging, frequency encoding is used in one direction and phase encoding in the other two. A line of data is stored on a computer as a sequence of integers for each TR. This process is continued until the whole data set has been assembled. This data does not correlate with the image, so it must be translated from the time domain to the frequency domain via a mathematical procedure called the Fast Fourier Transform (FFT). The image is made up of a matrix (the number of pixels) and a field of view (FOV) that defines the size of the area under investigation. The FOV is calculated by multiplying the number of pixels by the voxel size (FOV = number of pixels * voxel size).

- ***Signal-to-Noise Ratio***

The Signal-to-Noise Ratio (SNR) is a metric that compares signal intensity to background noise. SNR is the ratio of the mean voxel signal (from a homogenous area with high signal intensity inside the object of interest) divided by the Standard Deviation (SD) of the background signal (measured from several regions outside the object). The unwanted signal produced by the MR equipment, the surroundings, and the patient is known as "noise". It may happen at any moment

and field strength, proton density, coil type and position, TR, TE, flip angle, number of signal averages and receive bandwidth all impact the SNR [161].

- ***Contras- to-Noise Ratio***

The Contrast-to-Noise Ratio (CNR) is the ratio of signal intensity difference between areas with different tissues and background noise. Clinically, CNR is the most significant image quality parameter since the goal of any examination is to generate an image that clearly shows disease in relation to normal anatomy[162]. When the CNR between a lesion and the surrounding normal tissue is high, the visibility of the lesion improves. CNR may be boosted by T_1 or T_2-weighting, injection of a contrast agent, magnetization transfer contrast, and chemical suppression procedures. CNR is also influenced by the same factors that affect SNR.

3.2 Ultra-High-Field MRI

Ultra-Hi-Field (UHF) MRI includes the use of scanners with a field strength of 7T or even more to 11.7T, which are primarily used for research purposes. As of 2021, there were approximately 90 centres with access to UHF scanners worldwide and this number is expected to have increased [163].

The field strength of a scanner refers to the static magnetic field created by its magnet; this can be measured using units of Tesla (T). Increasing the scanner's magnetic field strength results in improved quality of the MR images. Due to the increase in field strengths, SNR and CNR increase, resulting in MR images with higher resolution, smaller voxel sizes and improved contrast. 7T MRI also leads to decreased scanning times [164].

UHF MRI offers a unique opportunity to study MS pathology in greater detail than possible through clinically available scanners. Previous research has found that 23% more WMLs were detected on 7T scans compared to 1.5T scans [165]. Similarly, 7T studies were able to detect 40 % more IRLs compared to 1.5T and 3T studies[166–170]. This is most likely due to the lower resolution of images and higher noise at lower field strength which reduces the detection of lesions details[170]. 7T scanners have also proven unparalleled at cortical lesion detection compared to conventional scanners [171]. It was believed that cortical lesions remained largely undetected on MRI, even when using UHF scanners, however, it has been demonstrated that with long enough scanning times it is possible to visualise virtually the majority of cortical lesions present on the corresponding histopathology sections[172].

Despite the high cost of roughly 10 million USD (approximately 7.7 million GBP) [173] per scanner, UHF imaging has limitations as well. The use of 7T MRI is limited by high Specific Absorption Rates (SARs) and field inhomogeneities. A SAR is a measurement of the human body's energy absorption rate in response to an RF electromagnetic pulse. Simply, part of the radio frequency energy emitted during scanning may be absorbed by the human body, resulting in tissue overheating. SAR increases as field strength increases along with using different MR sequences that apply 180°RF pulses, such as T_2-weighted images, that could exceed SAR safety limitations estimated by scanner manufacturers [174]. Field inhomogeneities may occur in both the main magnetic field (B_0) and the RF field (B_1), resulting in regional signal fluctuation and/or the appearance of susceptibility in the image.

In 2016, the first clinical 7T MRI in the UK was launched in Scotland. However, due to the high cost of UHF MRI and high sensitivity of 1.5T and 3T scanners in diagnosing brain disorders the high expense of UHF MRI machines, it is unlikely that 7T scanners will be routinely

used in clinics in the near future. Any study results at UHF must thus be proved and utilized at lower field strengths in a typical hospital context.

3.3 MRI in MS

3.3.1 MRI in MS diagnosis

MRI has been part of the diagnostic criteria since 2001. Today MRI plays a key role in several aspects of MS including diagnosis, monitoring progression and assessing treatment response [175].

MS is a multifocal, progressive, inflammatory disease of the CNS, and MRIs can show these changes. The changes seen on MRI are based on the changes in proton density (water content). MRI provides an evaluation of the anatomy (location), size, and detailed vascular information on MS lesions [176]. The most commonly used sequences include T_1W, T_1W post-contrast, T_2W, and FLAIR [177].

T_1W shows brain atrophy and lesions as hypointense or "black holes" representing areas of oedema and axonal loss [87,178]. T_1 black holes are of two types: transient and permanent. Transient black holes are seen in areas of acute inflammation, and probably represent focal oedema and resolve within days/weeks while permanent black holes are darker with an indication of focal axonal loss area. The presence of such black holes in the MRI of MS patients suggests a more destructive pattern of disease, one that can lead to another change on MRI, namely atrophy [78]. **T_1W-post contrast** allows the identification of any BBB deficit associated with acute inflamed MS lesions [76]. In a healthy brain, the contrast agent (CA) is confined to the vasculature and does not cross the BBB. However, due to MS pathophysiology, the BBB is disrupted causing CA to reach brain lesions and give signal enhancement in T_1W, which indicates that the lesion is less

than eight weeks old [74,78]. The pathological changes of lesions with CA are thought to be related to active inflammation and are usually associated with tissue distraction. Occasionally contrast-enhancing lesions may indicate areas of remyelination[179]. Over time, lesions lose their enhancement and are only visible on T_2/FLAIR and possibly on T_1W sequence.

T_2/FLAIR reflects the prolongation of transverse relaxation times related to increased tissue water content. T_2/FLAIR are highly sensitive in detecting focal WML, and the lesions are hyperintense representing areas of acute inflammation, demyelination, remyelination and chronic scarring. T_2/FLAIR lesions are usually more located around the ventricles or in the cortex (surface) of the brain. MS patients with multiple T_2/FLAIR or T_1 lesions are at a higher risk of physical disability [180]. Spinal cord lesions are also commonly found in approximately 50-90% of MS patients [181,182].

Currently, in clinical practice, brain or spinal cord atrophy, Central Vein Sign (CVS) and IRLs are not used widely during the diagnostic process. Although atrophy can be detected early, even at MS diagnosis stage, it is not commonly used as a part of the diagnosis process[105]. Similarly, CVS is proposed as a specific MS diagnostic imaging biomarker, which can successfully distinguish between MS and other conditions resulting in WM lesions. Studies using UHF MRI have reported around 80% of lesions as having a CV, with periventricular lesions having the highest number- a total of 94% [170,183]. CVS has been reported in all MS phenotypes[184] and all brain regions [184,185], and the proportion of lesions with CVS decreases with distance away from the ventricles[186–188] and patient age [184]. Studies using clinically available lower field strength scanners, including 1.5T and 3T, have also successfully visualised the CV sign. A number of different criteria for positive central vein sign have been used, including 40% of all lesions having central

veins, rule of 6 and rule of 3[166,189,190]. The optimal threshold that can be applied in clinical practice is still to be determined.

Similar to the CVS, IRL has also been proposed as an MS diagnostic biomarker. Both CVS and IRL reflect specific biological features of MS lesions, as the CVS relays on the pathological specificity of perivenular distribution of MS lesions [191] while the IRL reflects the iron-laden activated microglia/macrophages accumulation at the lesion's edge. The previous characteristic feature of MS (presence and location of WMLs) can be detected using conventional MRI sequences such as FLAIR and T_2- weighted imaging. However, the detection of CVS and IRL requires additional imaging sequences. IRL is one of the main focuses of this thesis which will be discussed in depth in section 3.4.1.

3.3.2 MRI in MS Prognosis

MRI has a high value in predicting disease conversion and disability progression. Multiple studies have focused on the predictive value of T_2-hyperintense lesions, T_1-hypointense lesions "black holes", as well as the implication of overall atrophy seen on MRI on disease progression. These MRI features were used for predicting the disease conversion from CIS to MS, together with the general prediction of long-term disability [192–194].

T_2/FLAIR hyperintense lesions accumulation in the CNS at the disease onset is a good predictor of clinical disability [178]. Longitudinal studies demonstrated that the increased number and volume of T_2-hyperintense were associated with disability [46,195]. Additionally, within the first 5 years of the disease, the number of new T_2-hyperintense lesions was the strongest predictor of increased EDSS at 14 years, and the follow-up study confirmed an association between early

lesion accumulation and subsequent 20-year disability [196]. Further discussion about this predictor will be discussed in section 3.4.2. and chapters 7 and 8.

The topographic distribution of the lesions has been associated with disability and in particular periventricular, brainstem and spinal cord lesions correlate with disease progression [197–199]. The impact of infratentorial lesions in long-term prognosis has been evaluated in patients with CIS and brainstem rather than cerebellar lesions were responsible for increased disability.

T_1 hypointense lesions persist for six months after the initial enhancement [200] and show significant demyelination and axonal loss [201]. They are associated with neurodegeneration and are known to correlate with disability in MS patients [194]. A ten-year follow-up study found that the number of T_1 hypointense lesions at baseline scan, and the increase in T_1-hypointense lesion volumes could predict worsening EDSS. New or enlarging T_1-hypointense lesions also correlated with EDSS change [202].

Recent studies aimed to quantify cord lesions showed their association with disability especially cervical lesions in both relapsing and progressive forms of MS and a higher lesion load was detected in patients with progressive MS [199,203].

IRL, brain and spinal cord atrophy are other MRI biomarkers with predictive prognostic value. These markers could indicate more severe, destructive inflammatory responses and their presence correlate better with subsequent disability [102,178,192–194]. IRL will be discussed further in detail in section 3.4.1. Thus, the above-mentioned biomarkers have the potential to predict disease progression, and long-term disability and could be used as a guide for treatment initiation.

3.3.3 MRI in disease monitoring

Most MRI studies investigating treatment efficacy focus on changes in the number and size/enlarge of T_2-hyperintense and contrast-enhanced T_1-hypointense lesions. A recent meta-analysis examined the effect of treatment on lesion load and found that treatment effects on MRI lesions over short periods (6–9 months) have a predictive value on relapses over longer follow-up periods (12–24 months) [204]. The overall analysis of these 31 studies showed that new or enlarging T_2-hyperintense lesions and contrast-enhanced T_1-hypointense lesions were associated with the number of relapses and disease activity, and the use of MRI was proposed as a primary endpoint for treatment trials.

In addition to relapses, and disease disability NEDA has been promoted by some as a target for patients with MS. NEDA incorporates relapses, clinical disability and development of brain atrophy, indicating the significance many clinicians put on atrophy [205].

3.4 Exploring MRI Biomarkers in MS in this thesis

Since MRI principally is showing the changes in the state of water in the CNS, such MRI-detected lesions are intrinsically pathologically nonspecific. Typically, MRI imaging the tissue response macroscopically rather than the pathology itself; many different pathologies or diseases can have a similar appearance/response. Thus, MRI T_2 hyperintense lesions are non-specific to MS with a long list of conditions, ranging from migraine, stroke, infection, normal ageing, and high blood pressure, to MS, causing brain "spots". Thus, changes on MRI should never be used in isolation to make an MS diagnosis. Confirming the diagnosis and identifying patients with a high-risk of developing a severe disability could impact the disease course positively[206]. It is believed

that early treatment with high effective DMTs could delay disease progression[8,207]. Currently, searching for imaging biomarkers that could accurately diagnose MS and predict long-term disease progression is clinically important, especially in the ear of new highly effective DMTs[208].

More recently, the study of lesions with paramagnetic/iron rim (PR/IR), which appear as a dark, ring-like feature on the edges of some MS lesions, has gained research attention. Other patterns of iron accumulation, including scattered iron deposits, which appear as hypointense 'dots' have also been described, and they could indicate the initial stages of iron deposition to form IRs[209]. The total WML count, volume and linear measurements of brain atrophy also have the potential to predict disease progression and long-term disability. Due to the overall focus of this thesis, CVS and iron dots will not be discussed in detail. Below I will introduce IR corresponding to the work in chapters 4, 5 and 6, WMLs in chapters 7 and 8, and linear measurements of brain atrophy in chapter 8.

3.4.1 Paramagnetic/ Iron Rim Lesions

The significance of iron presence in MS lesions is still unclear; however, MRI lesions with IRs are speculated to reflect what is termed in pathology Chronic Active Lesions (CAL). In MRI, we detect Slowly Expanding Lesions (SELs) and we assume that this reflects failure to remyelinate. SELs have been proposed to be a marker of tissue destruction, continuing inflammation and failure to repair [210–212].

Early data from the Reich group (2016) followed Gd-enhancing lesions over a one-year course and showed that IRL tent to form in newly formed T_2 lesions, being larger and more destructive than rimless lesions [211]. IRLs are 5-20 times larger than non-IRL at the time of

formation and the size difference persists long-term [211]. Long-term changes take place at a very slow pace taking several years to be unequivocally observed. The reported time for IRL to disappear differs among studies. In a 7T MRI study of 7 MS patients most IRLs enlarge/expand, and non-IRL shrink over 3.5 years[213]. However, another study from the USA yearly followed 10 MS patients using different methods assessing the T_2 * phase component of the rims at 7T, and showed that IRL slowly fades over 6-8 years leaving behind a (large) T_2 lesion [214].

The most extensive histological analysis of lesion phenotypes in MS (2476 WM plaques from 120 patients) showed that smouldering plaques were mainly seen in patients with disease duration of more than 10 years, and peaked at approximately 20 years of disease duration and in patients 50 years of age [215,216]. Studies have reported different findings on the presence of IRs in different MS subtypes. It has been reported that IRLs were commonly found in patients with progressive MS and higher disability[213,217] while others found more rims in RRMS patients [216].

IRLs might be specific features of MS lesions, which could be used not only as biomarkers of disease progression but also diagnostically [218]. Furthermore, the presence of at least one rim was shown to have an association with lowering thalamic and GM volumes [219–227]. There has been preliminary evidence showing an association between IRL and spinal cord lesions, atrophy [220,221]and greater load of cortical lesions [222].

Yet, there is no universal/agreed nomenclature for the rim in the MS imaging community, some refer to these lesions as iron rim lesions while others prefer to use a broader term such as paramagnetic rim lesions. The rim lesions were originally called paramagnetic rim lesions in view of the signal drop-out detected around some lesions, due to the paramagnetic shift on MRI acquisition. A number of studies [189,190,211,213,228,229] recently detected iron deposition as the main

contributor to these paramagnetic rims, hence, many investigators start using the term IRLs. In this thesis, both terms were used.

- ***Imaging and Analysing IRL***

A recent study found that almost all of the IR visible on 7T MRI could be seen on 3T phase images [230]. MRI offers different techniques and sequences which are sensitive to brain iron; the most common ones include, T_2W fast spin-echo (FSE) imaging, T_2*W gradient-echo (GE) imaging, SWI, and QSM. MRI acquisition and post-processing techniques for IRL detection and/or quantification are compared in *Table 3.1*. However, it is essential to bear in mind that iron-sensitive sequences are also sensitive to changes in tissue density, water and fibre orientation [231,232]. These techniques should be carefully chosen based on the context of use (ease of interpretation, need for quantification).

After having the images, IRL can be analyzed by looking at the (i) burden of IRL (IRL count and volume) [219], and (ii) ongoing microstructural damage in IRL (inside or at the edge of the lesion). Inside the lesion, by the change in normalized T_1 intensity, myelin water fraction, diffusion imaging or other available markers [233]. At the lesion's edge, by the change in phase signal intensity and QSM susceptibility to see the iron deposition or disappearance [234,235].

Although manual detection of IRL is still the common approach, a classical solution for automated IRL detection has been recently proposed. A fully automated IRL detection that employs classical machine learning with a random forest classifier to extract radiomic features provides good rim detection. This method detects lesions automatically with the removal of confluent lesions [236]. Another group used deep learning and achieved an excellent performance to

identify IRL using a conventional neuronal network [237]. This technique relies on manual cluster subdivisions to deal with the challenges of confluent lesions (semi-automated). However, like any advanced technique, it has not yet been implemented in clinics.

*Table 3.*1. Summarises the pros and cons of different acquisition and post-processing techniques in detecting and quantifying paramagnetic rim lesions [238]**.**

	T_2*-GRE	Fast GRE	mGRE	T_2*-EPI	R2* Relaxometry	SWI	Filters Phase	QSM
Pros	-Available on all vendors. -Ideal T_2*W -Easy optimization (contrast, resolution…)	-Available from all vendors. -Short scan time at high in-plane (axial)resolution -Whole-brain coverage	-Available from all vendors. -Multiple echoes (quantitative) -T_2*W at late echoes -Whole-brain coverage.	-Short scan time at high isotopic resolution (submillimeter isotopic) -IRL can be viewed in any orthogonal planes -Adequate T_2*W -Whole-brain coverage.	-Quantitative of T_2*/R2* -Relatively fast execution -Can incorporate multi-parametric fitting (e.g., GEPCI post-processing)	-Available on all vendors. Image sharpness improved -Very fast execution and can provide filtered phase	-Available from all vendors. -Image sharpness preserved -Easy optimization, fast execution.	- Quantitative of (apparent) tissue magnetic susceptibility -Remove dipole field effects (veins and lesions)
Cons	-Long scan time at high resolution -Partial brain coverage	-Mixture of T_2*/T1 W -Difficult to visualize IRL in orthogonal planes; thick slice (≥3mm) to reduce scan time -Scan time at a high isotopic resolution is not compatible with clinical workflow -Limited optimization (short TR...)	-Difficult to visualize IRL in orthogonal planes; thick slice (≥3mm) to reduce scan time -Scan time at a high isotopic resolution is not compatible with clinical workflow -Limited optimization (# echoes ≥ TR...)	-Limited vendor availability* Limited optimization (single-echo, trade-off distortions vs speed)	-Require multi-echo acquisition Accuracy of quantitation affected by noise (feasible at 1.5T) -Typically, offline post-processing	-Different post-processing methodologies across vendors (SWI: Siemens, SWIp: Philips, SWAN: GE). -Optimization locked by vendors -Risk of false-negative IRL due to thick slice acquisitions.	-Phase signal is highly dependent on imaging acquisitions /post-processing parameters -Risk of false-positive IRL due to diploe field effects.	-Offline, slow post-processing -Risk of false-negative IRL due to thick slice acquisitions & smoothing -Accuracy of quantification affected by noise (feasible at 1.5T)

GRE: Gradient-Echo, mGRE: Multi-Echo GRE, EPI: Echo-Planer-Imaging. SWI: Susceptibility Weighted Imaging, QSM: Quantitative Susceptibility Mapping.

** Siemens and Philips only.*

- ***IRL evolution: Can it be altered?***

Given the rising interest in IRL in MS patients, researchers and clinicians are raising different questions about these rims; (1) whether we could do anything about these rims, for example, early treatment to slow down the expansion of these lesions, (2) what is the natural history and the most biological relevance of these rims, (3) is it the IRL intensity as a whole, count or size? All these issues need further investigation.

Recently, a study from Absentia *et al.* suggested that measuring the intensity of the rim itself might be a promising outcome measure for disability progression [214]. Their data showed that IRL faded over time but there was a period of stability and long-lasting, so potentially they have a wide window in which to measure/intervene in this outcome marker. They estimated 16 patients per arm (112 IRL in total) to test the efficacy of drugs to accelerate the resolution of IRL over a year and found there was a 10% difference in IRL fading/disappearing.

A recent case-control analysis used QSM values on IRL of patients who were on Glatiramer Acetate (GA) and Dimethyl Fumarate (DMF) and found that DMF patients had more rapid QSM reduction on IRL compared to GA patients [239]. There was a slight imbalance between groups (16 GA, 18 DMF), however, this is certainly a promising finding.

In summary, IRLs can be a quantifiable early biomarker of lesion inflammatory activity although uncertainty remains about which aspects of these lesions represent the most sensitive and biologically relevant target (size, count, or intensity).

3.4.2 White Matter Lesion Counts and Volume

WMLs at baseline MRI scans are considered relevant by most clinicians and researchers in predicting disability, disease progression and guiding DMTs choice [10,240–244]. Most clinicians

monitor WMLs and note any change in T_2 lesion load when assessing treatment success. Concerns about the Gadolinium deposition in the brain made Gadolinium no longer routinely used for surveillance imaging [245,246].

- ***T_2 / FLAIR Hyperintensities WMLs***
    - ***Lesions Count***

The total WMLs number was proposed early in the MRI in MS research as an important predictive biomarker, as a high number of WMLs were associated with disease conversion, progression [247] and predicting disability after 20 years [87,248]. The baseline WMLs showed an association with EDSS, and also the changes in WMLs number were associated with the changes in EDSS [195,249,250].

Fisniku and colleagues conducted one of the most important investigations of WMLs in MS by following CIS patients for 20 years. This UCL cohort showed that patients with abnormal baseline MRI were more likely to develop CDMS. In the same study, patients who converted to SPMS had a higher yearly lesion growth rate than those who remained RRMS (almost $3cm^3$/year vs. $0.80cm^3$/year) [46]. It has also been shown that the early accumulation of WMLs in the first five years was associated with greater disability ($R=0.69$, $p<0.001$)[46]. Similarly, another group showed that new lesions in the first 3 years were associated with an increased risk of developing SPMS after 15 years [251]. These findings add further evidence that high lesion load is linked to poor clinical outcomes. A meta-analysis of prospective studies found a moderate association between the number of Gd-enhancing lesions in the first six months and longitudinal clinical outcomes [252]. Another meta-analysis assessed treatment effects in randomized clinical trials extended on these results, showing that short-term (6–9 month) follow-up of WMLs predicted the yearly relapse rate

long-term (year one to two; slope=0.52; R_2=0.71) [253]. All of the aforementioned points to WML's importance in predicting long-term disease progression in MS patients.

Despite this, the relationship between MRI-detected lesions and clinical outcomes remains modest at best, which has led to the formation of the phrase "clinical-radiological paradox." It is likely that this discrepancy between individual MRI biomarkers, such as WM lesion load, and clinical outcomes exists because of the vast heterogeneity of the pathophysiological processes taking place simultaneously in the MS brain. For example, T_2 lesions give information on ongoing, localized neuroinflammatory processes in the brain but do not represent the irreversible axonal damage caused by the disease.

Nevertheless, WMLs load is taken into account when evaluating new patients in clinics. For example, for newly diagnosed patients, the choice of DMTs is often determined by the appearance of their baseline MRI, as patients with more abnormal scans might be offered higher efficacy treatment.

- ***Lesions Volume***

The count of WMLs was not only associated with disease progression but also the lesion volume showed a better association with long-term disability [254]. The first UCL cohort found a strong correlation between lesion volume and EDSS score at 14 years [250], lesion counts revealed broadly similar relationships but were less reliable than volumes as an indicator of disease progression. This could be because of the difference in lesion size as expansion and confluent lesions are not accounted for [250]. There is a controversy about which of those two features of WMLs (numbers of volumes) holds more predictive power [131,255–258].

The location of WMLs also plays a role in explaining the disease outcome in MS. The baseline MRI assessment in CIS and MS patients showed that the infra-tentorial WMLs [247,259,260] and spinal cord lesions [199,261,262] have been demonstrated to predict disability in the short and medium term. For PPMS, lesions localised around motor tracts were shown to be the best predictor of disability [263].

MRI scanners are improving in detecting WMLs [264,265], especially at higher field strengths with a better resolution [266]. A significant number of lesions on MRI go undetected clinically [267]. It has been shown that the subclinical pathological processes might be 5 to 10 times more active than clinically expected, even when assessing conventional sequences at 1.5T MRI scans [268].

Although different automated WMLs detecting software is available with reasonable accuracy in research, an expert reviewer is still advised for the majority of scans and cannot be used in clinics [245,269]. Another challenge is identifying and quantifying new lesions for patients with large, confluent lesions. A confluent lesion might involve two lesions attached by a single edge or dozens of attached lesions forming large areas of white matter; in this situation, a new lesion joining this confluence could be easily missed [270]. Longitudinal follow-up MRIs, even when properly administrated, might be a long- period between scans and yet might show multiple new lesions that overlap in space. Automated software analysis could hold the key in such cases [90,271]. Additionally, combining different MRI biomarkers, such as WML and brain atrophy, could offer better insight into the disease.

3.4.3 Linear Measurements of Brain Atrophy

Brain atrophy has been proposed as a possible marker of disease progression and disability in MS and is increasingly being involved in MS treatment trials [114,272–274]. Although atrophy was seen in the early stage of relapse-onset MS, it may be more visible in the later stages [275]. At different phases of MS**,** whole-brain atrophy, together with tissue-specific (i.e. GM and WM) and regional atrophy have been perceived [112,276–280]. The rate of atrophy has been shown to be the same across MS subtypes [281], whereas other studies have shown more atrophy in the progressive forms of MS [275,278].

Two [106], five [282], and eight years later, the annual atrophy rate was found to be a good predictor of physical disability, with patients with the highest decrease in brain volume being four times more likely to reach an EDSS score ≥ 6 in 8 years of follow-up [283]. Similarly, a ten-year follow-up study of 176 RRMS reported that patients with a disability had a higher yearly atrophy rate, with the percentage of brain volume change (PBVC) at year two being predictive of disability in year ten [113].

Global brain measurements are not yet commonly used in clinics. Although in the future, computer power and IT development might give accurate measurements of brain atrophy, the reality is that currently, very few centres are quantifying brain atrophy outside research settings. However, it remains unclear how this should be incorporated into decision making. It is possible that simple linear measurements of regional brain atrophy could be used instead.

Third ventricle, medulla, corpus callosum and inter-caudate are established linear measurements of the brain, that correlate with long-term disability progression in MS and easy to implement in clinics [284–290].

Ventricular enlargement is a potential indirect marker of neurodegeneration. The enlargement of the ventricles was associated with brain atrophy and may be seen on MRI scans, even on 2D scans with poor contrast and clarity, particularly in MS patients who have had the disease for a long time[291]. Third ventricle is a sensitive marker of disability and disease worsening [292,293284,287,288]. This might be due to its easy-to-measure form, insensitivity to magnetic field inhomogeneities, and high tissue contrast [105]. The ventricular system consists of four linked CSF-filled chambers, also known as ventricles, which play a role in CSF production; the lateral ventricles are the biggest and are connected to the third ventricle through the interventricular foramina. The thalami surround the third ventricle, which connects to the fourth ventricle, a diamond-shaped chamber in the pons, through the cerebral aqueduct [294].

Medulla width (MEDW) has been demonstrated to be a sensitive indicator of atrophy in MS [295] and may be used instead of cervical spinal cord volume in predictive diagnoses [287,296]. A longitudinal study over 30 years of CIS patients showed that linear measurements of brain atrophy (specifically MEDW and TVW), within the first 5 years could predict progressive MS and disability 25 years later [191]. The medulla oblongata is the brain stem's most caudal component, which connects to the spinal cord. The lower medulla oblongata's ventral, dorsal, and lateral funiculi are connected to the spinal cord. As a result, it has been proposed that upper spinal cord volume measures give information on disease progression that is complimentary to brain atrophy assessment [296].

Corpus Callosum Index (CCI) is a normalized measurement that reflects the changes in brain volume and is a marker of brain atrophy in MS[289,297]. CCI is easily manually measured using clinical/conventional MRI scans. A moderate correlation of CCI with the EDSS has been reported in many studies [287,289,295,298,299]. [300,301]. CCI was measured by segmenting the anterior, medium, and

posterior segments of the CC were then measured and normalised to the greatest anteroposterior diameter of the CC, according to the formula shown in (*Appendix E.2.Figure 2*).

The Inter Caudate Distance (ICD) is a practical marker of MS-related brain atrophy that might be used in standard clinical practice to track MS progression [302]. Different studies showed a significant association between ICD and disease progression in MS [286]. ICD was defined as the minimum distance between the caudate indentations on the frontal horns of the lateral ventricles.

PART 2

IRON RIMS LESIONS in MS

Chapter 4 . A Systematic Mapping Review of Iron Rim as an Imaging Biomarker in Multiple Sclerosis

Abstract

Background: MS is an autoimmune, inflammatory, demyelinating, and degenerative disease of the CNS. To date, there is no definitive imaging biomarker for diagnosing MS. The current diagnostic criteria are mainly based on clinical relapses supported by the presence of white matter lesions (WMLs) on MRI. However, misdiagnosis of MS is still a significant clinical problem. The paramagnetic, iron rims (IRs) around WMLs have been proposed to be an imaging biomarker in MS. This study aimed to carry out a systematic mapping review to explore the detection of Iron Rim Lesions (IRLs), on MR scans, and describe the characteristics of IRLs presence in MS versus other MS-mimic disorders.

Methods: Publications from 2001 on IRs lesions were reviewed in three databases: PubMed, Web of Science and Embase. From the initial result set of 718 publications, a final total of 38 papers were selected.

Results: The study revealed an increasing interest in iron/paramagnetic rims lesions studies. IRs were more frequently found in periventricular regions and appear to be absent in MS-mimics.

Conclusions: IR is proposed as a promising imaging biomarker for MS.

4.1 Introduction

Unlike systematic reviews, mapping reviews aim to graphically map the key concepts that underpin a research area and examine a broader area to identify gaps in the research knowledge[303–305]. In general, mapping reviews are commonly used for 'reconnaissance' – to clarify working definitions and conceptual boundaries of a topic and disseminate research findings, identify research gaps, and make recommendations for future studies. Mapping reviews are focused on a visual synthesis of the data graphically or by using tables instead of using descriptive texts like scoping reviews.

MS is an autoimmune, inflammatory, demyelinating and degenerative disease of the CNS[21]. It is associated with focal inflammatory demyelinating lesions in both white and grey matter [22].

MRI has an important role in determining the diagnosis of MS. MS diagnostic criteria using MRI are dependent on the number of spread WM lesions throughout the CNS, in both time and space [306,307]. MRI is proven to be sensitive in detecting focal WM lesions; however, it lacks specificity as neuroinflammation, and cerebrovascular abnormalities may mimic MS WM [308,309].

To date, there is no established and uniformly used imaging biomarker for diagnosing MS, and the diagnostic criteria are based mainly on clinical relapses, the presence of lesions on MRI and Oligoclonal Bands (OCBs) in the cerebrospinal fluid. However, misdiagnosis with MS-mimicking disorders is not uncommon [208]. The presence of central veins in WMLs and paramagnetic iron rims (IRs) have been proposed as MRI biomarkers that can discriminate MS

from non-MS disorders. These new MRI signs could potentially provide a more accurate diagnosis of MS [166,310]. This review summarizes the literature surrounding IRs in MS.

Iron rims appear as dark, ring-like features on the edges of some MS lesions have gained recent research attention [209]. Lesions with IRs are believed to be Chronic Active Lesions (CALs), also known as smouldering or Slowly Expanding Lesions (SELs), which fail to remyelinate and have subsequently been proposed to be a marker of tissue destruction, continuing inflammation and failure to repair [210–212]. Indeed, evidence from pathology and 7T MRI has shown that rimmed MS lesions were found to be significantly larger and underwent expansion by almost 30%, unlike non-rimmed lesions whose size shrinks by 10% [213]. Contrarily, the non-rimmed lesions may disappear or return to a similar contrast of the NAWM over time, which may affect their clinical usefulness [166,311].

Several studies found that IRs are commonly seen in RRMS [217] while others found it in progressive MS. Also, some publications found IRs were more common in elderly patients with a higher EDSS score ≥5 [213,217,219,312], contrary to Dal-Bianco et al. who found them more common in young MS patients. Importantly, several studies reported the absence of IRs in MS mimics, such as NMOSD [313] Susac's syndrome [314] and ischemic lesions [315]. This suggests that IR might be a specific feature of MS lesions, not only diagnostically but also to predict disease progression. However, these initial findings are from few studies, as such they need further validation before being incorporated into clinical practice. IRLs were detected in different parts of the brain but were more commonly detected in the periventricular regions.

The present study aimed to explore the detection of IRLs, on variable MR scans, and describe the characteristics of IRLs presence in MS versus MS-mimics with highlighting the main

findings. This study followed a systematic mapping review approach, to provide researchers and clinicians with a global picture of using IRs as an imaging biomarker in MS.

4.2 Material and Methods

4.2.1 Search Strategy and Eligibility Criteria

This systematic mapping review was conducted on the detection of IRLs on MRI scans in MS for several reasons. The first is to overview the existing evidence on using IRLs as a proposed imaging biomarker in MS. The second is to describe the characteristics of IRLs found in MS versus MS-mimics. The third is to identify specific research topics in using IRLs as an MRI biomarker in MS for future systematic reviews and meta-analysis.

A systematic search was performed in January 2020 using the databases: PubMed, EMBASE and Web of Science to identify articles that evaluated the presence of IR in WMLs using MRI. The identified search terms were framed in PICO concepts. Patients/Population (P): multiple sclerosis OR MS. Intervention (I): magnetic resonance imaging OR MRI. Comparison (C) was not taken into account as there was not any comparison needed. Outcome (O): diagnosis OR differentiate. However, from this search, no results related to iron rim lesions were found. Thus, a search using broader keywords was used in all the databases, including ((Multiple sclerosis OR MS) AND (rims OR rim) AND (lesion OR lesions)). The search strategy is provided in the study protocol *Appendix B.1*. Review of the papers and analysis of results was conducted from January to July 2020.

4.2.2 Inclusion and Exclusion Criteria

The search was restricted to original articles on in vivo studies of human subjects published in peer-reviewed journals, written in English and featured an available full-text. The databases mentioned above were searched from 2001—the first time the MRI has been part of the MS diagnostic criteria [316,317]. Grey literature was individually searched, including internet resources, theses, and conferences (*Table 4.1*). All duplications were removed using Mendeley.

Table 4.1. Illustrates the selection criteria of the studies

Inclusion	Exclusion
MRI studies on WMLs with rims presence OR Pathology studies	Studies published before 2001
Studies published in peer-review journals or grey literature	Animal studies
Literature is written in English	Case reports, reviews or systematic literature reviews and qualitative studies, opinion pieces, editorials comments, and news

4.2.3 Data Extraction

Relevant articles that fulfilled the inclusion and exclusion criteria (*Table 4.1*) were assessed by three reviewers (A.A., A.O. and G.F.)[1]independently. The complete extraction and assessment were conducted in three phases.

[1] A.A.: Amjad Altokhis (MSc), Mental Health and Clinical Neurosciences Academic Unit, School of Medicine, University of Nottingham, Nottingham, UK.
A.O.: Abdulmajeed Alotaibi (MSc), Mental Health and Clinical Neurosciences Academic Unit, School of Medicine, University of Nottingham, Nottingham, UK.
G.F.: Ghadah Felmban (MSc), Mental Health and Clinical Neurosciences Academic Unit, School of Medicine, University of Nottingham, Nottingham, UK.

In the first phase, the three reviewers independently screened the titles and abstracts and removed the articles that did not fulfil the predefined inclusion/exclusion criteria.

In the second phase, all selected papers were reviewed by A.A. to select eligible studies for inclusion. Papers were read to determine if they contained data useful to the aim of this review. Disagreements between reviewers were resolved via discussion. The following details about each study were extracted by one reviewer (A.A.): study (author, date), type of the study, sample size, demographics, the aim of the paper, type of magnet strength, data analysis method, full MRI protocol procedure and main results and limitations.

In the third phase, a general quantitative overview of study characteristics was reported using descriptive statistics, median/mean and interquartile range (IQR) values. However, because of the heterogeneity of aims, the dataset used, techniques applied, and evaluation metrics specified in the selected publications, the results were stratified by pursuing clinical aim/key findings.

4.3 Results

4.3.1 Literature Search and Study Characteristics

The literature search is illustrated in a flowchart (*Figure 4.1*). From the initial search and after removing duplicate studies, 628 articles were identified. Out of these, 532 articles were excluded as they did not meet the criteria. An additional 58 studies were excluded after reading the full text. Finally, a total of 38 studies were included in this systematic mapping review.

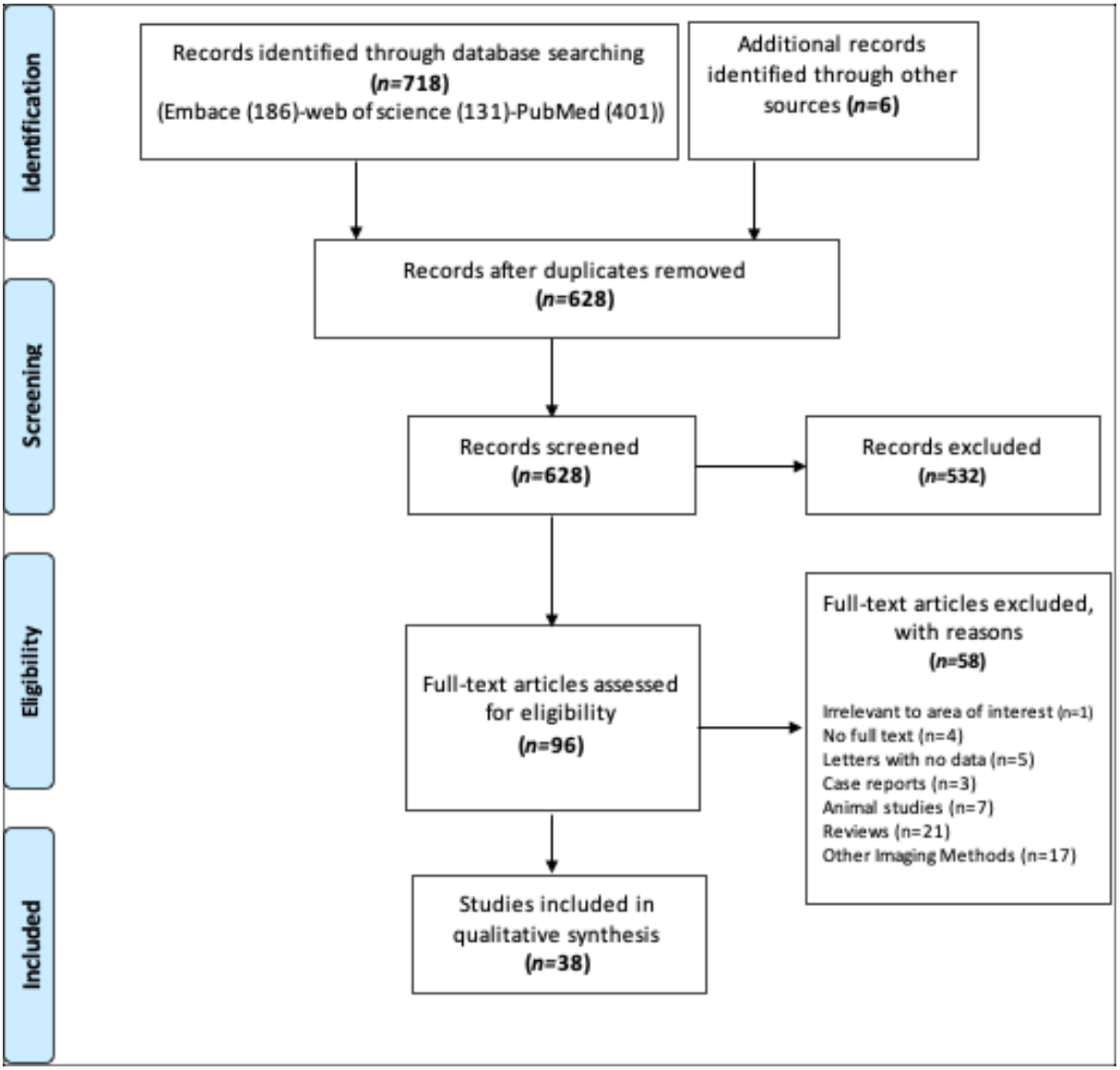

Figure 4.1. PRISMA flowchart of studies selection

Of all the literature that was reviewed, seven studies (18%) were conference presentations/or posters. Six studies (15%) had a retrospective design, while the remaining 32 studies (84%) had a prospective design. Eleven studies were longitudinal with both retro/prospective designs; 15 years was the longest study duration *(Appendix. B.2).*

Seven Tesla MRI was used alone in 15 studies (39%), while 3T was used in 13 studies (34%) whereas four studies (11%) used both 3T and 7T. Two studies used 1.5T, and one used 4.7T, while some studies did not provide this information.

Of the different MRI sequences used for WMLs, especially when detecting IRLs, SWI and T_2*-FLAIR (combined) were used most often. In particular, SWI was combined with T_2* and FLAIR in 52% of the studies. Additionally, SWI was combined with other sequences, such as T_1-, T_2-, and proton density-weighted images *(Appendix. B.2)*.

The aims and key findings of reported studies were sub-grouped into (1) IRLs presence in MS subtypes, (2) the spatial distribution of WMLs with IR, (3) gender differences in the presence of IRLs, (4) the clinical relevance of IRLs (i.e., rim lesions linked with a disability and psychological impairment), (5) the prevalence of IRLs presence based on lesions and patients count (6), the evolution of IRLs over time, and (7) the pathological nature of IRLs. Due to the nature of this report, the results will be highlighted and discussed briefly.

4.3.2 IR in Patients with MS and MS Subtypes

Sixteen papers reported the presence of IRLs in MS subtypes [213,215,323–328,216,217,313,318–322] (*Appendix. B.3*). Most of the publications examined patients with RRMS [216,318–321,323,325,329]. Three papers looked at RRMS and SPMS [318,323,325], while other studies compared MS with controls [213,215–217,318,320,325,329] or MS-mimics diseases [330,331]. The highest rate of IRL presence was found in RRMS (36%) followed by SPMS (27%) while benign MS and CIS had the lowest percentage of (5%). One study each was found reporting on benign MS [329]and Radiologically Isolated Syndrome (RIS)[328] while RRMS was most frequently reported in eight studies [216,319,320,323,325,329,332,333]

followed by SPMS in six studies [217,322–325,332]. Interestingly, IRLs were absent in NMOSD [313], Susac's syndrome [314] and ischemic lesions [315].

Llufriu et al. (2010) scanned 257 patients with the four MS subtypes; the IRLs detected were 7% in CIS, 11% in RRMS and 13% in SPMS with no rims detected in PPMS patients [324]. Similar work by Clarke et al. (2019) detected IRLs in 48% CIS, 59% RRMS and 39% SPMS [318]. In contrast, Chawla et al. (2018), scanned only nine patients (4 RRMS, 5 progressive) at 7T, and found that 5 out of 9 had IRLs, and 4 of these were progressive [167]. Although IRs are not commonly found in MS mimics [219,313,314], other brain disorders might have IRL. IRL has been reported to be present in brain abscess [330]. Clinically and radiologically, they are not frequently encountered in the differential diagnosis of MS, but worth noting.

4.3.3 IRLs and Lesion Localization

Only four studies [216,318,329,334] reported the anatomical location of the IRLs, indicating that periventricular (in direct contact with the lateral/third ventricles), was found to be the most common site of lesions with rims in 2 publications. The other two papers found the cortical/juxtacortical (in direct contact with the cerebral cortex) and the deep white matter (not in direct contact with the cortex or ventricles) to be the preferential location (*Figure.4.2*).

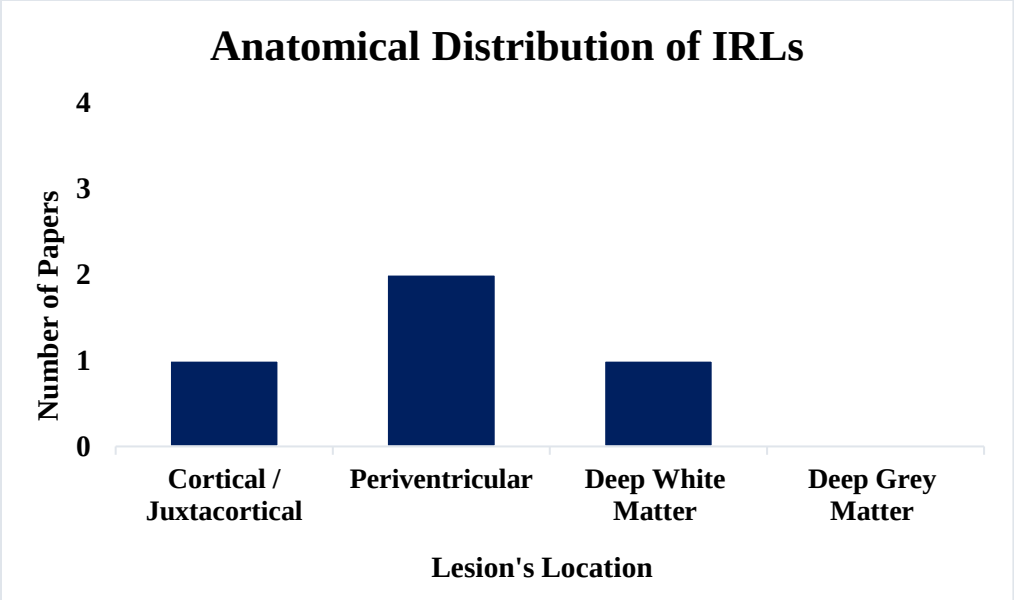

Figure 4.2. Illustrates the main anatomical location of the iron rim lesions (IRLS) in MS lesions when reported (total of 4 papers).

4.3.4 IRLs and Gender-specific Differences

Only seven papers reported the gender-specification related to IRLs presence[215,216,318,322,324,329,335]. IRLs were reported to be more common in males than females [322,335]. Clarke et al. (2019) provided more details relating to gender-specific differences; suggesting male gender is the most important predictor of the proportion of IRLs in CIS and MS patients [318]. Males are 40% more likely to have IRs compared to females.

4.3.5 Clinical Relevance of IRLs

IRLs presence was related to poor cognitive performance and disability in 9 of 10 papers[213,215,220,312,323,328,329,335–337], see *Figure 4.3*. However, Kilsdonk et al. (2014) reported a lack of relationship between IRLs and physical disability [322]. This drawn conclusion was derived from

scanning 33 MS patients at 7T MRI, and 8 patients had rims. In contrast, Dal-Bianco et al. (2019) analysed 33 MS patients, 24 had IRLs, and the presence of IRLs was associated with higher FLAIR lesion load, which was related to poorer cognitive performance on the symbol digit modalities test[329]. No significant difference in disease progression was found between the two groups (IRLs and non-IRLs), four patients switched disease courses during the study (3 RRMS into SPMS, 1 benign MS into RRMS), while three of these patients had IRLs.

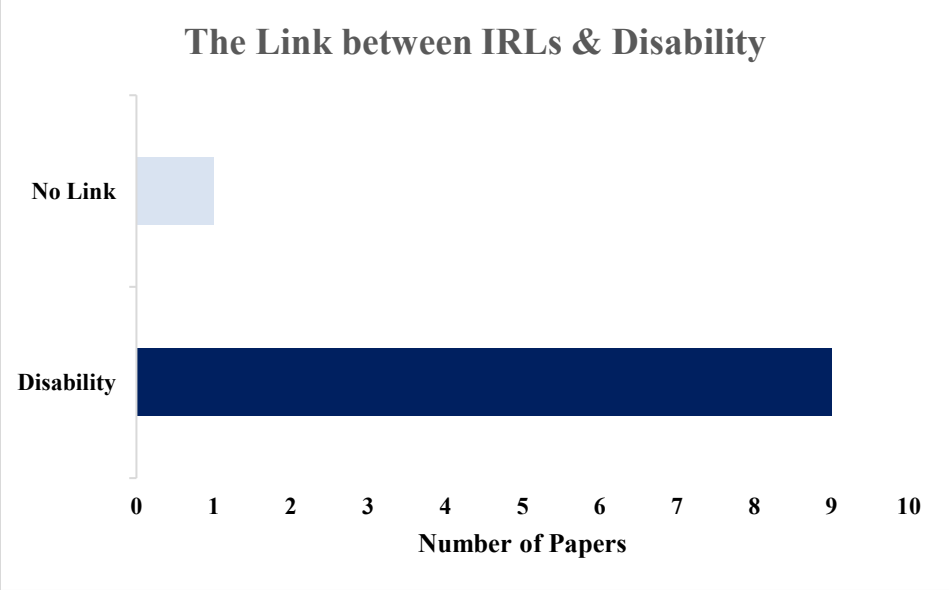

Figure 4.3. Illustrates the number of papers that found a link between iron rim lesions (IRLs) presence and Disability**.**

4.3.6 IRLs Prevalence

- ***As a proportion of total white matter lesions detected on MRI***

Figure.4.4 Shows the proportion of lesions with IRs reported between studies. The total lesion counts across studies ranged from 44 to 3211 lesions. Four studies showed a similar prevalence of IRLs presence, approximately ~10% [312,322,328,338]. However, Absinta et al. (2013) using a 7T scanner found IRLs in acute gadolinium-enhancing lesions and found their presence in 97% (43/44 lesions), but in 2018 the same group reported in their 3T and 7T longitudinal study the presence of IR in chronic lesions was 50% (27/54 lesions) [339,340]. Both Harrison and Blindenbacher shared a similar prevalence of 5% (16/306; 28/611 respectively) in acute gadolinium-enhancing lesions[217,328]. The MRI techniques used to detect rims in these studies were different, namely, Quantitative Susceptibility Mapping (QSM), SWI and R2*on their own or combined with FLAIR for clearer identification of lesions, using both 3T and 7T MRI scanners.

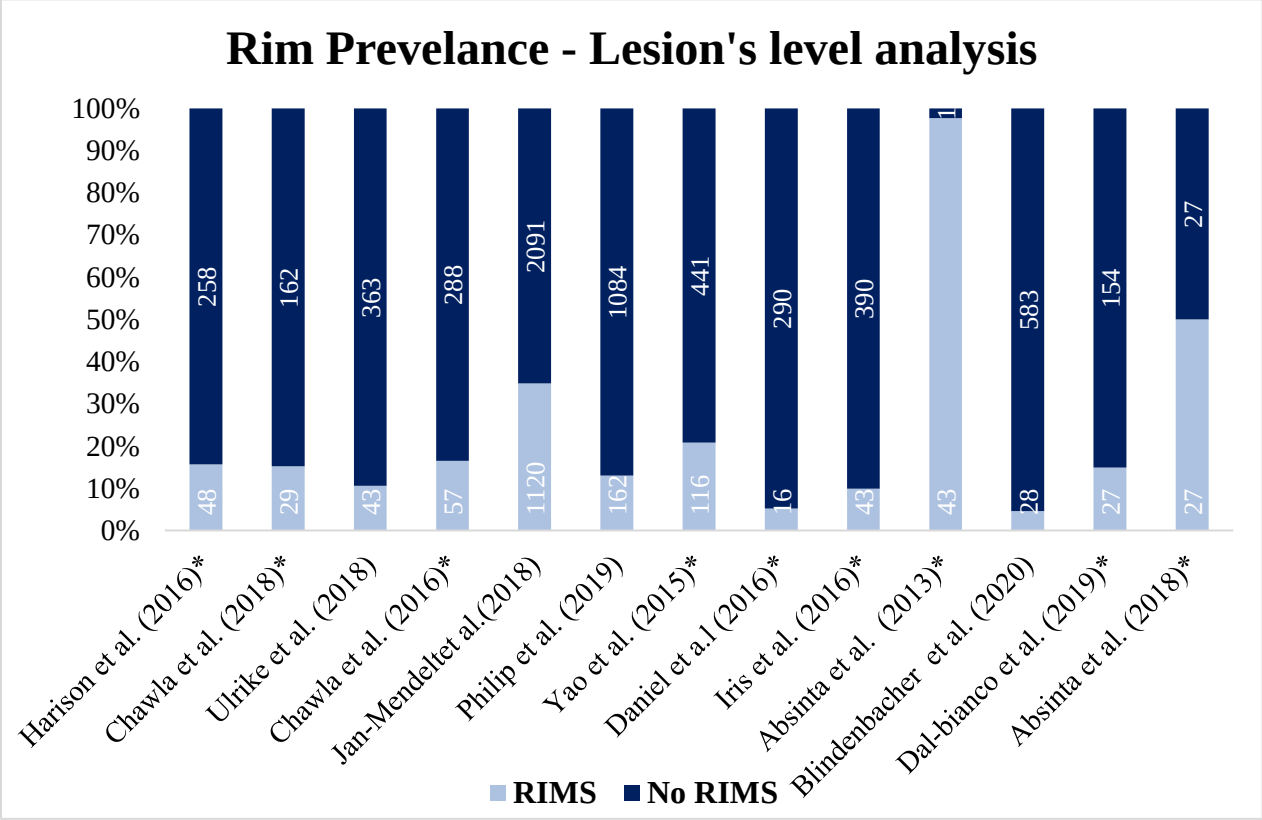

Figure 4.4. Illustrates the prevalence of iron rim presence in MS patients, the percentage based on the total lesion number. The presented studies used 3T and 7T MRI, and the symbol (*) shows the studies using 7T MRI.

- ***As a proportion of patients studied***

Ten papers reported the proportion of patients with at least one IRL, the mean of the total number of MS patients was 97.3 (range 9–257) [167,318,323,325,330,341,342]. Eighty percent of the studies stated that rims could be detected in 50% to 70% of MS patients examined. Jiwon Oh et al. (2019) reported the highest percentage of IRLs presence which was 72% (8/11 MS patients) [334] while only ~10%with IRs reported by Llufriu et al. (2010) scanning (24/233 MS patients) [324]. Similarly, Chawla et al. scanned nine patients (4 RRMS, 5 Progressive) at 7T, and 55.5% of patients had rims[313] (*Figure 4.5*). To sum up, histopathology or MRI studies (with details in appendix B.2) showed that ~8-70% of MS lesions are surrounded by IRLs, which could be seen in both 3T and 7T [213,219].

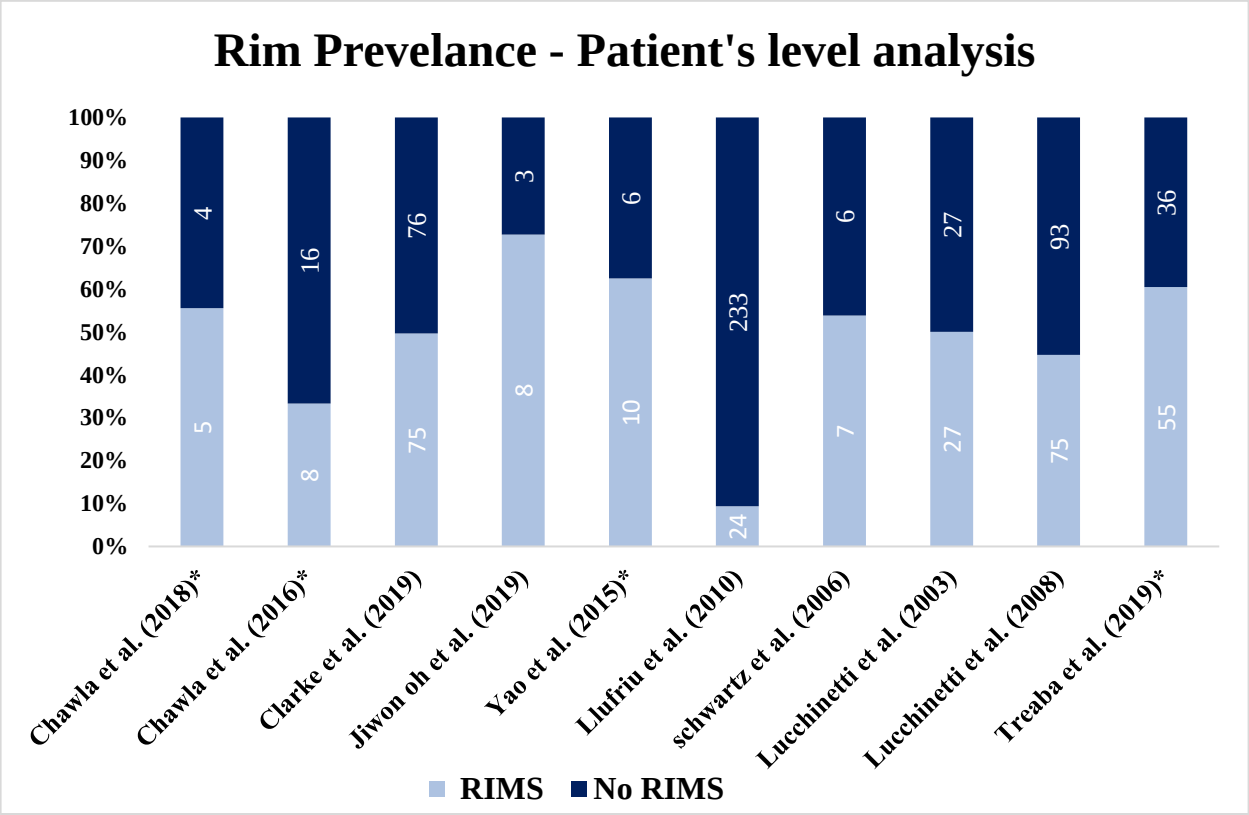

Figure 4.5. Illustrates the prevalence of iron rim lesions detected in MS patients. The percentage based on the total number of patients. The presented studies used 3T and 7T MRI, and the symbol (*) shows the studies using 7T MRI.

4.3.7 Rim Evolution Overtime

Eleven papers reported whether the IRLs expand or shrink without accurately specifying the time frame [167,213,346,229,321,328,329,336,343–345]. However, six papers reported a different duration for expansion and shrinkage [211,213,219,329,336,344] (*Figure 4.6*). Longitudinal studies with a mean follow-up of 3.5 years, observed a slow expansion of IRLs that persist over time [167,213,344], then gradually the hypointense rim disappeared, returning to contrast NAWM after seven years [211,321]. IRLs are frequently detected in young lesions and early disease [319,347].

Some studies showed that rimmed lesions were larger and expanded by almost 29.33%. In comparison, lesions without rims were smaller in size by 10% [213]. IRLs significantly enlarge over time [213] while non-rims lesions disappear in a period of 2.5 to 4.7 years. In short, lesions with IRLs tend to grow slowly and without rim shrinking over time.

An ECTRIMS presentation by Dal-Bianco et al. (2019) provided more insight into rim evolution [329]. They found that IRLs appear newly, enlarge slowly, then stabilise and gradually lose the iron rim. IRLs had a substantially larger initial volume, and the rim became thinner after 3.5 years before partially disappearing. The IRLs volume showed a gradual increase in size and fused with neighbouring rim lesions within 3.5 years.

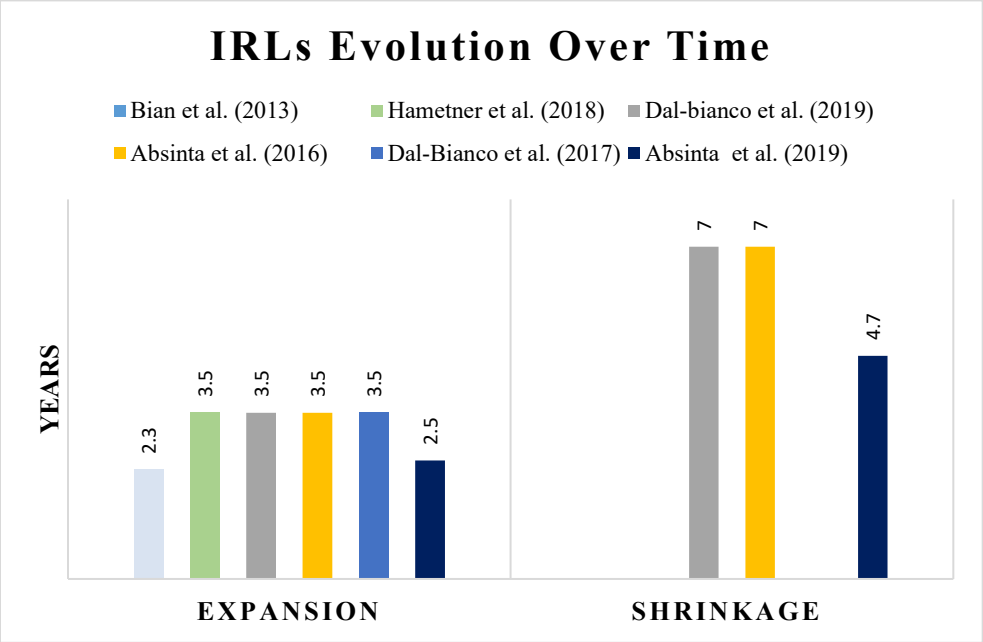

Figure 4.6. The figure shows on the left that when lesions were measured early (2.3-3.5 years) after lesion formation there was an overall expansion of IRL in all 6 publications. In the three publications that followed up lesions for longer (4.7- 7 years) IRLs were seen to shrink.

4.3.8 Nature of Rims – Pathology

Rims likely reflect iron accumulation within a subset of macrophages/activated microglia at the lesion edge [336,344]. Lesions with IRLs are believed to be CALs, also known as smouldering or SELs, which fail to remyelinate and have subsequently been proposed to be a marker of tissue destruction, continuing inflammation and failure to repair [168,210]

CALs are identified by gliotic, hypocellular centres and rims of activated microglia cells, macrophages, and iron. However, these rims cannot be found in remyelinated or shadow plaques[348].

Pathological studies investigating chronic MS lesions reported that up to 57% of these lesions are active or mixed [84,215,216] The chronic active lesions are thought to represent those that are slowly expanding in size causing continuous tissue loss. [84,213,215,216]. CALs are commonly

detected in patients with a disease duration of 10 years or more and peak at 20 years [216]. Colm et al. [349] found that when comparing RRMS with PPMS patients, RRMS had higher numbers of SELs.

Summary of the Results

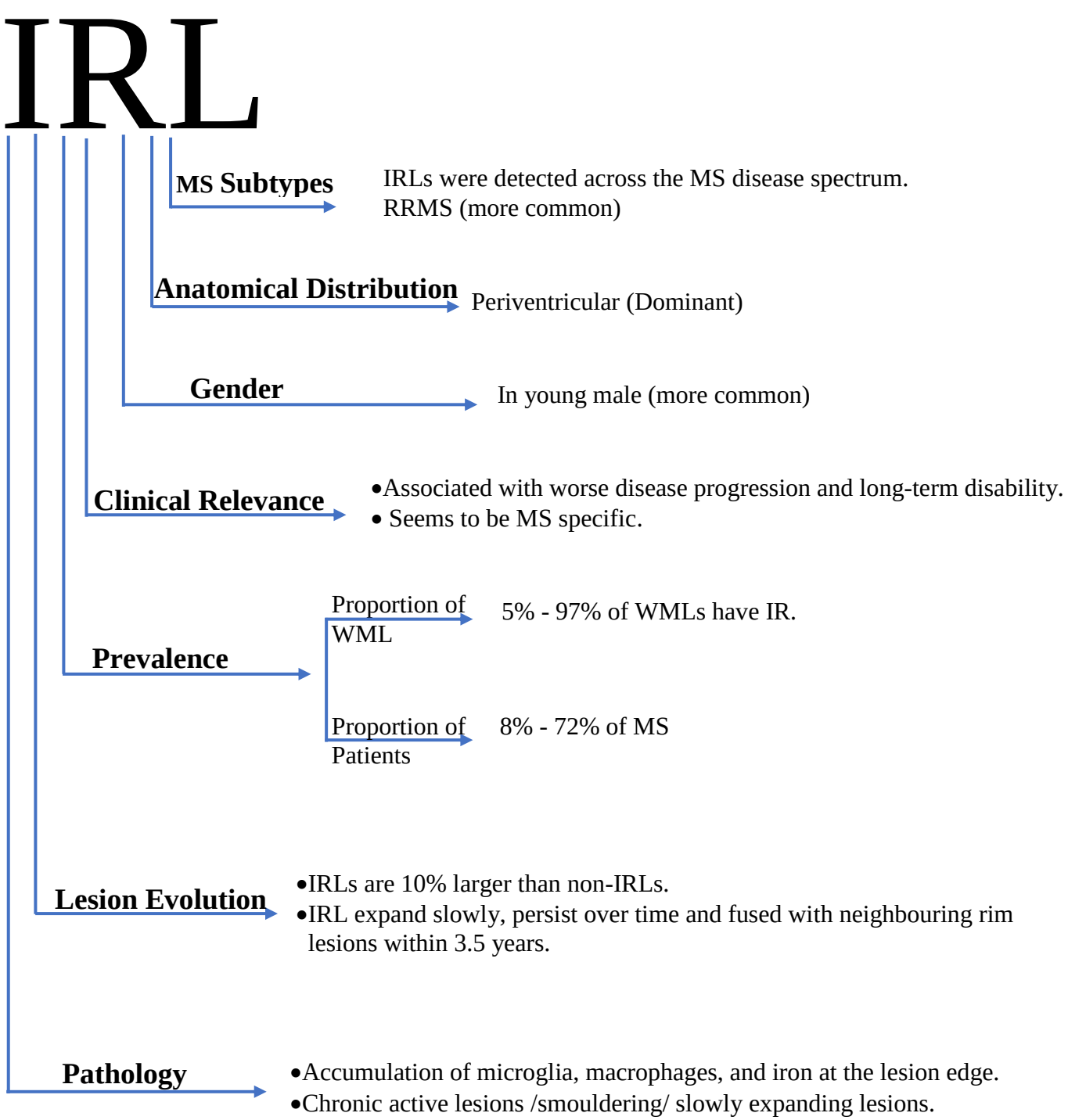

4.4 Discussion

This is the first systematic mapping review carried out on the presence of IRs in MS patients when using MRI. This review aimed to explore the detection of IRLs, on variable, clinical-quality MR scans, and describe the characteristics of IRLs presence in MS versus MS-mimics with highlighting the main findings. We primarily focused on study aims for which IRLs have been reported. Three different databases were searched, and after the screening, 38 studies were included in this review. Characteristics of the studies and IRLs were described.

In the past decade, several studies have focused on IRLs in MS and non-MS. Researchers around the world are working to exploit MRI data to improve MS diagnosis and treatment. Thus, an increase in the number of published IRLs studies was observed, reflecting the scientific community's growing interest in the clinical value of IRLs presence in MRI.

Although T_2*/FLAIR and phase imaging, including SWI, hold promise for identifying IRLs, yet there is no ideal technique to use in vivo. SWI is sensitive to iron detection which accumulates in normal-appearing brain tissue and in lesions in MS patients [228,350]. IR is best appreciated on phase (rather than T_2*) images [211]. However, for large lesion and vessel detection, Sati et al. suggested using T_2* and FLAIR combined [351]. Many sequences can detect iron but one of the challenges when comparing IRLs studies in MS is the different MRI sequences used. Only by utilizing different sequences for the same individual can the value of each sequence be demonstrated. This has rarely been done in the reported studies. Based on the included studies, 7T was found to be a useful tool for tracking the evolution of MS lesions, especially concerning changes in iron content but 3T would be more practical to use in clinical settings [167]. This explains the higher number of 7T studies compared to 1.5T when exploring IRs.

The key findings from this review are that IRLs, which appear as dark, ring-like features on the edges of some MS lesions, are believed to be CALs/SELs. These lesions fail to remyelinate and have subsequently been proposed to be a marker of tissue destruction, continuing inflammation and failure to repair [210,211]. Indeed, evidence from pathology and 7T MRI has shown that rimmed MS lesions were found to be significantly larger and underwent expansion by almost 30%, unlike non-rimmed lesions which reduced their size by 10% [213]. IRs were more frequently found in periventricular regions of young males with RRMS and linked with higher disability (EDSS score ≥5) [213,217] but appear absent in NMOSD [313], Susac´s syndrome [314] and ischemic lesions [315]. Thus, it seems that IRs have the potential to be a successful imaging marker for MS. More details about these results will be discussed in the next section.

○ The Presence and Spatial Distribution of IRLs

IRLs seem to be more common in RRMS; this might be due to the fact that RRMS patients were used more in studies compared to other MS subtypes. Besides, not all the studies included all MS subtypes in their studies. In contrast, Two studies tested four types of MS and both found IRLs were more common in SPMS than RRMS; however, the sample size was too small (9 patients) [352]. IRLs elevated in R2* were seen in both RRMS patients with low disability and those with long-standing SPMS [323].

It is hard to conclude from these studies as the heterogeneity of the sample size/MS types, as well as MRI scanners between studies, was high. However, the study by Schwart et al. compared IRLs presence in different diseases (glioma, metastases, abscess, MS) and found IRLs were more in abscess than MS; this could be from the higher number of abscess patients compared to MS

(18,11 patients respectively) [330]. Interestingly, in terms of neuroinflammatory conditions, it seems IRLs are MS-specific as they are absent in NMO [313], Susac´s syndrome [314]and ischemic lesions[315].

Lastly, the periventricular region was the highest anatomical location of IRLs presence while the cortical was the least. This is to be expected as MS lesions are commonly seen around the ventricles [353].

○ *The Gender Differences in IRLs*

Few studies tested the gender specification of IRLs. Although IRLs could be detected in women, men had a higher prevalence, especially young men. Men are 10% to 40% more likely than women to have IRLs [318,335]. The reason is still unknown and needs further investigation.

○ *The Prevalence of IRLs*

Different prevalence was reported for IRLs; the prevalence was calculated from the included studies based on lesions and patients counts. Overall, IRLs prevalence based on lesion counts ranges from 5–97% while 8–72% was based on patients' numbers. The differences seen between the results could be explained by the different scanners/sequences used, which have a significant impact on lesion/rim detection. However, the large range of reported prevalence of IRL in different MS studies is concerning. Larger studies are needed to confirm the prevalence of IRLs based on both the patient-level and lesion-level and also to determine the factors that affect the presence of IRLs.

MRI ring-enhancing lesions are among the recognized patterns in MS and occur in one-quarter of all MRI-enhancing lesions [324]. In contrast, few studies observed the peripheral hypointense rims on T_2-weighted images. The relation of the ring enhancement with hypointense T_2-weighted rims

was found in 54% (7/13) of the included MS patients [330]. A pathological study investigating the correlation of biopsy MS subtypes with MRI reported that the hypointense T_2-weighted rims were observed in 50% (27/54) of cases [342].

○ *The Evolution of IRLs over time*

The lesion volume of IRs showed a gradual increase in size and fusion with neighbouring IR lesions within 3.5 years, and this was proven in both 3T and 7T studies. IRLs gradually decline over time and disappear in a few years.

IRLs expand in 3 to 4 years compared to non-IRLs, and the size stabilises after. IRLs had larger initial volumes and became thinner after 3.5 years and partially disappeared over time. New IRLs appear with an increased iron load of the entire lesion, transforming into IRLs within a year.

7T-MRI showed that the area around IRLs has a diffuse hyperintense signal. Although the nature of these changes is still unknown, the 7T post-mortem study suggested that the hyperintensity signals could be an indication of demyelination and axonal degeneration.

Regarding the evolution of the iron rims, Dal-Bianco *et al.* reported some lesions started as a diffuse iron across the whole lesion and then within the 3.5 years, iron accumulated at the lesion's border forming an IR. Other lesions started with the rim without the "diffusion phase" [326]. It is possible that there are two different types of rim formation. Similarly, the disappearance of IRL might suggest that inflammatory cells are present in lesions early but might not be present a few years later. So, the margin of demyelination remains static and detected on T_2W, but not the presence of iron loaded inflammatory cells might wane and hence lesions lose their rims on SWI. To sum up, IRLs are a dynamic feature in MS, within 7 years IRLs enlarge slowly, then stabilise and gradually disappear.

○ *The Pathological Nature of IRLs and Disability*

Rims have a characteristic “pencil-thin” appearance at the junction of the lesion and adjacent normal-appearing WM. Combined MRI-pathology studies showed that IR lesions are composed of iron-containing macrophages and microglia at the lesion edge. They display a phenotype of pro-inflammatory activation and in part contain early myelin degeneration products. IRLs have been suggested to label a subset of CALs [213,228,229]. Chronic lesion activity driven by smouldering inflammation is a pathological hallmark of progressive forms of MS. Pathological studies showed that the smouldering demyelination occurs to a similar extent in both PPMS and SPMS.

Assessing new lesions with 7T MRI indicates that a persistent phase rim had lower quantitative T_1 signal intensities over time and could predict poor tissue outcomes. These interpretations were accordant with the pathological correlation of progressive MS and the concept of slowly expanding demyelination.

Recently, it has been recognized that iron and myelin are primarily contributing to WM MRI susceptibility. Iron has the properties of paramagnetic materials which allows a positive susceptibility for water content. However, myelin has the properties of diamagnetic materials which show negative susceptibility [348]. As a part of the demyelination process, it is believed that the inactive iron and pro-inflammatory microalga are obtained from the myelin and the debris of oligodendrocytes. Alternatively, another hypothesis states that the oligodendrocytes may contribute to releasing the iron in WM adjacent to plaques, which are thought to be produced by the inflammatory cytokines and discharged by microglia.

Hypointense rim lesion is a promising predictor of the continuation of tissue injuries and inflammation in progressive MS. Thus, detecting the inflammation activity could be used to

identify patients' responses to anti-inflammatory treatments. This might be valuable in improving disease prognosis as these lesions correlate with MS severity [218].

Disability scores tended to be worse in patients with rims. Despite that, the exact clinical significance of rim lesions in MS is still not clear.

This study has some interpretations of risks and limitations. One of the risks affecting all systematic mapping reviews is related to selective reporting bias [354]. To minimize this risk, three different databases were used which provide a comprehensive list of articles covering the various aspects of this mapping review. It is also worth noting that although it was decided to exclude reviews from the study, however, the reference list for the reviews was checked and all relevant papers were included. Another selection bias risk relates to the criteria used to select the articles to be analysed during the study. To mitigate such a risk, both the inclusion and exclusion criteria were clearly defined. One of the limitations is the limited number of papers available covering the same topic of interest of this review. There was much heterogeneity between studies, for example, different MRI magnetic strength, different aims, different samples size and disease types. Additionally, not all studies reported the needed information.

4.5 Conclusion

Based on the results of the present study it seems that IRLs were more frequently found in periventricular regions of young males with RRMS. Additionally, IRLs could be linked with a higher disability and appear to be absent in MS-mimicking disorders. Different prevalence was reported for IRLs; the prevalence was calculated from the included studies based on the level of lesion and patient (5–97% and 8–72% respectively). The lesion volume of IRs showed a gradual increase in size and fusion with neighbouring IR lesions within 3.5 years. Pathologically, IRLs are

a sign of chronic active inflammation and persisting demyelinating activity. Although IRs have a promising potential to be a proposed diagnostic imaging biomarker and disease progression, there is still much to learn about the aetiology and mechanisms underlying IRLs, especially regarding the link between IRLs and clinical impact and IRLs evolution and prevalence. To answer these questions, more extended observation in larger cohorts is required. Meta-analysis may further be considered.

4.6 Review's Update

Since the publication of the mapping review[1], which was at the beginning of my PhD in 2020, new papers have been published related to IRLs. I will briefly address the new papers and whether the new data confirm or add new knowledge to what has been discussed in the review.

Similar to the findings from the review, IRL could be a specific feature of MS lesions, which could be used not only as biomarkers of disease progression but also diagnostically [218]. Three new studies specifically investigated the diagnostic utility of IRLs by looking at rim lesions in MS and MS-mimicking disorders including small vessel disease, migraine, NMO, etc. [355–357]. These new studies confirmed the previous findings of IRLs having high specificity but low sensitivity in diagnosing MS. The larger studies by Clarke and Maggi investigating the diagnostic utility of IRLs, reported a sensitivity of around 50-60% for MS compared to other neuroinflammatory conditions [355,356].

Clarke's study also reported the prognostic utility of these rims in 112 CIS patients, and found that the presence of 1 or more IRLs has a higher sensitivity predicting the onset of relapsing disease course within 4.5 years [355]. A table summary of these studies is in *Appendix B.4.*

MRI findings showed that IRLs were strongly associated with MRI pathology. This is shown by the increase in T_1 and T_2 lesion volume/number when ≥1 IRL was present and usually increases with an additional IRL [3,224,357–360].

In late 2019, IRLs research was an active area of research and even more active in the past three years. Reviewing the literature on chronic active lesions, slowly expanding lesions, and paramagnetic rim lesions using clinicaltrials.gov or PubMed showed that IRL is active in cooperating in a wide variety of ongoing clinical trials. IRLs have been investigated in several monoclonal antibody trials or using IRL as an outcome measure in trials of high-dose corticosteroids, Anti-IL-1, and BTK inhibitors. A summary of the trials found in these sources (clinicaltrials.gov or PubMed) is presented in *Appendix B.5*.

Chapter 5 . Paramagnetic Rim Lesions are a promising diagnostic imaging biomarker in Multiple Sclerosis: a multi-centre MAGNIMS study

Abstract

Background: White matter lesions (WML) on brain MRI are universal in multiple sclerosis (MS) but can contribute to misdiagnosis. In chronic active lesions, peripheral iron-laden macrophages appear as paramagnetic rims (PRLs).

Objective: To evaluate the sensitivity and specificity of PRL in differentiating MS from mimics using clinical 3T MRI scanners.

Method: This retrospective international study reviewed MRI scans of patients with MS (n=254), MS mimics (n=91) and older healthy controls (n=217). WMLs, detected using fluid-attenuated inversion recovery MRI, were analysed with phase-sensitive imaging. Sensitivity and specificity were assessed for PRLs.

Results: At least one PRL was found in 22.9% of MS and 26.1% of clinically isolated syndrome patients. Only one PRL was found elsewhere. The identification of ≥1 PRL was the optimal cut-off and had a high specificity (99.7%, CI = 98.20%-99.99%) when distinguishing MS and CIS from mimics and healthy controls, but lower sensitivity (24.0%, CI 18.9%-36.6%). All patients with a PRL showing a central vein sign (CVS) in the same lesion (n=54) had MS or CIS, giving a specificity of 100% (CI 98.8% - 100.0%) but equally low sensitivity (21.3%, CI 16.4%-26.81%).

Conclusion: PRL may reduce diagnostic uncertainty in MS by being a highly specific imaging diagnostic biomarker, especially when used in conjunction with the central vein sign.

5.1 Introduction

The need for accurate, early diagnosis and consideration of early treatment of MS, introduces challenges for clinicians [361]. The 2017 modified McDonald diagnostic criteria[51] necessitate typical clinical symptoms and the presence of WMLs on MRI. These criteria shorten time to diagnosis [362] and improve the sensitivity of diagnosing MS [52]. Yet misdiagnosis is still common [208,363], especially when the MRI criteria are incorrectly applied outside of a typical clinical presentation or when there is incorrect interpretation of MRI findings. It has been suggested that recent changes to the MRI criteria decreased the diagnostic specificity [364–368], as WMLs can be present in other conditions such as migraine [369], NMOSD [370], and central nervous system vasculitis[371].

There is growing acceptance of the role of the Central Vein Sign (CVS) in diagnosing MS[1] leading to increased use of phase-sensitive imaging at the time of first clinical presentation [310,372].

Some chronic MS lesions have persistent active demyelination, the products of which are engulfed within activated microglia/macrophages on the periphery of the lesion. One such product is ferrous iron released into the extracellular space during the destruction of oligodendrocytes [336]. This can be detected in vivo with phase-sensitive imaging where it presents as a paramagnetic rim (PR). Paramagnetic rim lesions (PRLs) appear as hypointense, ring-like structures that surround WML on phase-sensitive MRI sequences. PRLs may increase in size whereas non-PRLs decrease in size or remain unchanged[219,336].

This imaging marker has been studied in detail using 7 T MRI[184,219,373,374]. Importantly 3T MRI studies have also detected PRLs in MS [346,348,375,376] and corroborated the possible diagnostic and prognostic value. However, there are reservations on the clinical utility as PRLs are only seen in a minority of WMLs [1,318].

This retrospective international, multicentre study within the Magnetic Resonance Imaging in MS (MAGNIMS) study group aimed to test the potential for PRLs in clinical practice. MRIs for patients with MS and MS mimics (including cerebral small vessel disease, migraine and NMOSD were compared. This dataset was originally collected by Sinnecker et al. [310] to evaluate the value of CVS in MS.

5.2 Material and Methods

5.2.1 Participants

The study included 562 participants scanned at seven MS centres across Europe between 2010 and 2016. The participants were enrolled in ongoing observational studies or included in neuroimaging research databases, all of which were approved by the institutional review board at each centre. All patients provided written informed consent prior to MRI. The inclusion criteria, diagnostic criteria and patient demographics have been reported previously[310]. All patients with NMOSD had antibodies against aquaporin 4 [310]. SWI and 3-dimensional (3D) FLAIR scans acquired at 3T of sufficient quality were analysed. Scan acquisition details for each centre can be found in *Appendix C.1* of Sinneker et al.[310] with more details about the method.

5.2.2 Image Post-processing

FLAIR images from each participant were co-registered to the SWI using the ITK registration library (Insight Software Consortium), which was implemented in 3D Slicer, version 4.6.2 (Slicer Community). Insufficient co-registration resulted in exclusion from analysis. The registered

images were then sectioned into 8 equal-sized 3-D blocks to ensure the blinding of assessors to the patients' diagnosis [310] (*Appendix C.2*).

5.2.3 Image Analysis

All image analysis was performed by two trained investigators (A.A. and I.M.)[2] using 3D Slicer (version 4.11.2). The trainer, an experienced researcher with publications record of IRL (M.C.)[3] demonstrated the criteria of IRL detection and used 10 practical MRI scans to identify these rims lesions. The trainees analysed 10 new practical scans individually then check them with M.C. Additionally, a neuroradiologist checked the IRL detection criteria, and advised on the image quality and window viewer standardisation. Each 3-D block was reviewed by A.A. and I.M. and results were collated after all image analysis was performed to avoid lesion classification in one part of a brain influencing the assessment of other regions of the same brain. The supratentorial regions of the FLAIR MRI scans were analysed for WMLs with a long axis ≥3 mm. Lesions were classified based on their location as cortical/juxtacortical (in direct contact with the cerebral cortex), periventricular (in direct contact with the lateral/third ventricles), deep WML (not in direct contact with the cortex or ventricles) or in direct contact with DGM structures [377].

The SWI scans were then analysed for the presence of PRLs. A PRL was defined as a hypointense, ring-like structure on phase-sensitive imaging. The rim had to correspond to the WML edge on the FLAIR scan, encircle it fully or partially and must be visible on at least two consecutive image slices (*Figure 5.1*). As part of this study, CVS was also analysed using the North American Imaging in MS Cooperative (NAIMS) criteria [166].

[2] I.M. Isobel Meaton (MD), School of Medicine, University of Nottingham, Nottingham, UK.
[3] M.C. Margareta Clarke (PhD), Division of Clinical Neuroscience, University of Nottingham, Nottingham, UK.

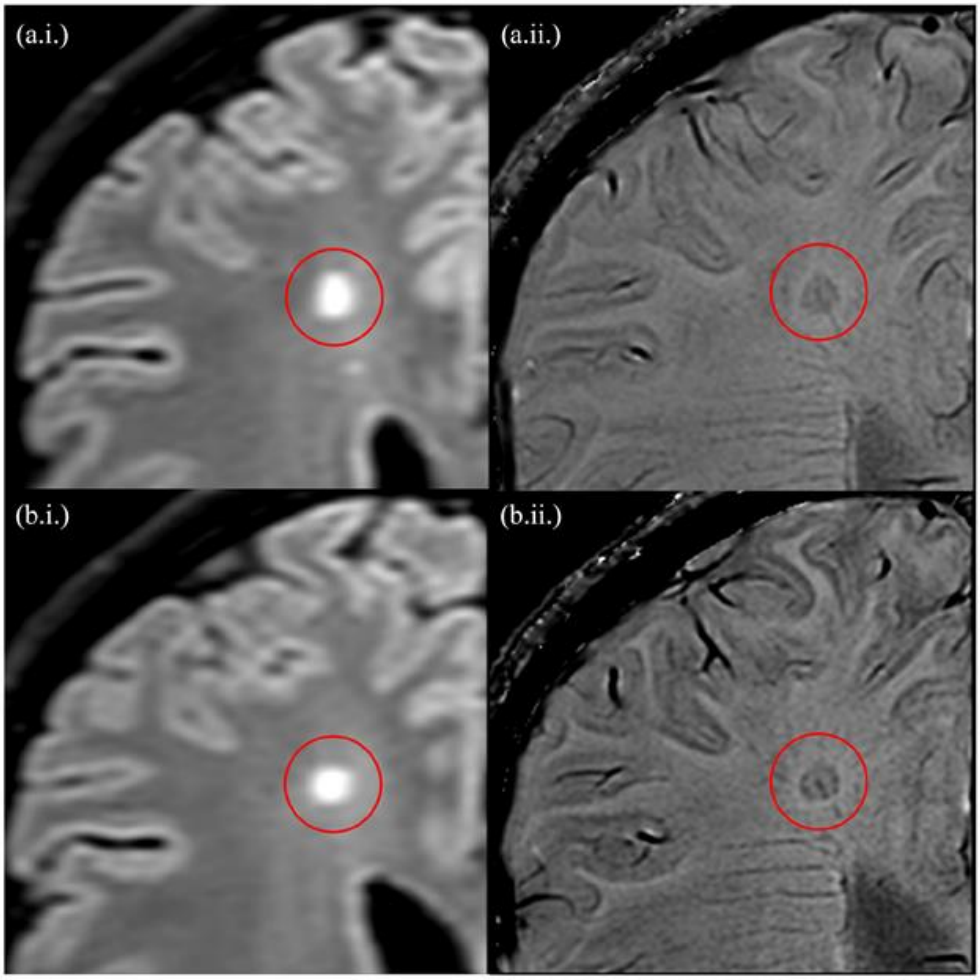

Figure 5.1 . Consecutive slices of a Paramagnetic Rim Lesion (with a central vein) detected using the fluid-attenuated inversion recovery (a.i and b.i) and phase-sensitive imaging (a. ii. and b.ii.), at 3T MRI. As per the study protocol, the lesions demonstrate a hypointense, ring-like structure corresponding to the lesion edge which is present on at least two consecutive slices.

5.2.4 Quality Assessment

Each block was assessed for artefacts and co-registration quality of FLAIR and SWI before the detection of WMLs (*Appendix.C.2.3*). A total of 18 out of 5196 blocks failed this quality test and were excluded from the analysis. Once image analysis was completed the blocks were de-anonymised and matched to patient data.

5.2.5 Statistical Analysis

The statistical analysis was performed using IBM SPSS statistics, version 20 (IBM). Sensitivity and specificity were calculated for having at least one PRL per complete scan and presented with 95% confidence intervals (CIs). A secondary analysis was performed, only considering lesions that demonstrated both the PRL and CVS; this was also presented as sensitivity and specificity with 95% CIs. Then, a sequential analysis was performed that first checks for PRL and then, if no PRL is detected, checks for CVS across the entire scan. A chi-square test was performed to investigate the location of PRL and WMLs (deep white matter vs all other locations).

The logistic regression was used to produce Receiver Operating Characteristic (ROC) curves. In the logistic model, diagnosis (MS vs MS-mimics) was set as a dependent variable and PRL (or CVS) as an independent variable. The ROC curve is a plot of sensitivity against 1-specificity. The sensitivity and specificity values were obtained by varying the cut-off to dichotomize PRL (or CVS).

5.2.6 Inter-rater Reliability

Inter-rater and intra-rater reliability for lesion identification and PRL detection was assessed in a randomly selected enriched data set of 100 blocks (53 with PRL and 47 without) containing MS and non-MS lesions. Reliability was calculated using Cohen's Kappa.

5.3 Results

5.3.1 Cohort Description

The demographics of the 562 participants (182 males and 380 females) are shown in *Table 5.1*.

Table 5.1. Overview of patients' clinical characteristics and analysed lesions.

	MS	CIS	Cluster Headache	Migraine	SLE	NMOSD	Diabetes Mellitus	Ageing Healthy Controls	Total
Number of patients (F)	166 (110)	88 (59)	3 (1)	21 (18)	19 (16)	30 (26)	18 (10)	217 (140)	562 (380)
Mean Age (SD)	37.3 (7.4)	32.6 (7.7)	49.3 (12.6)	40.8 (8.7)	32.5 (9.5)	46.5 (11.8)	68.3 (14)	64.2 (18.1)	48.4 (17.8)
Symptom Duration, Mean (range)	6.5 (0-30.5)	0.3 (0-2.5)	-	-	-	2.9 (0-9.6)	-	-	-
White Matter Lesions Analysed									
No. of patients with ≥ 1 WML, (%)	164 (98.9)	84 (95.8)	2 (66.7)	21 (100)	15 (78.9)	18 (60)	18 (100)	163 (75.1)	485 (86.3)
No. of lesions	3065	922	19	266	77	171	355	1142	6017
Median no. per patient (range)	17 (0-61)	7 (0-54)	9.5 (4-15)	10 (1-38)	4 (0-12)	1 (0-38)	17 (1-66)	3 (0-30)	7 (0-66)
Paramagnetic Rim Lesions									
No. of patients with ≥ 1 PRL, (%)	38 (22.9)	23 (26.1)	0	0	0	0	1 (5.6)	0	62 (11.3)
No. of lesions (%)	72 (2.3)	57 (6.2)	0	0	0	0	1 (0.3)	0	130 (2.2)
Median no. per patient (range)	0 (0-6)	0 (0-8)	0	0	0	0	1 (0-1)	0	0 (0-8)

MS: Multiple Sclerosis; CIS: Clinically Isolated Syndrome; NMOSD: Neuromyelitis Optica Disorder; SLE: Systematic Lupus Erythematosus; EDSS: Expanded Disability Status Scale (score range: 0-10, with the highest score indicating death from MS); SD: Standard Deviation; WMLs: White Matter Lesions; PRL: Paramagnetic Rim Lesions.

5.3.2 Lesion Count and Distribution

A total of 6,017 WMLs were analysed, with 3,987 in MS or CIS patients. The median and interquartile ranges of WML per patient found in each condition are represented in *Figure 5.2* Across the analysis, interrater reliability for lesion and PRL detection between investigators showed a substantial agreement with a Cohen's Kappa value of 0.640 and 0.696 respectively.

Furthermore, interrater reliability had a Cohen's Kappa value of 0.827, which indicate a moderate agreement.

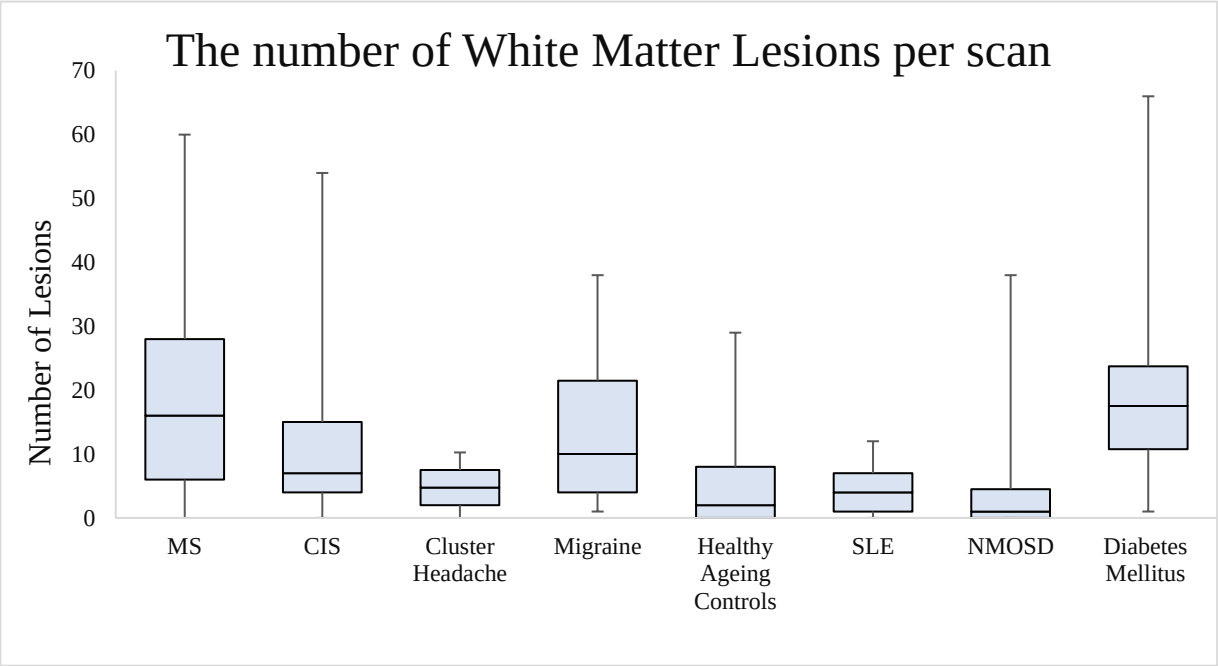

Figure 5.2. A box and whisker plot showing the mean and interquartile ranges of the number of white matter lesions per patient in each condition analysed.

MS: Multiple Sclerosis; CIS: Clinically Isolated Syndrome; SLE: Systematic Lupus Erythematosus; NMOSD: Neuromyelitis Optica Spectrum Disorder.

5.3.3 Paramagnetic Rim Lesions

PRLs were detected in 130 lesions across 62 patients. Within the MS cohort 38 patients (22.9% (CI 16.7%-30.0%) had at least one PRL. In the CIS cohort, the proportion of individuals with at least one PRL was 26.1% (CI 17.3%-36.6%), or 23 patients. Half of the PRL-positive scans had a single PRL (*Figure 5.3*). A single PRL was found in the scan of a diabetic patient, and this was the only PRL detected outside of the MS/CIS cohorts. Although the combined sensitivity of PRL for MS/CIS was 24.0%, (CI 18.9% -29.8%), PRLs had a very high specificity of 99.7% (CI 98.2%-99.99%) and positive predictive value (PPV) of 98.39.

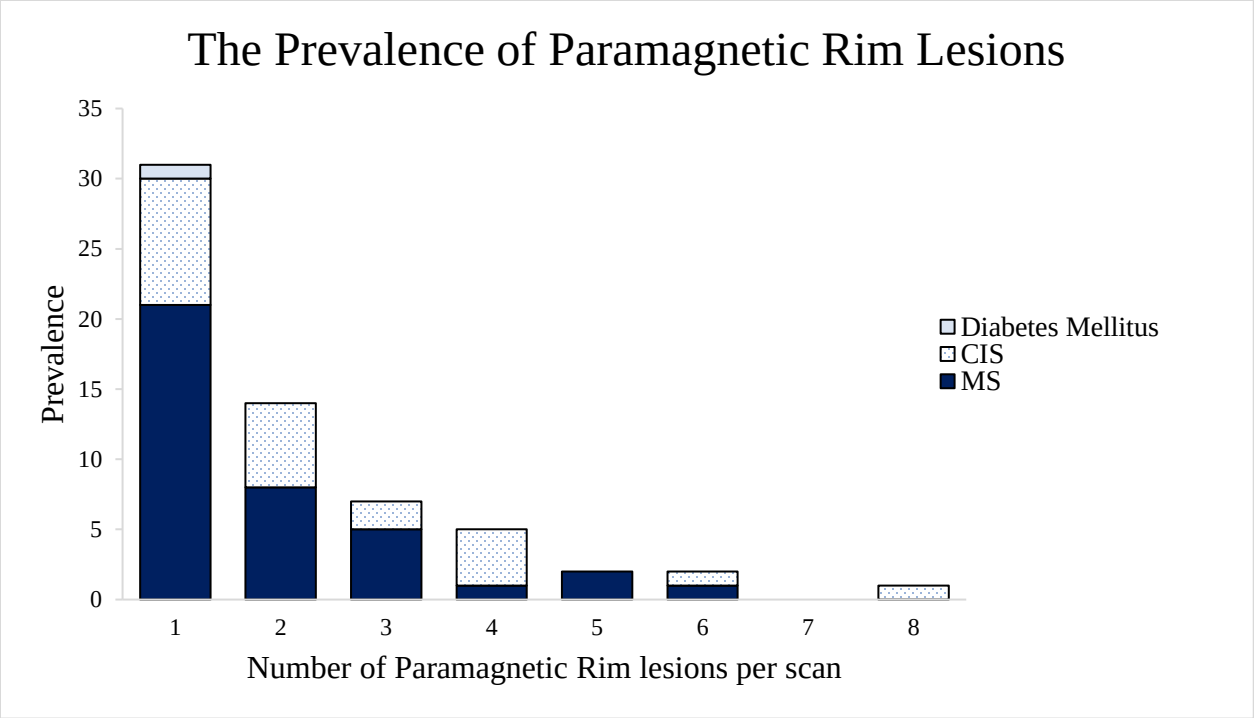

Figure 5.3. The number of paramagnetic rim lesions (PRLs) per patient for each cohort with ≥ 1 PRL. CIS: Clinically Isolated Syndrome, MS: Multiple Sclerosis

All patients with a PRL showing a CVS in the same lesion (n=54) had MS or CIS, giving a specificity of 100% (CI 98.8% - 100%) and a PPV of 100%. The sensitivity of PRL with a CVS for MS was 20.5% (CI 12.9% -25.4%) and 22.7% (CI 14.5% - 32.3%) in the CIS patients. In all MS/CIS patients displaying a PRL, 88.5% had a lesion displaying both PRL and CVS. The single PRL detected in the patient with diabetes did not display the CVS.

The identification of ≥ 1 PRL (optimal cut-off) was associated with a high specificity of 99.7%, but low sensitivity of 24.0%, and overall accuracy: area under the curve (AUC) = 0.71, 95% CI=0.64-0.78). CVS detection alone (optimal cut-off of ≥ 4 CVS) had a specificity of 88.3%, sensitivity of 56.7% and AUC = 0.82, 95% CI=0.79-0.86.

The combination of the two biomarkers (fulfilment of either ≥ 1 PRL or ≥ 4 CVS) further improved the specificity (90.6%), and a relative increase in the sensitivity (57.9%). The AUC= 0.83 (95% CI=0.79 - 0.87) *(Appendix C.3).*

We also performed a sequential analysis of the two signs: identification of any PRLs first, and if no PRL was identified followed by assessment of the presence of ≥ 4 CVS. The sensitivity of this two-stage analysis was 79.55% (95% CI 74.6 – 83.9) and 70.9% (95% CI 64.8 – 76.4).

Across the cohort, 73.1% of WMLs were found in the deep white matter, 19.4% in the periventricular region, 7.2% were juxtacortical and only 0.3% adjacent to DGM structures. In the MS and CIS cohorts, 70.1% and 66.5% of WMLs were located in the deep white matter respectively. Yet in the MS cohort, 84.2% of PRLs were identified in the deep white matter. The chi-square test investigating the location of the PRLs and WMLs found PRLs to be more common in the deep white matter (p =0 .003).

Summary of the Results

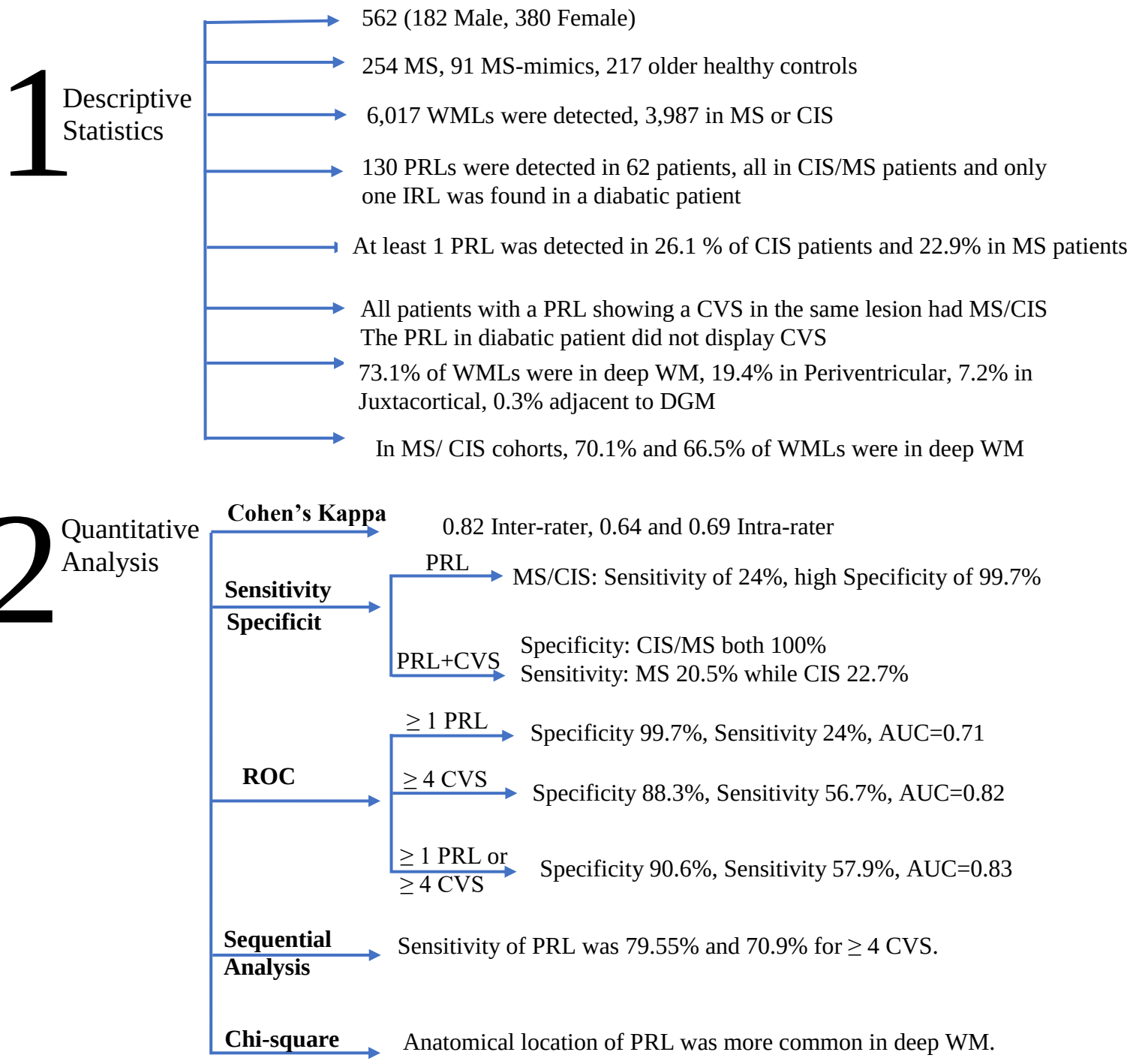

5.4 Discussion

The PRLs detected in phase-sensitive imaging have the potential to aid MS diagnosis. In this article, we expand beyond our original MAGNIMS study of the central vein sign [310] to evaluate PRLs using clinically determined 3T MRI protocols. We found the presence of any PRL highly specific for MS/CIS. Furthermore, the combination of PRL with CVS was found only in patients with MS or CIS and not in any other diseases studied with WMLs.

Maggi et al. [356] also reported in their large study low sensitivity and high specificity of PRL in MS. Our study, conducted in different centres, supports their findings. It further adds value as we examine a higher number of MS mimics and ageing controls with brain scans showing white matter lesions, which more commonly cause diagnostic difficulties for MS clinicians.

In addition to the analysis of the value of PRL and CVS, we performed a sequential analysis (first looking for the presence of PRL, and in the absence of any PRL assessing for ≥4 CVS). Although this did not lead to an improvement in sensitivity and specificity of the diagnosis of MS, it may prove popular with MS clinicians as it is time efficient while reviewing MRI scans with WMLs. This sequential analysis of course needs to be tested in a prospective study.

In both Sinnecker et al., 2019 [310]and this analysis we have recognised that the spatial distribution of the MS lesions and lesion characteristics may inadvertently un-blind the observer to the diagnosis and influences subsequent lesion characterisation on the same scan. For that reason, we have tried to improve the blinding by parcellating the brain into eight blocks and randomising the order of blocks analysis. In this way, we are certain that the investigators assessed individual lesions without the influence of other brain/lesion characteristics.

Although CVS is sensitive to MS, it was found to be less specific than PRL. Both of these imaging biomarkers are acquired on the same MRI sequence and may reduce the need for Oligoclonal Band testing which many patients find unpleasant. Our study strengthens the evidence for the role of phase-sensitive imaging in the diagnostic pathway of MS.

Our study is pragmatic, with clinical scans acquired by many centres, resulting in variability of scan quality, sequences, and operators. The results are therefore representative of the performance of this radiological biomarker in clinical practice. The patient-level prevalence of PRLs is within the range previously described by K.C. Ng Kee Kwong et. al.[359].

In this cross-sectional study, we did not aim to report on the natural history of PRLs but found that the percentage of lesions with an iron rim was higher in CIS compared to MS. This corroborates previous longitudinal studies which have suggested that PRLs may eventually dissipate as neuroinflammation is replaced by neurodegenerative pathology [211,219].

While in our study we examined the role of PRLs in the diagnosis of MS, the debate continues on whether most smouldering lesions produce a visible PR. Expanding lesion volume is important since it may be predictive of long-term clinical disability [336]. Our results suggest that one PRL is enough to help the diagnosis of MS, but counting the number of PRLs might be important as a prognostic factor for long-term disability. Studies suggest that some PRLs shrink after seven years, at which point the IR has faded along with the diffuse hyperintensity outside the rim [166]. It would be useful to examine the effect of disease-modifying treatments on PRLs. Unfortunately, data about the multiple disease-modifying treatments used in our cohort is unavailable. Furthermore, the scans available were not taken at the time of diagnosis of MS, thus we have been unable to determine at what point in the disease progression PRLs may be most prevalent.

As this cohort was previously reported the limitations are similar[310]. This study relied on the investigators' clinical diagnosis, and we did not independently assess the accuracy of the MS diagnosis or MS by subtype. Some publications suggest that relapsing-remitting and secondary progressive MS have a differing prevalence of PRLs [213,323]. The parcellated nature of the blocks, although essential for blinding, may also have resulted in lesions not being counted if they were dissected by the border of the blocks. This may account for why not all MS patients had lesions found on their scans, although we also excluded lesions smaller than 3mm in their longest axis. The moderate reproducibility we report is a concern. In clinical practice, clinicians will be influenced also by other MRI diagnostic features of the WML, concealed in our analysis by the parcellation method we used. Using automated, possibly image intensity based segmentation techniques may improve the accuracy of PRL detection and eliminating human errors. Once again only prospective studies can assess the true diagnostic value of a test.

5.5 Conclusions

Paramagnetic rims are a potential imaging biomarker, with high diagnostic specificity for MS. They have a clinical role to play in decreasing the diagnostic uncertainty in MS. In this large study a quarter of MS/CIS patients had at least one PRL. Furthermore, 3T phase-sensitive MRI is widely available and has already been proven to reliably identify the CVS. The combination of these radiological markers detected with the same MRI sequence shows great promise and requires further prospective evaluation, perhaps with added improvements to sequence optimisation.

Chapter 6 . Longitudinal Clinical Study of Patients with Iron Rim Lesions in Multiple Sclerosis

Abstract

Background: Iron rims (IR) surrounding white matter lesions (WML) are suggested to predict a more severe disease course. Only small longitudinal cohorts of patients with and without Iron Rim Lesions (IRLs) have been reported so far.

Objective: To assess whether the presence and number of IRLs in patients with clinically isolated syndrome (CIS) and MS are associated with long-term disability or progressive disease.

Methods: Ninety-one CIS/MS patients were recruited between 2008 and 2013 and scanned with 7T MRI. Expanded Disability Status Score (EDSS) was used to calculate Age Related Multiple Sclerosis Score (ARMSS) at the time of scan and the latest clinical follow-up after 9 years. WMLs were assessed for the presence of IRL using Susceptibility Weighted Imaging (SWI)-filtered phase images.

Results: In all, 132 IRLs were detected in 42 patients (46%). Nine percent of WMLs had IR. 54% of the cohort had no rims, 30% had 1-3 rims and 16% had ≥4. Patients with IRL had a higher EDSS and ARMSS. Presence of IRL was also a predictor of long-term disability, especially in patients with ≥4 IRLs. IRLs have a greater impact on disability compared to the WML number and volume.

Conclusion: The presence and number of perilesional IR on MRI scans hold prognostic value for long-term clinical disability in MS.

6.1 Introduction

MS is one of the leading causes of disability in young adults [378]. Given the availability of multiple DMTs and different approaches to MS treatment, there is a need to predict long-term disability [379]. Neurologists frequently select DMT based on the presence of prognostic factors [380]. Yet, there are still few prognostic markers that can be easily used in a routine clinical setting [381].

Iron accumulation at the edge of WMLs represents an emerging imaging biomarker that reflects iron-laden microglia and macrophages present in perilesional chronic inflammation[211,213,214,356,382]. IRLs are associated with remyelination failure and subsequent axonal loss. They appear as hypointense, ring-like structures on 7T or 3T MRI susceptibility imaging sequences[1,215].

MRI [356] and neuropathological [215,216] studies have reported that IRLs are present in more than half of MS patients and have been associated with clinical disability. It has been speculated that IRLs could serve as an imaging biomarker to predict future physical disability in MS [219,224] Two recent studies reported that patients with IRLs had a more aggressive disease course but their conclusions are tempered by either their sample size or follow-up duration [219,223].

In this large retrospective study, we aim to evaluate the association of IRLs on 7T SWI-filtered phase images [382] with clinical outcomes after a long clinical follow-up. Specifically, we aim to explore (i) whether the presence and number of IRL on an MRI scan is a predictor of worse clinical disability, (ii) IRL presence in different MS disease phenotypes and (iii) the association between IRL number and WML count and volume.

6.2 Materials and Methods

6.2.1 Clinical Cohort

Between August 2008 and July 2013, 156 patients with neuroinflammatory conditions were recruited from the outpatient neurology clinic at the Queen's Medical Centre in Nottingham to participate in ultra-high field MRI research studies.

Inclusion criteria used in this longitudinal clinical follow-up were age 18 years or older, diagnosis of CIS or clinically definite MS according to the revised McDonald criteria [307,383], up-to-date clinical records and the availability of 7T MRI scans including SWI *(Figure 6.1).* CIS and MS patients were included independently of their MRI findings. Patient demographics and clinical characteristics were collected by the research MS team (experienced MS neurologists and their MS fellows) at the time of their 7T MRI scan: age, sex, disease duration, treatment duration, disease subtype and EDSS [63]. ARMSS [67] was calculated. The latest clinical follow-up data were collected from hospital records in July 2021 to assess disability change. All studies contributing data to this longitudinal clinical follow-up received local ethics committee approvals, and all participants consented to have their clinical records reviewed.

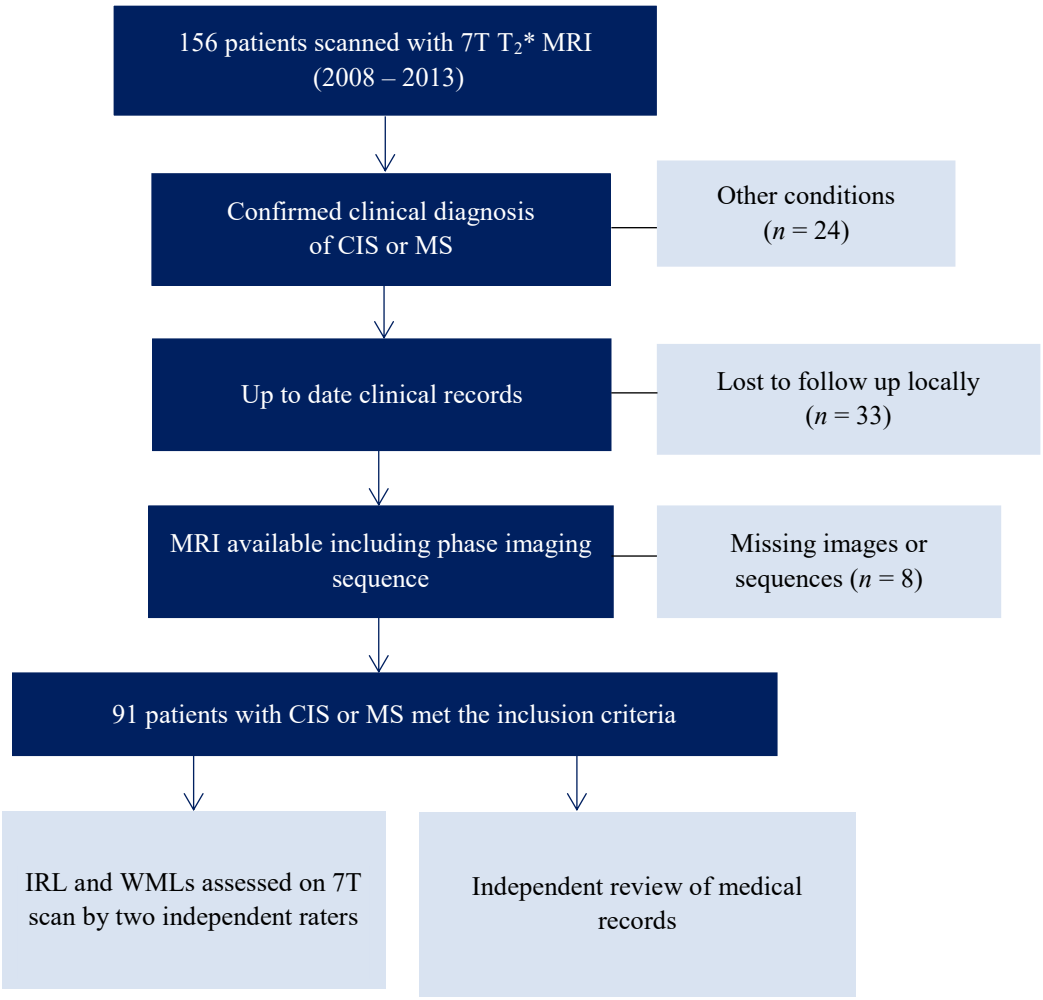

Figure 6.1. Flowchart summarises the study selection

6.2.2 MRI Acquisition

MRI scans were performed on a 7T MRI scanner (Philips Medical Systems, The Netherlands). We used T1- TFE (IR-TFE) sequence (also known as Magnetisation-Prepared Rapid Gradient-Echo (MPRAGE)) and 3D-FFE (3D-FLASH). High-resolution MPRAGE images were acquired with a tailored inversion pulse to reduce the effects of B1 inhomogeneity [384](Inversion Time TI=1070ms, FA=8˚, TE/TR=7/15ms for a total of 280 slices at a resolution 60 of 0.5x0.5x0.5mm^3 isotropic, for a total FOV of 205×215×140mm and acquisition time of 11 minutes). 3D T_2* weighted Echo Planner Images (EPI) were acquired with a 3D FLASH-T_2*

weighted spoiled Gradient Echo sequence (TR/TE=150/20ms, flip angle=14˚, FOV of 216×216×85mm, with a resolution of 0.5×0.5×0.5mm^3 and acquisition time of 9 minutes). Both magnitude and phase were saved, and the SWI-filtered phase images were reconstructed off-line using a high-pass filter as described in this study[382].

6.2.3 Lesion identification

For each patient, the number and volume of WML [385,386] were detected on T_1 (MPRAGE) sequence. Previous work identified the superior sensitivity of 7T MPRAGE in detecting MS WML compared to 3T FLAIR MRI [71]. The total lesion volume was recorded in mm$^{3.}$ After two-stage training by a neuroradiologist with MS experience, A. A. used the SWI-filtered phase images for rim detection. Inter-rater reproducibility was calculated on 10 random scans. A rim-positive lesion (IRL+) was defined as a hypointense rim that surrounds more than 50% of the lesion margin and is visible on at least 3 slices [387,388] (*Figure 6.2*). Total IRLs number and volume were calculated for each participant. ITK-SNAP [389] was used for the image analysis, detecting lesions and manually calculating the volumes. First, T_1 (MPRAGE) images were reviewed to detect and calculate the total volume of WML. Then, each lesion was individually checked for IRL presence on SWI images. The presence of rims was checked twice, by displaying two windows of SWI and T_1 images side by side and by co-registering/overlapping the two images, to check for co-registration errors. Manual segmentation of the IRL was then performed to calculate the volume

using the polygon feature. The IRLs were manually segmented in all the slices where the rim was visible. The volume of each rim lesion was then calculated.

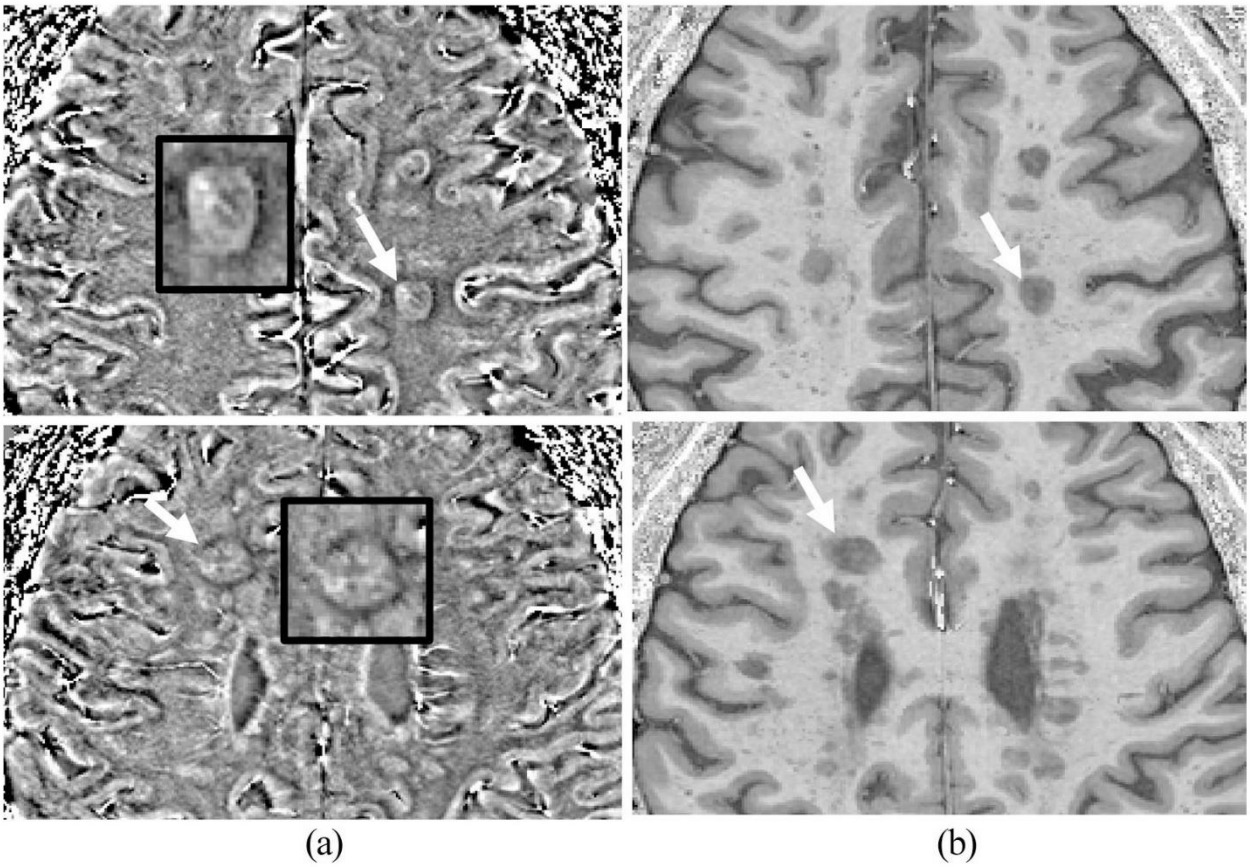

Figure 6.2. (A) Typical appearance of two lesions with rims on SWI-filtered phase image corresponding with (B) T1-weighted (MPRAGE). Enlarged images of the lesions indicated using white arrows from different patients are shown in the black box with the characteristic hypointense rim surrounding most of the lesion.

6.2.4 Statistical Analysis

Statistical analysis was performed using Jamovi (Version 1.6) and SPSS software package (version 27.0). Reported summary statistics include means, odds ratios, and relative risks along with associated 95% confidence intervals. Shapiro tests and visual inspection of histograms were used to assess the normality of the variables. The association between IRLs presence and disability

was initially assessed using Spearman's rank correlation coefficient. Disease subtypes and IRLs presence and number were assessed with sample *t-test*. The association between the presence and number of IRLs and disability (EDSS/ARMSS) was assessed using linear regression. In line with a previous IRLs study [219], we classified all patients into 3 groups based on the number of IRLs (0, 1-3, and ≥4) to test their association with disability using linear regression. Receiver Operating Characteristic (ROC) analysis was used to assess, for a given IRLs threshold, the sensitivity and specificity to classify two patient groups: either an increase in or a decrease or unchanged ARMSS at follow-up. We calculated the change in ARMSS from baseline to follow-up and dichotomised patients into two groups; those with positive "increased" change (ARMSS at follow-up was greater than baseline) and those with negative "reduced" or stable change (ARMSS at follow-up was either lower or the same as baseline).

Mediation analysis is a method used to explain the process by which one variable affects another [390]. A bootstrapping of 5000 samples was performed to explore whether IRLs number or WML number/volume has a greater direct effect on long-term disability. Statistical significance was set at $P<0.05$. Intraclass correlation coefficient (ICC) was used to assess the agreement between quantitative measurements of the number of IRLs in 10 randomly selected scans.

6.3 Results

6.3.1 Clinical Cohort and IRLs

Of 156 patients with neuroinflammatory conditions scanned on 7T MRI, data from 91 CIS and MS patients met the study inclusion criteria. Patients had a median of 7 years (IQR 2-15) from disease onset to the MRI scan; the median clinical follow-up after the MRI scan was 9 years (IQR

7-10). Nine percent of the 1468 WMLs had IR. Eighteen CIS patients had MS diagnosis at follow-up. Sex and age did not appear to affect the presence of IR. Study cohort demographic and clinical characteristics are presented in *(Table 6.1).* Forty-nine patients (53.8%) had no rims (IRL-), 27 (29.6%) had 1 to 3 rims and 15 (16.4%) had four or more rims *(Table 6.2, Figure 6.3).* IRL+ patients had a median number of 2 IRLs (IQR 1- 4). The intra and inter-rater agreement was ICC 0.95 and 0.81, respectively, conducted by (A.A. and A.O.).

Table 6.1. Baseline demographic, clinical and imaging data of the study cohort

	Total cohort	CIS	RRMS	SPMS	PPMS	>1 IRL+	IRL-
Clinical and demographic data							
Patients, n	91	22	34	17	18	42	49
Female sex, n (%)	53 (58%)	13 (59%)	25 (74%)	9 (53%)	9 (50%)	27 (64%)	29 (59%)
Age, y	46 (18-75)	39(18-64)	41 (20-58)	50 (33-61)	51 (32-75)	48 (23-75)	40 (18-65)
Disease duration, y	7 (0-40)	1 (0-22)	9 (0-32)	17 (4-40)	6 (1-17)	8 (0-40)	5 (0-32)
EDSS	4 (0-7)	1 (0-7)	2.5 (0-6.5)	6 (4.5-7.5)	5.5 (2.5-6.5)	4 (0-7)	3 (0-7)
ARMSS	5.4 (0.2-9.7)	1.8 (0.4-8.3)	4.9 (0.2-9.6)	7.4 (5.3-9.7)	6.25 (3.1-9.0)	6.7 (0.3-9.3)	5.0 (0.2-9.7)
DMT, n (%)	27 (30%)	0	16 (47%)	11 (65%)	0	16 (38%)	11 (22%)
DMT Duration before baseline, m	0 (0-140)	0	0.5 (0-130)	12 (0-140)	0	0 (0-130)	0 (0-140)
MRI Data							
>1 IRL, n	42	11	13	12	6	42	NA
Total number of IRL, (F/M)	132 (88/44)	25 (16/9)	41 (30/11)	58 (37/21)	8 (5/3)	132 (88/44)	NA
Total WML, n (% IRL)	1468 (9%)	171 (15%)	463 (9%)	526 (11%)	308 (3%)	1076 (12%)	392 (NA)
Total WML volume mm^3, (% with IRL)	135179 (12%)	19296 (20%)	38019 (14%)	50828 (9%)	27036 (2%)	97610 (19%)	37279 (NA)
Total IRL volume mm^3, n	15509	4003	5412	4732	596	18582	NA

All data presented as medians and ranges; IRL+: Iron Rim Lesion positive, IRL-: Iron Rim Lesion negative, EDSS: Expanded Disability Status Scale, ARMSS: Age-Related Multiple Sclerosis Severity; DMT: Disease-Modifying Treatment; CIS: Clinically Isolated Syndrome, RRMS: Relapsing-Remitting Multiple Sclerosis, SPMS: Secondary Progressive Multiple Sclerosis, PPMS: Primary Progressive Multiple sclerosis. DMT patients treated refer to individuals who ever received treatment prior to scan.NA: not applicable

Table 6.2. Cohort characteristics and their lesion analysis at baseline scan

Characteristic	IRL-	1-3 IRL+	≥4 IRL+
No. (%)	49 (53.8%)	27 (29.6%)	15 (16.4%)
Sex, F, n (%)	29 (58%)	18 (66.7%)	10 (66.7%)
Age, y	40 (18-65)	40 (21-75)	48 (23-64)
EDSS	3 (0-7)	2.5 (0-6.5)	6 (0-7)
ARMSS	6.5 (0.30-9.30)	4.9 (0.7-8.86)	8.1 (0.30-9.30)
Disease duration, y	5 (0-32)	6 (0-28)	9 (2-40)
Total rim lesion volume mm^3, n	NA	6550	8115
Total lesion volume mm^3, n	37279	44307	53593

All data were presented as medians and ranges; IRL+: Iron Rim Lesion positive, IRL-: Iron Rim Lesion negative, EDSS: Expanded Disability Status Scale, ARMSS: Age Related Multiple Sclerosis Severity Scale.

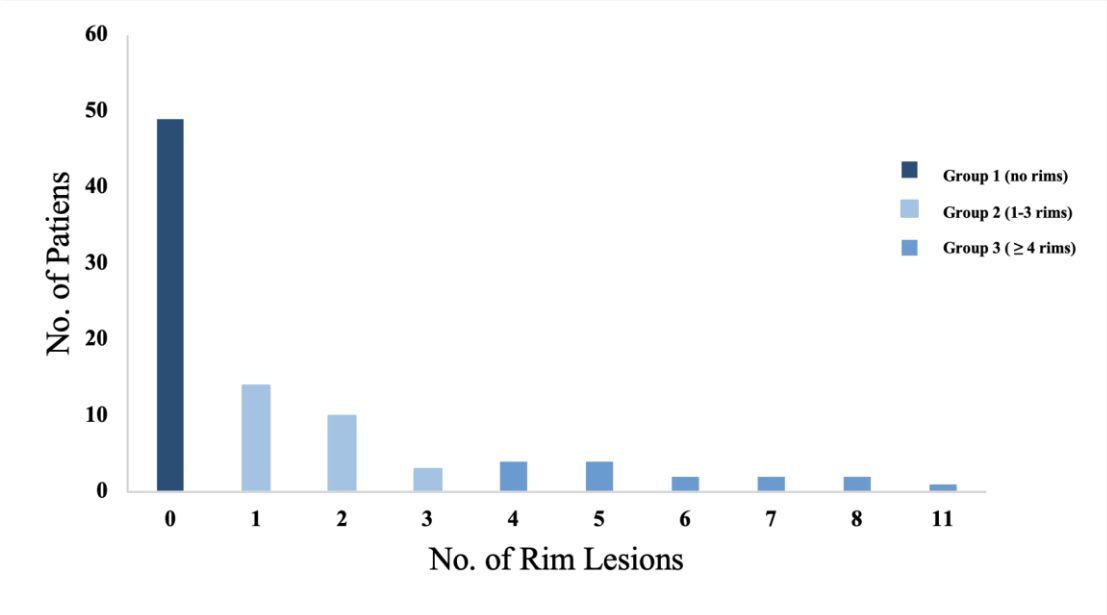

Figure 6.3. Histogram illustrating the number of Iron Rim Lesions (IRLs). Lesions were classified into three groups based on rim presence.

6.3.2 Association between IRLs and disease phenotype/evolution

The presence of IRLs was affected by disease subtype. A higher proportion of patients with SPMS had at least 1 IRL (*Table 6.1*), SPMS patients also had more rims per patient compared to all the other disease subtypes (P=0.007). Development of RRMS/SPMS was not affected by the presence of IRLs in those with an initial diagnosis of CIS patients (9/11 vs 9/11; a risk ratio of 1). IRL+ RRMS patients had a higher rate of progression to SPMS during the follow-up period compared to IRL- (7/13 vs 7/21), giving a risk ratio of 1.6 (95% CI 0.74 -3.44). Both at baseline and follow-up the ARMSS (and EDSS) were higher in IRL+ patients *(Figure 6.4).*

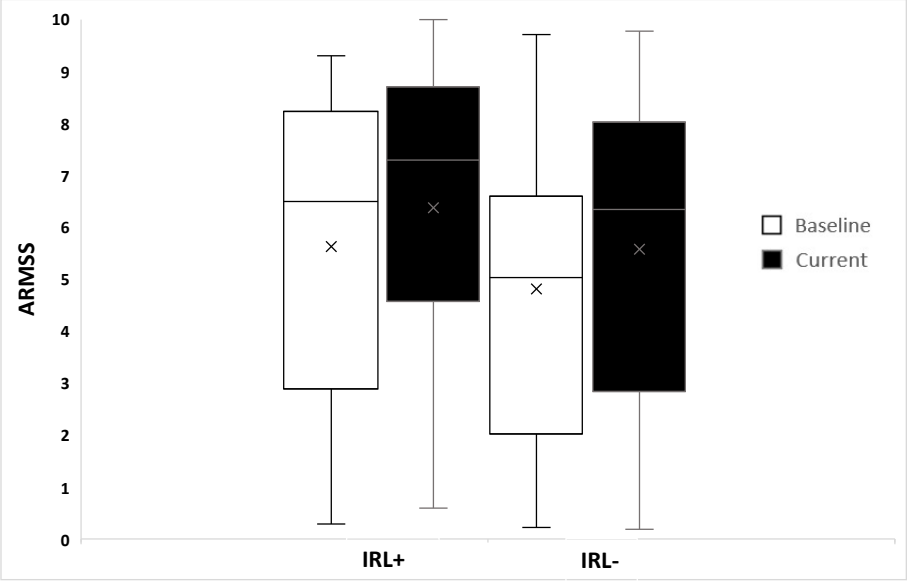

Figure 6.4. ARMSS at baseline and current clinical follow-up in patients with and without IRL. The median baseline ARMSS of the whole cohort was 5.4 (IQR 2.8-7.6). Patients with at least one IRL had a higher baseline ARMSS (6.7; IQR 3.1-8.1) compared to those without IRL (5.0; IQR 2.2-6.5)

**ARMSS: Score Age-Related Multiple Sclerosis Severity Score, IRL: Iron Rim Lesions*

6.3.3 Association between clinical disability and the number of IRLs

The number of IRLs correlated with the baseline ARMSS ($p<0.006$) even when accounting for total WML volume ($p<0.04$). Similarly, it correlated with current ARMSS ($P<0.003$). However, due to the high correlation between IRLs and WML number ($r=0.58$) and volume ($r=0.48$), they were not modelled in the same regression analysis. Therefore, mediation analysis was performed and showed that the direct effect of IRLs number on current ARMSS was greater (63%) than lesion count (0.23 (Bootstrap CI: 0.007-0.46)), and even greater (77%) than lesion volume (0.30 (Bootstrap CI: 0.10-0.09).

Patients with ≥4 IRLs had higher ARMSS at baseline (5.9) and follow-up (8.1) compared to those with <4 IRLs with ARMSS at baseline (5.4) and (6.7) at follow-up *(Figure 6.5).* Therefore, to explore whether it was a better prediction of disease progression in patients with ≥4 IRLs, ROC analysis showed that a threshold of ≥4 IRLs has a high specificity (95%) but showed low sensitivity (12%) to the rate of progression. The Area Under the Curve (AUC) was 0.66 ($P<0.05$) demonstrating poor prognostic accuracy *(Figure 6.6).* Thresholds lower than 4 IRL (not reported here) were less useful.

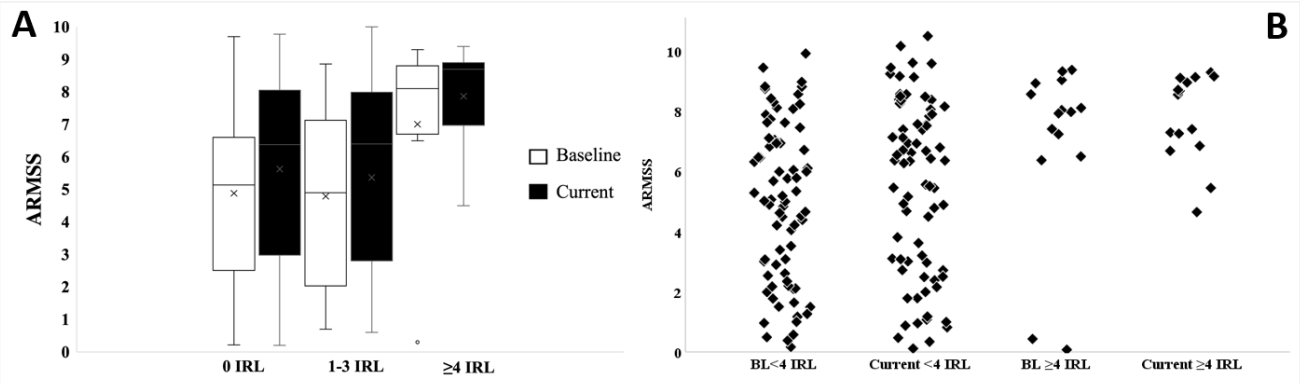

Figure 6.5. ARMSS at baseline and current clinical follow-up in IRL patients. The number of IRLs was grouped to (A; 0 IRL, 1-3 IRL and ≥4 IRL), (B; less than 4 IRL and 4 or more rims).

**ARMSS: Score Age-Related Multiple Sclerosis Severity Score, IRL: Iron Rim Lesions*

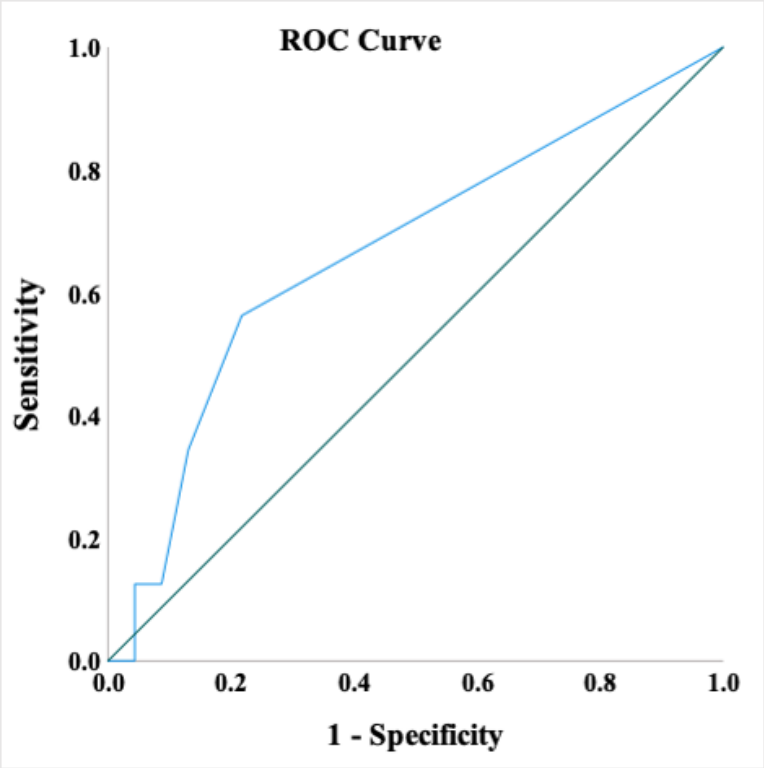

Figure 6.6. Receiver Operating Characteristic (ROC) curve for the cut-offs of iron rim lesions number. Reference line (in green)

6.3.4 IRLs and DMTs

IRLs were present despite prior treatment with DMT (Copaxone, beta interferon and natalizumab). The odds of being IRL+/IRL- among previously treated patients was 16/26 and 12/37 in untreated patients, giving an odds ratio of 1.9 (95% CI 0.77 – 4.67); the mean DMT duration prior to scanning was 16.8 months (SD 32.8). Only two patients were treated with monoclonal antibody therapy (both natalizumab) prior to the scanning (both IRL+). The mean total DMT duration of treatment, prior to scanning and during clinical follow-up was 45.5 (SD 63.8) months.

Summary of the Results

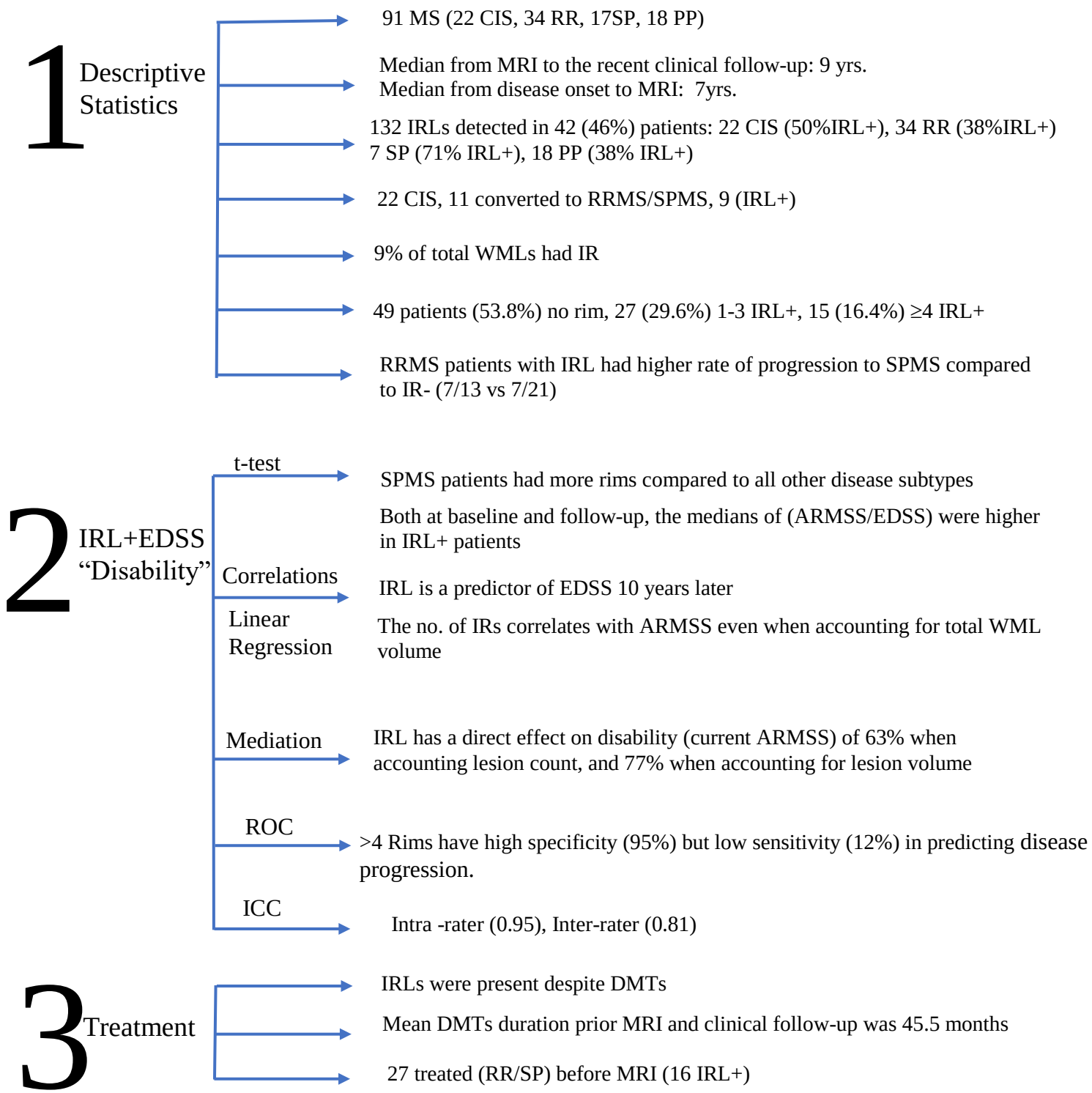

6.4 Discussion

The role chronic active inflammation, reflected in the presence of IRLs in this study, plays in determining disability in MS patients has been a topic of interest in recent years.

In this retrospective study, we explored the association between the presence and number of IRLs on 7T MRI with clinical outcomes, over a follow-up period of up to 12 years. We found that the presence of IRLs was associated with worsened clinical disability in a cohort of 91 patients, particularly if patients had more than 4 IRLs at their MRI scan, supporting the notion of unfavourable prognosis associated with IRLs presence [219,223,224].

In line with others, at least 1 IRL was detected in almost half of our patients [221,356], and IRLs were more prevalent in SPMS patients compared to CIS and all other MS subtypes[215,223,328,355,356,391,392].

We found patients with IRLs had a more aggressive disease (greater WML number and volume, higher disability scores at baseline and follow-up), corroborating findings from earlier studies [216,219,223]. The contribution of our longer clinical follow-up study of 9 years validates the previously reported association of IRLs presence and long-term disability. We report patients with at least one rim lesion had higher disability [63] and MS severity (accounting for patient age [global ARMSS]) [307], comparable to two recent studies, Blindenbacher *et al.* followed-up 66 CIS and MS patients for a median of 2.9 years [328] and Dal-bianco *et al.* who followed-up 8 MS patients for 7-years follow-up [223].

Although as a group of patients with IRLs do worse, we have found that the presence of one IRL does not appear to be sensitive in detecting patients with the worse outcome. In line with a recent report [223], we found that patients with ≥4 IRLs had the worst disability scores, with high specificity.

As on average 9% of WM lesions have IR, we tested if identifying IRLs had an advantage over assessing the total WML load (count or volumes) in determining clinical disability. Previous studies did not explicitly account for this in their analysis. We performed mediation analysis and found that the number of IRLs had the most direct effect on disability compared to WML count and volume, supporting its role as an independent prognostic imaging biomarker.

Detecting and counting IRLs are much easier than assessing all WML in clinical settings. We have found IRLs present in DMT-treated and untreated patients. We have to treat this observation very cautiously as the duration of DMT treatment was only 17 months and most patients were treated with first-line agents. Although IRLs number was higher in patients ever treated with DMTs, this might also be reflected by the number/volume of WMLs, as patients with more extensive disease are more likely to be treated. It remains to be seen if long-term use of DMTs, or higher effectiveness DMTs influence IRLs and more importantly whether long-term clinical disability can be mediated through IRLs.

We have found that iron-sensitive MRI may become an additional tool for monitoring and predicting disease progression, above what can be achieved through the study of gadolinium-enhanced lesions and brain atrophy alone [223].

6.5 Limitations and Future Direction

This study has limitations that include the exclusion of a large subset of patients due to the lack of clinical follow-up data. Also due to the retrospective study design, we were not able to accurately record all previous DMT data. Detecting IRLs on brain MRI is subjective and requires clear guidelines on manual assessment or automatic algorithms before these findings can be translated to clinical practice.

Our results support the need for (i) prospective studies using IRLs as a prognostic imaging biomarker in MS, (ii) longitudinal studies to capture the long-term IRLs evolution, and (iii) study of the association between IRLs presence and disease progression in the spinal cord, (iv) clinical trials to assess to what extent IRLs can practically contribute to monitoring disease progression, and (v) validation of our results using 3T clinical scanners as 7T MRI is still limited to tertiary MS research centres.

6.6 Conclusions

The presence and number of IRLs at MRI scan, especially the presence of ≥4 rims, hold prognostic value for long-term clinical disability in MS. The effect of IRLs on disability was greater than WML number or volume. This supports the role of IRLs as an imaging biomarker for disease severity, which could be easily implemented in clinical practice.

PART 3

WHITE MATTER LESIONS in MS

Chapter 7 . Magnetic Resonance Imaging as a Prognostic Disability Marker in Clinically Isolated Syndrome and Multiple Sclerosis: a systematic review and meta-analysis

Abstract

To date, predicting disability progression in MS is still a challenge. Although MRI is helpful and white matter lesions (WML) counts and volume are reported to be of value, their exact role in long-term disability prediction has not been systematically and quantitatively assessed. A meta-analysis was conducted using studies from four databases to assess whether MS lesion count and volume at baseline MRI scans could predict long-term disability, assessed by the Expanded Disability Status Scale (EDSS). 15 studies were eligible for the qualitative analysis and 3 studies for meta-analysis. T_2 brain lesion count and volume after the disease onset was associated with disability progression after 10 years. Four or more lesions at baseline showed a highly significant association with EDSS 3 and EDSS 6 with a pooled OR of 4.10 and 4.3 respectively. The risk increased when more than 10 lesions were present. This review and meta-analysis confirmed that lesion counts and volume could be associated with disability and might offer additional valid guidance in treatment decision-making. Future work is essential to determine whether these prognostic markers have a high predictive potential.

7.1 Introduction

MRI has an essential role in MS diagnosis and prognosis, estimating the risk of developing MS [307] and assessing MS disease activity when making treatment decisions [393–395]. Neurological disability varies among patients, from practically asymptomatic patients[396,397] to those with severe neurological disability and shortened life. Recently, early treatment initiation has gained an interest to prevent/eliminate long-term disability and induce remission. However, DMTs might be associated with life-changing side effects [398,399].

The majority of the first presentation of MS is referred to as CIS. patients present with an episode of neurological symptoms that at least partially resolves [400]. However, 85% of CIS patients develop RRMS[400]. Following a CIS, a higher initial brain WMLs load and volume over the first 5 years, were thought to be associated with increasing the risk of developing disability in 20 years[46,247]. Given this, assessing the association between WML lesion load and volume and their prediction of long-term disability is crucial[401].

Different reviews have been performed on MRI factors and their association with the risk of developing MS[402,403]; however, most do not fulfil systematic review criteria[354,404,405]. To our knowledge, this is the first systematic review with meta-analysis assessing the prognostic value of MRI in MS and predicting long-term physical disability.

7.2 Material and Methods

7.2.1 Study Registration

This systematic review and meta-analysis were conducted according to the Preferred Reporting Items for Systematic reviews and Meta-Analysis (updated PRISMA) guidelines [405] and were registered in the International Prospective Register of Systematic Reviews (PROSPERO) database (CRD42021249236) in May 2021.

7.2.2 Sources, Search Strategy, and Screening

Four electronic databases were searched (Medline, Embase, Web of Science, and PubMed) with the keywords ["Magnetic Resonance Imaging" or "MRI"], ["Lesion" or "lesions"], ["Count or Counts"], and ["Multiple Sclerosis" or "MS"]. The Medline search strategy (*Appendix D.1*). Mendeley was used for bibliographic management, including duplicate removal.

The search strategy was conducted by three reviewers (A.A., A.M., and A.O.)[4], who also verified the database selections, study screening/identification, study eligibility/inclusion, and quality assessments independently and blindly.

7.2.3 Study Selection (Eligibility Criteria)

Studies were considered for inclusion if they: (i) were longitudinal prospective and retrospective studies; (ii) reported the association between baseline MRI lesion count or volume and MS disability (iii) included ≥ 10 years of follow-up to assess disease progression, as disability

[4] A.M. Abrar Alamrani (MSc), Faculty of Health, York University, Toronto, Canada

is usually a slow process from the disease onset, and the predictive value of the short-term disability evolution within the first years is low [406]; (iv) investigated the association between white matter lesions counts/volume in MS and disability, with at least one of the MRI measurement (T_1/ T_2 lesion number or count) at the baseline; (v) reported EDSS as an outcome; (vi) were published in peer-reviewed journals; (vii) were written in English.

Studies were considered for exclusion if: (i) they were placebo arms of randomised controlled MS immunotherapy treatment studies because the placebo arms often convert to treatment after 2 years; (ii) the participants were under 18 years old; (iii) they reported on different MRI techniques (e.g., spectroscopy), or only reported prognostic models; and/or (iv) they were reviews, opinion pieces, editorials, comments, no-full text articles, technical, or animal studies. A manual search of the reference lists of the included studies was performed to detect further eligible studies.

7.2.4 Data Extraction

In April 2021, full texts were examined independently by three reviewers (A.T., A.A., and A.O.) according to the predefined inclusion criteria. Disagreement of including or excluding a study was resolved by discussion.

The same reviewers independently extracted demographics, disease-specific data, and outcome data (including age, gender, disease duration, EDSS score, population groups, and sample size), and then the results were compared. All included studies assessing disability, MS or SPMS in relation to baseline MRI data were extracted.

7.2.5 Outcome Measures

The primary outcome was disability assessed by EDSS. Thus, studies that evaluated the mean EDSS and time to reach EDSS 3 or 6 were included.

7.2.6 Quality Assessment

To assess the validity of included studies, the Quality In Prognosis Studies (QUIPS) tool[407] was used. It contains six domains to appraise the following: (i) participation; (ii) attrition; (iii) prognostic factor measurement (MRI in this study); (iv) outcome measurement; (v) study confounding; and (vi) analysis. A judgment concerning the related risk of bias was assigned for each domain (yes, partly, no), and a checklist was used to assess the quality and completeness of MRI reporting. Citation chaining from reviews and other papers discovered by reviewers was carried out, and the searches were re-run before the final analysis in June 2021. Disagreement between reviewers was solved by mutual discussion.

7.2.7 Statistical analysis

Study characteristics and extracted variables were summarized using standard descriptive statistics. Continuous variables were expressed as means and SD, and categorical variables were expressed as frequencies or percentages. Meta-analysis of binary outcomes was expressed as OR with 95% CI. A random-effects model and the Mantel–Haenszel method were used to pool the study odd ratios and compute an overall P-value. Heterogeneity tests were conducted as a chi-square variate (assumption of homogeneity of effect sizes). The I^2 statistic was used to assess the extent of between-study heterogeneity. Study heterogeneity I^2 values > 50% were considered

substantial and those >75% were deemed considerable heterogeneity. All P-values were two-tailed, with values < 0.05 considered statistically significant. Review Manager 5.4.1 software (Cochrane organisation, London, UK) implemented all analyses.

7.3 Results

7.3.1 Literature Search and Study Characteristics

The systematic search retrieved 1108 studies. A total of 424 studies remained after removing duplicate studies and ineligible studies such as case studies and letters, using an automated tool on each database; screening the title and abstract excluded 399 studies that did not meet the eligibility criteria. A total of 25 studies remained for full-text assessment. Of those, 15 studies[15,46,408–412,130,202,247,249,250,385,386,401] fulfilled the eligibility criteria for qualitative synthesis, while three studies[46,202,247] were included in the meta-analysis (*Figure 7.1*).

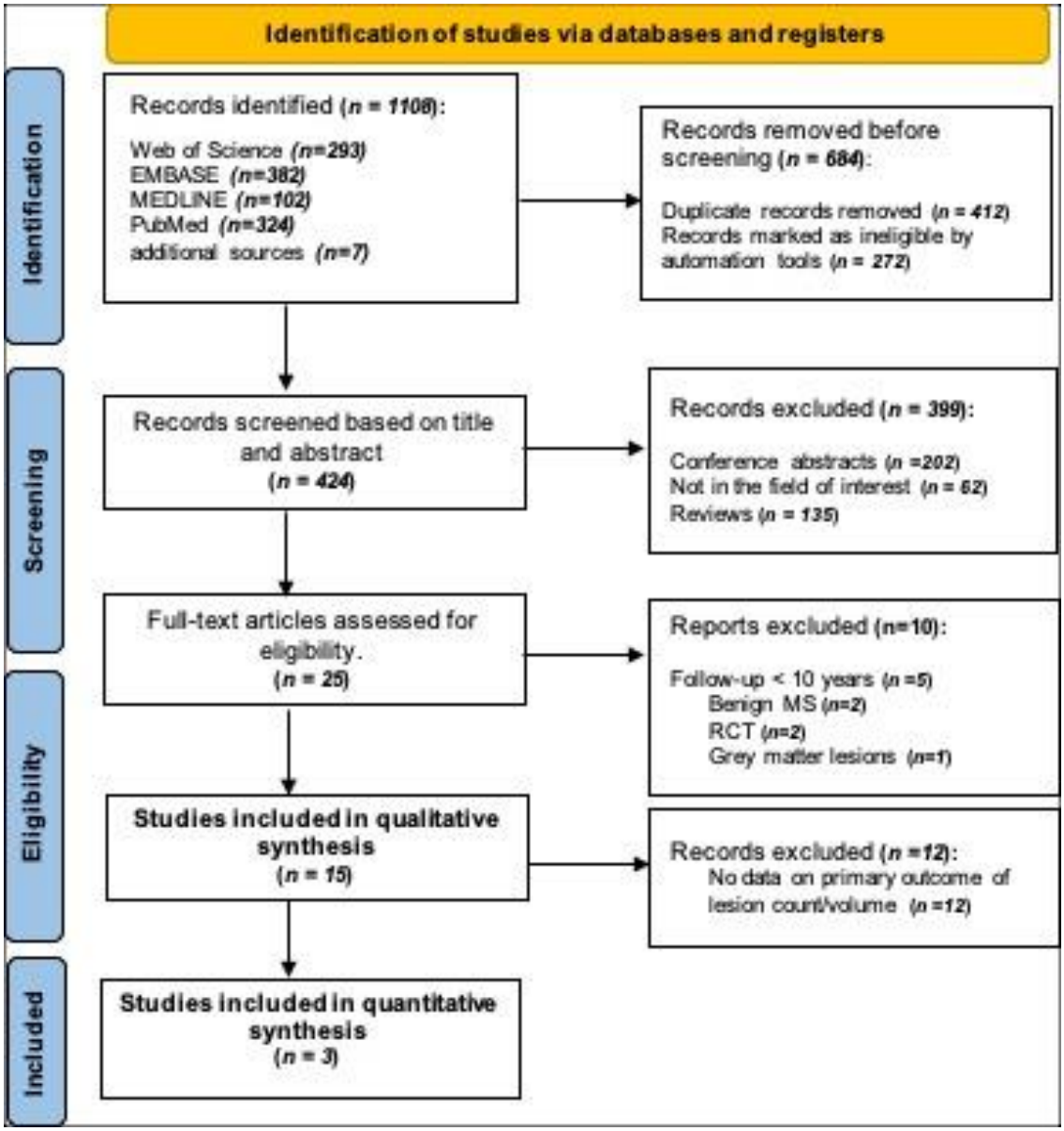

Figure 7.1. PRISMA flow diagram, illustrating the systematic search strategy and study selection.

7.3.2 Cohort Description

London (The National Hospital, Queen Square; Moorfields Eye Hospital) has two different cohorts, namely London 1 in 1984–1987 and London 2 in 1995–2004[46,250,410,411]. The London 1 cohort[46,411] included 140 patients scanned at baseline[46] and followed clinically after 5[413], 10[410], 14[250], and 20 years[46] by assessing the EDSS changes throughout the years.

Filippi[414] performed a reanalysis of the 5-years cohort data[413]. Similarly, Sailer[411] and colleagues used the data of 58 patients from the 5- and 10-years London 1 cohort. Filippi and Sailer used semi-automated MRI analysis techniques, and Chung et al. (2020) used the same data after 30 years of follow-up[401]. In London 2, the cohort was part of a follow-up study of 143 patients and the EDSS was assessed at 5 years.

Barcelona (Vall d'Hebron University Hospital) has a centre-based cohort that started in 1995 and is ongoing[247,260,415]. CIS patients are included consecutively with an assessment of the EDSS and relapse every 3-6 months[247,260,415] or annually[247]. MRI scans were performed at baseline (3-5 months after CIS diagnosis), 12 months after, and then every 5 years[247]. The EDSS was assessed at each visit[247,260,415]. Several studies were published from this cohort, including the first[415], which was a 7-year longitudinal study of 175 patients. In contrast, the study in 2010 focused on the prognostic role of infratentorial lesions at baseline by analysing retrospectively 77 patients with infratentorial lesions out of 246 patients[260]. Another study in 2015 included 1058 patients[247]. The latest publication[412] from 2019 reports on 401 patients. All cohorts used the Poser criteria for MS diagnosis [46,131].

7.3.3 Quality Assessment

There was high heterogeneity between studies due to several causes, namely, different study designs (centre or multi-centre-based cohort), prospective and retrospective studies, and the broad spectrum of study duration starting from 1984 to ongoing studies (*Table 7.1*).

There was no systematic way of reporting the findings, making the comparison between the findings challenging. A striking observation was made of the way the results were reported

between the studies, mainly, the raw data related to the primary outcome was not reported and cannot be accessed. For example, the lesion counts and volumes at baseline and follow-up were not reported, making it challenging to compare. Additionally, different findings that were not essential to the primary or secondary outcomes were reported instead of illustrating that no significant results were found.

Quality assessment for potential bias showed mixed results. Specifically, quality was not consistent for "prognostic factor" (MRI measurements), "outcome measurement (i.e., EDSS) and "confounding measurement and account" (immunotherapy). Detailed information about essential and raw data was often missing including lesion counts/volume at baseline and their association with EDSS 3 or EDSS 6.

Additionally, variability in MRI sequences, field strengths, and rater blinding strategies led to more heterogeneity between studies. The MRI data synthesis showed that most of the studies provided information on field strength and scan resolution. However, the clinical data blinding was only reported in eight studies, and the number of raters was reported in 11 studies. The most common sequence used in lesion detection was T_2-weighted images using a semi-automated tool. Complete information can be found in *Appendix D.2*.

Table 7.1. Quality assessment and potential bias: No: □, Partly: ▫ Yes: ■

	Potential Bias (QUIPS) tool					
Study, y	**Study participation**	**Study attrition**	**Prognostic factor**	**Outcome measurement**	**Confounding measurement and account**	**Analysis**
Tintore, 2020 [412]				▫		
Chung, 2020 [401]				▫		
Brownlee, 2019 [249]				▫		
Tintore, 2015 [247]	▫	▫	▫	▫	▫	
Jacobsen, 2014 [416]	■	■	■	▫		■
Kearney, 2014 [130]	▫	▫	▫		▫	
Giorgio, 2014 [386]					▫	
Popescu, 2013 [15]		▫	▫	▫	▫	■
Rovaris, 2011 [408]	▫	▫	▫		▫	
Renard, 2010 [385]	▫			▫		▫
Fisniku, 2008 [46]			▫	▫	▫	
Chard, 2003 [409]	▫	▫		▫		■
Brex, 2002 [250]				▫	▫	
Sailer, 1998 [411]	▫	▫	▫	▫	▫	
O'Riordan, 1998 [410]	▫	▫		▫	▫	

7.3.4 Study Results

At baseline, the patients' mean age ranged from 29-32 years, and 67% were female across all cohorts. However, no data were given regarding the mortality rate after the onset and its correlation with MRI parameters/findings. To predict disability after CIS, we compared different MRI prognostic features, namely lesion counts and volumes. Additionally, we assessed how these MRI features could also predict the conversion to MS. Limited information about the SPMS transition was reported. Besides disability and the conversion of MS - which are the main endpoints of this review—different prognostic factors were also mentioned in the included studies such as brain atrophy and Gd- enhancing lesions. For further details of the included studies see Table 7.2.

Table 7.2. Characteristics of the included studies (qualitative and quantitative).

Author, y	Centre and design	Clinical features	Study length	Sample size	T2 lesion count	Lesion volume	EDSS
Tintore et al. (2020) [412]	Barcelona centre-based prospective cohort 1995-2016	CIS	21 y	401 analysed	0: 80 (20%) 1-3: 67 (17%) 4-9: 56 (14%) ≥10 188 (48%)	⦸	DMT after CDMS: EDSS= 3 74 of 156 (47%), EDSS= 6 11 of 156 (7%) DMT before CDMS: EDSS=3 11 of 55 (20%), EDSS=6 4 of 55 (7%)
Chung et al. (2020) [401]	UCL, London Prospective cohort 1984-1987	CIS	30 y	132 120 analysed	0-16 (86%) 17-20+ (17%)	⦸	⦸
Brownlee et al. (2019) [417]	UCL, London Prospective cohort 1995-2004	CIS	15 y	178 164 analysed	⦸	⦸	BL: EDSS= 5 (15.25) FU= 0 (range 0-1) in CIS FU=2 (range 0-10) in MS
Tintore et al. (2015) [247] *****	Barcelona centre-based prospective cohort 1995-2013	CIS	18 y	1058 1015 analysed	0: 299 (31%) 1-3: 137 (14%) 4-9: 137 (14%) ≥10: 378 (40%)	⦸	EDSS >3 12 of 299 (4%) with 0 les, 10 of 137 (7%) with 1-3 les, 13 of 137 (10%) with 4-9 les, 83 of 378 (22%) with ≥10 les. EDSS≥6 2 of 299 (0.7%) with 0 les, 0 (0%) of 137 with 1-3 les, 0(0%) of 137 with 4-9 les, 20 of 378 (5.3%) with ≥10 les
Jacobsen et al. (2014) *	2 centres in Norway, Prospective cohort 1998-2000	MS	10 y	81 analysed	BL: (16.0± 12.3)	⦸	EDSS >3 (50/81) 0 of 50 (0%) with 0 les, 0 of 50(0%) with 1-3 les, 6 of 50 (12%) with 4-9 les, 44 of 50 (88%), with ≥10 les. EDSS ≥6 (3/81) 0 of 0 (0%) with 0 les, 0 of 0 (0%) with 1-3 les, 1 of 3 (33.33 %) with 4-9 les, 2 of 3 (6.06 %) with ≥10 les
Kearney et al. (2014)	MAGNIMS (7 centres), retrospective	MS subtypes (CIS, RRMS, SPMS)	26 y	159 analysed	⦸	⦸	EDSS BL:4 (range 0-8)
Giorgio et al. (2014) [386]	Siena, Italy Prospective cohort 2000-2001	RRMS	10 y	73 57 analysed	BL: (22.4± 18.5) 17 (2 -80) New/enlarge: (+1.5±1),1.3 (0.01 to 4.3)	BL: (5.8±6.4) cm^3 FU: (8.3±8.1) cm^3 Annualized 10y rate of T2 lesion growth (LV change/y) of: (0.25±0.5) cm^3	EDSS BL: (1.8± 1.1) 10 y FU: (2.5± 1.7)

Popescu et al. (2013) [15]	MAGNIMS (8 centres), retrospective (before Jan. 2000).	MS subtypes (CIS, RRMS, SPMS, PPMS)	10 y	261 analysed	⊘	BL: 5.91 (2.07-13.82) 1yr FU: 9 (4.2-19) Difference/yr 2 (0.5-3.9)	EDSS for the whole group [median (IQR)] BL: [4 (2-6)], 10 y FU: [6 (4-7.5)] EDSS for CIS BL: [0 (0-1)],10y FU: [1.5 (1-3)] EDSS for RRMS BL: [2 (1-3)] 10y, 10y FU: [3.5 (2-5.5)] EDSS for SPMS BL: [5.5 (4-6)], 10y FU: [7 (6-7.5)] EDSS for PPMS BL: [5.5 (3.5-6.5)], 10y FU: [7(6-8)]
Rovaris et al. (2011) [408]	MAGNIMS (7centers), retrospective	MS	15 y	369 analysed	⊘	12.4 (0.4-61.1)	EDSS BL: 2 (0-3)
Renard et al. (2010) [385]	3 centres in France, retrospective	RRMS, PPMS	10 y	84 analysed	1-8: 8% 9-20: 12% ≥20: 80%	⊘	EDSS > 6 Of our 84 included patients: 3 had (1-3) les, 4 (4-9) les and 77 had (³10) les.
Fisniku et al. (2008) [46] *****	London centre-based prospective cohort 1984-1987	CIS	20 y	140 107 analysed	⊘	0.43 cm^3 (median)	EDSS >3 9 of 34 (26%) with 0 les, 8 of 22 (36%) with 1-3 les, 10 of 20 (50%) with 4-9 les, 20 of 31(65%), with ≥10 les. EDSS ≥6 2 of 34 (6%) with 0 les, 4 (18%) of 22 with 1-3 les, 7 (35%) of 20, with 4-9 les, 14 (45%) of 31 with ≥10 les
Chard et al., (2003) [409]	London centre-based (1984-1987)	CIS	14 y	28 analysed	⊘	BL: 1 (0.1-3.7) 5yr FU: 2.8 (0-36.6) 10yr FU: 5.8 (0.6-46.1 14yr FU: 9.4 (1-46.8)	EDSS BL: 2.5 (0-9.5)
Brex et al. (2002) [250]	London centre-based prospective cohort 1984-1987	CIS	14 y	81 71 analysed	⊘	0.43 cm^3 (median)	EDSS >3 0 of 21 (0%) with 0 les, 5 of 18 (28%) with 1-3 les, 7 of 15 (47%), with 4-10 les, 12 of 17 (71%) with >10 lesion. EDSS ≥6 0 of 21 (0%) with 0 les, 2 of 18 (11%) with 1-3 les, 4 of 15 (27%) with 4-10 les, 9 of 17 (53%) with >10 lesion. T2-LV EDSS >3 0 of 21 (0%) with 0 cm^3, 5 of 18 (28%) with 0.6 cm^3, 7 of 15 (47%) with 0.9 cm^3, 12 of 17 (71%) with 5.6 cm^3. EDSS ≥6 0 of 21 (0%) with 0 cm^3, 2 of 18 (11%) with 0.6 cm^3, 4 of 15 (27%) with 0.9 cm^3, 9 of 17 (53%) with 5.6 cm^3.
Sailer et al. (1998) [411]	UCL, London centre-based prospective cohort 1984-1987	CIS	10 y	71 58 analysed	BL: 2.0 (0-74.0) 5y FU: 7.5 (0-103) 10y FU: 10.5 (0-105)	BL: 0.43 (0-13.7) 5 y FU:1.84 (0-36.5) 10 y FU: 3.39 (0-88.6)	EDSS>3 0-5 y= 1.5 (0-8.5) EDSS >3 5-10 y=0.5 (-1.0-5.0) 0-10 y =2 (01-10)

O'Riordan et al. (1998) [410]	UCL, London centre-based prospective cohort 1984-1987	CIS	10 y	129 81 analysed	⃠	⃠	10 y FU EDSS >3 0 of 27 (0%) with 0 les, 0 of 3 (0%) with 1 les 5 of 16 (31%) with 2-3 les, 4 of 15 (27%) with 4-10 les, 14 of 20 (75%) with >10 les. EDSS >5.5 1 of 27 (4%) with 0 les, 0 of 3 (0%) with 1 les, 2 of 16 (13%) with 2-3 les, 3 of 15 (20%) with 4-10 les, 7 of 20 (35%) with >10 les.

** Studies included in the meta-analysis (quantitative). The data are presented as median (range), (mean ±SD) otherwise stated, Y.: years, BL: Baseline, FU: Follow-up, ⃠ not report, les: Lesion, LV: Lesion Volume.*

7.3.5 Baseline MRI Lesions

- ***Ten to Fourteen years***

London 1 cohort showed a moderate correlation between the number of T_2 lesions at baseline and EDSS after a mean of 10 and 14 years of follow-up ($r = 0.54$, $P < 0.001$)[410] ($r = 0.47$, $P < 0.001$)[250] respectively. In the 14-years follow-up cohort, three-time points (5, 10, and 14 years) were studied for both lesion counts and volumes. They followed four MS patients with a normal MRI scan having a median EDSS of 1.75, and 44 MS patients with an abnormal MRI having a median EDSS of 3.5. Additionally, a moderate correlation of newly formed lesions with disability was also reported ($r = 0.59$, $P < 0.001$). For lesion volume, there was a moderate correlation between lesion volume and EDSS at 10 years ($r = 0.48$, $P < 0.001$), while a weak correlation was found in the change of lesion volume over 10–14 years of follow-ups with disability ($r = 0.35$, $P < 0.02$)[250]. Baseline lesion count and volume seem to be larger and increase over time in patients with worse clinical outcomes[250].

- ***Fifteen to Twenty years***

In Fisniku London 1, T_2 lesion volume (baseline, 5, 10, 14, and 20 years) correlated moderately after 20 years of follow-ups ($r = 0.48$ to 0.67, $P < 0.001$). The change in T_2 lesion volume over 10–14 years ($r = 0.40$, $P < 0.004$), over 14–20 years ($r = 0.49$, $P < 0.001$) correlated weakly to moderately with the change in EDSS after 20 years[46]. Only one study reported brain atrophy and gadolinium-enhancing lesions as MRI measurements rather than lesion count and volume [249].

7.3.6 MS Progression

To capture disease conversion, this was only reported in London cohort [46,250,410,411]. Fisniku reported that 28 (42%) patients with MS converted to SPMS 20 years later[46]. There was a significant trend for the development of SPMS to be associated with a higher T_2 lesion volume increase over 20 years than in patients who remained RRMS (P = 0.007), and T_2 lesion volume increase in patients diagnosed with SPMS appeared higher than those with RRMS (P = 0.08)[46]. Results on MRI and mortality were not reported.

7.3.7 Meta-Analysis Results

- ***Lesions Count and Disability in MS patients***

Two centres reported the same cohorts but with different follow-ups, namely London cohort [46,250,401,411,417,418] and Barcelona [247,412]. Thus, for forest plots, we included the study that reported the needed data; London [46], Barcelona [247], and Norway[416]. Renard's [385] cohort was also excluded from the quantitative analysis as all their patients reached EDSS 6. Three studies reported on WML count and EDSS 3 and showed a significant association between the increased WML and higher odds of EDSS 3 (*Figure 7.2A*). After pooling, 4 or more lesions at baseline showed a highly significant association with EDSS 3 (P<0.001) with a pooled OR of 4.10 (95% CI 2.73–6.18). Detection of ten or more lesions had even a higher pooled OR of 4.15 (95% CI 2.89–5.95) and was highly significant (P<0.001) (*Figure 7.2B).* The heterogeneity was very low for both analyses. A diagram illustrates the key elements of the forest plot *(Appendix D.3).*

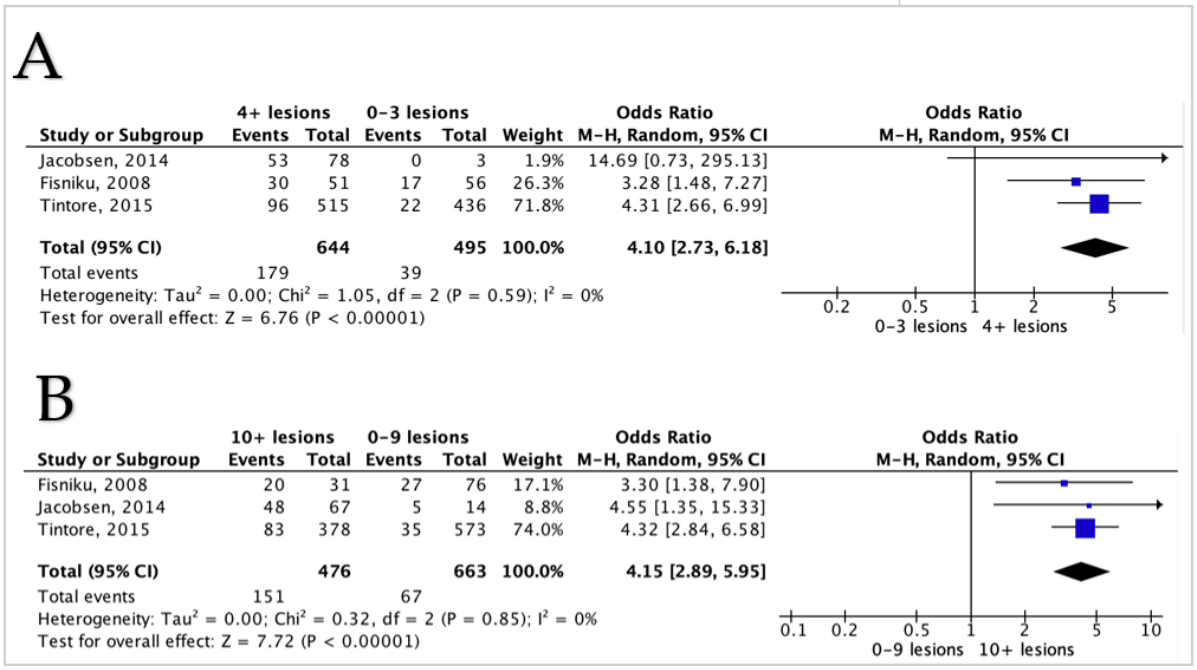

F*igure 7.2.* Forest plot demonstrating the odds of EDSS 3 comparing different lesion counts.
**CI = confidence interval, I^2 = heterogeneity index, df = degree of freedom.*

Three studies reported on WML count and EDSS 6 and all three showed a significant association between the higher number of WML and higher odds of EDSS 6 (*Figure 7.3A).* After pooling, 4 or more lesions at baseline showed a highly significant association with EDSS 6 (P<0.001) with pooled OR of 4.3 (95% CI 1.094–16.89). Detection of ten or more lesions also showed a highly significant association with EDSS 6 (P<0.001) and the pooled OR was 5.54 (95%CI 1.61-19.06) (*Figure 7.3B*). The heterogeneity between studies was moderate to fair (I2 =53%, I2 =47% respectively).

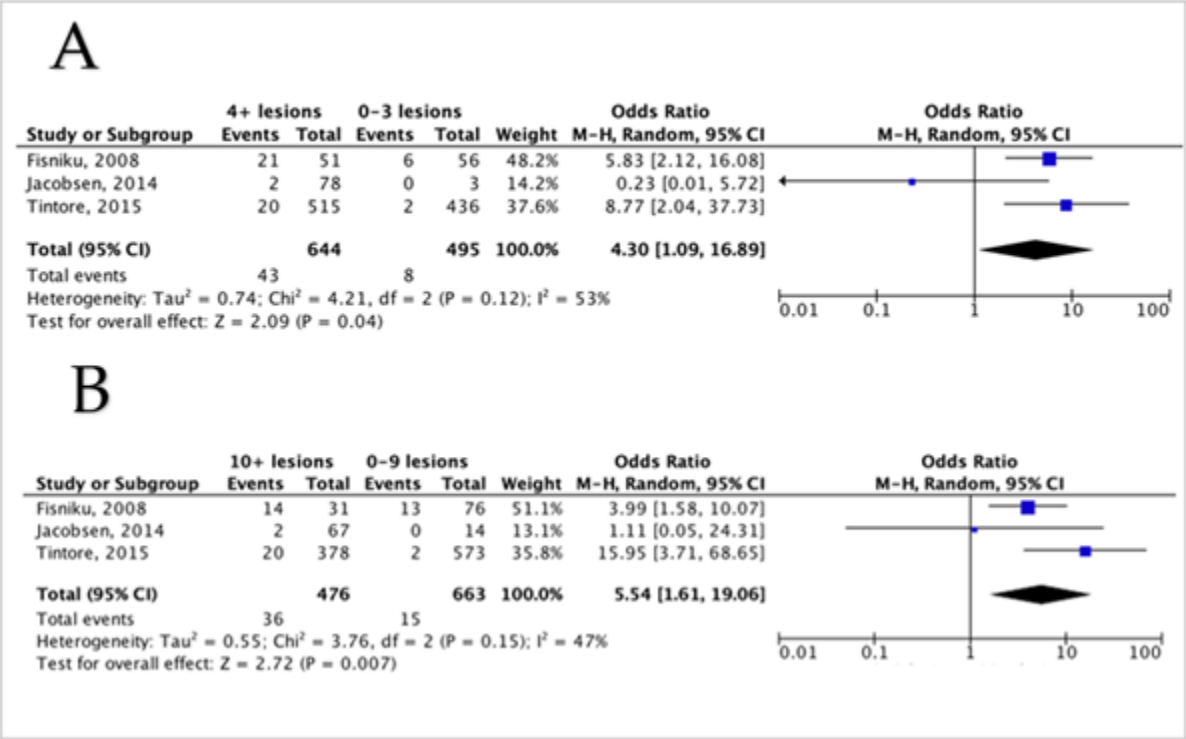

Figure 7.3. Forest plot demonstrating the odds of EDSS 6 comparing between different lesion counts. **CI = confidence interval, I^2 = heterogeneity index, df = degree of freedom***.**

Lesions Volume and Disability in MS Patients

Three studies reported on WML volume and disability; however, due to missing raw data it was impossible to generate forest plots, thus, descriptive analysis was performed. In the Sailer et al. study they found a significant correlation between baseline WML volume and disability at 10 years (r=0.81, P<0.001) but the change in lesion volume during the first 5 years did not show any association with long-term disability [411]. In contrast, Brex and colleagues found that in CIS patients during the first 5 years increases in the lesion volume correlate with the degree of long-term disability[250]. This relation was moderate, so they conclude that the volume of the lesions alone may not be an adequate basis for decisions about the use of DMT. Lastly, in Italy's cohort, EDSS worsening over 10 years was best correlated with the combination of baseline lesion count and increasing lesion volume (R = 0.61, p < 0.001)[386].

Summary of the Results

WML

- **Study Characteristics** → 15 studies for qualitative, 3 studies for quantitative
- **Studies Cohorts** → The mean age of the patients included in the studies ranged from 29-32 years, 67% were female
- **Baseline MRI lesions**
  - **10- 14 years**
    - Moderate correlation was found between the number/ volume of T_2 lesions and EDSS after up to 14 yrs. of FU.
    - Weak correlation was found between the change in lesion volume and EDSS.
  - **15- 20 years**
    - Moderate correlation was found between lesion volume and EDSS after 20 yrs. of FU.
    - Weak to moderate correlations were found between the change in lesion volume and change in EDSS.
- **MS progression**
  - 42% of RRMS patients converted to SPMS 20 years later.
  - T_2 lesion volume is higher in SPMS patient's versus RRMS after 20 years.
- **Meta-Analysis**
  - **Lesion count & Disability**
    - A significant association was found between the increased number of WMLs and higher odds of reaching EDSS 3 and EDSS 6.
    - 4 or more lesions at baseline showed a highly significant association with EDSS 3 and EDSS 6.
    - The detection of 10 or more lesions had higher pooled odd ratio and was highly significant
  - **Lesion volume & Disability**
    - Due to missing raw data, it was impossible to generate forest plots.
    - A significant correlation was found between baseline lesion volume and disability.
    - The change in lesion volume during the first 5 years demonstrated a weak to moderate correlation with long-term disability.

7.4 Discussion

To our knowledge, this is the first systematic review and meta-analysis that assess the prognostic value of MRI for disability in MS. The results illustrate that few studies assessed the prognostic MRI value beyond 10 years in MS patients. Previous work presented some evidence that baseline lesions are associated with EDSS after 10 years[260]. The larger cohort from Barcelona, which was followed up after a median of 6.8 years, showed that the risk of an increase EDSS was higher in patients with 10 or more lesions[247]. The London cohort reported that T_2 lesion volume correlated moderately with EDSS after 20 years[46]. Similarly, 14 years of follow-up showed a correlation between EDSS and lesion count at baseline[250].

These findings are in line with our analysis which showed that both EDSS 3/EDSS 6 showed a strong positive association with the accumulation of WML at baseline. Therefore, it can be concluded that lesion number and volume could be predictors for MS long-term disability. Contrarily, a study of 15 years of follow-up showed no association between baseline MRI lesion count/volume and long-term physical disability[249], still, the conversion to another MS subtype was strongly correlated to baseline MRI. A longitudinal observation study with a longer follow-up period is needed to capture disease conversion, only reported in London cohort[46,250,410,411].

Data were derived from only three different cohorts in Barcelona, London and Norway. A quantitative assessment of these data shows a consistent relationship between early brain lesion loads and subsequent disability. All cohorts were restricted to one city, a fact that might bias the findings and not allow generalization to the other centres.

Lesion segmentation and analysis is a vulnerable process, as it depends potentially on the rater's experience, software used, criteria of lesion selection, and image quality. Thus, having a

harmonized and standard procedure for lesion segmentation such as the state of art automatic segmentation tool (e.g. HyperMapper) [419] could be beneficial for future studies.

Around 70% of the study population of the included studies in this review were females with a mean age of 30. These population is inline with the epidemiology of early MS [23,24].

Two studies reported that spinal cord lesions (≥ 1 lesion) could predict disability in patients converting to MS[131,247]. However, recent findings highlighted the uncertainty of the prognostic and diagnostic value of spinal cord lesions[420]. Further work is needed to clarify the independent and interaction impact of brain and upper cervical cord atrophy as promising prognostic markers[421].

Although higher brain lesion load could link with long-term disability, the correlation between early lesion loads and later disability still only explains a small proportion of disabilities. It is also difficult in clinical practice to utilise a certain threshold of disability and disease progression milestones.

7.5 Limitations

There were several limitations to the data that we could access for our review. Relatively few of the included studies were conducted prospectively, such that the others were potentially vulnerable to various biases due to their retrospective design. In addition, the primary study aims varied considerably, and this could contribute to differences in the observed lesion counts and volume. Treatment information was not available in the publications. Therefore, the potential differential treatment effect on the disability outcome could not be assessed. Few studies were included in the meta-analysis, this could cause a publication bias and only positive findings were published. Additionally, measuring and defining disability is subjective, and EDSS is prone to

human-error. Lastly, it should be emphasised that subgroup and meta-analysis are by their nature observational, and results must therefore be interpreted with caution.

7.6 Conclusion

This systematic and meta-analysis have confirmed that the number or the volume of WML detected with MRI has the potential to be a prognostic imaging marker for long-term disability. Nevertheless, there is considerable heterogeneity in their assessment, detection, and reporting across studies. While the meta-analysis presented here highlights their potential of playing a prognostic role in MS, patient and lesion levels may limit sensitivity for initial diagnosis. We believe there is a need to establish clear criteria for evaluating and reporting WML, which would improve the interpretation and comparison of data acquired across studies. Such criteria would thus allow validation and potential translation of this imaging marker into future clinical practice. Further work with longer clinical follow-up is required to determine whether lesion count, volume, and regional brain atrophy can be used as predictive imaging biomarkers in MS.

Chapter 8 . Predictors of Long-term Disability in Multiple Sclerosis Patients Using Routine MRI data: a 15-year retrospective study

Abstract

Introduction: Early identification of patients at high risk of progression could help with a personalised treatment strategy. MRI measures have been proposed to predict long-term disability in MS, especially the accumulation of WMLs in the first 5 years of the disease, but a reliable predictor that can be easily implemented clinically is still needed.

Aim: Assess MRI measures during the first 5 years of the MS disease course for the ability to predict progression at 10+ years.

Methods: Eighty-two MS patients (53 females), with ≥10 years of clinical follow-up and having two MRI scans, were included. Clinical data were obtained at baseline, follow-up and at ≥10 years. WML counts and volumes, and four linear brain sizes were measured on T_2/FLAIR and T_1-weighted images.

Results: Baseline and follow-up inter-caudate-diameter (ICD) and third ventricular width (TVW) measures correlated positively with EDSS ≥10 years. A steeper rate of lesion volume increase was observed in subjects converting to secondary progressive MS. The sensitivity and specificity of both ICD and TVW, to predict disability at ≥10 years were 60% and 64% respectively.

Conclusion: Despite advances in brain imaging and computerised volumetric analysis, ICD and TVW remain relevant as they are simple, fast and have the potential in predicting long-term disability. However, in this study, despite the statistical significance of these measures, the clinical utility is still not reliable.

8.1 Introduction

MS is a chronic inflammatory, demyelinating and neurodegenerative disease of the CNS[422]. The early identification of MS high -risk patients with a greater disability is crucial and it would be effective for determining an early personalised treatment strategy. Studies have shown that more than half of MS patients are likely to develop a significant disability after 15-30 years[287,401,412], however, some cohorts showed that many maintained a mild disease state.

In a largely untreated cohort of people with CIS, it has been found that up to 42% of patients remained fully ambulatory (EDSS ≤3.5) 30 years later, while 58% developed disability and may have benefitted from early treatments[401]. It has also been reported that patients who accumulated lesions over the first five years of their disease were more likely to develop SPMS 20 years later [401], especially when 10 or more lesions are present at the baseline scan [412]. It is therefore important to examine if there is an easily applicable measurement that could predict long-term disability in an era the DMTs have been used [423]. EDSS 4 and EDSS 6 are routinely used as disease progression cut-offs because EDSS 4 is the first point in the scale at which walking is limited/restricted, and EDSS 6 is the first point at which unilateral walking aids are required [247,412].

Despite advances in brain imaging and computerised volumetric analysis, manual brain measurements of the lesions and linear measures of brain atrophy remain relevant as they are simple, fast, and can be performed on non-digitised data. In addition, for brain atrophy measures, linear two-dimensional methods do not require extensive training or expensive and time-intensive computer software necessary for complex quantitative and volumetric analyses. Furthermore, imaging protocols do not always include three-dimensional brain imaging (required for voxel-based morphometry) due to time constraints while two-dimensional scans have shorter acquisition

times and are easily available. For these reasons, simple linear measurements are applicable to clinical practice, especially in regions with no access to advanced imaging technology.

Different MRI predictors of MS disability which can be easily implemented in clinics have been proposed [10,251,424,425]. To date, these predictors have not been approved to be implemented in clinical practice. Predictors These include WMLs accumulation and linear measurements of brain atrophy[15,195,250,426,427]. Amongst the many proposed linear measures of brain atrophy, the most widely reported are Third Ventricular Width (TVW) [286,287], Medullary Width (MEDW) [287], Corpus Callosum Index (CCI)[289] and Inter-Caudate Distance (ICD)[286]. These measurements are established and practical techniques that correlate with long-term disability in MS [286,428,429]. However, the reliability and strength to use these measures in clinics are yet to be confirmed in clinical MS cohort.

This study aims to assess the role and reliability of measures, that can feasibly be implemented within a clinical setting in the first 5 years of the disease, for predicting long-term (>10 years) outcomes. This assessment is needed to facilitate and implement reliable and practical MRI metrics in clinics.

8.2 Material and Methods

8.2.1 Patient Selection

This is a retrospective study from the MS clinic database at the Queen's Medical Centre in Nottingham. In this study, data collected up to January 2021 were included. A total number of 3801 patients with different MS subtypes were registered with the clinic with the date of disease onset $\leq$ 2011.

Inclusion criteria were (1) baseline brain MRI scan in 2011 or earlier (2) follow-up scan acquired between 4-6 years from the baseline scan (3) both sets of scans had a T_2-FLAIR and T_1 sequences of brain MRI (4) patients with a confirmed diagnosis of MS on the McDonald criteria 2010 (5) consented to have their MRI and clinical data used for research purposes.

Exclusion criteria were (1) PPMS due to the different nature of the disease (2) more than one year between the disease onset and 1st MRI scan (3) MRI scans with bad quality images or (4) scans with missing required images.

Patients' demographic data were captured at baseline and follow-up MRI, and clinical data were extracted from the clinical notes. Data include age, sex, date of MS onset, date of MS diagnosis, MS subtypes, EDSS, date of reached EDSS 4 and 6 if applicable and details of DMTs used. The number and volume of T2-FlAIR lesions at baseline and follow-up scans were measured by a researcher blind to their clinical characteristics.

Disability was evaluated according to the EDSS at three times; baseline, follow-up (4-6 years interval), and last visit (≥10 years). Disability milestones were defined as reaching an EDSS score ≥ 4.0 or 6.0, respectively, in addition to disease conversion to SPMS. A confirmed diagnosis of SPMS was defined by steady progression rather than relapse as the major cause of increasing disability in the preceding 2 years; and evidence of progression-either an increase of at least one point in EDSS or clinical documentation of increasing disability in patient notes. The follow-up duration was computed as the time between the date of the disease onset and the date of the most recent last visit.

We divided treatments into high-efficacy treatments (HET): Tysabri (natalizumab), Lemtrada (alemtuzumab, Campath), Ocrevus (ocrelizumab); and non-HET: beta-Interferons, Copaxone (glatiramer acetate), Aubagio (teriflunomide), Tecfidera (dimethyl fumarate), Gilenya (Fingolimod), Mavenclad (Cladribine)[379].

8.2.2 MRI Protocol

Clinical brain MRI scans were performed as part of the service provided at the MS clinic at the Queen's Medical Centre using 1.5T and 3T MRI. These scans included sagittal T_2-FLAIR and T_1-weighted spin-echo. All the sequences were obtained using a contiguous 3-5 mm slice thickness covering the whole brain. Having a normal brain MRI scan was not an exclusion criterion, since patients were included based solely on their clinical diagnosis (i.e., patients with normal baseline brain scans were included).

8.2.3 Image Analysis

- ***Lesion Count and Volume***

All measurements were performed using 3D slicer version 4.13.0 (http://www.slicer.org)[430]. Inter-rater and intra-rater reliability statistics were provided in *Appendix E.1*. Lesions with long axis diameter ≥ 3mm were included in line with MRI in MS diagnostic criteria[218]. The total number and volume of WML for each scan were calculated. The level tracing segmentation tool on a 3D slicer was used to trace around each lesion on the scan, then computed into a volume measured in cm^3. Volumes were added together to produce a total lesion volume measurement for each scan. Annualised change in total lesion volume was calculated between the first and follow-up scans to adjust for the differences in length of time between the two scans [431].

- ***Atrophy***

Four linear measures were used: TVW [286,287], MEDW [287], CCI [289] and ICD [286]. TVW was measured as the width of the third ventricle at the midpoint of a line running parallel to the long axis of the ventricle on axial T_2-weighted MRI scans. MEDW was measured as the dorsoventral diameter of the medulla on a mid-sagittal image. The level of medullary measurement was determined by the craniocaudal pontine length mirrored caudally from the inferior pontine notch. CCI was obtained on a conventional best mid-sagittal FLAIR image, by manually drawing a straight line at the greatest anteroposterior diameter of CCI and a perpendicular at its midline. Anterior, posterior, and medium segments of CCI were measured and normalized to their greatest anteroposterior diameter. ICD was measured on axial T1-weighted when the frontal horn reached the maximum width. ICD width is the minimum distance between the medial borders of the head of the caudate nuclei [286,300]. All measurements were explained in-depth in (*Appendix E.2*).

8.2.4 Statistical Analysis

Shapiro tests and visual inspection of histograms were used to assess the normal distribution of the variables. Spearman's correlation coefficient was used to assess the relationship between EDSS at ≥10 years/change in EDSS and the six brain MRI metrics (lesion count, lesion volume, TVW, CCI, ICD, MEDW) at baseline, follow-up and changes in MRI parameters were computed as an annualized measure (e.g., CCI change/y).

To assess the extent to which MRI brain metrics can be used to predict worsening disability over 10 years, we performed an ordinal regression analysis, as EDSS is an ordinal categorical variable with a scale from 0 to 10. The EDSS scores at ≥10 years were set as the dependent variable while MRI predictors (lesion count, lesion volume, TVW, CCI, ICD, MEDW) at baseline or follow-up were set as the independent variables, including a factor variable with three levels (HET,

non-HET and untreated) in the model. The Wilcoxon test was used to compare EDSS and MRI predictors between baseline, follow-up, and yearly change.

For the binary logistic regression, the EDSS models were EDSS≥ 4 or ≥6 (dependent variables), while MRI predictors (lesion count, lesion volume, TVW, CCI, ICD, MEDW) at baseline or follow-up were set as the independent variable, including a factor variable with three levels (HET, non-HET and untreated) in the model. We calculated the sensitivity and specificity of different cut-offs of T_2 lesions count. Inter and intra-rater errors were assessed in a sample of 10 randomly chosen scans. A brief descriptive statistics were also highlighted to show the differences between patients who converted to SPMS and to those who remained RRMS. Statistical analysis was undertaken with *Jamovi* (Version 1.6), and statistical significance was reported at $P<0.05$. The statisticians (A.V. and P.M)[5] provided a statistical guidance throughout this chapter.

8.3 Results

8.3.1 Patients' characteristics.

Of the 3801 MS patients that were recorded, 82 RRMS patients were included based on the inclusion criteria (*Figure 8.1)*. MRI brain scans of the 82 patients were 29 male and 53 female, with a mean age (± SD) of 35.4 (± 10.3) years.

The mean clinical follow-up was 12.1 (± 1.31) years, and the mean time between scans was 5.33 (± 1) years. The baseline MRI scan was acquired with a median of 3 months (IQR 6)

[5]A.V.: Andrea Venn (PhD), School of Medicine, University of Nottingham, Nottingham, UK.

P.B.: Paul Bassett (MSc), Statsconsultancy Ltd, Hamel Hampstead, UK.

after disease onset. A wide range of physical disabilities encompassing all levels of the EDSS was seen across the cohort (*Figure 8.2*). EDSS worsened from a mean of 1.95 (± 1.59) at baseline to 4.48 (± 2.17) after 10 years (P<0.001). Out of 82 patients, 70 remained RRMS and 12 progressed to SPMS. During the follow-up, 51 RRMS patients reached EDSS 4 at the last visit while 31 patients reached EDSS 6. Two RRMS patients deceased and only one due to MS.

Table 8.1 illustrates the characteristics of this cohort. The median time from the disease onset to DMTs initiation was 36 months (IQR 59.5). In terms of treatment, 23 patients received HET, 44 received non-HET, and 15 patients were untreated. From the 67 treated patients, the mean duration of treatment was 90.6 months (SD 45.3) with a range of (2–168). On average, patients were treated with DMTs in 61% of their disease duration. The follow-up scan was requested as a standard procedure in 41 patients, or with new or worsening symptoms in 48 patients. Treatment with different levels of DMTs did not appear to contribute significantly to any of the models and thus were removed from the model.

The numbers of slices and slice thickness were variable, both between patients and between the first and second scans. Of the 164 scans analysed (first and follow-up MRIs), the number of slices ranged from 15 to 60 and slice thickness ranged from 3 to 5 mm. The mean number of slices was 26.7 (± 5.94) and the mean slice thickness was 3.91 mm (± 0.76).

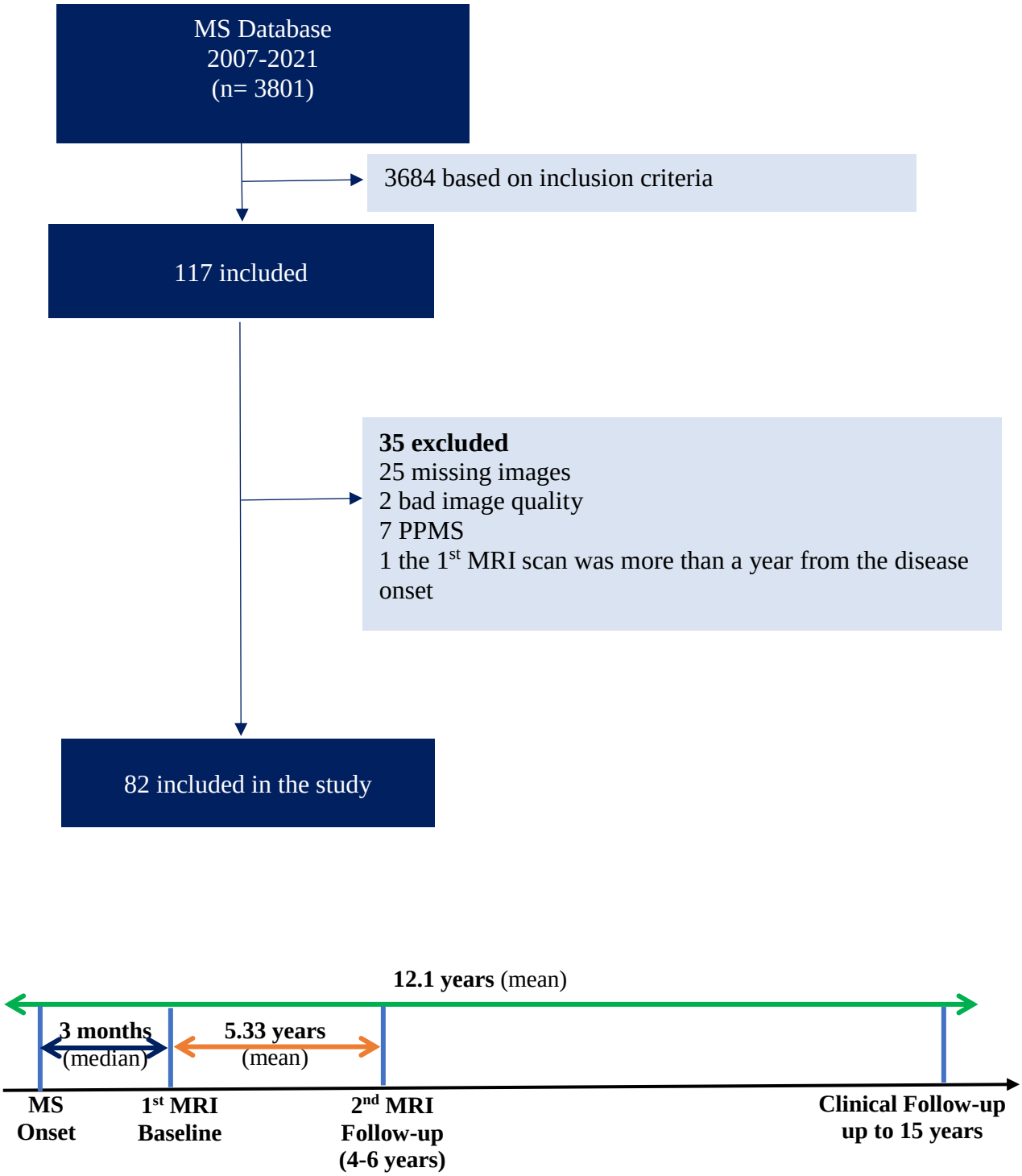

Figure 8.1. Flowchart illustrates the process of patient selection, and the timeline of the study.

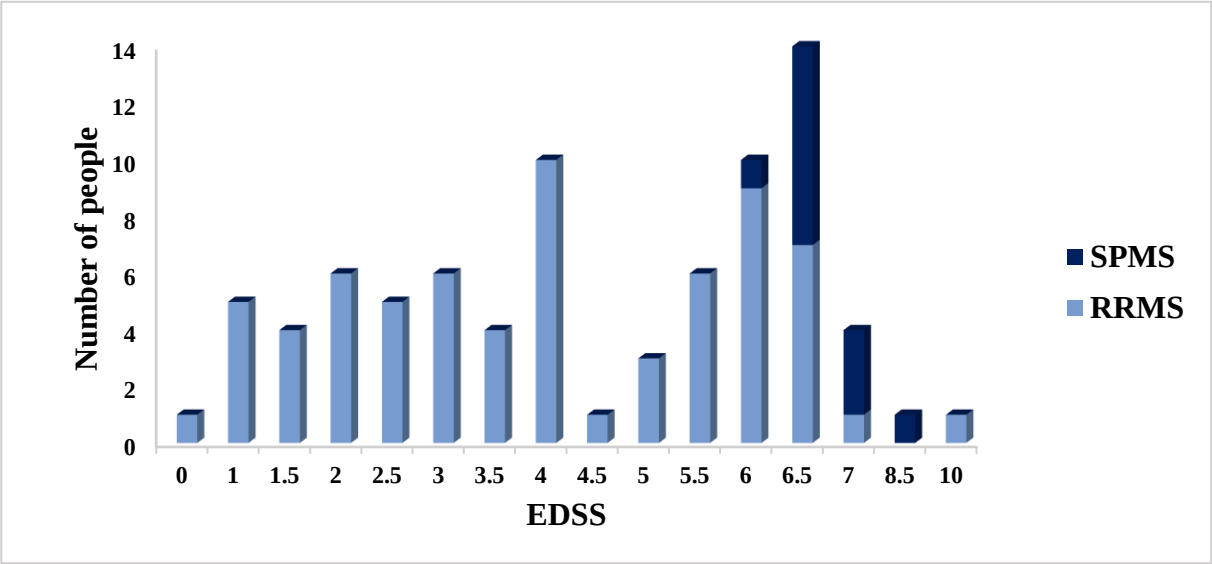

Figure 8.2. Expanding Disability status scale (EDSS) scores after more than 10 years of follow up. EDSS were obtained from 82 patients at the last visit >10 years. An EDSS of 10 was assigned to those where Multiple sclerosis (MS) was known to contribute to death.

**RRMS: Relapsing remitting multiple sclerosis; SPMS: Secondary progressive multiple sclerosis*

Table 8.1. Demographic characteristics, clinical classification, and data availability at each follow-up time point.

Characteristic	Baseline (n=82)	Follow-up MRI (n=82)	Last visit (n=82)
Female sex, n (%)	53 (64.6%)	53 (64.6%)	53 (64.6%)
Age, Mean (SD)	35.4 (10.3)	40.8 (10.2)	47.5 (10.1)
EDSS	1.5 (0-7)	3.25 (1-7.5)	4.25 (0-10)
Number DMT treated, n (%)	0	51 (62.1%)	72 (87.0%)
Onset of Treatment	-	2011 (2006-2016)	-
T_2 hyperintense lesion count	15.0 (0-58)	25.0 (2-99)	-
Total lesion volume (cm^3)	2.44 (0 – 26.7)	4.44 (0.6 -31.4)	-
Third Ventricle Width(mm)	2.79 (1.27-7.31)	3.58 (1.69-8.85)	-
Corpus Callosum Index (mm)	0.39 (0.23-0.48)	0.36 (0.20-0.44)	-
Medulla Width (mm)	8.19 (5.77-12.4)	7.72 (5.77-11.9)	-
Inter- Caudate Distance (mm)	13.5 (7.08-22.4)	15.2 (8.65-26.8)	-
Clinical follow-up (Mean)**:** 12.1 years (10-15)		**Time between scans**(Mean)**::** 5.33 years (3.25-7.92)	

All data are presented as medians and ranges, unless otherwise stated; EDSS: Expanded Disability Severity Status Scale, DMT: disease-modifying treatment

8.3.2 Baseline Brain MRI and new lesions

Only one patient did not have T_2 lesions at the baseline MRI scan; 30 % had between 1– 9 T_2 WML, and 68 % had more than 10 T_2 WML. Three patients did not develop any new lesions over the period of observation. The new lesions and the yearly change in lesion counts are illustrated in *Table 8.2*.

Table 8.2. New lesions and the change rate in lesions on the follow-up MRI scan

New lesions in the follow-up scan (4-6 years)	Number of patients
0 - 3	25
4 - 6	18
7 - 9	10
10 - 13	10
14 - 16	4
17 - 20	4
> 21	14
Fewer lesions	4
The rate change in lesion count/year	Number of patients (%)
<1	39 (47.6%)
1 - <2	16 (19.5%)
2 - <3	8 (9.8%)
3 - <4	5 (6.1%)
4 - <5	4 (4.9%)
5 - <6	4 (4.9%)
6 - <7	1 (1.2%)
7 -<8	3 (3.7%)
8 - <9	0
9 - <10	1 (1.2%)
10 - <11	0
11 - <12	1 (1.2%)

8.3.3 MRI predictors and long-term physical disability

- ***Correlations between MRI predictors and clinical disability***

No correlations were found between WML counts or volumes and clinical disability at both baseline and follow-up. Alternatively, some linear brain measurements showed a positive correlation with EDSS at the last visit. This included ICD (r=0.25, r=0.27, P<0.01 at baseline and follow-up) and TVW (r=0.28, r=0.24, P<0.01 at baseline and follow-up).

All correlations of MRI metrics with clinical disability are listed in *Table 8.3*. Considering the correlation between changes in EDSS from the follow-up scan, and the yearly change in MRI predictors, over the first 5 years, it was only significant in the case of CCI, but with weak, positive correlations (r=0.31, r= 0.30, P<0.01).

Table 8.3. Correlations between MRI predictors and disease severity (EDSS).

EDSS last visit	Spearman's (95% CI)	P-value
T_2 Lesion		
BL lesion count FU lesion count Change rate in lesion count	r_s= 0.30, (-0.18-0.24) r_s= 0.06, (-0.15-0.27) r_s=0.10, (-0.12-0.34)	P=0.78 P=0.57 P = 0.35
BL total lesion volume FU total lesion volume Change rate in total lesion volume	r_s=0.56, (-0.16-0.27) r_s= 0.07, (-0.15-0.30) r_s= 0.03, (-0.18-0.26)	P =0.61 P=0.49 P=0.73

Linear Measures of Brain Atrophy		
BL CCI FU CCI Change rate in CCI	r_s= -0.07, (-0.28-0.12) r_s= -0.01, (-0.23-0.19) r_s=0.12, (-0.11-0.34)	P=0.49 P=0.90 P=0.26
BL MEDW FU MEDW Change rate in MEDW	r_s=0.13, (-0.21-0.24) r_s= 0.02, (-0.33-0.11) r_s= -0.05, (-0.12-0.32)	P= 0.21 P =0.84 P=0.58
BL ICD FU ICD Change rate in ICD	r_s= 0.21, (0.05-0.49) r_s=0.28, (0.02-0.47) r_s= 0.25, (-0.17-0.29)	P=0.04* P<0.01* P=0.14
BL TVW FU TVW Change rate in TVW	r_s=0.29, (0.08-0.49) r_s=0.19, (-0.14-0.40) r_s= 0.15, (-0.05-0.37)	P<0.01* P<0.01* P=0.16
Change in EDSS (from 1st MRI to the last visit)	**Spearman's (95% CI)**	**P-value**
T_2 Lesion		
BL lesion count FU lesion count Change rate in lesion count	r_s= -0.10, (-0.32-0.09) r_s= 0.03, (-0.26-0.17) r_s=0.17, (-0.13-0.34)	P=0.36 P=0.72 P = 0.10
BL total lesion volume FU total lesion volume Change rate in total lesion volume	r_s=-0.13, (-0.28-0.15) r_s= -0.12, (-0.24-0.23) r_s= 0.01, (-0.22-0.28)	P = 0.23 P=0.25 P=0.89
Linear Measures of Brain Atrophy		
BL CCI FU CCI Change rate in CCI	r_s= -0.10, (-0.04-0.33) r_s=0.31, (0.10- 0.49) r_s=0.30, (0.09-0.48)	P=0.36 P<0.01* P<0.01*
BL MEDW FU MEDW Change rate in MEDW	r_s=-0.06, (-0.18-0.24) r_s=-0.08, (-0.29-0.14) r_s=-0.001, (-0.15-0.30)	P= 0.54 P =0.45 P=0.99
BL ICD FU ICD Change rate in ICD	r_s=0.09, (-0.03-0.38) r_s=0.13, (-0.55-0.37) r_s=0.11, (-0.19-0.26)	P=0.38 P=0.21 P=0.31
BL TVW FU TVW Change rate in TVW	r_s=-0.007, (-0.16-0.24) r_s=-0.02, (-0.19-0.23) r_s-0.03, (-0.19-0.24)	P=0.94 P=0.85 P=0.77

*BL: Baseline, FU: Follow up, EDSS: Expanded Disability Status Score, CCI: Corpus Callosum Index, MEDW: Medulla Width, ICD: Inter-Caudate Distance, TVW: Third Ventricular Width. * Significance at P-value of <0.05.*

8.3.4 T_2 Lesions and Brain changes

The lesion count at the follow-up scan was greater than baseline (median of 25 versus 15 lesions), with an annual rate of new lesions of 1.11 lesion/year. Similarly, the lesion volume was greater in the follow-up scan (median 1.48 versus 1.44 cm^3), with an annual lesion growth rate of 0.16 cm^3/year. Only 3 patients; 2 RRMS, and 1 SPMS did not have any new lesions, they had fewer visible lesions at the follow-up scan by 1 to 4 lesions.

Patients who remained RRMS or progressed to SPMS at the end of the observational period had similar medians of the baseline T_2 lesion volumes see *table 8.4.* However, observing the pattern of median T_2 lesion volume during the follow-up scan showed a steeper rate of lesion volume increase in SPMS compared to RRMS over the first 4 – 6 years of the disease.

Table 8.4. White matter lesions counts and volume in relapsing-remitting and secondary-progressive MS patients.

MS subtypes	Baseline		Yearly change		Follow-up	
	Number	**Volume**	**Number**	**Volume**	**Number**	**Volume**
Remained RRMS	16 (0-58)	2.44 (0-26.7)	1.06 (0-11.8)	0.15 (-6.38-9.63)	25.5 (2-99)	4.47 (0.60-31.4)
Converted to SPMS	13 (3-48)	2.34 (0.17-24)	1.22 (0.14 -9.71)	0.23 (-1.35 1.10)	24 (6-58)	4.44 (0.65 -25.8)

All data presented as medians and ranges RRMS: Relapsing-Remitting Multiple Sclerosis, SPMS: Secondary Progressive Multiple Sclerosis.

For the total population, baseline and follow-up brain linear measurements showed that MEDW and CCI had a greater median at baseline, while ICD and TVW had a greater median at the follow-up (*Table 8.1*). The medians of the yearly change of the four linear measurements of brain atrophy were as follows: TVW (3.12 mm/year), ICD (0.35 mm/year), MEDW (0.13 mm/year) and CCI (-0.005 mm/year).

8.3.5 EDSS at last visit (≥10 years)

The results from the ordinal regression showed that TVW and ICD at both baseline and follow-up could predict the long-term disability (EDSS ≥10 years). An increase of 1 unit at these MRI measurements whether at baseline or follow-up would increase one scale on EDSS at ≥10 years. All predictors are illustrated in the *Table 8.5.*

Table 8.5. *Ordinal regression for the MRI predictors of EDSS ≥10 years*

Predictors	Odd ratio	95% CI	P-value
BL lesion count	1.01	(0.98-1.04)	0.40
FU lesion count	1.01	(0.98-1.03)	0.37
BL lesion volume	1.04	(0.97-1.12)	0.24
FU lesion volume	1.03	(0.96-1.10)	0.45
BL CCI	0.01	(5.08e-6 -77.7)	0.34
FU CCI	0.28	(8.29e-5-1010)	0.76
BL Medulla	1.01	(0.73-1.40)	0.95
FU Medulla	0.89	(0.62-1.28)	0.56
BL ICD	1.18	(1.03-1.36)	0.01*
FU ICD	1.14	(1.02-1.28)	0.02*
BL TVW	1.48	(1.11-2.00)	<0.001**
FU TVW	1.29	(1.02-1.63)	0.03*

*BL: Baseline, FU: Follow-up, EDSS: Expanded Disability Status Score, CCI: Corpus Callosum Index, MEDW: Medulla Width, ICD: Inter-Caudate Distance, TVW: Third Ventricular Width. * Significance at P-value of <0.05.*

8.3.6 EDSS of 4.0 and 6.0 at 10 years

It seems irrespective of the baseline lesions, the same proportion of patients reached EDSS 4 whereas a higher proportion of patients needed a stick to walk (EDSS 6) if they have more lesions at baseline, see *Table 8.6*.

Table 8.6. Baseline MRI lesion number and clinical status at ≥10 years.

White matter lesion number	0-3 (n= 13)	4-9 (n=13)	10+ (n=56)
EDSS ≥4	8 (61.5%)	8 (61.5%)	35 (62.5%)
EDSS ≥ 6	3 (23.0%)	4 (30.7%)	24 (42.8%)

Similar to the ordinal regression findings, the binary logistic regression also showed that TVW at baseline could predict EDSS≥4 and EDSS≥6 after 10 years (*Table 8.7*). For EDSS ≥ 6, TVW at baseline/follow-up and ICD at baseline were significant predictors of disability while TVW at baseline was the only predictor for EDSS ≥4. In other words, the odds of TVW at follow-up was 0.75 higher with patients with EDSS ≥6.

Table 8.7. Binary logistic regression for the MRI predictors and EDSS≥4 or EDSS≥6

Predictors	Odd ratio	95% CI	P-value
	EDSS≥4		
BL lesion count	0.98	(0.95-1.02)	0.39
FU lesion count	0.99	(0.96-1.02)	0.60
BL lesion volume	0.92	(0.81-1.02)	0.16
FU lesion volume	0.96	(0.88-1.05)	0.35
BL CCI	12.98	(4.6e-4-361645.2)	0.62
FU CCI	3.97	(0.0-499510.6)	0.85
BL Medulla	0.84	(1.25e-4-46171.8)	0.86
FU Medulla	2.40	(0.53-1.20)	0.27
BL ICD	0.89	(0.76-1.05)	0.16
FU ICD	0.95	(0.84-1.08)	0.48
BL TVW	0.67	(0.45-1.01)	0.05*
FU TVW	0.90	(0.68-1.18)	0.44
	EDSS≥6		
BL lesion count	0.97	(0.94-1.01)	0.13
FU lesion count	0.98	(0.96-1.01)	0.33
BL lesion volume	0.92	(0.83-1.02)	0.10
FU lesion volume	0.95	(0.88-1.03)	0.24
BL CCI	7963.91	(0.27-2.32e+8)	0.08
FU CCI	1165.00	0.06-2.15e+7)	0.15
BL Medulla	1.02	(0.71-1.46)	0.90
FU Medulla	0.95	(0.65-1.41)	0.82
BL ICD	0.86	(0.73-1.00)	0.05*
FU ICD	0.90	(0.79-1.02)	0.09
BL TVW	0.57	(0.38-0.84)	0.005**
FU TVW	0.75	(0.58-0.99)	0.04*

*BL: Baseline, FU: Follow-up, EDSS: Expanded Disability Status Score, CCI: Corpus Callosum index, MEDW: Medulla Width, ICD: Inter-Caudate Distance, TVW: Third Ventricular Width. * Significance at P-value of <0.05.*

8.3.7 Aggressive MS: EDSS of 6.0 at 10 years

There is no consensus on the definition of aggressive MS, however, as stated in the introduction the majority of previous studies set EDSS ≥6 as a millstone of aggressiveness and disease progression [247,412]. The risk of having aggressive MS in the group of more than 10 lesions at baseline was 18% higher compared to patients with less than 10 lesions and this difference was highly statistically significant (P=0.004). Furthermore, the median (IQR) number of baseline T2 lesions was 18 (0-58) in the aggressive group compared to 15 (1-38) in the non-aggressive group (*Figure 8.3*). In addition, the area under the curve was 0.60 (95% CI 0.48 – 0.72) which means poor prediction; the best cut point was 4 lesions at baseline with a high sensitivity of 88% but low specificity of 20% in predicting disability by reaching EDSS 6. A cut-point of ten lesions had better specificity of 43% but sensitivity was reduced to 74%.

A cut-point of 0.46 mm/year had the highest specificity of ~ 64% and sensitivity of ~ 60% for both ICD and TVW to predict the development of EDSS 6 with an accuracy of 62% and AUC was 0.70 (95% CI 0.16 – 0.94) which are considered as acceptable predictors.

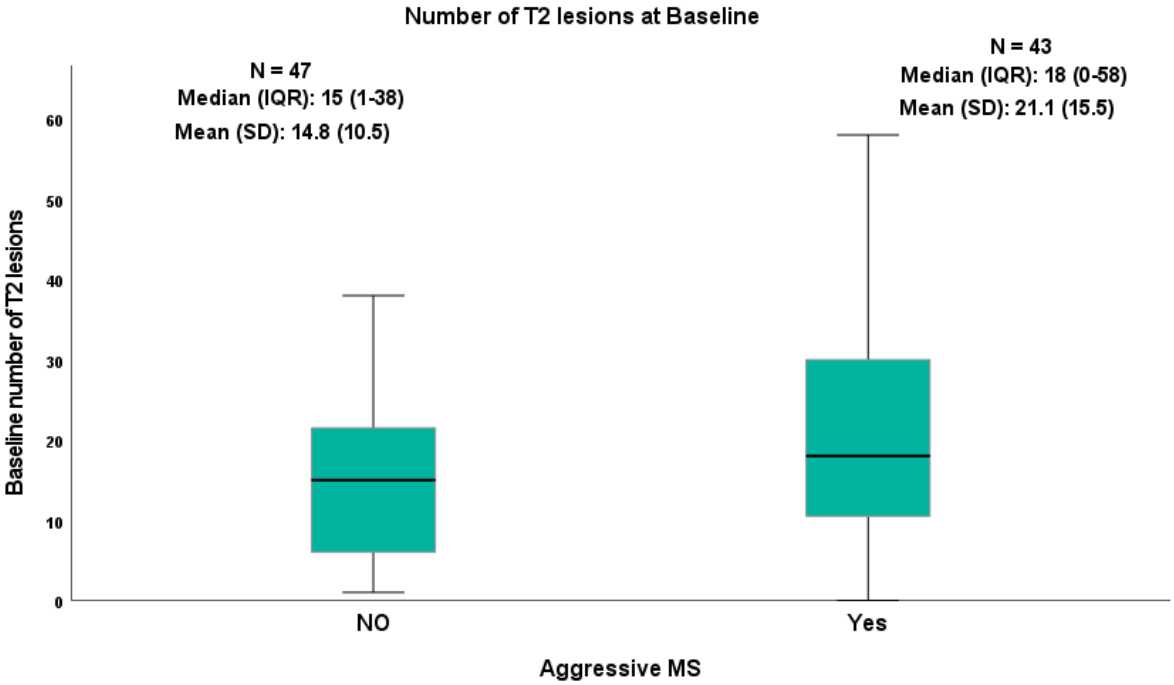

Figure 8.3. Number of T_2 lesions at baseline in two MS groups, aggressive MS patients who reached EDSS ≥6 and EDSS<6

Summary of the Result

1 Descriptive Analysis

- 82 RRMS (29 male, 53 female)
- Mean clinical FU: 12.1 years (± 1.31), Mean time between scans: 5.33 (± 1)
- EDSS worsened from mean 1.95 (SD 1.59) at BL to 4.48 (SD 2.17) after 10 yrs.
- •Median time from the disease onset to drug prescription was 36 months
  •23 patients had HET, 44 non-HET and 15 patients were untreated.
  •Mean of the overall treatment duration in months was 90.6 months
- 1-9 WMLs in 30% of the patients, ≥10 WMLs in 68% of the patients

2 Quantitative Analysis

Correlation (Pearson's)

- Lesion count / Volume
  - •No significant correlation was found btw lesions count/volume and EDSS
  - •Weak correlation was found btw ICD/TVW at BL&FU with EDSS at last visit.
  - •No significant correlation was found in CCI nor MEDW at BL&FU with EDSS at last visit.
- Atrophy
  - •Weak correlation was found btw the changes in EDSS and yearly change in CCI over the first 5 years.

Wilcoxon

- Lesion count / Volume
  - •Lesion count/volume in FU scan had a greater median than BL
  - •Annualized rate of new lesions (1.11 lesion/year)
  - •Annualized lesion growth rate of (0.16 mm^3/year)
  - •Only 3 patients had fewer lesions at the FU scan
- Atrophy
  - •The medians of the yearly change were; TVW (3.12 mm/y), ICD (0.35 mm/y), MEDW (0.13 mm/y), CC (-0.005 mm/y).

Ordinal/Binary Regression

- Lesion count / Volume
  - No associations were found between WML count /volume and predicting disability (10yrs EDSS).
- Atrophy
  - TVW and ICD both BL/FU had sig. associations with long-term disability

EDSS 4 / EDSS 6

- •The risk of disability was 18% higher in patients with at least 10 BL lesions vs less than 10.
- •A cut point of 10 WML had a specificity of 43% but sensitivity of 74%.
- •A cut point of 0.46 mm/year had a specificity and sensitivity of both ICD and TVW 64% – 60% respectively.

8.4 Discussion

This study assesses the role and reliability of different MRI measures during the first 5 years of the disease, which can be easily used in routine clinics and could reliably predict MS disability. The current study demonstrated that linear brain atrophy metrics related to ICD and TVW have an independent impact in predicting disability after 10 years, whereas WML counts or volumes showed no association with clinical disability.

More than 37% of our patients developed an aggressive MS (reaching an EDSS of 6 or more at 10 years). It is important to note that in patients with an aggressive phenotype, the baseline characteristics such as age and sex did not contribute to identifying patients at risk.

Contrary to previous findings [15,46,195], in our study, the counts and volume of WMLs were not associated with disability either at baseline or during the follow-up period. This could be due to the small sample size compared to other studies. Having said that, the correlation coefficient (R-value) was smaller compared to other studies and that should not be affected by study size.

It is more likely that our results are due to the patients included, which had definite MS, rather CIS and by definition a more active disease with different lesions evolution characteristics. A recent study included 548 placebo-treated RRMS patients, the multivariable analysis indicated EDSS score and T_2 lesion load as factors that independently predict clinical progression. Nonetheless, these two variables taken together were able to account for only 3% of the probability to have an EDSS increase over follow-up time. Thus, confirming the limited value of these metrics in predicting disability changes in RRMS [432]. Such a finding is in line with previous cross-sectional and longitudinal studies conducted on a smaller group of patients with different clinical characteristics, which have shown only a modest correlation between T_2 lesions and changes in disability [192,433].

The presence of 10 or more of WMLs in the baseline scan has attracted attention since the Barcelona group reported as being very predictive of how aggressive the disease appears to be 10 years later [247], our cohort was of longer duration (> 15 years). In the recent Barcelona study [412]the median number of baseline T_2 lesions in the aggressive group (EDSS 6 at 10 years) was very high (71) which can be explained as they are the most severe patients 13 out of 401 patients. In our longer cohort, we had a much higher number of patients developing EDSS 6 (43) but after 15 years.

Furthermore, lesion load continues to increase in RRMS patients and the rate of lesion growth in those who developed SPMS was higher than those who remained RRMS, in line with a previous finding [46]. Several reasons might explain the weak or absent association of WML and/or regional atrophy with clinical changes. This might be related to some technical limitations such as the difference in slice thickness and noise as manual measurements are generally more susceptible to it.

There are no previous studies investigating critical cut-off values for MRI volumetric predictors of disability, such as TVW. Therefore, a direct comparison of our findings with the existing literature's cut-off values was not possible.

In the current study, the MEDW was measured as part of our dataset as a previous study showed that brainstem measures are sensitive to atrophy in MS [288] and might act as a replacement for cervical spinal cord volume in predicting MS diagnosis [287]. MEDW measures were correlated with disease severity in MS patients [296]. However, in our study, the similar metric of MEDW did not produce any statistical significance as a prognostic predictor. These findings could suggest that there is some independence of the MS pathology in these regions, as this lack of correlation between the brainstem and spinal cord measurements has been reported previously [434].

Similarly, CCI was demonstrated in a previous study to be correlated to disease progression in MS patients but was not itself an independent predictor [290]. Accordingly, CCI showed an annual decrease in patients following MS diagnosis, and the severity of CCI decrease was double in SPMS compared to RRMS patients with identifying a trend for a slower rate of CCI in patients using DMTs. Consistent with this line of thinking, the use of CCI as a measure of disease progression may not have been as statistically robust.

A great proportion of our patients received DMTs during the follow-up and for the majority, there was a short time between the first clinical event and treatment initiation. This might indicate that the patients included in our study had more severe symptoms/disease, therefore, were readily treated.

This study has limitations that include the exclusion of a large subset of patients when patients with MS were not routinely scanned annually during the first years of their disease. Additionally, due to the retrospective study design, we were not able to accurately record all previous DMTs data. A further caveat is the estimated odds ratios, although statistically significant should be interpreted with caution, particularly where all confidence intervals were very wide. The lack of data on spinal cord lesions and atrophy is another major limitation, in knowing the association of spinal lesions with long-term disability[435].

8.5 Conclusion

Brain atrophy of ICD and TVW early in the cohort of MS could predict progressive disease and disability over 10 years of clinical follow-up, as measured by simple, fast linear measurements which are applicable to clinical practice. The current clinical monitoring relies on T_2 lesions development, but this study suggests that simply counting the number of lesions does not have a direct effect on clinical disability 10 years later in the current DMTs treated cohorts. This study also shows that the predictive value of brain lesions and atrophy alone from

routine MRI scans may be not enough if used as the sole predictor of outcome. The use of more advanced MRI biomarkers, and especially the integration of these measures in prediction modelling using artificial intelligence platforms, either by way of the use of machine learning (vector) programs with pre-defined features or deep learning techniques, could improve in the future this prediction ability.

Chapter 9 . Thesis Conclusions and Future Direction

This thesis aimed to contribute to refining the role of MRI as a diagnostic and prognostic tool for MS patients. I was fortunate enough to work with multiple datasets from many international centres. The different data gathered were unique as they were (1) multi-centre large data sets including subjects with MS and MS-mimicking disorders to determine whether IRLs could be reliably used to classify patients as MS and non-MS. (*See Chapter 5).*

To assess MS disease prognosis and disability, two different data sets were collected (2) long-term clinical follow-up up to 12 years to evaluate IRLs in MS patients and whether they can be used as an imaging predictor of long-term disability, *Chapter 6,* and (3) 15 years of clinical follow-up to assess WMLs and linear measurements of brain atrophy in MS and their role in predicting disability, *Chapter 8.*

I confirmed the hypotheses indicating that the presence of IRLs was highly specific in diagnosing MS. The number of IRL and the atrophy measurements of TVW, and ICD were helpful in predicting long-term disability in MS patients. With the hope that the results from this work will have direct implications for the care of MS patients particularly as MRI biomarkers could accelerate an accurate MS diagnosis and predict the long-term prognosis of the disease for individual patients.

- ***MS Diagnosis***

Diagnosis of MS is typically straightforward. The use of Oligoclonal Bands (OCBs) has been used for many years and now is used for diagnostic purposes in patients with CIS (current diagnostic criteria) [362]. Still, misdiagnosis remains prevalent and is an increasing

concern. In the absence of a single marker for MS, more diagnostic markers have been proposed that could possibly replace the need for invasive lumbar puncture and confirm an MS diagnosis, especially when the OCBs are negative. The CVS is a promising marker, however, in several conditions, only a small number of lesions appear to have a central vein.

The role of iron, principally in the form of IRs surrounding some MS lesions, has demonstrated promising results in the study of CIS/MS and MS-mimicking patients. In this thesis, I confirmed the hypothesis that rim lesions were quite specific to MS patients. Various studies using a similar MRI protocol at 3T demonstrated that IRLs were observed across the entire course of the MS disease spectrum [355,356,436,437]. The prevalence of at least one IRL was 50% in MS disease-related patients, and it was relatively uniform across diagnostic phenotypes [355,356,436,437]. I tested the detectability of IRLs in a large, multi-centre study of over 500 patients, and IRLs were proven to be a useful diagnostic biomarker of MS. The identification of ≥1 IRL was the optimal cut-off and had a high specificity of 99.7% when distinguishing MS and CIS from mimics and healthy controls. All patients with an IRL showing a CVS in the same lesion had MS or CIS, giving a specificity of 100%. Therefore, IRLs may reduce the diagnostic uncertainty in MS by being a highly specific imaging diagnostic biomarker, especially when used in conjunction with the CVS. The confirmation of our hypothesis that IRLs were highly specific to MS suggests their utility as an additional imaging feature used in MS diagnostic criteria. The combination of IRLs and CVS (fulfilment of either ≥ 1 IRL or ≥ 4 CVS) further improved the sensitivity from ~23% to 57.9%. Moreover, combining IRLs and CVS with evidence of DIS, demonstrated a promising alternative to DIT or OCBs at the time of the baseline scan. Concerns over Gadolinium accumulation in the brain and side effects from lumbar punctures make the integration of these two MS lesion features in clinical diagnosis promising.

The multicentre nature of our study with the lack of a specific scanner and protocol standardization helps translate our research findings into clinical practice. This study reinforces the value of assessing IRLs using conventional protocols utilised by major European MS centres and as a result, can be considered a robust biomarker of MS lesions.

At the North America Imaging in Multiple Sclerosis (NAIMS-ACTRIMS) meeting in 2021, multiple guidelines regarding IRLs were highlighted. These include the clinical utility of IRLs if observed in the context of co-morbid conditions that contribute to non-specific WML (e.g., small vessel disease, migraine, etc.). IRLs could help to "rule in" the diagnosis of MS. At the same time, however, they should not be used to "rule out" any disease, especially for NMO or Susac syndrome. Future directions should aim to increase the sample size for MS-mimics in order to build a reliable clinical utility. However, these guidelines were suggested before publishing our work. Based on our findings, the next step is to independently confirm our findings, and if similar results are found, IRLs could be incorporated into future MS diagnostic criteria. Additionally, a comparison of the diagnostic performance of the IRLs against the use of positive OCBs, in a larger cohort of patients with MS-mimics would help determine which of the tests is the most accurate, well-tolerated by patients, and financially viable.

- ***MS Prognosis***

Once the diagnosis is confirmed, the next important question patients commonly ask is if they are at a higher risk than average to develop a clinical disability. As previously discussed, many studies over the years attempted to answer that and so far, we are aware of different proposed prognostic factors, which are ranging from demographic, clinical, imaging and laboratory-based. However, the most sensitive para-clinical test to predict conversion from suspected demyelinating disease to definite MS is MRI.

The role of iron accumulation in MS lesions has been linked to chronic lesion activity and disease progression [210,219]. Over 36 studies including more than 1300 MS cases in total, concluded that there is a pathological directionality of IRL with clinical outcomes. It has been shown that the presence of ≥1 IRL characterizes an MS phenotype of greater disease severity, with 'dose-dependent' effects, meaning the more rims, the worse clinical outcome [219,222,224,360]. Additionally, the presence of ≥1 IRL overall is not clearly associated with age, disease duration, or clinical phenotypes.

To test the hypothesis of the prognostic role of IRLs, 91 MS patients were assessed retrospectively for up to 12 years of clinical follow-up. The IRLs proved to be a useful biomarker in predicting disease progression and disability in MS. I found that the presence and number of IRLs hold a prognostic value for long-term clinical disability in MS, especially the presence of ≥4 IRLs with a high specificity of 95%. I also found that there is a strong association between IRLs and T_2 lesion count and volume, which raises the question of what is more related to disability. I reported that there is an independent effect of IRLs on predicting disability. The number of IRLs had the most direct effect on disability compared to WML count and volume, supporting its role as an independent prognostic imaging biomarker.

In addition, I looked at the role of WMLs accumulation and linear measurements of brain atrophy, especially at an early stage of the disease, as they have been suggested to be imaging predictors for disease progression, disease conversion, and long-term disability[196,247,401,412,438]. They are important measurements of demyelination and neurodegeneration that can simply be used in clinics. I aimed to verify whether WML counts, volumes, and linear measurements of brain atrophy could reliably predict disease progression and disability in MS using simple, fast measures that can be implemented in clinics. Previous studies tested this hypothesis on untreated cohorts [46]. In this thesis, the prognostic role of these biomarkers was tested retrospectively in 82 MS patients with up to 15 years of clinical follow-

up. I have found that when applied these measures in treated cohort clinical conditions, no association was found between WMLs count/volume and predicting disability, therefore, I was not able to confirm our hypothesis. Despite advances in brain imaging and computerised volumetric analysis, ICD and TVW remain relevant as they are simple, fast and could predict long-term disability. The reliability of these measures, however, still needs further validation to be authorised for clinical use. Although WML count and volume seem to be weak predictors for long-term disability, the conversion to SPMS has been shown to correlate with a higher number of T_2 lesions.

The baseline MRI data could help in MS diagnosis and in predicting disease progression in a way that is not dependent on the initial clinical presentation. Indeed, MRI studies have shown that IRLs and some linear measurements of brain atrophy have a predictive role in disability progression in MS. This thesis, not only confirms these findings but also suggests that the number of IRL is a more important predictor compare to WML number or volume. Moreover, TVW and ICD measures also showed their potential in predicting disability.

- ***Future Direction***

Whilst our data showed that findings as few as one to four lesions with IRs can provide high specificity in diagnosing and predicting disability in MS, future studies should determine the ideal threshold for MS diagnosis and disease progression using a fixed number of lesions. This is especially important in CIS patients, who might present with very few lesions on their baseline scan.

The IRLs remain unreported in the spinal cord, due to methodological issues. As the presence of spinal cord lesions at the baseline scans significantly increases the risk of a subsequent MS diagnosis, it would be rather interesting to determine if there is a reliable way to visualise rims outside of the brain.

There are still open questions and some concerns that ought to be addressed in future studies. It is now known that IRLs are likely to form in the stage of newly formed T_2-lesions, and most persist for many years. Over time, IRLs can but do not always enlarge, and may also persist or fade. In this work, I have explored the IRLs association with disability, however, other longitudinal clinical metrics, e.g., cognition, fatigue, upper extremity dexterity and quality of life should also be tested. Additionally, the clinical impact of preventing and/or resolving IRLs need further studies for validation, together with specifying the optimal follow-up duration to capture the evolution of rims.

Our findings were not based on a large sample of patients, so confirmation in another cohort is needed to test if any of the current DMTs influence the prognostic value of rims. They might affect IRLs development or absorption. In addition, we need to test if clinicians treat patients with IRLs more aggressively than rimless patients. Answering these questions might clarify if IRL can be used as an outcome measure in clinical trials, possibly studying if DMTs prevent the development of new IRL or speed up the disappearance of Rimmed lesions.

Different acquisition and post-processing methods have been proposed for IRLs detection (e.g., unwrapped/filtered phase, T_2*), further studies are nonetheless needed to compare them against each other in terms of IRLs detection and quantification. Also, given the fact that most clinical scans are 1.5T, it is important to evaluate the performance of each technique at a lower field. It is also essential to know the proportion IRLs which might be missed by the highest-sensitivity in vivo imaging method. Still, there are no well-validated techniques for the identification of chronic inflammation in GM lesions, future studies should focus on the cortex or other GM structures.

We have not observed yet the widespread use of deep learning or radiomics studies in clinical practice. These studies could be complementary to automated analysis of images at the source. Implementation of any research findings into clinical practice is very important and

possibly less attention is paid. It has been reported that it takes an average of 17 years for research evidence to reach clinical practice [439–441].

Additionally, current methods need to be tested with a standardised acquisition in a large-scale validation study. As Artificial Intelligence (AI) uses huge data, it provides more reliable findings in terms of the most relevant and useful biomarker to use in clinics. Our study showed that the predictive value of brain lesions and linear measurements of brain atrophy taken from routine MRI scans might not be enough if used as the sole predictor of outcome. The use of more advanced MRI biomarkers, and especially the integration of these measures in prediction modelling using artificial intelligence platforms, either by using machine learning (vector) programs with pre-defined features or deep learning techniques, could improve the future prediction ability. Such a study is underway at the University of Nottingham and other MS centres.

SELs are an emerging area of research, and they represent concentrically expanding areas of focal tissue damage with high tissue destruction and are thought to be associated with disability. SELs can be detected using conditional T_1 and T_2- based sequences and do not require high-field MRI platforms. However, the pathological correlates of SELs are not yet definitively known. It remains to be determined if IRLs originate from existing chronic lesions. Genetic studies are also needed which could help to identify people that are more likely to develop rims and whether this provides us with more insight into MS biology. Finally, a reliable estimation of linear measures of brain atrophy values obtained from clinical scans also needs further investigation.

This work was not devoid of limitations which are addressed in detail in each discussion chapter. Even with the overarching limitations such as the known shortcomings of MRI technology and the acknowledged issues with disability scales, the data in this thesis shed some light on our understanding of MS. Knowledge is accumulated at an accelerated pace, I explored

some of the new imaging biomarkers and how they fit into what we know already about MS in the last seventy years. The hope and potential of research are to continue working towards the aim of curing MS.

Appendices

Appendix A

A.1 Kurtzke's Expanded Disability Status Scale (EDSS)[63]

EDSS score	Definition
0	Normal neurological examination (all FS normal)
1	No disability, minimal signs in one FS
1.5	No disability, minimal signs in more than one FS
2	Minimal disability in one FS
2.5	Minimal disability in two FS
3	Moderate disability in one or mild disability in up to four FS though fully ambulatory
3.5	Fully ambulatory but with a moderate disability in one FS and mild disability in one or two others; or moderate disability in two FS; or mild disability in five FS
4	Fully ambulatory without aid; self-sufficient; up and about some 12 hours a day despite relatively severe disability in one FS or combinations of exceeding the limits of previous step. Able to walk without aid or rest for 500m.
4.5	Fully ambulatory without aid; up and about much of the day; may otherwise have some limitation of full activity or require minimal assistance. Able to walk without aid or rest for 300m.
5	Ambulatory without aid or rest for 200m; disability severe enough to impair full daily activities.
5.5	Ambulatory without aid or rest for 100m; disability severe enough to impair full daily activities.
6	Intermittent or unilateral constant assistance required to walk 100m
6.5	Constant bilateral assistance to walk 20m without rest.
7	Unable to walk 5m even with aid. Essentially restricted to a wheelchair. Transfers alone.
7.5	Unable to walk more than few steps. May need aid with transfers.
8	Restricted to bed or chair or perambulated in wheelchair. Generally, has effective use of arms. Out of bed for much of the day
8.5	Essentially restricted to bed for much of the day. Retains some self-care functions
9	Helpless bed patient; can communicate and eat
9.5	Totally helpless, unable to communicate effectively or eat/swallow
10	Death due to MS

FS: Functional system

Appendix B

B.1 Study protocol was submitted to the Nottingham Research data management repository.

The protocol was not registered in PRISMA as they don't accept mapping review, so the university repository was chosen instead https://rdmc.nottingham.ac.uk/handle/internal/8308

A systematic Mapping Review of Paramagnetic Rims as a Diagnostic Imaging Biomarker in Multiple Sclerosis (MS)

Amjad Altokhis, Rebecca Stevenson, Cris Tench, Abdulmajeed AlOtaibi, Ghadah Felmban, Cris Constantiscu, Nikos Evangelou

Review question
To assess the detection of iron rims, on variable, clinically-quality MR scan, and investigate the characteristics of rim presence in MS versus MS-mimics.

Searches
We will search the following electronic bibliographic databases: PubMed, EMBASE and Web of science. All databases will be searched from the date of the first MS diagnostic use of MRI in 2001. We will hand search reference lists of eligible studies, key journals will be individually searched as well as grey literature: internet resources, these and conferences. Duplications will be removed.

Types of study to be included
MRI studies detecting rims of MS alone or MS in comparison to healthy or other disease populations (MS-mimicking disorders)

Condition or domain being studied
MS

Participants/population
Inclusion:
MRI studies in brain lesions with rims.
MS defined as World health organisation and The McDonald criteria
Pathological studies will also be included
Exclusion:
Studies published before 2001
Animal studies
Non- English publications

Intervention(s), exposure(s)
none

Comparator(s)/control
Health control group or none or MS- mimicking disorders (migraine, vascular disease etc.)
Context

The review will focus on the contribution of MRI to the understanding of rims in MS.

Data extraction (selection and coding)
Two reviewers will independently assess titles and abstracts of identified records to determine eligibility using pre-specified inclusion and exclusion criteria. Those titles that are irrelevant will be discarded. Full text articles of potentially relevant references (as deemed by at least one reviewer) will be retrieved. The retrieved full text articles will be assessed independently by two reviewers based on pre-stated inclusion criteria. Using an iterative approach, papers will be read and re-read to determine if they contain data useful to the aims of this review. Disagreements between reviewers will be resolved via discussion. The following details about each study will be extracted by one reviewer: Study (Author, date), type of the study, number of participants, demographics, aim of paper, type of magnet strength, data analysis method, full MRI protocol procedure and main results and limitations.

Risk of bias assessment Mapping review does not require a bias assessment

Strategy for data synthesis
Map the data 1) type of MS 2) study design 3) inductive approach to any other category.

Analysis of subgroups or subsets
The review will focus on the evidence of rims in brain lesions, especially in MS.

Contact details for further information
Ms Amjad Altokhis
Amjad.Altokhis@nottingham.ac.uk

Organisational affiliation of the review
University of Nottingham
www.nottingham.ac.uk

Type and method of review
Systematic Mapping Review

Anticipated or actual start date
01 Jan 2020

Anticipated completion date
01 Feb 2021

Funding sources/sponsors
NA

Conflicts of interest
Nothing to declare.

Language
English

Country
England

Stage of review
The review has not started.

Subject index terms
Rims; Humans; Magnetic Resonance Imaging; Multiple Sclerosis, lesions

Date of registration in
March 2020

Date of publication of this version
N/A

Revision notes for this version
If there is no comparable quantitative, a descriptive synthesis will be looked at.

Search strategy and key works (assessed by librarians)- Ms Alison Ashmore

Web of science
("multiple sclerosis" OR "MS") AND ("rim" OR "rim*") AND ("lesion" OR "lesion*") AND

Embase
("multiple sclerosis"[MeSH Terms] OR "multiple sclerosis"[All Fields] OR "MS"[All Fields]) AND ("rim" [All Fields] OR "rims""[All Fields]) AND ("lesion" "[All Fields] OR "lesions""[All Fields])

PubMed
Below is a sample search I ran in PubMed database. The number of results I got was 401.

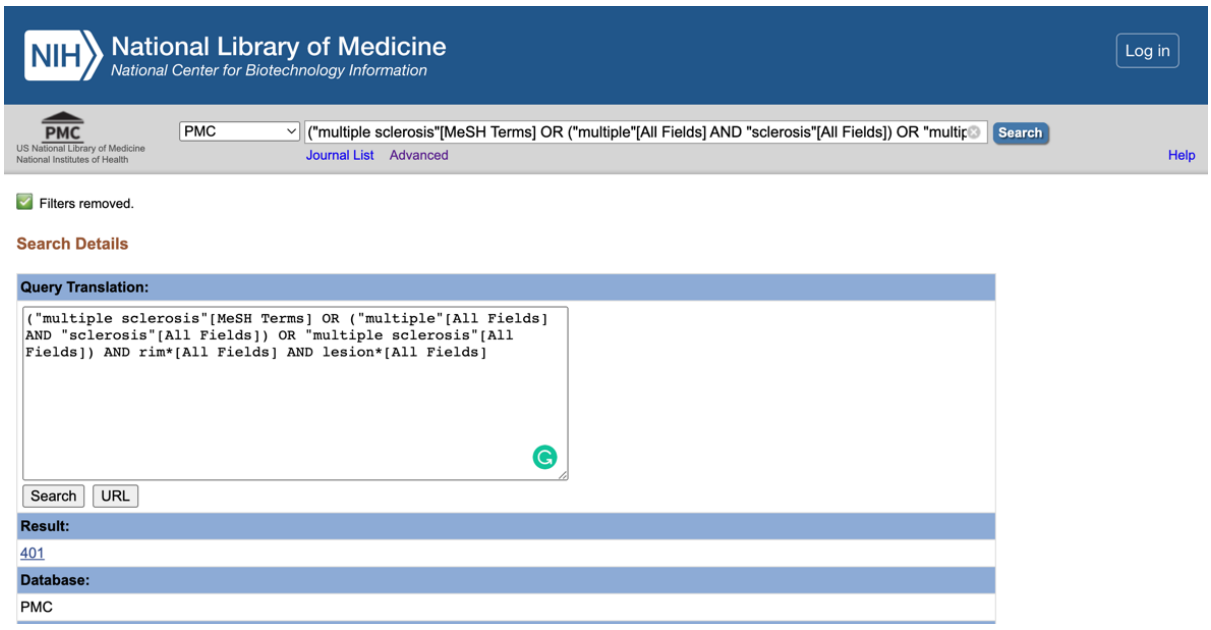

B.2 Details of the included studies

Studies	Study Type	Scanner Strength	MRI Sequences
Blindenbacher et al. (2020)[328]	Observational, prospective, longitudinal 5 years	3T	SWI, T2 FLIR
Suthiphosuwan *et al.* (2020)[220]	Cross-sectional, Prospective, observational longitudinal	3T	3D T1W, 3D T2 FLAIR, and 3D T2-segmented echo-planar imaging results (with magnitude and phase images) T1-phase sensitive inversion recovery
Tolaymat *et al.* (2020)[335]	Cross-sectional	7T	FLAIR
Clarke *et al.* (2019) (unpublished/ECTRIMS)[318]	Presentation	3T	FLAIR, SWI, T2
Dal-Bianco *et al.* (2019) (unpublished, ECTRIMS)	Prospective, longitudinal	7T	FLAIR, SWI, MPRAGE
C. Treaba *et al.* (2019)[325]	Cross-sectional	7T	T2*, 3D T1W DWI, phase images
Jiwon oh *et al.* (2019)[334]	Cross-sectional	3T	3D-T2-FLAIR, 3D-T1-MPRAGE 3D-T2*EPI, T2* and phase images.
Philip *et al.* (2019)[442]	Cross-sectional	3T	T2W, FLAIR, T1W, SWI
Dal-Bianco *et al.* (2019) [329]	Cross-sectional	7T	SWI, FLAIR
Absinta *et al.* (2019)[219]	Retrospective, longitudinal, including pathological data	3T,7T	SWI, T2*, 3D FLAIR, pre-post contrast T1
Luchetti *et al.* (2018)[215]	Pathology study	Pathology autopsy	NA
Absinta *et al.* (2018)[340]	Longitudinal (10 years)	7T,3T	T2*w, T2-FLAIR
Constantina et al. (2018)[443]	Poster	7T	T2*w, T1W
Yao *et al.* (2018)[375]	Retrospective longitudinal	3T	QSM, T1W, T2W
Jan-Mendelt *et al.* (2018)[346]	Cross-sectional	3T	double-inversion-recovery sequence (DIR)
Chawla *et al.* (2018)[167]	Longitudinal	7T	3D-SWI, 2D-GE-T2*W
Ulrike *et al.* (2018)[348]	Cross-sectional retrospective	3T	T1W pre and post contrast T2W, T2-FLAIR

Elliot *et al.* (2018)[349]	Phase 3 trial, multi-centre, randomised, double-blind, placebo-control	3T, 7T	T1W and T2W
Dal-Bianco *et al.* (2017)[213]	longitudinal 3.5 yrs., including pathological data	7T	SWI, FLAIR
Chawla *et al.* (2016)[313]	Cross-sectional	7T	SWI, QSM, T2*, FLAIR, T1W
Harrison *et al.* (2016)[217]	Cross-sectional	7T	SWI, R*, FLAIR, QSM
Iris *et al.* (2016)[337]	Prospective, cross-sectional	7T	3D FLAIR, T2*, FLAIR* (combination of T2 and FLAIR)
Absinta *et al.* (2016)[211]	A prospective follow-up study every 3 months for a year, including pathological data	7T	SWI, T1W pre/post-Gd, DCE
Daniel *et al.* (2016)[217]	Cross-sectional	7T	R2*, QSM, FLAIR, phase
Yao *et al.* (2015)[323]	Cross-sectional	3T,7T	T1W, T2W, R2*
Frischer *et al.* (2015)[216]	Pathology study	3T	NA
Chen W *et al.* (2014) [321]	Retrospective	3T (GE)	T1, T2W, QSM
Kilsdonk *et al.* (2014)[184]	Cross-sectional	7T	3D FLAIR, T2*, FLAIR* (combination of T2 and FLAIR)
Wiggermann *et al.* (2013)[319]	Longitudinal (6 months)	3T	Gd, FLAIR, SWI, T1W
Bian et al. (2013)[344]	longitudinal	7T	T2*W
Walsh *et al.* (2013)[444]	Pathology study	4.7T	T2W, R2 mapping, and R2* mapping and phase imaging
Absinta *et al.* (2013)[445]	Longitudinal, a year	7T	T2*, phase scans, T1 before/after gadolinium contrast injection, dynamic contrast-enhanced (DCE) T1W
Yablonskiy *et al.* (2012)[320]	cross-sectional	3T	T1W, T2*, FLAIR, phase Imaging
Llufriu *et al.* (2010)[324]	Retrospective 2000-2009	1.5 T	PD, T2W, T1W pre and post Gd, DWI
Lucchinetti, (2008)[341]	Retrospective, including pathological data	1.5T	T1, T2, FLAIR
Schwart *et al.* (2006)[330]	Retrospective	not mention (but probably 1.5 or 3T)	T1W-Gd, T2W, DWI
Lucchinetti *et al.* (2003)[342]	Presentation	1.5T	T1, T2, FLAIR

FLAIR: Fluid-attenuated inversion recovery, SWI: Susceptibility weighted imaging, QSM: Quantitative susceptibility mapping, Gd: Gadolinium, T: Tesla.

B.3 The pie chart shows the percentage of studies reported iron rim lesions (IRLs) presence in different MS subtypes

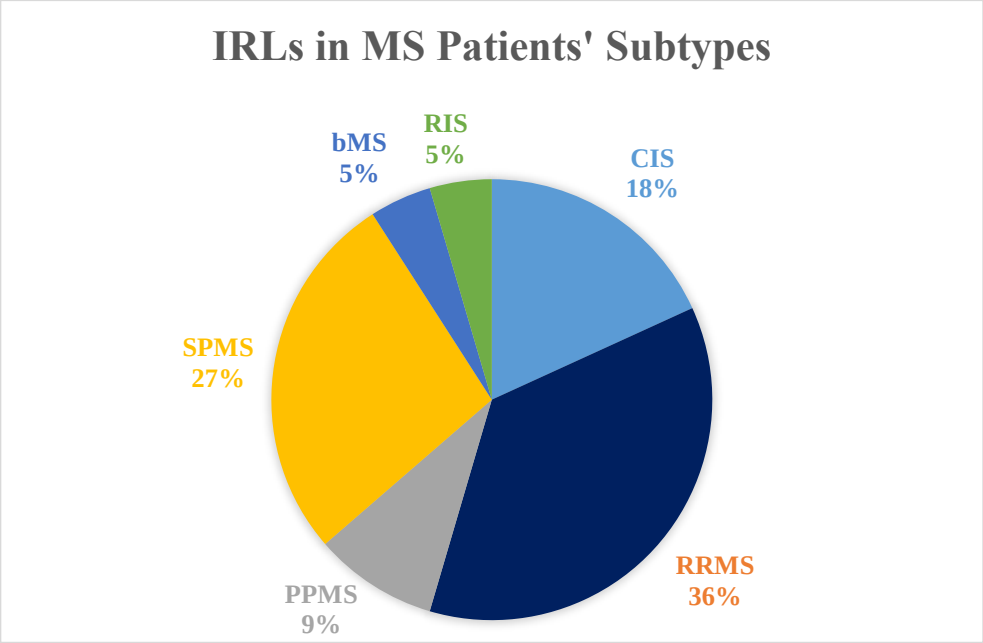

IRLs: Iron rim lesions, RIS: Radiologically isolated syndrome, CIS: Clinically isolated syndrome, bMS: Benign Multiple Sclerosis, SPMS: Secondary progressive MS, PPMS: Primary progressive MS.

B.4 The table summarises the sensitivity and specificity of IRL detection across different studies**.**

Author/Year	N (MS)	N (Comparison)		Specificity ≥ 1 PRL	Sensitivity ≥ 1 PRL	Field
Hagemeier 2012[446]	135	49	Incidental	98%	22%	3T
Hosseini 2018[315]	17	18		100%	NR	7T
Wuerfel 2012[314]	10	5	Susac	20%	100%	7T
Chawla 2016[313]	21	21	NMO	100%	10%	7T
Sinnecker 2016[447]	10	10		80-90%	90%	7T
Jang 2020[357]	32	21		95%	81%	3T
Clarke 2020[355]	112 (CIS)	35	OIND, NIND & other mimics)	100%	59%	3T
Maggi 2020[356]	329	83		93%	52%	3T

MS: Multiple Sclerosis, NMO: Neuromyelitis Optica, PRL: paramagnetic Rim Lesions, T: Tesla, OIND: other inflammatory neurological diseases, NIND: non-inflammatory neurological diseases.

B.5 Reported and ongoing studies of treatment effect on PRL (clinicaltrials.gov or PubMed)

- NCT 03222973 (AFFINITY)-opicinummab in RMS; some data reported at American Academy of Neurology (AAN) 2021
- NCT 03523858 (CONSONANCE)-ocrelizumab in PMS; recruiting
- NINDS internal: High dose corticosteroids; recruiting
- NIND internal: Atac-MS: Anti-IL-1 (anakinra)
- NIND internal: BRaKe-MS: BTK inhibitor (tolebrutinib)

Appendix C

C.1. Overview of MRI Protocol and Multicenter Design

Center	GRE sequence			IR sequence		Study participants
	type	resolution (mm)	TE/TR (ms)	type	resolution (mm)	
Amsterdam	SWI	0.49x0.49x3.0	23/31	3-D FLAIR	0.98x0.98x1.2	RRMS, n=40
Barcelona	SWI	0.65x0.65x3.0	24.6/33	TIRM, tra	0.49x0.49x2.99	CIS, n=29 RRMS, n=2 Migraine, n=20 SVD, n=24 SLE, n=7
Berlin	SWI	0.78x0.78x3.0	24.6/33	3-D FLAIR	0.98x0.98x1.0	CIS, n=2 RRMS, n=28 NMOSD, n=44
Graz	SWI	0.9x0.9x4.0	59/68	TIRM, tra	0.86x0.86x3.0	CIS, n=73 RRMS, n=71 SVD, n=102
Poznan	SWI	0.86x0.86x1.5	20/28	3-D FLAIR	0.49x0.49x1.0	RRMS, n=73 SLE, n=18 SVD, n=22
Siena	SWI	0.3x0.3x1.0	13.4/31	3-D FLAIR	1.0x1.0x1.0	RRMS, n=15 Migraine, n=9
						Cluster headache, n=5
Verona	SWI	0.55x0.55x0.55	29/51	3-D FLAIR	1.0x1.0x1.0	CIS, n=19 RRMS, n=13 Migraine, n=1 NMOSD, n=1

*GRE: gradient echo, IR: inversion recovery, TE: echo time, TR: repetition time, TI: inversion time, SWI: susceptibility-weighted imaging, T2*w: T2* weighted imaging, FLAIR: fluid attenuated inversion recovery*

C.2. Further details about the method are provided in this section.

C.2.1. Patient Selection

Patients (n=562) were enrolled in this cross-sectional, multicentre study at seven neuroimaging centres across Europe. The centres included Vall d'Hebron University Hospital (Barcelona), Universitätsmedizin (Berlin), Medical University of Graz (Graz), Poznan University of Medical Sciences (Poznan), University of Siena (Siena), University of Verona (Verona), VU University Medical Centre Amsterdam (Amsterdam).

Patients between the ages of 18 and 85 with various conditions that result in brain WMLs were retrospectively included in the study. These included CIS with documented evidence of one demyelinating episode (excluding optic neuritis), RRMS; NMOSD; cerebral vasculitis; cluster headache; episodic migraine; small vessel disease; systemic lupus erythematosus (SLE); and diabetes mellitus (DM).

Patients were eligible for inclusion in this study if they had a 3T MRI scan, including SWI sequence or T2*-weighted and 3D FLAIR sequence. Exclusion criteria were insufficient SWI and/or FLAIR image quality and inadequate coregistration of SWI and FLAIR images. Clinical disability was assessed using the EDSS (score range: 0-10, with the highest score indicating death from MS) in patients with MS and NMOSD. Patients with RRMS with a disease duration shorter than five years were considered to have early MS.

C.2.2. MRI Acquisitions

Scans were performed on different 3T MRI scanners/head coils and protocols, reflecting the multicentre setting of the study. Image acquisition and pre-processing details have been published by Sinnecker et al. (2019). Here, a summary for completeness is provided. The imaging protocols included 3D T2-FLAIR and a high-resolution gradient-echo sequence,

which was either an SWI sequence or an optimised 3D T2*-weighted sequence. The T2*-weighted protocol covered only the supratentorial areas and upper part of the cerebellum.

Image Post-processing

T2*-FLAIR images were co-registered to the SWI using Insight Segmentation and Registration Toolkit (ITK) library, which was implemented in 3D Slicer, version 4.6.2.

Each co-registered pair of images was then split into 8 equal-sized 3D blocks (*figure below).* The parcellation of the brain was performed to restrict the field of view of the investigators and hence blind them to the global information about the lesion load, the distribution pattern of lesions, and the presence or absence of PR in other lesions in the same individual. This procedure was done to prevent inference of the disease type on the PR assessment. All the blocks were subsequently randomised across centres, subjects, and blocks (individual ID for each block). This step was performed by Tim Sinnecker from the Basel group.

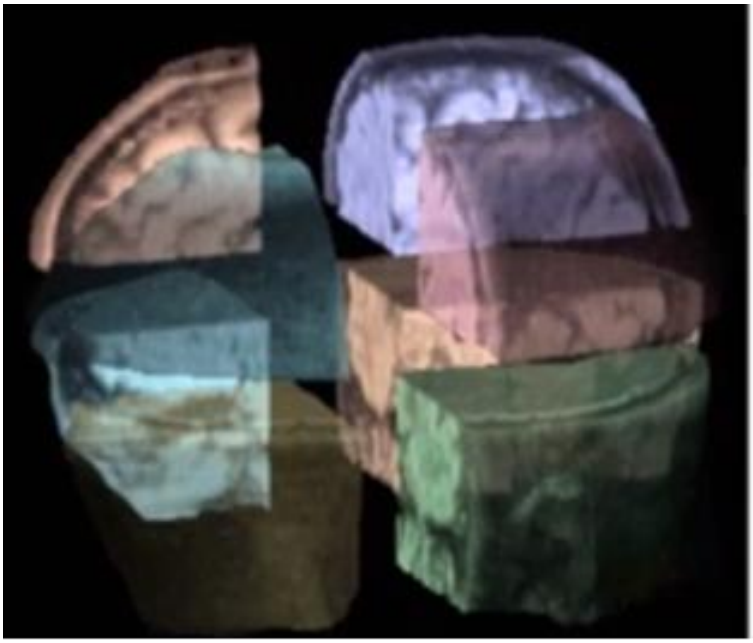

Figure. Parcellation of brains to achieve disease-type blinding

C.2.3. Image Analysis

3D Slicer version 4.6.2 was then used to view an overlay of the SWI and FLAIR images to help detect the presence of individual lesions, veins, rims and dots in each of the blocks *(figure below).*

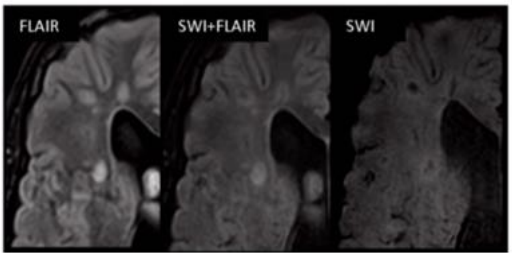

Figure. Overlay of SWI and FLAIR using 3D-slicer

Each WM lesion needs to be larger than (3 mm) alongside the long axes using the annotations option and classified based on their location as cortical/juxtacortical (in direct contact with the cerebral cortex), periventricular (in direct contact with the lateral/third ventricles), deep WM lesion (not in direct contact with the cortex or ventricles) and deep grey matter. Lesions that were poorly contrasted (e.g., owing to motion artefacts, sequence-specific

artefacts, or bad overall image quality) were excluded. The window viewer was standardised where possible to W481/L210 for FLAIR and W619/L254 for SWI.

Each WM lesion was checked for three primary markers (CVS, PR). **CVS** was marked if they satisfied the pre-specified criteria defined in accordance with the North American Imaging in MS (NAIMS) guidelines [166], that is, a) appears as a hypointense line on SWI/FLAIR scans vein b) entering and/or exiting lesion c) vein run through the centre of the lesion. **PR** was marked if a) FLAIR/SWI scan showed an area of a hypointense ring-like signal corresponding to the lesion's edge, b) encircle the lesion fully or partially c) visible on two or more slices.

C.3

Receiver operating characteristic curves (ROC) for prediction the diagnosis of MS vs MS-mimics based on Central Vein Sign (CVS) and Paramagnetic Rim Lesion (PRL).
Figure 1. Illustrates the ROC curve analysis for the Central vein sign and Figure 2. Illustrates the CVS and PRL combined which has no significant difference.

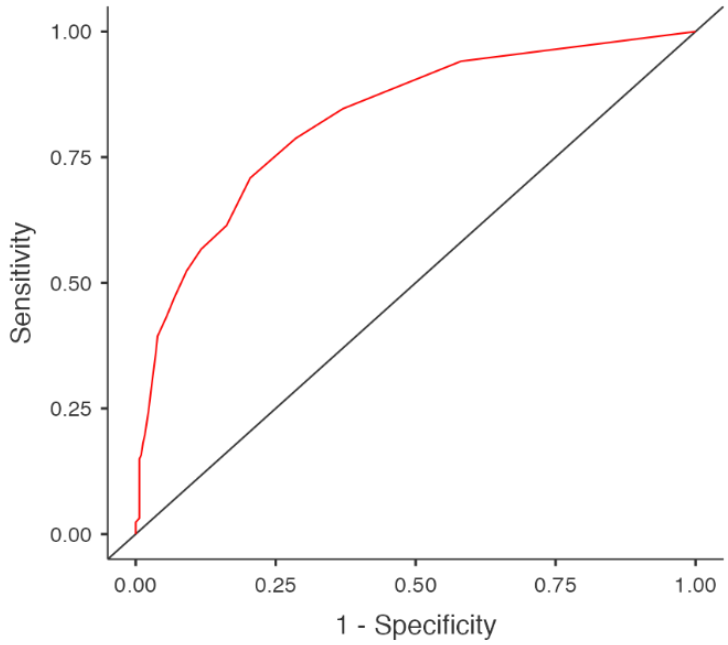

Figure 1. ROC for the dependent variable of diagnosis (MS vs MS-mimics) against the independent variable of Central Vein Sign

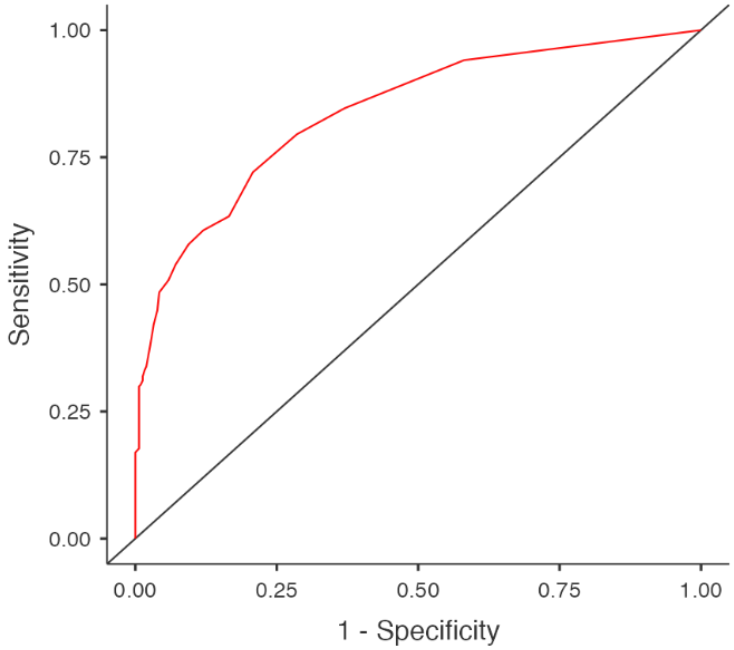

Figure 2. ROC for the dependent diagnosis (MS vs MS-mimics) against the independent variable of Paramagnetic Rim Lesions or Central Vein Sign

Appendix D

D.1 Search strategy and key works (assessed by librarians)

Web of science

("multiple sclerosis" OR "MS") AND ("Magnetic resonance imaging" OR "MRI") AND (white matter lesion OR lesions) AND (long*) AND (Disability) AND (T2 or FLAIR)

PubMed

("multiple sclerosis" OR "MS") AND ("Magnetic resonance imaging" OR "MRI") AND (white matter lesion OR lesions) AND (long*) AND (Disability) AND (T2 or FLAIR)

Embase:

("multiple sclerosis"[MeSH Terms] OR "multiple sclerosis"[All Fields] OR "MS"[All Fields]) AND ("magnetic resonance imaging"[MeSH Terms] OR "magnetic"[All Fields] OR "imaging"[All Fields]) AND ("lesion" [All Fields] OR "lesions"[All Fields]) AND (white matter [All Fields]) AND ("disability"[All Fields]) AND (long* [All Fields]) AND ("T2" [All Fields] OR "FLAIR" [All Fields])

Below is a sample search I ran in Ovid MEDLINE. Notice that both MeSH terms *and* keywords (the lines ending in **.mp.**) have been used. The MeSH terms have been 'exploded' (**exp** Magnetic Resonance Imaging/) and included all their sub-headings. The number of results I got was **102**

1	exp Magnetic Resonance Imaging/	470430
2	(MRI or "magnetic resonance imaging").mp. [mp=title, abstract, original title, name of substance word, subject heading word, floating sub-heading word, keyword heading word, organism supplementary concept word, protocol supplementary concept word, rare disease supplementary concept word, unique identifier, synonyms]	603156
3	(WML or "white matter lesion*").mp. [mp=title, abstract, original title, name of substance word, subject heading word, floating sub-heading word, keyword heading word, organism supplementary concept word, protocol supplementary concept word, rare disease supplementary concept word, unique identifier, synonyms]	5290
4	(count* or number*).mp. [mp=title, abstract, original title, name of substance word, subject heading word, floating sub-heading word, keyword heading word, organism supplementary concept word, protocol supplementary concept word, rare disease supplementary concept word, unique identifier, synonyms]	3384137
5	volume*.mp. [mp=title, abstract, original title, name of substance word, subject heading word, floating sub-heading word, keyword heading word, organism supplementary concept word, protocol supplementary concept word, rare disease supplementary concept word, unique identifier, synonyms]	771624
6	exp Multiple Sclerosis/	60809
7	(MS or "multiple sclerosis").mp. [mp=title, abstract, original title, name of substance word, subject heading word, floating sub-heading word, keyword heading word, organism supplementary concept word, protocol supplementary concept word, rare disease supplementary concept word, unique identifier, synonyms]	400696
8	exp Disability Evaluation/	53879
9	(EDSS or "Expanded Disability Status Scale").mp. [mp=title, abstract, original title, name of substance word, subject heading word, floating sub-heading word, keyword heading word, organism supplementary concept word, protocol supplementary concept word, rare disease supplementary concept word, unique identifier, synonyms]	6415
10	(disabilit* or disabled).mp. [mp=title, abstract, original title, name of substance word, subject heading word, floating sub-heading word, keyword heading word, organism supplementary concept word, protocol supplementary concept word, rare disease supplementary concept word, unique identifier, synonyms]	334935
11	1 or 2	623201
12	4 or 5	4032476
13	6 or 7	400696
14	8 or 9 or 10	339822
15	3 and 11 and 12 and 13 and 14	102

D.2 MRI data, raters, and lesion segmentation.

Study	T2 Lesion Sequence	T2/PD Slice Thickness	MRI -Tesla	Blinded to Clinical Details	No. of raters	Lesion Segmentation	Software
Tintore 2020 [412]	T2, PD, FLAIR	3-5mm	1.5T or 3T	⃠	⃠	⃠	⃠
Chung 2020 [401]	T2, PD	5-10mm	1.5T or 3T	⃠	3	⃠	⃠
Brownlee,2019 [417]	T2, PD	3mm	1.5T	Yes	1	Semi-automated	JIM6, Xinapse systems, Aldwincle, UK
Tintore 2015* [247]	T2, PD, Flair	3-5mm	1.5T or 3T	⃠	⃠	⃠	⃠
Jacobsen 2014* [202]	T2, PD	5mm	1.5T	⃠	⃠	Semi-automated	⃠
Kearney 2014 [130]	T2	1-3mm	1.5T or 3T	⃠	2	Semi-automated	JIM6, Xinapse systems, Aldwincle, UK
Giorgio 2014 [386]	T2, PD	3mm	1.5T	Yes	1	Semi-automated	Jim 5.0, Xinapse System, Leicester, UK
Popescu 2013 [15]	T2	3-5mm	1T or 1.5T	Yes	1	Semi-automated	Jim 5.0, Xinapse System, Leicester, UK
Rovaris 2011 [408]	T2	3-5mm	1T or 1.5T	Yes	1	Semi-automated	Jim, Xinapse System, Leicester, UK
Renard 2010 [385]	T2, PD, Flair	3mm	1.5T	Yes	2	Semi-automated	⃠
Fisniku 2008* [46]	T2	5-10mm	0.5T	Yes	1	Semi-automated	DispImage
Chard 2003 [409]	T2	5-10mm	1.5T	Yes	2	Semi-automated	DispImage
Brex. 2002 [250]	T2	5-10mm	0.5T	⃠	⃠	Semi-automated	DispImage
Sailer 1999 [411]	T2	5-10mm	0.5T	⃠	1	Semi-automated	DispImage
O'Riordan 1998 [410]	⃠	5-10mm	0.5T	Yes	2	Semi-automated	DispImage
Reported (%)	**14 (93%)**	**15 (100%)**	**15 (100%)**	**8 (53%)**	**11 (73%)**	**12 (80%)**	**10 (66%)**

*⃠: not reported, T2: T2 weighted images, PD: proton density, *studies included in the Mata-analysis, No: Number.*

D.3 Key elements for forest plot interpretation.

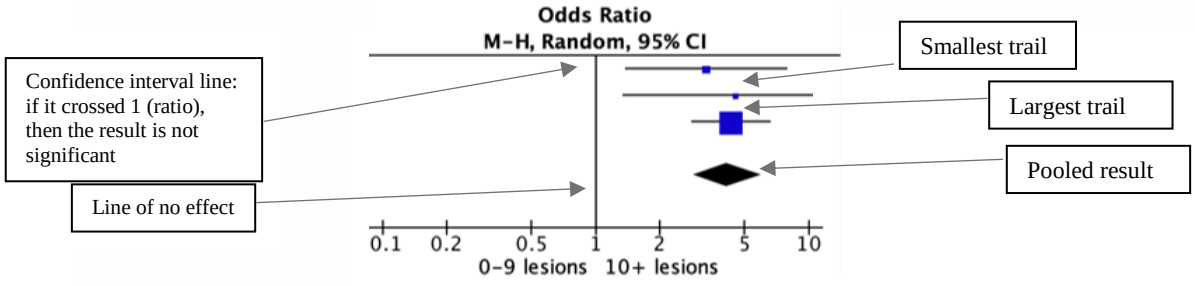

Legend:

■ This square represents the individual studies effect. The size varies to reflect the weight a specific study has in the overall analysis (larger "symbol" has more weight).

The black line represents the CIs of the study; the smaller "symbol" which has less weight generally has larger CIs than the larger "symbol".

The diamond represents the overall or summary effect. The outer edges of the diamond represent the CIs.

Appendix E

E.1

The table illustrates the correlation coefficients, inter-class correlations (ICC) for Inter and intra-rater reliability for all MRI measures. These measurements were conducted between two reviewers (A.A. and A.O.).

Measures	Intra-rater	Inter-rater
Lesion counts	0.88 (P < 0.05)	0.80 (P < 0.05)
Lesion volume	0.80 (P < 0.05)	0.83 (P < 0.05)
Third ventricle	0.99 (P < 0.05)	0.86 (P < 0.05)
Corpus Callosum	0.65 (P < 0.05)	0.66 (P < 0.05)
Medulla	0.81 (P < 0.05)	0.64 (P < 0.05)
Inter-caudate distance	0.97 (P < 0.05)	0.70 (P < 0.05)

P<0.05 was set as significant.

E.2

1. **Third Ventricle Width** [286,287]

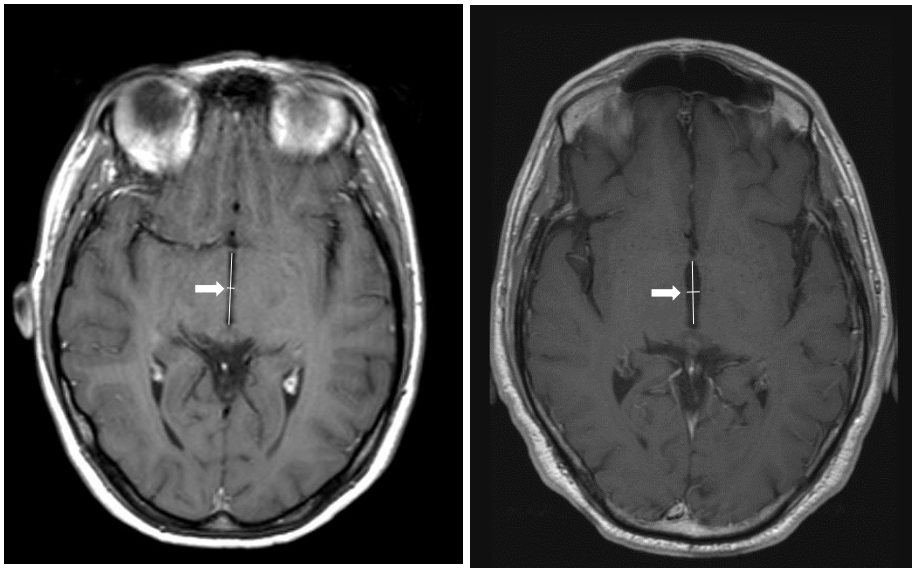

Figure 1. Third Ventricular Width (TVW) was measured as the width of the third ventricle at the midpoint (see white arrow) of a line running parallel to the long-axis of the ventricle on axial T_1- weighted MRI scans.

2. **Corpus Callosum Index** [289,290,448]

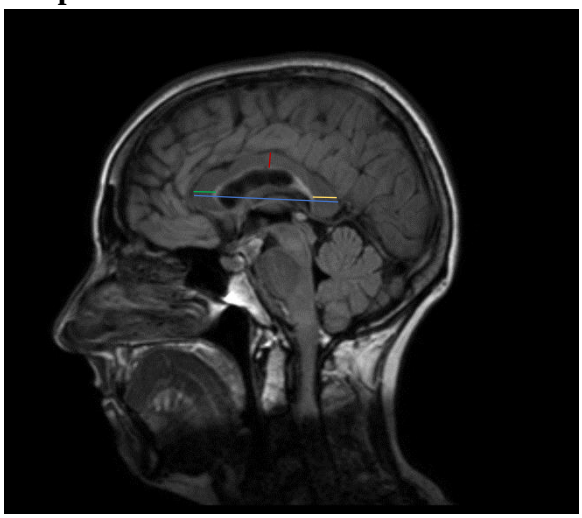

Figure 2. Sagittal FALIR MRI scan.

Corpus Callosum Index (CCI) was obtained on a conventional best mid-sagittal FLAIR image, by drawing a straight line at the greatest anteroposterior diameter of CC and a perpendicular at its midline, owing to points a, b and c. Anterior (green line), posterior (yellow line) and medium (red line) segments of CC were measured and normalized to its greatest anteroposterior diameter (blue line).

$$CCI = \frac{\text{Anterior} + \text{Posterior} + \text{medium}}{\text{Anteroposterior diameter}}$$

3. **Medulla Width** [287]

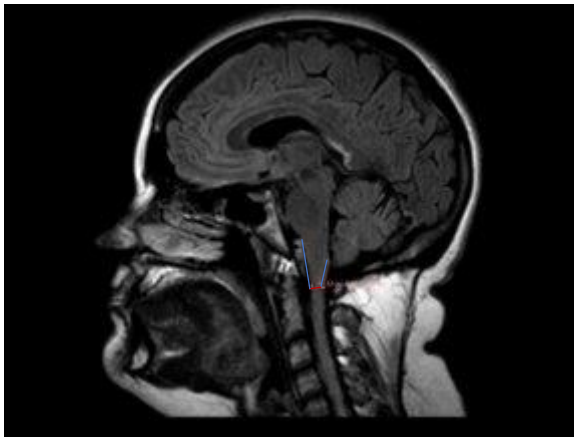

Figure 3. Sagittal FLAIR image and the red line shows the medulla width measure.

- Medulla width (MEDW) was measured as the dorsoventral diameter of the medulla on a mid-sagittal image.
- The level of medullary measurement was determined by the craniocaudal pontine length mirrored caudally from the inferior pontine notch.

4. Inter-caudate distance [286]

Figure 4. Axial T_{1}- weighted brain MRI, the black arrow shows the ICD measure.

- Inter-caudate distance (ICD) was measured on an axial T_1-weigted image when the frontal horn (white arrow) reached the maximum width.
- ICD width is the minimum distance between medial boarders of the head of the caudate nuclei.

References

1. Altokhis AI, Alamrani A, Alotaibi AM, et al. diagnostics Iron Rims as an Imaging Biomarker in MS: A Systematic Mapping Review. *Diagnostics*. 2020;10(11):968. doi:10.3390/diagnostics10110968

2. Altokhis AI, Alamrani A, Alotaibi A, Podlasek A, Constantinescu CS. Magnetic Resonance Imaging as a Prognostic Disability Marker in Clinically Isolated Syndrome and Multiple Sclerosis: A Systematic Review and Meta-Analysis. *Diagnostics*. 2022;12(2):270. doi:10.3390/Diagnostics12020270

3. Altokhis AI, Hibbert AM, Allen CM, et al. Longitudinal clinical study of patients with iron rim lesions in multiple sclerosis. *Mult Scler J*. Published online August 24, 2022. doi:10.1177/13524585221114750

4. Meaton I, Altokhis A, Allen CM, et al. Paramagnetic rims are a promising diagnostic imaging biomarker in multiple sclerosis. *Mult Scler J*. Published online August 26, 2022:135245852211186. doi:10.1177/13524585221118677

5. Altokhis A, Alotaibi A, Morgan P, Tanasescu R, Evangelou N. Predictors of long-term disability in multiple sclerosis patients using routine magnetic resonance imaging data: A 15-year retrospective study. *Neuroradiol J*. Published online 2023. doi:10.1177/19714009221150853

6. Sartori A, Abdoli M, Freedman MS. Can we predict benign multiple sclerosis? Results of a 20-year long-term follow-up study. *J Neurol*. 2017;264(6):1068-1075. doi:10.1007/S00415-017-8487-Y

7. Hollen CW, Soldán MMP, Rinker JR, II, Spain RI. The Future of Progressive Multiple Sclerosis Therapies. *Fed Pract*. 2020;37(Suppl 1):S43.

8. Cerqueira JJ, Compston DAS, Geraldes R, et al. Time matters in multiple sclerosis: can early treatment and long-term follow-up ensure everyone benefits from the latest advances in multiple sclerosis? *J Neurol Neurosurg Psychiatry*. 2018;89(8):844-850. doi:10.1136/JNNP-2017-317509

9. Ontaneda D, Tallantyre EC, Raza PC, et al. Determining the effectiveness of early intensive versus escalation approaches for the treatment of relapsing-remitting multiple sclerosis: The DELIVER-MS study protocol. *Contemp Clin Trials*. 2020;95:106009. doi:10.1016/J.CCT.2020.106009

10. Gajofatto A, Calabrese M, Benedetti MD, Monaco S. Clinical, MRI, and CSF Markers of Disability Progression in Multiple Sclerosis. *Dis Markers*. 2013;35(6):687. doi:10.1155/2013/484959

11. Rzepí Nski Ł, Zawadka-Kunikowska M, Maciejek Z, Newton JL, Zalewski P. Early Clinical Features, Time to Secondary Progression, and Disability Milestones in Polish Multiple Sclerosis Patients. *Medicina (B Aires)*. 2019;55(232). doi:10.3390/medicina55060232

12. Horakova D, Dwyer MG, Havrdova E, et al. Gray matter atrophy and disability progression in patients with early relapsing-remitting multiple sclerosis A 5-year longitudinal study. *J Neurol Sci*. 2009;282(1-2, SI):112-119. doi:10.1016/j.jns.2008.12.005

13. Charcot M. Histologie de la sclerose en plaque. In: Gaz. Hôsp.; 1868:41, 554-556.

14. Charcot JM, Marie P. Sur une forme particulière d'atrophie musculaire progressive : souvent familiale débutant par les pieds et les jambes et atteignant plus tard les mains. In: Félix Alcan; 1886:96-138.

15. Popescu V, Agosta F, Hulst HE, et al. Brain atrophy and lesion load predict long term disability in multiple sclerosis. *J Neurol Neurosurg Psychiatry*. 2013;84(10):1082-1091. doi:10.1136/jnnp-2012-304094

16. Zivadinov R, Sepcic J, Nasuelli D, et al. A longitudinal study of brain atrophy and cognitive disturbances in the early phase of relapsing-remitting multiple sclerosis. *J Neurol Neurosurg Psychiatry* . 2001;70(6):773-780. doi:10.1136/jnnp.70.6.773

17. Calabrese M, Agosta F, Rinaldi F, et al. Cortical lesions and atrophy associated with cognitive impairment in relapsing-remitting multiple sclerosis. *Arch Neurol*. 2009;66(9):1144-1150. doi:10.1001/Archneurol.2009.174

18. Tomic D, Kappos L, Meier DP, et al. Predictors of Conversion to Secondary Progressive Multiple Sclerosis in Patients With Relapsing–Remitting Multiple Sclerosis (P2.393). *Neurology*. 2018;90(15 Supplement).

19. Tur C, Grussu F, Kanber B, et al. Spatial distribution of MS lesions: New insights into white matter damage. *Mult Scler J*. 2018;24(2 Supplement):246. doi:10.1177/1352458518798582

20. Giovannoni G. Disease-modifying treatments for early and advanced multiple sclerosis: a new treatment paradigm. *Curr Opin Neurol*. 2018;31(3):233-243. doi:10.1097/WCO.0000000000000561

21. Compston A, Coles A. Multiple sclerosis. *Lancet*. 2008;372(9648):1502-1517. doi:10.1016/S0140-6736(08)61620-7

22. Frischer JM, Bramow S, Dal-Bianco A, et al. The relation between inflammation and neurodegeneration in multiple sclerosis brains. *Brain*. 2009;132(5):1175-1189. doi:10.1093/brain/awp070

23. Szczepaniak M, Dowden K, Jackson M, Verne J, Foster S, Sandhu S. Multiple sclerosis: prevalence, incidence and smoking status - data briefing. Gov.UK. Published 2020.

https://www.gov.uk/government/publications/multiple-sclerosis-prevalence-incidence-and-smoking-status/multiple-sclerosis-prevalence-incidence-and-smoking-status-data-briefing#content

24. Walton C, King R, Rechtman L, et al. Rising prevalence of multiple sclerosis worldwide: Insights from the Atlas of MS, third edition. *Mult Scler J*. 2020;26(14):1816-1821. doi:10.1177/1352458520970841

25. Trojano M, Lucchese G, Graziano G, et al. Geographical Variations in Sex Ratio Trends over Time in Multiple Sclerosis. Paul F, ed. *PLoS One*. 2012;7(10):e48078. doi:10.1371/journal.pone.0048078

26. Pugliatti M, Sotgiu S, Rosati G. The worldwide prevalence of multiple sclerosis. *Clin Neurol Neurosurg*. 2002;104(3):182-191. doi:10.1016/s0303-8467(02)00036-7

27. Kingwell E, Marriott JJ, Jetté N, et al. Incidence and prevalence of multiple sclerosis in Europe: a systematic review. *BMC Neurol*. 2013;13(1):128. doi:10.1186/1471-2377-13-128

28. Coles A. Multiple sclerosis: The bare essentials. *Pract Neurol*. 2009;9(2):118-126. doi:10.1136/jnnp.2008.171132

29. Nourbakhsh B, Mowry EM. Multiple sclerosis risk factors and pathogenesis. *Contin Lifelong Learn Neurol*. 2019;25(3):596-610. doi:10.1212/CON.0000000000000725

30. Ward M, Goldman MD. Epidemiology and Pathophysiology of Multiple Sclerosis. *Contin Lifelong Learn Neurol*. 2022;28(4):988-1005. doi:10.1212/CON.0000000000001136

31. Leray E, Moreau T, Fromont A, Edan G. Epidemiology of multiple sclerosis. *Rev Neurol (Paris)*. 2016;172(1):3-13. doi:10.1016/J.Neurol.2015.10.006

32. Taan M, Al Ahmad F, Ercksousi MK, Hamza G. Risk Factors Associated with Multiple Sclerosis: A Case-Control Study in Damascus, Syria. *Mult Scler Int*. 2021;2021:1-5. doi:10.1155/2021/8147451

33. Adamczyk- Sowa M, Gębka- Kępińska B, Kępiński M. MULTIPLE SCLEROSIS – RISK FACTORS. *Wiadomości Lek*. 2020;73(12):2677-2682. doi:10.36740/WLek202012122

34. Dendrou CA, Fugger L, Friese MA. Immunopathology of multiple sclerosis. *Nat Rev Immunol*. 2015;15(9):545-558. doi:10.1038/nri3871

35. Orrell RW. Multiple Sclerosis: The History of a Disease. *J R Soc Med*. 2005;98(6):289-289. doi:10.1177/014107680509800616

36. Ford H. Clinical presentation and diagnosis of multiple sclerosis. *Clin Med (Northfield Il)*. 2020;20(4):380. doi:10.7861/Clinmed.2020-0292

37. Dutta R, Trapp BD. Relapsing and progressive forms of multiple sclerosis. *Curr Opin Neurol*. 2014;27(3):271-278. doi:10.1097/WCO.0000000000000094

38. Lublin FD, Reingold SC, Cohen JA, et al. Defining the clinical course of multiple sclerosis: the 2013 revisions. *Neurology*. 2014;83(3):278-286. doi:10.1212/WNL.0000000000000560

39. Ghasemi N, Razavi S, Nikzad E. Multiple Sclerosis: Pathogenesis, Symptoms, Diagnoses andCell-Based Therapy. *Cell J*. 2017;19(1):1. doi:10.22074/Cellj.2016.4867

40. Efendi H. Clinically Isolated Syndromes: Clinical Characteristics, Differential Diagnosis, and Management. *Nöro Psikiyatr Arşivi*. 2015;52(Suppl 1):S1. doi:10.5152/NPA.2015.12608

41. Brownlee WJ, Miller DH. Clinically isolated syndromes and the relationship to multiple sclerosis. *J Clin Neurosci*. 2014;21(12):2065-2071. doi:10.1016/j.jocn.2014.02.026

42. Kim S-H, Hyun J-W, Blackburn K, Blackburn KM, Greenberg BM. Revisiting Transverse Myelitis: Moving Toward a New Nomenclature. *Front Neurol*. 2020;11:519468. doi:10.3389/fneur.2020.519468

43. Moraal B, Pohl C, Uitdehaag BMJ, et al. Magnetic Resonance Imaging Predictors of Conversion to Multiple Sclerosis in the BENEFIT Study. *Arch Neurol*. 2009;66(11):1345-1352. doi:10.1001/Archneurol.2009.243

44. Patrucco L, Rojas JI, Miguez JS, Cristiano E. Application of the McDonald 2010 criteria for the diagnosis of multiple sclerosis in an Argentinean cohort of patients with clinically isolated syndromes. *Mult Scler*. 2013;19(10):1297-1301. doi:10.1177/1352458513475492

45. Marcus JF, Waubant EL. Updates on Clinically Isolated Syndrome and Diagnostic Criteria for Multiple Sclerosis. *The Neurohospitalist*. 2013;3(2):65. doi:10.1177/1941874412457183

46. Fisniku LK, Brex PA, Altmann DR, et al. Disability and T2 MRI lesions: a 20-year follow-up of patients with relapse onset of multiple sclerosis. *Brain*. 2008;131(3):808-817. doi:10.1093/brain/awm329

47. Confavreux C, Aimard G, Devic M. Course and prognosis of multiple sclerosis assessed by the computerized data processing of 349 patients. *Brain*. 1980;103(2):281-300. doi:10.1093/Brain/103.2.281

48. Scalfari A, Neuhaus A, Daumer M, Muraro PA, Ebers GC. Onset of secondary progressive phase and long-term evolution of multiple sclerosis. *J Neurol Neurosurg Psychiatry*. 2014;85(1):67-75. doi:10.1136/jnnp-2012-304333

49. Scalfari A, Neuhaus A, Degenhardt A, et al. The natural history of multiple sclerosis, a

geographically based study 10: relapses and long-term disability. *Brain*. 2010;133(7):1914-1929. doi:10.1093/brain/awq118

50. Trojano M, Paolicelli D, Bellacosa A, Cataldo S. The transition from relapsing-remitting MS to irreversible disability: clinical evaluation. *Neurol Sci*. 2003;24(0):s268-s270. doi:10.1007/s10072-003-0171-6

51. Thompson AJ, Banwell BL, Barkhof F, et al. Diagnosis of multiple sclerosis: 2017 revisions of the McDonald criteria. *Lancet Neurol*. 2018;17(2):162-173. doi:10.1016/S1474-4422(17)30470-2

52. Beesley R, Anderson V, Harding KE, et al. Impact of the 2017 revisions to McDonald criteria on the diagnosis of multiple sclerosis. *Mult Scler*. 2018;24(13):1786-1787. doi:10.1177/1352458518778007

53. Lechner-Scott J, Spencer B, De Malmanche T, et al. The frequency of CSF oligoclonal banding in multiple sclerosis increases with latitude. *Mult Scler*. 2012;18(7):974-982. doi:10.1177/1352458511431729

54. Hansen K, Cruz M, Link H. Oligoclonal Borrelia burgdorferi-specific IgG antibodies in cerebrospinal fluid in Lyme neuroborreliosis. *J Infect Dis*. 1990;161(6):1194-1202. doi:10.1093/Infdis/161.6.1194

55. Bergamaschi R, Tonietti S, Franciotta D, et al. Oligoclonal bands in Devic's neuromyelitis optica and multiple sclerosis: differences in repeated cerebrospinal fluid examinations. *Mult Scler*. 2004;10(1):2-4. doi:10.1191/1352458504MS988OA

56. Ernerudh J, Olsson T, Lindstromt F, Skogh T. Cerebrospinal fluid immunoglobulin abnormalities in systemic lupus erythematosus. *J Neurol Neurosurg Psychiatry*. 1985;48(8):807. doi:10.1136/Jnnp.48.8.807

57. Weinshenker BG, Bass B, Rice GPA, et al. The natural history of multiple sclerosis: a geographically based study. I. Clinical course and disability. *Brain*. 1989;112 (Pt 1(1):133-146. doi:10.1093/Brain/112.1.133

58. Eriksson M, Andersen O, Runmarker B. Long-term follow up of patients with clinically isolated syndromes, relapsing-remitting and secondary progressive multiple sclerosis. *Mult Scler*. 2003;9(3):260-274. doi:10.1191/1352458503MS914OA

59. Wingerchuk DM, Banwell B, Bennett JL, et al. *International Consensus Diagnostic Criteria for Neuromyelitis Optica Spectrum Disorders*. Vol 85.; 2015. doi:10.1212/wnl.0000000000001729

60. Confavreux C, Vukusic S. Age at disability milestones in multiple sclerosis. *Brain*. 2006;129(3):595-605. doi:10.1093/brain/awh714

61. Weinshenker BG, Bass B, Rice GPA, et al. The natural history of multiple sclerosis: A geographically based study: 2 predictive value of the early clinical course. *Brain*. 1989;112(6):1419-1428. doi:10.1093/brain/112.6.1419

62. Miller D, Barkhof F, Montalban X, Thompson A, Filippi M. Clinically isolated syndromes suggestive of multiple sclerosis, part I: natural history, pathogenesis, diagnosis, and prognosis. *Lancet Neurol*. 2005;4(5):281-288. doi:10.1016/S1474-4422(05)70071-5

63. Kurtzke JF. Rating neurologic impairment in multiple sclerosis. *Neurology*. 1983;33(11).

64. Kremenchutzky M, Rice GPA, Baskerville J, Wingerchuk DM, Ebers GC. The natural history of multiple sclerosis: A geographically based study 9: Observations on the progressive phase of the disease. *Brain*. 2006;129(3):584-594. doi:10.1093/brain/awh721

65. Confavreux C, Vukusic S, Moreau T, Adeleine P. Relapses and Progression of Disability in Multiple Sclerosis. *N Engl J Med*. 2000;343(20):1430-1438. doi:10.1056/Nejm200011163432001

66. Roxburgh RHSR, Seaman SR, Masterman T, et al. Multiple Sclerosis Severity Score: using disability and disease duration to rate disease severity. *Neurology*. 2005;64(7):1144-1151. doi:10.1212/01.WNL.0000156155.19270.F8

67. Manouchehrinia A, Westerlind H, Kingwell E, et al. Age Related Multiple Sclerosis Severity Score: Disability ranked by age. *Mult Scler*. 2017;23(14):1938. doi:10.1177/1352458517690618

68. Ebers GC, Daumer M. Natural history of MS. *Eur J Neurol*. 2008;15(9):881-882. doi:10.1111/J.1468-1331.2008.02245.X

69. Harding K, Anderson V, Williams O, et al. A contemporary study of mortality in the multiple sclerosis population of south east Wales. *Mult Scler Relat Disord*. 2018;25:186-191. doi:10.1016/J.MSARD.2018.08.001

70. Rolak LA. Multiple sclerosis: it's not the disease you thought it was. *Clin Med Res*. 2003;1(1):57-60. doi:10.3121/cmr.1.1.57

71. Mistry N, Tallantyre EC, Dixon JE, et al. Focal multiple sclerosis lesions abound in normal appearing white matter. *Mult Scler J*. 2011;17(11):1313-1323. doi:10.1177/1352458511415305

72. Calabrese M, Favaretto A, Martini V, Gallo P. Grey matter lesions in MS: from histology to clinical implications. *Prion*. 2013;7(1):20-27. doi:10.4161/pri.22580

73. Evangelou N, Konz D, Esiri MM, Smith S, Palace J, Matthews PM. Regional axonal loss in the corpus callosum correlates with cerebral white matter lesion volume and distribution in multiple sclerosis. *BRAIN*. 2000;123(9):1845-1849. doi:10.1093/brain/123.9.1845

74. Trip SA, Miller DH. Imaging in multiple sclerosis. *J Neurol Neurosurg Psychiatry*. 2005;76 Suppl 3(suppl 3):iii11-iii18. doi:10.1136/jnnp.2005.073213

75. Popescu BFG, Lucchinetti CF. Pathology of demyelinating diseases. *Annu Rev Pathol*. 2012;7:185-217. doi:10.1146/annurev-pathol-011811-132443

76. Giorgio A, De Stefano N, A. G, Giorgio A, De Stefano N, A. G. Advanced Structural and Functional Brain MRI in Multiple Sclerosis. *Semin Neurol*. 2016;36(2):163-176. doi:10.1055/s-0036-1579737

77. Dawson J. *The Histology of Disseminated Sclerosis* . Vol 50. Trans R Soc; 1916.
78. Birnbaum G. *Multiple Sclerosis : Clinician's Guide to Diagnosis and Treatment.* Oxford University Press, USA; 2013.

79. Keirstead HS, Blakemore WF. The role of oligodendrocytes and oligodendrocyte progenitors in CNS remyelination. Matsas, R and Tsacopoulos M, ed. *Adv Exp Med Biol*. 1999;468:183-197. doi:10.1007/978-1-4615-4685-6_15

80. Brück W, Porada P, Poser S, et al. Monocyte/macrophage differentiation in early multiple sclerosis lesions. *Ann Neurol*. 1995;38(5):788-796. doi:10.1002/ANA.410380514

81. Lucchinetti C, Brück W, Parisi J, Scheithauer B, Rodriguez M, Lassmann H. A quantitative analysis of oligodendrocytes in multiple sclerosis lesions. A study of 113 cases. *Brain*. 1999;122 (Pt 1(12):2279-2295. doi:10.1093/Brain/122.12.2279

82. Brück W, Sommermeier N, Bergmann M, et al. Macrophages in Multiple Sclerosis. *Immunobiology*. 1996;195(4-5):588-600. doi:10.1016/S0171-2985(96)80024-6

83. Laron M, Han Cheng, Bin Zhang, Schiffman JS, Tang RA, Frishman LJ. Comparison of multifocal visual evoked potential, standard automated perimetry and optical coherence tomography in assessing visual pathway in multiple sclerosis patients. *Mult Scler J*. 2010;16(4):412-426. doi:10.1177/1352458509359782

84. Kuhlmann T, Ludwin S, Prat A, Antel J, Brück W, Lassmann H. An updated histological classification system for multiple sclerosis lesions. *Acta Neuropathol*. 2017;3:13-24. doi:10.1007/s00401-016-1653-y

85. Wu E, Raine C. Multiple sclerosis. Interactions between oligodendrocytes and hypertrophic astrocytes and their occurrence in other, nondemyelinating conditions - PubMed. *Lab Invest*. 1992;67:88-99.

86. Lassmann H. Neuropathology in multiple sclerosis: new concepts. *Mult Scler*. 1998;4(3):93-98. doi:10.1177/135245859800400301

87. Sahraian MA, Radue E-WW, Haller S, Kappos L. Black holes in multiple sclerosis: definition, evolution, and clinical correlations. *Acta Neurol Scand*. 2009;122(1):1-8.

doi:10.1111/j.1600-0404.2009.01221.x

88. Barkhof F. The clinico-radiological paradox in multiple sclerosis revisited. *Curr Opin Neurol*. 2002;15(3):239-245. doi:10.1097/00019052-200206000-00003

89. Lai M, Hodgson T, Gawne-Cain M, et al. A preliminary study into the sensitivity of disease activity detection by serial weekly magnetic resonance imaging in multiple sclerosis. *J Neurol Neurosurg Psychiatry*. 1996;60(3):339-341. doi:10.1136/JNNP.60.3.339

90. Guttmann CRG, Rousset M, Roch JA, et al. Multiple sclerosis lesion formation and early evolution revisited: A weekly high-resolution magnetic resonance imaging study. *Mult Scler*. 2016;22(6):761-769. doi:10.1177/1352458515600247

91. Barkhof F, Scheltens P, Frequin ST, et al. Relapsing-remitting multiple sclerosis: sequential enhanced MR imaging vs clinical findings in determining disease activity. *AJR Am J Roentgenol*. 1992;7:1041.

92. Filippi M, Horsfield MA, Hajnal J V, et al. Quantitative assessment of magnetic resonance imaging lesion load in multiple sclerosis. *J Neurol Neurosurg PSYCHIATRY*. 1998;64(1):S88-S93.

93. Narayana PA, Doyle TJ, Lai D, Wolinsky JS. Serial proton magnetic resonance spectroscopic imaging, contrast-enhanced magnetic resonance imaging, and quantitative lesion volumetry in multiple sclerosis. *Ann Neurol*. 1998;43(1):56-71. doi:10.1002/ana.410430112

94. Werring DJ, Brassat D, Droogan AG, et al. The pathogenesis of lesions and normal-appearing white matter changes in multiple sclerosis: a serial diffusion MRI study. *Brain*. 2000;123 (Pt 8(8):1667-1676. doi:10.1093/Brain/123.8.1667

95. Wuerfel J, Bellmann-Strobl J, Brunecker P, et al. Changes in cerebral perfusion precede plaque formation in multiple sclerosis: a longitudinal perfusion MRI study. *Brain*. 2004;127(Pt 1):111-119. doi:10.1093/Brain/AWH007

96. De Groot CJA, Bergers E, Kamphorst W, et al. Post-mortem MRI-guided sampling of multiple sclerosis brain lesions: increased yield of active demyelinating and (p)reactive lesions. *Brain*. 2001;124(Pt 8):1635-1645. doi:10.1093/BRAIN/124.8.1635

97. Van Der Valk P, Amor S. Preactive lesions in multiple sclerosis. *Curr Opin Neurol*. 2009;22(3):207-213. doi:10.1097/WCO.0B013E32832B4C76

98. Kemper TL. Neuroanatomical and neuropathological changes during aging and dementia. - PsycNET. *Clin Neurol aging*. Published online 1994:3-67.

99. Hedman AM, van Haren NEM, Schnack HG, Kahn RS, Hulshoff Pol HE. Human brain changes across the life span: a review of 56 longitudinal magnetic resonance imaging

studies. *Hum Brain Mapp*. 2012;33(8):1987-2002. doi:10.1002/hbn.21334

100. Svennerholm L, Boström K, Jungbjer B. Changes in weight and compositions of major membrane components of human brain during the span of adult human life of Swedes. *Acta Neuropathol*. 1997;94(4):345-352. doi:10.1007/S004010050717

101. Vollmer T, Signorovitch J, Huynh L, et al. The natural history of brain volume loss among patients with multiple sclerosis: a systematic literature review and meta-analysis. *J Neurol Sci*. 2015;357(1-2):8-18. doi:10.1016/J.jns.2015.07.014

102. De Stefano N, Stromillo ML, Giorgio A, et al. Establishing pathological cut-offs of brain atrophy rates in multiple sclerosis. *J Neurol Neurosurg Psychiatry* . 2016;87(1):93-99. doi:10.1136/jnnp-2014-309903

103. De Stefano N, Giorgio A, Battaglini M, et al. Assessing brain atrophy rates in a large population of untreated multiple sclerosis subtypes. *Neurology*. 2010;74(23):1868-1876. doi:10.1212/WNL.0B013E3181E24136

104. Pérez-Miralles F, Sastre-Garriga J, Tintoré M, et al. Clinical impact of early brain atrophy in clinically isolated syndromes. *Mult Scler*. 2013;19(14):1878-1886. doi:10.1177/1352458513488231

105. Miller DH, Barkhof F, Frank JA, Parker GJM, Thompson AJ. Measurement of atrophy in multiple sclerosis: pathological basis, methodological aspects and clinical relevance. *Brain*. 2002;125(8):1676-1695. doi:10.1093/brain/awf177

106. Sormani M, Arnold D, De Stefano N. Treatment effect on brain atrophy correlates with treatment effect on disability in multiple sclerosis. *Ann Neurol*. 2014;75(1):43-49. doi:10.1002/ana.24018

107. Bartzokis G, Cummings JL, Sultzer D, Henderson VW, Nuechterlein KH, Mintz J. White matter structural integrity in healthy aging adults and patients with Alzheimer disease: a magnetic resonance imaging study. *Arch Neurol*. 2003;60(3):393-398. doi:10.1001/Archneur.60.3.393

108. Bartzokis G, Sultzer D, Lu PH, Nuechterlein KH, Mintz J, Cummings JL. Heterogeneous age-related breakdown of white matter structural integrity: implications for cortical "'disconnection'" in aging and Alzheimer's disease. *Neurobiol Aging*. 2004;7(25):843-851. doi:10.1016/j.neurobiolaging.2003.09.005

109. Sachdev P, Wen W, Chen X, Brodaty H. Progression of white matter hyperintensities in elderly individuals over 3 years. *Neurology*. 2007;68(3):214-222. doi:10.1212/01.WNL.0000251302.55202.73

110. Pantoni L, Garcia JH. The significance of cerebral white matter abnormalities 100 years after Binswanger's report. A review. *Stroke*. 1995;26(7):1293-1301.

doi:10.1161/01.str.26.7.1293

111. Madden DJ, Bennett IJ, Burzynska A, Potter GG, Chen N kuei, Song AW. Diffusion tensor imaging of cerebral white matter integrity in cognitive aging. *Biochim Biophys Acta*. 2012;1822(3):386-400. doi:10.1016/j.bbadis.2011.08.003

112. Dalton CM, Chard DT, Davies GR, et al. Early development of multiple sclerosis is associated with progressive grey matter atrophy in patients presenting with clinically isolated syndromes. *BRAIN*. 2004;127(5):1101-1107. doi:10.1093/brain/awh126

113. Zivadinov R, Uher T, Hagemeier J, et al. A serial 10-year follow-up study of brain atrophy and disability progression in RRMS patients. *Mult Scler*. 2016;22(13):1709-1718. doi:10.1177/1352458516629769

114. Maghzi A-H, Revirajan N, Julian LJ, et al. Magnetic resonance imaging correlates of clinical outcomes in early multiple sclerosis. *Mult Scler Relat Disord*. 2014;3(6):720-727. doi:10.1016/j.msard.2014.07.003

115. Sastre-Garriga J, Pareto D, Rovira À. Brain Atrophy in Multiple Sclerosis: Clinical Relevance and Technical Aspects. *Neuroimaging Clin N Am*. 2017;27(2):289-300. doi:10.1016/J.NIC.2017.01.002

116. Thorpe JW, Kidd D, Kendall BE, et al. Spinal cord MRI using multi-array coils and fast spin echo. *Mult Scler J*. 1993;43(12):2625-2625. doi:10.1212/WNL.43.12.2625

117. Thorpe JW, Kidd D, Moseley IF, et al. Spinal MRI in patients with suspected multiple sclerosis and negative brain MRI. *Brain*. 1996;119 (Pt 3(3):709-714. doi:10.1093/brain/119.3.709

118. Oppenheimer DR. The cervical cord in Multiple Sclerosis. *Neuropathol Appl Neurobiol*. 1978;4(2):151-162. doi:10.1111/J.1365-2990.1978.TB00555.X

119. Evangelou N, DeLuca GC, Owens T, Esiri MM. Pathological study of spinal cord atrophy in multiple sclerosis suggests limited role of local lesions. *BRAIN*. 2005;128(1):29-34. doi:10.1093/brain/awh323

120. Ganter P, Prince C, Esiri MM. Spinal cord axonal loss in multiple sclerosis: a post-mortem study. *Neuropathol Appl Neurobiol*. 1999;25(6):459-467. doi:10.1046/J.1365-2990.1999.00205.X

121. Bot JCJ, Barkhof F, Polman CH, et al. Spinal cord abnormalities in recently diagnosed MS patients. *Neurology*. 2004;62(2):226-233. doi:10.1212/WNL.62.2.226

122. Bergers E, Bot JCJ, De Groot CJA, et al. Axonal damage in the spinal cord of MS patients occurs largely independent of T2 MRI lesions. *Neurology*. 2002;59(11):1766-1771. doi:10.1212/01.WNL.0000036566.00866.26

123. Losseff NA, Wang L, Lai HM, et al. Progressive cerebral atrophy in multiple sclerosis - A serial MRI study. *BRAIN*. 1996;119(6):2009-2019. doi:10.1093/brain/119.6.2009

124. Lukas C, Bellenberg B, Popescu V. Relevance of Spinal Cord Abnormalities to Clinical Disability in Multiple Sclerosis: MR Imaging Findings in a Large Cohort of Patients Neurobiology of heroin-assisted therapy View project Burden of disability View project. *Radiology*. Published online 2013. doi:10.1148/radiol.13122566

125. Lukas C, Knol DL, Sombekke MH, et al. Cervical spinal cord volume loss is related to clinical disability progression in multiple sclerosis. *J Neurol Neurosurg Psychiatry*. 2015;86(4):410-418. doi:10.1136/JNNP-2014-308021

126. Edan G, Comi G, Le Page E, et al. Mitoxantrone prior to interferon beta-1b in aggressive relapsing multiple sclerosis: a 3-year randomised trial. *J Neurol Neurosurg PSYCHIATRY*. 2011;82(12):1344-1350. doi:10.1136/jnnp.2010.229724

127. Rocca MA, Horsfield MA, Sala S, et al. A multicenter assessment of cervical cord atrophy among MS clinical phenotypes. *Neurology*. 2011;76(24):2096-2102. doi:10.1212/wnl.0B013E31821F46B8

128. Brex PA, Leary SM, O'Riordan JI, et al. Measurement of spinal cord area in clinically isolated syndromes suggestive of multiple sclerosis. *J Neurol Neurosurg PSYCHIATRY*. 2001;70(4):544-547. doi:10.1136/jnnp.70.4.544

129. Daams M, Steenwijk MD, Wattjes MP, et al. Unraveling the neuroimaging markers of motor dysfunction in long-standing multiple sclerosis. *Mult Scler*. 2014;20(1 SUPPL. 1):277. doi:10.1177/1352458514546077

130. Kearney H, Rocca MA, Valsasina P, et al. Magnetic resonance imaging correlates of physical disability in relapse onset multiple sclerosis of long disease duration. *Mult Scler*. 2014;20(1):72-80. doi:10.1177/1352458513492245

131. Swanton JK, Fernando KT, Dalton CM, et al. Early MRI in optic neuritis: The risk for clinically definite multiple sclerosis. *Mult Scler*. 2009;16(2):156-165. doi:10.1177/1352458509353650

132. O'Connor P, Comi G, Montalban X, et al. Oral fingolimod (FTY720) in multiple sclerosis: two-year results of a phase II extension study. *Neurology*. 2009;72(1):73-79. doi:10.1212/01.wnl.0000338569.32367.3d

133. Beck RW, Chandler DL, Cole SR, et al. Interferon β-1a for early multiple sclerosis: CHAMPS trial subgroup analyses. *Ann Neurol*. 2002;51(4):481-490. doi:10.1002/ana.10148

134. Comi G, Filippi M, Barkhof F, et al. Effect of early interferon treatment on conversion to definite multiple sclerosis: a randomised study. *Lancet*. 2001;357(9268):1576-1582.

doi:10.1016/S0140-6736(00)04725-5

135. Comi G. Shifting the paradigm toward earlier treatment of multiple sclerosis with interferon beta. *Clin Ther*. 2009;31(6):1142-1157. doi:10.1016/J.Clinthera.2009.06.007

136. Kappos L, Freedman MS, Polman CH, et al. Effect of early versus delayed interferon beta-1b treatment on disability after a first clinical event suggestive of multiple sclerosis: a 3-year follow-up analysis of the BENEFIT study. *Lancet (London, England)*. 2007;370(9585):389-397. doi:10.1016/S0140-6736(07)61194-5

137. La Mantia L, Di Pietrantonj C, Rovaris M, et al. Interferons-beta versus glatiramer acetate for relapsing-remitting multiple sclerosis. *Cochrane Database Syst Rev*. 2016;(11). doi:10.1002/14651858.CD009333.pub3

138. La Mantia L, Di Pietrantonj C, Rovaris M, et al. Interferons-beta versus glatiramer acetate for relapsingremitting multiple sclerosis. *Cochrane Database Syst Rev*. 2014;(7). doi:10.1002/14651858.CD009333.pub2

139. Kappos L, Radue E-W, O'Connor P, et al. A placebo-controlled trial of oral fingolimod in relapsing multiple sclerosis. *N Engl J Med*. 2010;362(5):387-401. doi:10.1056/Nejmoa0909494

140. Polman CH, O'Connor PW, Havrdova E, et al. A Randomized, Placebo-Controlled Trial of Natalizumab for Relapsing Multiple Sclerosis. *N Engl J Med*. 2006;354(9):899-910. doi:10.1056/Nejmoa044397

141. Rudick RA, Stuart WH, Calabresi PA, et al. Natalizumab plus Interferon Beta-1a for Relapsing Multiple Sclerosis. *N Engl J Med*. 2006;354(9):911-923. doi:10.1056/nejmoa044396

142. Lamb YN. Ocrelizumab: A Review in Multiple Sclerosis. *Drugs*. 2022;82(3):323-334. doi:10.1007/S40265-022-01672-9

143. Miller DH, Soon D, Fernando KT, et al. MRI outcomes in a placebo-controlled trial of natalizumab in relapsing MS. *Neurology*. 2007;68(17):1390-1401. doi:10.1212/01.WNL.0000260064.77700.FD

144. Kappos L, Bar-Or A, Cree BAC, et al. Siponimod versus placebo in secondary progressive multiple sclerosis (EXPAND): a double-blind, randomised, phase 3 study. *Lancet*. 2018;391(10127):1263-1273. doi:10.1016/S0140-6736(18)30475-6

145. Clifford DB, DeLuca A, Simpson DM, Arendt G, Giovannoni G, Nath A. Natalizumab-associated progressive multifocal leukoencephalopathy in patients with multiple sclerosis: lessons from 28 cases. *Lancet Neurol*. 2010;9(4):438-446. doi:10.1016/S1474-4422(10)70028-4

146. Yousry TA, Major EO, Ryschkewitsch C, et al. Evaluation of Patients Treated with Natalizumab for Progressive Multifocal Leukoencephalopathy. *N Engl J Med*. 2006;354(9):924-933. doi:10.1056/Nejmoa054693

147. Beck RW. Corticosteroid treatment of optic neuritis: a need to change treatment practices. The Optic Neuritis Study Group. *Neurology*. 1992;42(6):1133-1135. doi:10.1212/WNL.42.6.1133

148. Freeman JA, Langdon DW, Hobart JC, Thompson AJ. The impact of inpatient rehabilitation on progressive multiple sclerosis. *Ann Neurol*. 1997;42(2):236-244. doi:10.1002/ana.410420216

149. Thompson AJ, Toosy AT, Ciccarelli O. Pharmacological management of symptoms in multiple sclerosis: current approaches and future directions. *Lancet Neurol*. 2010;9(12):1182-1199. doi:10.1016/S1474-4422(10)70249-0

150. Westbrook C. *MRI at Aglance*. 2nd ed. wiley-blackwel; 2010.

151. Altokhis A. *What Are T1,T2,PD and How Do They Contribute to Image Contrast in Conventional Spin Echo and Inversion Recovery MR Imaging?*; 2017.

152. McRobbie DW, Moore EA, Graves MJ, Prince MR. *MRI From Picture to Proton*.; 2010.

153. Dale BM, Brown MA, Semelka RC. *MRI : Basic Principles and Applications*. fifth. Wiley Blackwell; 2015.

154. Maciver CL, Ebden S, Tallantyre EC. MRI: how to understand it. *Pract Neurol*. 2021;21(3):216-224. doi:10.1136/PRACTNEUROL-2020-002905

155. Westbrook C. *MRI at a Glance*. 3rd ed. Blackwell Science; 2015.

156. Westbrook C, Talbot J. *MRI in Practice*. 5th ed. Wiley-Blackwell; 2005.

157. Barnes SRS, Haacke EM. Susceptibility-weighted imaging: clinical angiographic applications. *Magn Reson Imaging Clin N Am*. 2009;17(1):47-61. doi:10.1016/j.mric.2008.12.002

158. Ashwal S, Babikian T, Gardner-Nichols J, Freier M-C, Tong KA, Holshouser BA. Susceptibility-Weighted Imaging and Proton Magnetic Resonance Spectroscopy in Assessment of Outcome After Pediatric Traumatic Brain Injury. *Arch Phys Med Rehabil*. 2006;87(12):50-58. doi:10.1016/j.apmr.2006.07.275

159. Haller S, Haacke EM, Thurnher MM, Barkhof F. Susceptibility-weighted imaging: Technical essentials and clinical neurologic applications. *Radiology*. 2021;299(1):3-26. doi:10.1148/radiol.2021203071/asset/images/large/radiol.2021203071.fig27.jpeg

160. Calvi A, Haider L, Prados F, Tur C, Chard D, Barkhof F. In vivo imaging of chronic active lesions in multiple sclerosis. *Mult Scler*. 2022;28(5):683-690. doi:10.1177/1352458520958589

161. Dietrich O, Raya JG, Reeder SB, Reiser MF, Schoenberg SO. Measurement of signal-to-noise ratios in MR images: Influence of multichannel coils, parallel imaging, and reconstruction filters. *J Magn Reson Imaging*. 2007;26(2):375-385. doi:10.1002/JMRI.20969

162. Magnotta VA, Friedman L. Measurement of Signal-to-Noise and Contrast-to-Noise in the fBIRN Multicenter Imaging Study. *J Digit Imaging*. 2006;19(2):140. doi:10.1007/S10278-006-0264-X

163. Cosottini M, Roccatagliata L. Neuroimaging at 7 T: are we ready for clinical transition? *Eur Radiol Exp*. 2021;5(1):1-5. doi:10.1186/S41747-021-00234-0/Metrics

164. Trattnig S, Bogner W, Gruber S, et al. Clinical applications at ultrahigh field (7 T). Where does it make the difference? *NMR Biomed*. 2016;29(9):1316-1334. doi:10.1002/nbm.3272

165. Kollia K, Maderwald S, Putzki N, et al. First Clinical Study on Ultra-High-Field MR Imaging in Patients with Multiple Sclerosis: Comparison of 1.5T and 7T. *Am J Neuroradiol*. 2009;19(8):1489-1493. doi:10.3174/ajnr.a1434

166. Sati P, Oh J, Constable RT, et al. The central vein sign and its clinical evaluation for the diagnosis of multiple sclerosis: a consensus statement from the North American Imaging in Multiple Sclerosis Cooperative. *Nat Rev Neurol*. 2016;12(12):714-722. doi:10.1038/nrneurol.2016.166

167. Chawla S, Kister I, Sinnecker T, et al. Longitudinal study of multiple sclerosis lesions using ultra-high field (7T) multiparametric MR imaging. Jiang Q, ed. *PLoS One*. 2018;13(9):e0202918. doi:10.1371/journal.pone.0202918

168. Absinta M, Sati P, Fechner A, Schindler MK, Reich DS. 3T MRI detection of 7T paramagnetic rims in multiple sclerosis lesions: A step toward the clinical application. *Mult Scler J*. 2017;23(3 Supplement 1):79-80. doi:10.1177/1352458517731283

169. Haacke EM, Liu S, Buch S, Zheng W, Wu D, Ye Y. Quantitative susceptibility mapping: current status and future directions. *Magn Reson Imaging*. 2015;33(1):1-25. doi:10.1016/j.mri.2014.09.004

170. Tallantyre EC, Morgan PS, Dixon JE, et al. A Comparison of 3T and 7T in the Detection of Small Parenchymal Veins Within MS Lesions. *Invest Radiol*. 2009;44(9):491-494. doi:10.1097/RLI.0b013e3181b4c144

171. Kilsdonk ID, Jonkman L, Klaver R, et al. Increased Cortical Grey Matter Lesion Detection in Multiple Sclerosis With 7 T MRI: A Post-Mortem Verification Study. *Brain*. 2016;139(Pt

5). doi:10.1093/BRAIN/AWW037

172. LassmannASSMANN H. From neuropathology to new patho-physiological concepts and clinical perspectives. In: ECTRIMS-ACTRIMS; 2017:202447; 92. doi:10/26/17

173. Balchandani P, Naidich T. Ultra-High-Field MR Neuroimaging. *AJNR Am J Neuroradiol*. 2015;36(7). doi:10.3174/AJNR.A4180

174. Biller A, Choli M, Blaimer M, Breuer FA, Jakob PM, Bartsch AJ. Combined Acquisition Technique (CAT) for Neuroimaging of Multiple Sclerosis at Low Specific Absorption Rates (SAR). Kleinschnitz C, ed. *PLoS One*. 2014;9(3):e91030. doi:10.1371/journal.pone.0091030

175. Mahajan KR, Ontaneda D. The Role of Advanced Magnetic Resonance Imaging Techniques in Multiple Sclerosis Clinical Trials. *Neurotherapeutics*. 2017;14(4):905-923. doi:10.1007/s13311-017-0561-8

176. Rees JH. Diagnosis and treatment in neuro-oncology: An oncological perspective. *Br J Radiol*. 2011;84(SPEC. ISSUE 2). doi:10.1259/bjr/18061999

177. Karakasis C, Bricker A, Stephen J. Magnetic Resonance Imaging in Multiple Sclerosis. In: Fox RJ, Rae-Grant AD, Bethoux F, eds. *Multiple Sclerosis and Related Disorders : Clinical Guide to Diagnosis, Medical Management, and Rehabilitation*. second. ; 2019:64-66.

178. Traboulsee A. MRI relapses have significant pathologic and clinical implications in multiple sclerosis. *J Neurol Sci*. 2007;256:S19-S22. doi:10.1016/J.JNS.2007.01.064

179. Karabudak R. Magnetic Resonance Imaging as a Major Milestone in Multiple Sclerosis Diagnosis and Treatment. *Noro Psikiyatr Ars*. 2015;52(Suppl 1):S16-S24. doi:10.5152/npa.2015.12576

180. Robert T. Naismith M. "Black Holes" and Long-Term Disability in Multiple Sclerosis. *NEJM J Watch*. 2013;2013. doi:10.1056/NEJM-JW.NA31801

181. Rovira Á, Wattjes MP, Tintoré M, et al. Evidence-based guidelines: MAGNIMS consensus guidelines on the use of MRI in multiple sclerosis-clinical implementation in the diagnostic process. *Nat Rev Neurol*. 2015;11(8):471-482. doi:10.1038/NRNEUROL.2015.106

182. Rovira A, Auger C. Spinal Cord in Multiple Sclerosis: Magnetic Resonance Imaging Features and Differential Diagnosis. *Semin Ultrasound CT MR*. 2016;37(5):396-410. doi:10.1053/J.SULT.2016.05.005

183. Kuchling J, Sinnecker T, Bozin I, et al. Ultrahigh field MRI in context of neurological diseases. *Nervenarzt*. 2014;85(4):445-458. doi:10.1007/s00115-013-3967-5

184. Kilsdonk ID, Lopez-Soriano A, Kuijer JPA, et al. Morphological features of multiple

sclerosis lesions on FLAIR* at 7 Tesla and their relation to patient characteristics. *J Neurol*. 2014;19:1356-1364. doi:10.1007/s00415-014-7351-6

185. Sati P, George IC, Shea CD, et al. Flair*: A Combined MR Contrast Technique for Visualizing White Matter Lesions and Parenchymal Veins 1. *Radiol n Radiol*. 2012;265(3):926-932. doi:10.1148/radiol.12120208

186. Kuchling J, Ramien C, Bozin I, et al. Identical lesion morphology in primary progressive and relapsing-remitting MS - an ultrahigh field MRI study. *Mult Scler*. 2014;20(14):1866-1871. doi:10.1177/1352458514531084

187. Tan IL, Van Schijndel RA, Pouwels PJW, et al. MR Venography of Multiple Sclerosis. *AJNR Am J Neuroradiol*. 2000;21(6):1039.

188. Tallantyre EC, Brookes MJ, Dixon JE, Morgan PS, Evangelou N, Morris PG. Demonstrating the perivascular distribution of MS lesions in vivo with 7-Tesla MRI. *Neurology*. 2008;70(22):2076-2078. doi:10.1212/01.WNL.0000313377.49555.2E

189. Chaaban L, Safwan N, Moussa H, El-Sammak S, Khoury SJ, Hannoun S. Central vein sign: A putative diagnostic marker for multiple sclerosis. *Acta Neurol Scand*. 2022;145(3):279-287. doi:10.1111/ANE.13553

190. Ontaneda D, Sati P, Raza P, et al. Central vein sign: A diagnostic biomarker in multiple sclerosis (CAVS-MS) study protocol for a prospective multicenter trial. *Neuroimage (Amst)*. 2021;32. doi:10.1016/J.NICL.2021.102834

191. Kutzelnigg A, Lucchinetti CF, Stadelmann C, et al. Cortical demyelination and diffuse white matter injury in multiple sclerosis. *BRAIN*. 2005;128(11):2705-2712. doi:10.1093/brain/awh641

192. Sailer M, Losseff NA, Wang L, Gawne-Cain ML, Thompson AJ, Miller DH. T1 lesion load and cerebral atrophy as a marker for clinical progression in patients with multiple sclerosis. A prospective 18 months follow-up study. *Eur J Neurol*. 2001;8(1):37-42. doi:10.1046/j.1468-1331.2001.00147.x

193. Parry A, Clare S, Jenkinson M, Smith S, Palace J, Matthews P. White Matter and Lesion T1 Relaxation Times Increase in Parallel and Correlate With Disability in Multiple Sclerosis. *J Neurol*. 2002;249(9). doi:10.1007/S00415-002-0837-7

194. Tam RC, Traboulsee A, Riddehough A, Sheikhzadeh F, Li DKB. The Impact of Intensity Variations in T1-hypointense Lesions on Clinical Correlations in Multiple Sclerosis. *Mult Scler*. 2011;17(8):949-957. doi:10.1177/1352458511402113

195. Rudick RA, Lee JC, Simon J, Fisher E. Significance of T2 lesions in multiple sclerosis: A 13-year longitudinal study. *Ann Neurol*. 2006;60(2):236-242. doi:10.1002/ana.20883

196. Fisniku LK, Chard DT, Jackson JS, et al. Gray matter atrophy is related to long-term disability in multiple sclerosis. *Ann Neurol*. 2008;64(3):247-254. doi:10.1002/ana.21423

197. Stankiewicz JM, Neema M, Alsop DC, et al. Spinal cord lesions and clinical status in multiple sclerosis: a 1.5T and 3T MRI study. *J Neurol Sci*. 2009;279(1-2):99. doi:10.1016/J.JNS.2008.11.009

198. Giorgio A, Battaglini M, Rocca MA, et al. Location of brain lesions predicts conversion of clinically isolated syndromes to multiple sclerosis. *Neurology*. 2013;80(3):234-241. doi:10.1212/WNL.0B013E31827debeb

199. Brownlee WJ, Altmann DR, Da Mota PA, et al. Association of asymptomatic spinal cord lesions and atrophy with disability 5 years after a clinically isolated syndrome. *Mult Scler J*. 2017;23(5):665-674. doi:10.1177/1352458516663034

200. Zivadinov R, Dwyer M, Barkay H, Steinerman J, Knappertz V, Khan O. Effect of glatiramer acetate three-times weekly on the evolution of new, active multiple sclerosis lesions into T1-hypointense "black holes": a post hoc magnetic resonance imaging analysis. *J Neurol*. 2015;262(3). doi:10.1007/S00415-014-7616-0

201. Kutzelnigg A, Lassmann H. *Pathology of Multiple Sclerosis and Related Inflammatory Demyelinating Diseases*. Vol 122. Handb Clin Neurol; 2014. doi:10.1016/B978-0-444-52001-2.00002-9

202. Jacobsen C, Hagemeier J, Myhr K-MM, et al. Brain atrophy and disability progression in multiple sclerosis patients: a 10-year follow-up study. *J Neurol Neurosurg PSYCHIATRY*. 2014;85(10):1109-1115. doi:10.1136/jnnp-2013-306906

203. Kearney H, Altmann DR, Samson RS, et al. Cervical cord lesion load is associated with disability independently from atrophy in MS. *Neurology*. 2015;84(4):367-373. doi:10.1212/WNL.0000000000001186

204. Sormani MP, Bruzzi P. MRI lesions as a surrogate for relapses in multiple sclerosis: a meta-analysis of randomised trials. *Lancet Neurol*. 2013;12(7):669-676. doi:10.1016/S1474-4422(13)70103-0

205. Kappos L, De Stefano N, Freedman MS, et al. Inclusion of brain volume loss in a revised measure of ``no evidence of disease activity' (NEDA-4) in relapsing-remitting multiple sclerosis. *Mult Scler J*. 2016;22(10):1297-1305. doi:10.1177/1352458515616701

206. Harding K, Williams O, Willis M, et al. Clinical Outcomes of Escalation vs Early Intensive Disease-Modifying Therapy in Patients With Multiple Sclerosis. *JAMA Neurol*. 2019;76(5):536-541. doi:10.1001/JAMANEUROL.2018.4905

207. Karampampa K, Gyllensten H, Murley C, et al. Early vs. late treatment initiation in multiple sclerosis and its impact on cost of illness: A register-based prospective cohort study in

Sweden. *Mult Scler J - Exp Transl Clin*. 2022;8(2). doi:10.1177/20552173221092411

208. Solomon A, Bourdette D, Cross A, et al. The contemporary spectrum of multiple sclerosis misdiagnosis: A multicenter study. *Neurology*. 2016;87(13):1393. doi:10.1212/WNL.0000000000003152

209. Hagemeier J, Weinstock-Guttman B, Bergsland N, et al. Iron deposition on SWI-filtered phase in the subcortical deep gray matter of patients with clinically isolated syndrome may precede structure-specific atrophy. *Am J Neuroradiol*. 2012;33(8):1596-1601. doi:10.3174/ajnr.A3030

210. Absinta M, Sati P, Filippi M, Ohayon J, Cortese I. Failure of early lesion repair in multiple sclerosis lesions with persistent phase rim. *Neurology*. 2015;84(SUPPL. 14).

211. Absinta M, Sati P, Schindler M, et al. Persistent 7-tesla phase rim predicts poor outcome in new multiple sclerosis patient lesions. *J Clin Invest*. 2016;126(7):2597-2609. doi:10.1172/JCI86198

212. Absinta M, Reich DS, Filippi M, et al. Spring cleaning: time to rethink imaging research lines in MS? *J Neurol*. 2016;263(10):1893-1902. doi:10.1007/s00415-016-8060-0

213. Dal-Bianco A, Grabner G, Kronnerwetter C, et al. Slow expansion of multiple sclerosis iron rim lesions: pathology and 7 T magnetic resonance imaging. *Acta Neuropathol*. 2017;133(1):25-42. doi:10.1007/s00401-016-1636-z

214. Absinta M, Maric D, Gharagozloo M, et al. A lymphocyte–microglia–astrocyte axis in chronic active multiple sclerosis. *Nature*. 2021;597(7878):709-714. doi:10.1038/s41586-021-03892-7

215. Luchetti S, Fransen NL, van Eden CG, Ramaglia V, Mason M, Huitinga I. Progressive multiple sclerosis patients show substantial lesion activity that correlates with clinical disease severity and sex: a retrospective autopsy cohort analysis. *Acta Neuropathol*. 2018;135(4):511-528. doi:10.1007/s00401-018-1818-y

216. Frischer JM, Weigand SD, Guo Y, et al. Clinical and pathological insights into the dynamic nature of the white matter multiple sclerosis plaque. *Ann Neurol*. 2015;78(5):710-721. doi:10.1002/ana.24497

217. Harrison DM, Li X, Liu H, et al. Lesion heterogeneity on high-field susceptibility MRI Is associated with multiple sclerosis severity. *Am J Neuroradiol*. 2016;37(8):1447-1453. doi:10.3174/ajnr.A4726

218. Filippi M, Preziosa P, Banwell BL, et al. Assessment of lesions on magnetic resonance imaging in multiple sclerosis: practical guidelines. *Brain*. 2019;142(7):1858-1875. doi:10.1093/brain/awz144

219. Absinta M, Sati P, Masuzzo F, et al. Association of Chronic Active Multiple Sclerosis Lesions With Disability In Vivo. *JAMA Neurol*. 2019;76(12):1474-1483. doi:10.1001/jamaneurol.2019.2399

220. Suthiphosuwan S, Sati P, Absinta M, et al. Paramagnetic Rim Sign in Radiologically Isolated Syndrome. *JAMA Neurol*. 2020;77(5):653-655. doi:10.1001/jamaneurol.2020.0124

221. Weber CE, Krämer J, Wittayer M, et al. Association of iron rim lesions with brain and cervical cord volume in relapsing multiple sclerosis. *Eur Radiol*. 2022;32(3):2012-2022. doi:10.1007/s00330-021-08233-w

222. Treaba CA, Conti A, Klawiter EC, et al. Cortical and phase rim lesions on 7 T MRI as markers of multiple sclerosis disease progression. *Brain Commun*. 2021;3(3). doi:10.1093/BRAINCOMMS/FCAB134

223. Dal-Bianco A, Grabner G, Kronnerwetter C, et al. Long-term evolution of multiple sclerosis iron rim lesions in 7 T MRI. *Brain*. 2021;144(3):833-847. doi:10.1093/brain/awaa436

224. Marcille M, Hurtado Rúa S, Tyshkov C, et al. Disease correlates of rim lesions on quantitative susceptibility mapping in multiple sclerosis. *Sci Reports 2022 121*. 2022;12(1):1-10. doi:10.1038/s41598-022-08477-6

225. Hemond CC, Baek J, Ionete C, Reich DS. Paramagnetic rim lesions are associated with pathogenic CSF profiles and worse clinical outcomes in multiple sclerosis: a retrospective cross-sectional study. *medRxiv*. Published online January 10, 2022:2022.01.08.22268838. doi:10.1101/2022.01.08.22268838

226. Pinto C, Cambron M, Dobai A, Vanheule E, Casselman JW. Smoldering lesions in MS: if you like it then you should put a rim on it. *Neuroradiology*. 2022;64(4):703-714. doi:10.1007/S00234-021-02800-0

227. Maggi P, Kuhle J, Schädelin S, et al. Chronic White Matter Inflammation and Serum Neurofilament Levels in Multiple Sclerosis. *Neurology*. 2021;97(6):e543-e553. doi:10.1212/WNL.0000000000012326

228. Bagnato F, Hametner S, Yao B, et al. Tracking iron in multiple sclerosis: A combined imaging and histopathological study at 7 Tesla. *Brain*. 2011;134(12):3599-3612. doi:10.1093/brain/awr278

229. Absinta M, Sati P, Reich DS. Advanced MRI and staging of multiple sclerosis lesions. *Nat Rev Neurol*. 2016;12(6):358-368. doi:10.1038/nrneurol.2016.59

230. Absinta M, Sati P, Fechner A, et al. Identification of Chronic Active Multiple Sclerosis Lesions on 3T MRI. *Am J Neuroradiol*. 2018;39(7):1233-1238. doi:10.3174/ajnr.A5660

231. Cronin MJMJ, Wharton S, Al-Radaideh A, et al. A comparison of phase imaging and quantitative susceptibility mapping in the imaging of multiple sclerosis lesions at ultrahigh field. *MAGMA*. 2016;29(3):543-557. doi:10.1007/s10334-016-0560-5

232. Wang Y, Spincemaille P, Liu Z, et al. Clinical quantitative susceptibility mapping (QSM): Biometal imaging and its emerging roles in patient care. *J Magn Reson Imaging*. 2017;46(4):951-971. doi:10.1002/jmri.25693

233. Rahmanzadeh R, Lu P-JJ, Barakovic M, et al. Myelin and axon pathology in multiple sclerosis assessed by myelin water and multi-shell diffusion imaging. *Brain*. 2021;144(6):1684-1696.

234. Liu C, Li W, Tong KA, Yeom KW, Kuzminski S. Susceptibility-weighted imaging and quantitative susceptibility mapping in the brain. *J Magn Reson Imaging*. 2015;42(1):23-41. doi:10.1002/jmri.24768

235. Hametner S. 7T MRI: Measuring white matter changes in MS and iron content in brain. *J Neurol Sci*. 2019;405(Supplement):35-36. doi:10.1016/j.jns.2019.10.099

236. Lou C, Sati P, Absinta M, et al. Fully automated detection of paramagnetic rims in multiple sclerosis lesions on 3T susceptibility-based MR imaging. *NeuroImage Clin*. 2021;32:102796. doi:10.1016/J.NICL.2021.102796

237. Barquero G, La Rosa F, Kebiri H, et al. RimNet: A deep 3D multimodal MRI architecture for paramagnetic rim lesion assessment in multiple sclerosis. *NeuroImage Clin*. 2020;28:102412. doi:10.1016/J.NICL.2020.102412

238. Sati P. Americas Committee for Treatment and Research in Multiple Sclerosis (ACTRIMS). In: *How to Image and Analyze Chronic Active Lesions*. ; 2022.

239. Zinger N, Ponath G, Sweeney E, et al. Dimethyl Fumarate Reduces Inflammation in Chronic Active Multiple Sclerosis Lesions. *Neurol Neuroimmunol neuroinflammation*. 2022;9(2). doi:10.1212/NXI.0000000000001138

240. Swanton J, Fernando K, Miller D. Early prognosis of multiple sclerosis. *Handb Clin Neurol*. 2014;122:371-391. doi:10.1016/B978-0-444-52001-2.00015-7

241. Barnett Y, Garber JY, Barnett MH. MRI biomarkers of disease progression in multiple sclerosis: Old dog, new tricks? *Quant Imaging Med Surg*. 2020;10(2):527-532. doi:10.21037/qims.2020.01.04

242. Filippi M, Brück W, Chard D, et al. Association between pathological and MRI findings in multiple sclerosis. *Lancet Neurol*. 2019;18(2):198-210. doi:10.1016/S1474-4422%2818%2930451-4

243. Filippi M, Rocca MA. New magnetic resonance imaging biomarkers for the diagnosis of

multiple sclerosis. *Expert Opin Med Diagn*. 2012;6(2):109-120. doi:10.1517/17530059.2012.657624

244. Reich DS, Lucchinetti CF, Calabresi PA. Multiple Sclerosis. Longo DL, ed. *N Engl J Med*. 2018;378(2):169-180. doi:10.1056/NEJMRA1401483

245. McKinley R, Wepfer R, Grunder L, et al. Automatic detection of lesion load change in Multiple Sclerosis using convolutional neural networks with segmentation confidence. *NeuroImage Clin*. 2020;25. doi:10.1016/J.NICL.2019.102104

246. Guo BJ, Yang ZL, Zhang LJ. Gadolinium Deposition in Brain: Current Scientific Evidence and Future Perspectives. *Front Mol Neurosci*. 2018;11. doi:10.3389/FNMOL.2018.00335

247. Tintore M, Rovira À, Río J, et al. Defining high, medium and low impact prognostic factors for developing multiple sclerosis. *Brain*. 2015;138(7):1863-1874. doi:10.1093/brain/awv105

248. Bagnato F, Jeffries N, Richert ND, et al. Evolution of T1 black holes in patients with multiple sclerosis imaged monthly for 4 years. *Brain*. 2003;126(Pt 8):1782-1789. doi:10.1093/brain/awg182

249. Brownlee WJ, Altmann DR, Prados F, et al. Early imaging predictors of long-term outcomes in relapse-onset multiple sclerosis. *Brain*. 2019;142(8):2276-2287. doi:10.1093/brain/awz156

250. Brex PA, Ciccarelli O, O'Riordan JI, Sailer M, Thompson AJ, Miller DH. A longitudinal study of abnormalities on MRI and disability from multiple sclerosis. *N Engl J Med*. 2002;346(3):158-164. doi:10.1056/NEJMoa011341

251. Davda N, Tallantyre E, Robertson NP. Early MRI predictors of prognosis in multiple sclerosis. *J Neurol*. 2019;266(12):3171-3173. doi:10.1007/s00415-019-09589-2

252. Kappos L, Moeri D, Radue EW, et al. Predictive value of gadolinium-enhanced magnetic resonance imaging for relapse rate and changes in disability or impairment in multiple sclerosis: a meta-analysis. *Lancet*. 1999;353(9157):964-969. doi:10.1016/S0140-6736(98)03053-0

253. Sormani M, Rio J, Tintorè M, et al. Scoring treatment response in patients with relapsing multiple sclerosis. *Mult Scler*. 2013;19(5):605-612. doi:10.1177/1352458512460605

254. Chiang GC. Atrophied T2 Lesion Volume in Multiple Sclerosis: Reducing the Focus on Lesion Counting. *Radiology*. 2019;293. doi:10.1148/radiol.2019191816

255. Sormani MP, Rovaris M, Comi G, Filippi M. A reassessment of the plateauing relationship between T2 lesion load and disability in MS. *Neurology*. 2009;73(19):1538-1542. doi:10.1212/WNL.0b013e3181c06679

256. Li DKB, Held U, Petkau J, et al. MRI T2 lesion burden in multiple sclerosis: a plateauing relationship with clinical disability. *Neurology*. 2006;66(9):1384-1389. doi:10.1212/01.WNL.0000210506.00078.5C

257. Pascual-Lozano AM, Martinez-Bisbal MC, Bosca-Blasco I, et al. Total brain T-2-hyperintense lesion-volume and the axonal damage in the normal-appearing white matter of brainstem in early relapsing-remitting multiple sclerosis. *Rev Neurol*. 2007;45(8):468-473. doi:10.33588/rn.4508.2007087

258. Mammi S, Filippi M, Martinelli V, et al. Correlation between brain MRI lesion volume and disability in patients with multiple sclerosis. *ACTA Neurol Scand*. 1996;94(2):93-96. doi:10.1111/j.1600-0404.1996.tb07036.x

259. Minneboo A, Barkhof F, Polman CH, Uitdehaag BMJ, Knol DL, Castelijns JA. Infratentorial Lesions Predict Long-term Disability in Patients with Initial Findings Suggestive of Multiple Sclerosis. *Arch Neurol*. 2004;61(2):217-221. doi:10.1001/archneur.61.2.217

260. Tintore M, Rovira A, Arrambide G, et al. Brainstem lesions in clinically isolated syndromes. *Neurology*. 2010;75(21):1933-1938. doi:10.1212/WNL.0b013e3181feb26f

261. Dekker I, Sombekke MH, Balk LJ, et al. Infratentorial and spinal cord lesions: Cumulative predictors of long-term disability? *Mult Scler*. 2020;26(11):1381. doi:10.1177/1352458519864933

262. Arrambide G, Rovira A, Sastre-Garriga J, et al. Spinal cord lesions: A modest contributor to diagnosis in clinically isolated syndromes but a relevant prognostic factor. *Mult Scler*. 2018;24(3):301-312. doi:10.1177/1352458517697830

263. Bodini B, Battaglini M, De Stefano N, et al. T2 lesion location really matters: a 10 year follow-up study in primary progressive multiple sclerosis. *J Neurol neurosurggery psychiatry*. 2011;82(1):72-77. doi:10.1136/jnnp.2009.201574

264. Sarbu N, Shih RY, Jones R V., Horkayne-Szakaly I, Oleaga L, Smirniotopoulos JG. White Matter Diseases with Radiologic-Pathologic Correlation. *RadioGraphics*. 2016;36(5):1426-1447. doi:10.1148/rg.2016160031

265. Fernando MS, O'Brien JT, Perry RH, et al. Comparison of the pathology of cerebral white matter with post-mortem magnetic resonance imaging (MRI) in the elderly brain. *Neuropathol Appl Neurobiol*. 2004;30(4):385-395. doi:10.1111/J.1365-2990.2004.00550.X

266. Tawfik AI, Kamr WH. Diagnostic value of 3D-FLAIR magnetic resonance sequence in detection of white matter brain lesions in multiple sclerosis. *Egypt J Radiol Nucl Med*. 2020;51(1):1-9. doi:10.1186/s43055-020-00247-6

267. Tiu VE, Enache I, Panea CA, Tiu C, Popescu BO. Predictive MRI Biomarkers in MS—A

Critical Review. *Medicina (B Aires)*. 2022;58(3). doi:10.3390/Medicina58030377

268. Van Waesberghe JHTM, Van Walderveen MAA, Castelijns JA, et al. Patterns of lesion development in multiple sclerosis: longitudinal observations with T1-weighted spin-echo and magnetization transfer MR. *AJNR Am J Neuroradiol*. 1998;19(4):675-683.

269. Dworkin JD, Linn KA, Oguz I, et al. An Automated Statistical Technique for Counting Distinct Multiple Sclerosis Lesions. *Am J Neuroradiol*. 2018;39(4):626-633. doi:10.3174/ajnr.A5556

270. Zivadinov R, Zorzon M, De Masi R, Nasuelli D, Cazzato G. Effect of intravenous methylprednisolone on the number, size and confluence of plaques in relapsing-remitting multiple sclerosis. *J Neurol Sci*. 2008;267(1-2):28-35. doi:10.1016/j.jns.2007.09.025

271. Harris JO, Frank JA, Patronas N, McFarlin DE, McFarland HF. Serial gadolinium-enhanced magnetic resonance imaging scans in patients with early, relapsing-remitting multiple sclerosis: implications for clinical trials and natural history. *Ann Neurol*. 1991;29(5):548-555. doi:10.1002/ANA.410290515

272. Barkhof F, Calabresi PA, Miller DH, et al. Imaging outcomes for neuroprotection and repair in multiple sclerosis trials. *Nat Rev Neurol*. 2009;5(5):256-266. doi:10.1038/nrneurol.2009.41

273. Kapoor R, Furby J, Hayton T, et al. Lamotrigine for neuroprotection in secondary progressive multiple sclerosis: a randomised, double-blind, placebo-controlled, parallel-group trial. *Lancet Neurol*. 2010;9(7):681-688. doi:10.1016/S1474-4422(10)70131-9

274. Furby J, Hayton T, Anderson V, et al. Magnetic resonance imaging measures of brain and spinal cord atrophy correlate with clinical impairment in secondary progressive multiple sclerosis. *Mult Scler J*. 2008;14(8):1068-1075. doi:10.1177/1352458508093617

275. Dalton CM, Miszkiel KA, O'Connor PW, Plant GT, Rice GPA, Miller DH. Ventricular enlargement in MS. *Neurology*. 2006;66(5):693-698. doi:10.1212/01.wnl.0000201183.87175.9F

276. Bakshi R, Dmochowski J, Shaikh ZA, Jacobs L. Gray matter T2 hypointensity is related to plaques and atrophy in the brains of multiple sclerosis patients. *J Neurol Sci*. 2001;185(1):19-26. doi:10.1016/S0022-510X(01)00477-4

277. Chard DT, Griffin CM, Rashid W, et al. Progressive grey matter atrophy in clinically early relapsing-remitting multiple sclerosis. *Mult Scler J*. 2004;10(4):387-391. doi:10.1191/1352458504ms1050oa

278. Fisher E, Lee J-C, Nakamura K, Rudick RA. Gray matter atrophy in multiple sclerosis: A longitudinal study. *Ann Neurol*. 2008;64(3):255-265. doi:10.1002/ana.21436

279. Sastre-Garriga J, Ingle GT, Chard DT, et al. Grey and white matter volume changes in early primary progressive multiple sclerosis: a longitudinal study. *Brain*. 2005;128(6):1454-1460. doi:10.1093/brain/awh498

280. Zivadinov R, Bakshi R. Role of MRI in multiple sclerosis I: Inflammation and lesions. *Front Biosci*. 2004;9:665-683. doi:10.2741/1251

281. Kalkers NF, Ameziane N, Bot JCJJ, Minneboo A, Polman CH, Barkhof F. Longitudinal brain volume measurement in multiple sclerosis - Rate of brain atrophy is independent of the disease subtype. *Arch Neurol*. 2002;59(10):1572-1576. doi:10.1001/archneur.59.10.1572

282. Zivadinov R, Bergsland N, Dolezal O, et al. Evolution of cortical and thalamus atrophy and disability progression in early relapsing-remitting MS during 5 years. *AJNR Am J Neuroradiol*. 2013;34(10):1931-1939. doi:10.3174/ajnr.A3503

283. Fisher E, Rudick RA, Simon JH, et al. Eight-year follow-up study of brain atrophy in patients with MS. *Neurology*. 2002;59(9):1412-1420. doi:10.1212/01.WNL.0000036271.49066.06

284. B Benedict RH, Weinstock-Guttman B, Fishman I, Sharma J, Tjoa CW, Bakshi R. Prediction of Neuropsychological Impairment in Multiple Sclerosis Comparison of Conventional Magnetic Resonance Imaging Measures of Atrophy and Lesion Burden. *Arch Neurol*. 2004;61(2):226-230. doi:10.1001/Archneur.61.2.226

285. Rocca MA, Ceccarelli A, Rodegher M, et al. Preserved brain adaptive properties in patients with benign multiple sclerosis. *Neurology*. 2010;74(2):142-149. doi:10.1212/WNL.0b013e3181c91a00

286. Pontillo G, Cocozza S, Di Stasi M, et al. 2D linear measures of ventricular enlargement may be relevant markers of brain atrophy and long-term disability progression in multiple sclerosis. *Eur Radiol*. 2020;30(7):3813-3822. doi:10.1007/s00330-020-06738-4

287. Haider L, Chung K, Birch G, et al. Linear brain atrophy measures in multiple sclerosis and clinically isolated syndromes: a 30-year follow-up. *J Neurol Neurosurg Psychiatry*. 2021;92(8):839-846. doi:10.1136/jnnp-2020-325421

288. Chivers T, Constantinescu C, Tench C. MRI-Based Measurement of Brain Stem Cross-Sectional Area in Relapsing-Remitting Multiple Sclerosis. *J Neuroimaging*. 2015;25(6):1002-1006. doi:10.1111/JON.12244

289. Gonçalves LI, dos Passos GR, Conzatti LP, et al. Correlation between the corpus callosum index and brain atrophy, lesion load, and cognitive dysfunction in multiple sclerosis. *Mult Scler Relat Disord*. 2018;20:154-158. doi:10.1016/j.msard.2018.01.015

290. Yaldizli O, Atefy R, Gass A, et al. Corpus callosum index and long-term disability in

multiple sclerosis patients. *J Neurol*. 2010;257(8):1256-1264. doi:10.1007/s00415-010-5503-x

291. Vrenken H, Jenkinson M, Horsfield MA, et al. Recommendations to improve imaging and analysis of brain lesion load and atrophy in longitudinal studies of multiple sclerosis. *J Neurol*. 2013;260(10):2458. doi:10.1007/S00415-012-6762-5

292. Berg D, Mäurer M, Warmuth-Metz M, Rieckmann P, Becker G. The correlation between ventricular diameter measured by transcranial sonography and clinical disability and cognitive dysfunction in patients with multiple sclerosis. *Arch Neurol*. 2000;57(9):1289-1292. doi:10.1001/Archneur.57.9.1289

293. Müller M, Esser R, Kötter K, Voss J, Müller A, Stellmes P. Third ventricular enlargement in early stages of multiple sclerosis is a predictor of motor and neuropsychological deficits: a cross-sectional study. *BMJ Open*. 2013;3(9):e003582. doi:10.1136/BMJOPEN-2013-003582

294. Sinnecker T, Ruberte E, Schädelin S, et al. New and enlarging white matter lesions adjacent to the ventricle system and thalamic atrophy are independently associated with lateral ventricular enlargement in multiple sclerosis. *J Neurol 2019 2671*. 2019;267(1):192-202. doi:10.1007/S00415-019-09565-W

295. Bakshi R, Neema M, Healy BC, et al. Predicting Clinical Progression in Multiple Sclerosis With the Magnetic Resonance Disease Severity Scale. *Arch Neurol*. 2008;65(11):1449-1453. doi:10.1001/archneur.65.11.1449

296. Liptak Z, Berger AM, Sampat MP, et al. Medulla oblongata volume: a biomarker of spinal cord damage and disability in multiple sclerosis. *AJNR Am J Neuroradiol*. 2008;29(8):1465-1470. doi:10.3174/AJNR.A1162

297. Faria Andrade Figueira F, Silva dos Santos V, Medeiros Andrade Figueira G, Correa Marques da Silva Â. *CORPUS CALLOSUM INDEX A Practical Method for Long-Term Follow-up in Multiple Sclerosis*.

298. Ozturk A, Smith SA, Gordon-Lipkin EM, et al. MRI of the corpus callosum in multiple sclerosis: association with disability. *Mult Scler J*. 2010;16(2):166-177. doi:10.1177/1352458509353649

299. Sugijono SE, Mulyadi R, Firdausia S, Prihartono J, Estiasari R. Corpus callosum index correlates with brain volumetry and disability in multiple sclerosis patients. *Neurosci J*. 2020;25(3):193-199. doi:10.17712/NSJ.2020.3.20190093

300. Kunchok A, Lechner-Scott J, Granella F, et al. Prediction of on-treatment disability worsening in RRMS with the MAGNIMS score. *Mult Scler*. 2021;27(5):695-705. doi:10.1177/1352458520936823

301. Garg N, Reddel SW, Miller DH, et al. The corpus callosum in the diagnosis of multiple sclerosis and other CNS demyelinating and inflammatory diseases. *J Neurol Neurosurg Psychiatry*. 2015;86(12):1374-1382. doi:10.1136/JNNP-2014-309649

302. Butzkueven H, Kolbe S, Jolley D, et al. Validation of linear cerebral atrophy markers in multiple sclerosis. *J Clin Neurosci*. 2008;15(2):130-137. doi:10.1016/J.JOCN.2007.02.089

303. Khalil H, Tricco AC. Differentiating between mapping reviews and scoping reviews in the evidence synthesis ecosystem. *J Clin Epidemiol*. 2022;149:175-182. doi:10.1016/J.JCLINEPI.2022.05.012

304. Grant MJ, Booth A. A typology of reviews: an analysis of 14 review types and associated methodologies. *Health Info Libr J*. 2009;26:91-108. doi:10.1111/j.1471-1842.2009.00848.x

305. Diane C. What is a "mapping study?" *J Med Libr Assoc*. 2016;104(1):76. doi:10.3163/1536-5050.104.1.013

306. Montalban X, Tintoré M, Swanton J, et al. MRI Criteria for MS in Patients With Clinically Isolated Syndromes. *Neurology*. 2010;74(5). doi:10.1212/WNL.0B013E3181CEC45C

307. Polman CH, Reingold SC, Banwell B, et al. Diagnostic criteria for multiple sclerosis: 2010 revisions to the McDonald criteria. *Ann Neurol*. 2011;69(2):292-302. doi:10.1002/ana.22366

308. Fazekas F, Barkhof F, Filippi M, et al. The contribution of magnetic resonance imaging to the diagnosis of multiple sclerosis. *Neurology*. 1999;53(3):448-456. doi:10.1212/wnl.53.3.448

309. Charil A, Yousry TA, Rovaris M, et al. MRI and the diagnosis of multiple sclerosis: expanding the concept of "no better explanation". *Lancet Neurol*. 2006;5(10):841-852. doi:10.1016/S1474-4422(06)70572-5

310. Sinnecker T, Clarke MA, Meier D, et al. Evaluation of the Central Vein Sign as a Diagnostic Imaging Biomarker in Multiple Sclerosis. *JAMA Neurol*. 2019;76(12):1446. doi:10.1001/jamaneurol.2019.2478

311. Yao B, Hametner S, van Gelderen P, et al. 7 Tesla magnetic resonance imaging to detect cortical pathology in multiple sclerosis. Antal A, ed. *PLoS One*. 2014;9(10):e108863. doi:10.1371/journal.pone.0108863

312. Li X, Harrison DM, Liu H, et al. Magnetic susceptibility contrast variations in multiple sclerosis lesions. *J Magn Reson Imaging*. 2016;43(2):463-473. doi:10.1002/jmri.24976

313. Chawla S, Kister I, Wuerfel J, et al. Iron and non-iron-related characteristics of multiple sclerosis and neuromyelitis optica lesions at 7T MRI. *Am J Neuroradiol*. 2016;37(7):1223-

1230. doi:10.3174/ajnr.A4729

314. Wuerfel J, Sinnecker T, Ringelstein EB, et al. Lesion morphology at 7 Tesla MRI differentiates Susac syndrome from multiple sclerosis. *Mult Scler*. 2012;18(11):1592-1599. doi:10.1177/1352458512441270

315. Hosseini Z, Matusinec J, Rudko DA, et al. Morphology-Specific Discrimination between MS White Matter Lesions and Benign White Matter Hyperintensities Using Ultra-High-Field MRI. *AJNR Am J Neuroradiol*. 2018;39(8):1473-1479. doi:10.3174/ajnr.A5705

316. Igra MS, Paling D, Wattjes MP, Connolly DJA, Hoggard N. Multiple sclerosis update: use of MRI for early diagnosis, disease monitoring and assessment of treatment related complications. *Br J Radiol*. 2017;90(1074):20160721. doi:10.1259/bjr.20160721

317. McDonald WI, Compston A, Edan G, et al. Recommended diagnostic criteria for multiple sclerosis: Guidelines from the international panel on the diagnosis of multiple sclerosis. *Ann Neurol*. 2001;50(1):121-127. doi:10.1002/ANA.1032

318. Clarke M, Ferreira LMP, Pareto D, et al. The central vein sign and iron rings: insights from a large cohort of patients with multiple sclerosis and mimicking disorders. In: *ECTRIMS*. Vol 25. 35th Congress of the European Committee for Treatment and Research in Multiple Sclerosis, ECTRIMS 2019. Sweden. ; 2019:38-39. doi:10.1177/1352458519868070

319. Wiggermann V, Torres EH, Vavasour IM, et al. Magnetic resonance frequency shifts during acute MS lesion formation. *Neurology*. 2013;81(3):211-218. doi:10.1212/WNL.0b013e31829bfd63

320. Yablonskiy DA, Luo J, Sukstanskii AL, Iyer A, Cross AH. Biophysical mechanisms of MRI signal frequency contrast in multiple sclerosis. *Proc Natl Acad Sci U S A*. 2012;109(35):14212-14217. doi:10.1073/pnas.1206037109

321. Chen W, Gauthier SA, Gupta A, et al. Quantitative Susceptibility Mapping of Multiple Sclerosis Lesions at Various Ages. *Radiology*. 2014;271(1):183-192. doi:10.1148/radiol.13130353

322. Kilsdonk ID, Lopez-Soriano A, Kuijer JPA, et al. Morphological features of MS lesions on FLAIR at 7 T and their relation to patient characteristics. *J Neurol*. 2014;261(7):1356-1364. doi:10.1007/s00415-014-7351-6

323. Yao B, Ikonomidou VN, Cantor FK, Ohayon JM, Duyn J, Bagnato F. Heterogeneity of Multiple Sclerosis White Matter Lesions Detected With T2*-Weighted Imaging at 7.0 Tesla. *J Neuroimaging*. 2015;25(5):799-806. doi:10.1111/jon.12193

324. Llufriu S, Pujol T, Blanco Y, et al. T2 hypointense rims and ring-enhancing lesions in MS. *Mult Scler*. 2010;16(11):1317-1325. doi:10.1177/1352458510377905

325. Treaba C, Granberg T, Herranz E, et al. The relevance of 7-Tesla paramagnetic rim lesions in patients with multiple sclerosis. *Mult Scler J*. Published online September 2019.

326. Dal-Bianco A, Grabner G, Kronnerwetter C, et al. Iron rim lesions in multiple sclerosis at 7 Tesla magnetic resonance imaging: a 7 year prospective longitudinal study. In: *Multiple Sclerosis Journal*. Vol 25. ; 2019:50-51.

327. Ontaneda D, Fox RJ. Progressive multiple sclerosis. *Curr Opin Neurol*. 2015;28(3):237-243. doi:10.1097/WCO.0000000000000195

328. Blindenbacher N, Brunner E, Asseyer S, et al. Evaluation of the "ring sign" and the "core sign" as a magnetic resonance imaging marker of disease activity and progression in clinically isolated syndrome and early multiple sclerosis. *Mult Scler J - Exp Transl Clin*. 2020;6(1):2055217320915480. doi:10.1177/2055217320915480

329. Dal-Bianco A, Kolbrink S, Pusswald G, et al. Do 7T observed iron rim lesions in patients with multiple sclerosis serve as a marker for neuropsychological deficits? In: *ECTRIMS*. ; 2019.

330. Schwartz KM, Erickson BJ, Schwartz KM, Erickson BJ, Lucchinetti C. Pattern of T2 hypointensity associated with ring-enhancing brain lesions can help to differentiate pathology. *Neuroradiology*. 2006;48(3):143-149. doi:10.1007/s00234-005-0024-5

331. Sinnecker T, Ruberte E, Schaedelin S, et al. New or enlarging T2 weighted lesions in the white matter near to the ventricle wall and thalamic atrophy are independently associated with lateral ventricular enlargement in multiple sclerosis. *Mult Scler J*. 2020;267(1):192-202. doi:10.1177/1352458519868081

332. Clarke MA, Samaraweera AP, Falah Y, et al. Single Test to ARrive at Multiple Sclerosis (STAR-MS) diagnosis: A prospective pilot study assessing the accuracy of the central vein sign in predicting multiple sclerosis in cases of diagnostic uncertainty. *Mult Scler J*. Published online October 31, 2019:135245851988228. doi:10.1177/1352458519882282

333. Chen JW. Imaging Neuroinflammation – from Bench to Bedside. *J Clin Cell Immunol*. 2014;05(03). doi:10.4172/2155-9899.1000226

334. Oh J, Suthiphosuwan S, Guenette M, Absinta M, Reich D, Bharatha A. The central vein sign and paramagnetic rim sign in white matter lesions of radiologically isolated syndrome. *Neurology*. 2019;92(15 Supplement 1).

335. Tolaymat B, Zheng W, Chen H, Choi S, Li X, Harrison D. Sex-specific differences in rim appearance of multiple sclerosis lesions on quantitative susceptibility mapping. *Mult Scler Relat Disord*. 2020;45(15, S):102317. doi:10.1016/j.msard.2020.102317

336. Hametner S, Dal Bianco A, Trattnig S, et al. Iron related changes in MS lesions and their validity to characterize MS lesion types and dynamics with Ultra-high field magnetic

resonance imaging. *Brain Pathol*. 2018;28(5):743-749. doi:10.1111/bpa.12643

337. Kilsdonk ID, Wattjes MP, Lopez-Soriano A, et al. Improved differentiation between MS and vascular brain lesions using FLAIR* at 7 Tesla. *Eur Radiol*. 2014;24(4):841-849. doi:10.1007/s00330-013-3080-y

338. Kang Y, Schlyer D, Kaunzner UW, et al. Comparison of two different methods of image analysis for the assessment of microglial activation in patients with multiple sclerosis using (R)-[N-methyl-carbon-11] PK11195. Guillemin GJ, ed. *PLoS One*. 2018;13(8):e0201289. doi:10.1371/journal.pone.0201289

339. Absinta M, Sati P, Gaitán MI, et al. Seven-tesla phase imaging of acute multiple sclerosis lesions: A new window into the inflammatory process. *Ann Neurol*. 2013;74(5):669-678. doi:10.1002/ana.23959

340. Absinta M, Bhagavatheeshwaran G, Sati P. Longitudinal MRI history of lesion repair based on the presence or absence of a 7t paramagnetic RIM. In: *Multiple Sclerosis Journal*. Vol 24. 3rd Annual Americas Committee for Treatment and Research in Multiple Sclerosis Forum, ACTRIMS 2018. United States. SAGE Publications Ltd; 2018:62. doi:10.1177/1352458517750967

341. Lucchinetti CF, Gavrilova RH, Metz I, et al. Clinical and radiographic spectrum of pathologically confirmed tumefactive multiple sclerosis. *Brain*. 2008;131(7):1759. doi:10.1093/BRAIN/AWN098

342. Lucchinetti C, Altintasm A, Wegner C, Silvia Menk S, Lassmann H, Andreas B. Magnetic Resonance Imaging Correlates of Multiple Sclerosis Pathologic Subtypes. In: *Ann Neurol*. ; 2003:54(Suppl 7): S37.

343. Blaabjerg M, Ruprecht K, Sinnecker T, et al. Widespread inflammation in CLIPPERS syndrome indicated by autopsy and ultra-high-field 7T MRI. *Neurol Neuroimmunol Neuroinflammation*. 2016;3(3):e226. doi:10.1212/NXI.0000000000000226

344. Bian W, Harter K, Hammond-Rosenbluth KE, et al. A serial in vivo 7T magnetic resonance phase imaging study of white matter lesions in multiple sclerosis. *Mult Scler J*. 2013;19(1):69-75. doi:10.1177/1352458512447870

345. Yao Y, Nguyen T, Pandya S, Rua SH, Kuceyeski A, Wang Y. MS lesions demonstrating a QSM hyperintense-rim have more myelin loss compared to those without a QSM hyperintense-rim. *Neurology*. 2017;88(16 Supplement 1).

346. Tillema J-MJ-MJ-M, Weigand SDD, Dayan M, et al. Dark Rims: Novel Sequence Enhances Diagnostic Specificity in Multiple Sclerosis. *AJNR Am J Neuroradiol*. 2018;39(6):1052-1058. doi:10.3174/ajnr.A5636

347. Li Y-X, Shi Z, Aibaidula A, et al. Not all 1p/19q non-codeleted oligodendroglial tumors are

astrocytic. *Oncotarget*. 2016;7(40):64615-64630. doi:10.18632/oncotarget.11378

348. Kaunzner UW, Kang Y, Zhang S, et al. Quantitative susceptibility mapping identifies inflammation in a subset of chronic multiple sclerosis lesions. *Brain*. 2019;142(1):133-145. doi:10.1093/brain/awy296

349. Elliott C, Wolinsky JS, Hauser SL, et al. Slowly expanding/evolving lesions as a magnetic resonance imaging marker of chronic active multiple sclerosis lesions. *Mult Scler*. 2019;25(14):1915-1925. doi:10.1177/1352458518814117

350. Haacke EM, Xu Y, Cheng Y-CN, Reichenbach JRJR. Susceptibility weighted imaging (SWI). *Magn Reson Med*. 2004;52(3):612-618. doi:10.1002/mrm.20198

351. Sati P, George IC, Shea CD, et al. FLAIR*: A combined MR contrast technique for visualizing white matter lesions and parenchymal veins. *Radiology*. 2012;265(3):926-932. doi:10.1148/radiol.12120208

352. Kister I, Chawla S, Wuerfel JT, Sinnecker T, Paulm F. Longitudinal study of MS lesions using multi-parametric ultra-high field (7Tesla) MRI. *Mult Scler*. 2016;22(Supplement 3):240. doi:10.1177/1352458516663081

353. Casini G, Yurashevich M, Vanga R, et al. Are Periventricular Lesions Specific for Multiple Sclerosis? *J Neurol Neurophysiol*. 4(2):150. doi:10.4172/2155-9562.1000150

354. Higgins J, Altman D. *Assessing Risk of Bias in Included Studies.Cochrane Handbook for Systematic Reviews of Interventions*. John Wiley & Sons, Ltd

355. Clarke MA, Pareto D, Pessini-Ferreira L, et al. Value of 3T Susceptibility-Weighted Imaging in the Diagnosis of Multiple Sclerosis. *Am J Neuroradiol*. 2020;41(6):1001-1008. doi:10.3174/AJNR.A6547

356. Maggi P, Sati P, Nair G, et al. Paramagnetic Rim Lesions are Specific to Multiple Sclerosis: An International Multicenter 3T MRI Study. *Ann Neurol*. 2020;88(5):1034-1042. doi:10.1002/ANA.25877

357. Jang J, Nam Y, Choi Y, et al. Paramagnetic Rims in Multiple Sclerosis and Neuromyelitis Optica Spectrum Disorder: A Quantitative Susceptibility Mapping Study with 3-T MRI. *J Clin Neurol*. 2020;16(4):562. doi:10.3988/JCN.2020.16.4.562

358. Dal-Bianco A, Schranzer R, Grabner G, et al. Iron Rims in Patients With Multiple Sclerosis as Neurodegenerative Marker? A 7-Tesla Magnetic Resonance Study. *Front Neurol*. 2021;12:2261. doi:10.3389/FNEUR.2021.632749/BIBTEX

359. Kwong KCNK, Mollison D, Meijboom R, et al. The prevalence of paramagnetic rim lesions in multiple sclerosis: A systematic review and meta-analysis. *PLoS One*. 2021;16(9):e0256845. doi:10.1371/JOURNAL.PONE.0256845

360. Hemond CC, Reich DS, Dundamadappa SK. Paramagnetic Rim Lesions in Multiple Sclerosis: Comparison of Visualization at 1.5-T and 3-T MRI. *AJR Am J Roentgenol*. 2022;219(1):120-129. doi:10.2214/AJR.21.26777

361. Solomon AJ, Corboy JR. The tension between early diagnosis and misdiagnosis of multiple sclerosis. *Nat Rev Neurol 2017 139*. 2017;13(9):567-572. doi:10.1038/nrneurol.2017.106

362. Gaetani L, Prosperini L, Mancini A, et al. 2017 revisions of McDonald criteria shorten the time to diagnosis of multiple sclerosis in clinically isolated syndromes. *J Neurol*. 2018;265(11):2684-2687. doi:10.1007/s00415-018-9048-8

363. Geraldes R, Ciccarelli O, Barkhof F, et al. The current role of MRI in differentiating multiple sclerosis from its imaging mimics. *Nat Rev Neurol*. 2018;14(4):199-213. doi:10.1038/nrneurol.2018.14

364. Wong YYM, De Mol CL, Van Der Vuurst De Vries RM, et al. Real-world validation of the 2017 McDonald criteria for pediatric MS. *Neurol Neuroimmunol NeuroInflammation*. 2018;6(2):528. doi:10.1212/NXI.0000000000000528

365. Gobbin F, Zanoni M, Marangi A, et al. 2017 McDonald criteria for multiple sclerosis: Earlier diagnosis with reduced specificity? *Mult Scler Relat Disord*. 2019;29:23-25. doi:10.1016/j.msard.2019.01.008

366. Van Der Vuurst De Vries RM, Mescheriakova JY, Wong YYM, et al. Application of the 2017 Revised McDonald Criteria for Multiple Sclerosis to Patients with a Typical Clinically Isolated Syndrome. *JAMA Neurol*. 2018;75(11):1392-1398. doi:10.1001/jamaneurol.2018.2160

367. Hyun JW, Kim W, Huh SY, et al. Application of the 2017 McDonald diagnostic criteria for multiple sclerosis in Korean patients with clinically isolated syndrome. *Mult Scler J*. 2019;25(11):1488-1495. doi:10.1177/1352458518790702

368. Habek M, Pavičić T, Ruška B, et al. Establishing the diagnosis of multiple sclerosis in Croatian patients with clinically isolated syndrome: 2010 versus 2017 McDonald criteria. *Mult Scler Relat Disord*. 2018;25:99-103. doi:10.1016/j.msard.2018.07.035

369. Liu S, Kullnat J, Bourdette D, et al. Prevalence of brain magnetic resonance imaging meeting Barkhof and McDonald criteria for dissemination in space among headache patients. *Mult Scler*. 2013;19(8):1101-1105. doi:10.1177/1352458512471874

370. Huh SY, Min JH, Kim W, et al. The usefulness of brain MRI at onset in the differentiation of multiple sclerosis and seropositive neuromyelitis optica spectrum disorders. *Mult Scler J*. 2014;20(6):695-704. doi:10.1177/1352458513506953

371. Kim SS, Richman DP, Johnson WO, Hald JK, Agius MA. Limited utility of current MRI criteria for distinguishing multiple sclerosis from common mimickers: Primary and

secondary CNS vasculitis, lupus and Sjogren's syndrome. *Mult Scler*. 2014;20(1):57-63. doi:10.1177/1352458513491329

372. Maggi P, Absinta M, Grammatico M, et al. Central vein sign differentiates Multiple Sclerosis from central nervous system inflammatory vasculopathies. *Ann Neurol*. 2018;83(2):283. doi:10.1002/ANA.25146

373. Suthiphosuwan S, Sati P, Guenette M, Absinta M, Reich DS, Bharatha A. The central vein sign and paramagnetic rim sign in white matter lesions of radiologically isolated syndrome: Perivenular and chronic active demyelination in asymptomatic individuals? *Mult Scler J*. 2018;24(2 Supplement):420. doi:10.1177/1352458518798590

374. Sinnecker T, Dorr J, Pfueller CF, et al. Distinct lesion morphology at 7-T MRI differentiates neuromyelitis optica from multiple sclerosis. *Neurology*. 2012;79(7):708-714. doi:10.1212/WNL.0b013e3182648bc8

375. Yao Y, Nguyen TD, Pandya S, et al. Combining Quantitative Susceptibility Mapping with Automatic Zero Reference (QSM0) and Myelin Water Fraction Imaging to Quantify Iron-Related Myelin Damage in Chronic Active MS Lesions. *Am J Neuroradiol*. 2018;39(2):303-310. doi:10.3174/ajnr.A5482

376. Pakpoor J, Seminatore B, Graves JS, et al. Dietary factors and pediatric multiple sclerosis: A case-control study. *Mult Scler J*. 2018;24(8):1067-1076. doi:10.1177/1352458517713343

377. Haacke EM, Mittal S, Wu Z, Neelavalli J, Cheng Y-CN. Susceptibility-Weighted Imaging: Technical Aspects and Clinical Applications, Part 1 From the Departments of Radiology (E. *Phys Rev AJNR Am J Neuroradiol*. 2009;30:19-30. doi:10.3174/ajnr.A1400

378. Rosati G. The prevalence of multiple sclerosis in the world: An update. *Neurol Sci*. 2001;22(2):117-139. doi:10.1007/s100720170011

379. Ontaneda D, Tallantyre E, Kalincik T, Planchon SM, Evangelou N. Early highly effective versus escalation treatment approaches in relapsing multiple sclerosis. *Pers View Lancet Neurol*. 2019;18(10):973-980. doi:10.1016/S1474-4422(19)30151-6

380. Rotstein D, Montalban X. Reaching an evidence-based prognosis for personalized treatment of multiple sclerosis. *Nat Rev Neurol 2019 155*. 2019;15(5):287-300. doi:10.1038/s41582-019-0170-8

381. Allen CM, Mowry E, Tintore M, Evangelou N. Prognostication and contemporary management of clinically isolated syndrome. *J Neurol Neurosurg Psychiatry*. 2021;92(4):391-397. doi:10.1136/JNNP-2020-323087

382. Haacke EMM, Makki M, Ge Y, et al. Characterizing iron deposition in multiple sclerosis lesions using susceptibility weighted imaging. *J Magn Reson Imaging*. 2009;29(3):537-544.

doi:10.1002/jmri.21676

383. Polman CH, Reingold SC, Edan G, et al. Diagnostic criteria for multiple sclerosis: 2005 revisions to the "McDonald Criteria." *Ann Neurol*. 2005;58(6):840-846. doi:10.1002/ANA.20703

384. Hurley A, Al-Radaideh A, Bai L, et al. Tailored RF pulse for magnetization inversion at ultrahigh field. *Magn Reson Med*. 2010;63(1):51-58. doi:10.1002/MRM.22167

385. Renard D, Castelnovo G, Bousquet P-JJ, et al. Brain MRI findings in long-standing and disabling multiple sclerosis in 84 patients. *Clin Neurol Neurosurg*. 2010;112(4):286-290. doi:10.1016/j.clineuro.2009.12.012

386. Giorgio A, Stromillo ML, Bartolozzi ML, et al. Relevance of hypointense brain MRI lesions for long-term worsening of clinical disability in relapsing multiple sclerosis. *Mult Scler J*. 2014;20(2):214-219. doi:10.1177/1352458513494490

387. Elliott C, Belachew S, Wolinsky JS, et al. Chronic white matter lesion activity predicts clinical progression in primary progressive multiple sclerosis. *Neurology*. 2012;142(4):2787-2799. doi:10.1093/brain/awz212

388. Yao B, Bagnato F, Matsuura E, et al. Chronic multiple sclerosis lesions: Characterization with high-field-strength MR imaging. *Radiology*. 2012;262(1):206-215. doi:10.1148/radiol.11110601

389. Yushkevich PA, Piven J, Hazlett HC, et al. User-guided 3D active contour segmentation of anatomical structures: Significantly improved efficiency and reliability. *Neuroimage*. 2006;31(3):1116-1128. doi:10.1016/j.neuroimage.2006.01.015

390. Mackinnon DP, Fairchild AJ, Fritz MS. Mediation Analysis. *Annu Rev Psychol*. 2007;58:593-614. doi:10.1146/annurev.psych.58.110405.085542

391. Zhang S, Nguyen TD, Hurtado Rúa SM, et al. Quantitative Susceptibility Mapping of Time-Dependent Susceptibility Changes in Multiple Sclerosis Lesions. *AJNR Am J Neuroradiol*. 2019;40(6):987-993. doi:10.3174/ajnr.A6071

392. Mehta V, Pei W, Yang G, et al. Iron Is a Sensitive Biomarker for Inflammation in Multiple Sclerosis Lesions. Reindl M, ed. *PLoS One*. 2013;8(3):e57573. doi:10.1371/journal.pone.0057573

393. MAGNIMS consensus guidelines on the use of MRI in multiple sclerosis—establishing disease prognosis and monitoring patients. *Nat Rev Neurol*. 2015;11(10):597-606. doi:10.1038/nrneurol.2015.157

394. Heesen C, Kasper J, Segal J, Köpke S, Mühlhauser I. Decisional role preferences, risk knowledge and information interests in patients with multiple sclerosis. *Mult Scler*.

2004;10(6):643-650. doi:10.1191/1352458504MS1112OA

395. Brand J, Köpke S, Kasper J, et al. Magnetic Resonance Imaging in Multiple Sclerosis – Patients' Experiences, Information Interests and Responses to an Education Programme. *PLoS One*. 2014;9(11):e113252. doi:10.1371/JOURNAL.PONE.0113252

396. Ramsaransing GSM, De Keyser J. Benign course in multiple sclerosis: a review. *Acta Neurol Scand*. 2006;113(6):359-369. doi:10.1111/J.1600-0404.2006.00637.X

397. Hawkins SA, McDonnell G V. Benign multiple sclerosis? Clinical course, long term follow up, and assessment of prognostic factors. *J Neurol Neurosurg Psychiatry*. 1999;67(2):148-152. doi:10.1136/JNNP.67.2.148

398. Soelberg Sorensen P. Safety concerns and risk management of multiple sclerosis therapies. *Acta Neurol Scand*. 2017;136(3):168-186. doi:10.1111/ANE.12712

399. Danchaivijitr N, Waldman AD, Tozer DJ, et al. Low-Grade Gliomas: Do Changes in rCBV Measurements at Longitudinal Perfusion-weighted MR Imaging Predict Malignant Transformation? 1. *Radiology*. 2008;247:170-178.

400. Miller DH, Chard DT, Ciccarelli O. Clinically isolated syndromes. *Lancet Neurol*. 2012;11(2):157-169. doi:10.1016/S1474-4422(11)70274-5

401. Chung KK, Altmann D, Barkhof F, et al. A 30-Year Clinical and Magnetic Resonance Imaging Observational Study of Multiple Sclerosis and Clinically Isolated Syndromes. *Ann Neurol*. 2020;87(1):63-74. doi:10.1002/ana.25637

402. Odenthal C, Coulthard A. The prognostic utility of MRI in clinically isolated syndrome: a literature review. *AJNR Am J Neuroradiol*. 2015;36(3):425-431. doi:10.3174/AJNR.A3954

403. Zhang W, Hou Y. Prognostic value of magnetic resonance imaging in patients with clinically isolated syndrome conversion to multiple sclerosis: a meta-analysis. *Neurol India*. 2013;61(3):231-238. doi:10.4103/0028-3886.115058

404. Moher D, Liberati A, Tetzlaff J, Altman DG. Preferred reporting items for systematic reviews and meta-analyses: the PRISMA statement. *BMJ*. 2009;339(7716):332-336. doi:10.1136/BMJ.B2535

405. Page MJ, Mckenzie JE, Bossuyt PM, et al. The PRISMA 2020 statement: an updated guideline for reporting systematic reviews. doi:10.1136/bmj.n71

406. Hayden JA, Côté P, Bombardier C. Evaluation of the quality of prognosis studies in systematic reviews. *Ann Intern Med*. 2006;144(6):427-437. doi:10.7326/0003-4819-144-6-200603210-00010

407. Hayden JA, van der Windt DA, Cartwright JL, Côté P, Bombardier C. Assessing bias in

studies of prognostic factors. *Ann Intern Med*. 2013;158(4):280-286. doi:10.7326/0003-4819-158-4-201302190-00009

408. Rovaris M, Rocca MA, Barkhof F, et al. Relationship between brain MRI lesion load and short-term disease evolution in non-disabling MS: a large-scale, multicentre study. *Mult Scler J*. 2011;17(3):319-326. doi:10.1177/1352458510388824

409. Chard DT, Brex PA, Ciccarelli O, et al. The longitudinal relation between brain lesion load and atrophy in multiple sclerosis: a 14 year follow up study. *J Neurol Neurosurg Psychiatry* . 2003;74(11):1551-1554. doi:10.1136/jnnp.74.11.1551

410. O'Riordan JI, Thompson AJ, Kingsley DPE, et al. The prognostic value of brain MRI in clinically isolated syndromes of the CNS. A 10-year follow-up. *Brain*. 1998;121 (Pt 3(3):495-503. doi:10.1093/brain/121.3.495

411. Sailer M, O'Riordan JI, Thompson AJ, et al. Quantitative MRI in patients with clinically isolated syndromes suggestive of demyelination. *Neurology*. 1999;52(3):599-606. doi:10.1212/WNL.52.3.599

412. Tintore M, Arrambide G, Otero-Romero S, et al. The long-term outcomes of CIS patients in the Barcelona inception cohort: Looking back to recognize aggressive MS. *Mult Scler J*. 2020;26(13):1658-1669. doi:10.1177/1352458519877810

413. Morrissey SP, Miller DH, Kendall BE, et al. The significance of brain magnetic resonance imaging abnormalities at presentation with clinically isolated syndromes suggestive of multiple sclerosis. A 5-year follow-up study. *Brain*. 1993;116(1):135-146. doi:10.1093/brain/116.1.135

414. Filippi M, Horsfield MA, Morrissey SP, et al. Quantitative brain MRI lesion load predicts the course of clinically isolated syndromes suggestive of multiple sclerosis. *Neurology*. 1994;44(4):635-641. doi:10.1212/wnl.44.4.635

415. Tintoré M, Rovira A, Río J, et al. Baseline MRI predicts future attacks and disability in clinically isolated syndromes. *Neurology*. 2006;67(6):968-972. doi:10.1212/01.wnl.0000237354.10144.ec

416. Jacobsen CO, Farbu E. MRI evaluation of grey matter atrophy and disease course in multiple sclerosis: an overview of current knowledge. *ACTA Neurol Scand*. 2014;129(198, SI):32-36. doi:10.1111/ane.12234

417. Brownlee WJ, Solanky B, Prados F, et al. Cortical grey matter sodium accumulation is associated with disability and secondary progressive disease course in relapse-onset multiple sclerosis. *J Neurol Neurosurg Psychiatry*. 2019;90(7):755-760. doi:10.1136/jnnp-2018-319634

418. Gawne-Cain ML, O'Riordan JI, Coles A, Newell B, Thompson AJ, Miller DH. MRI lesion

volume measurement in multiple sclerosis and its correlation with disability: a comparison of fast fluid attenuated inversion recovery (fFLAIR) and spin echo sequences. *J Neurol Neurosurg Psychiatry*. 1998;64(2):197-203. doi:10.1136/jnnp.64.2.197

419. Forooshani PM, Biparva M, Ntiri EE, et al. Deep Bayesian networks for uncertainty estimation and adversarial resistance of white matter hyperintensity segmentation. *bioRxiv*. Published online December 18, 2021:2021.08.18.456666. doi:10.1101/2021.08.18.456666

420. Gumberz J von, Mahmoudi M, Young K, et al. Short-term MRI measurements as predictors of EDSS progression in relapsing-remitting multiple sclerosis: grey matter atrophy but not lesions are predictive in a real-life setting. *PeerJ*. 2016;4(9). doi:10.7717/PEERJ.2442

421. Vidal-Jordana A, Sastre-Garriga J, Pareto D, et al. Brain atrophy 15 years after CIS: Baseline and follow-up clinico-radiological correlations. *Mult Scler*. 2018;24(6):721-727. doi:10.1177/1352458517707070

422. Lassmann H. The changing concepts in the neuropathology of acquired demyelinating central nervous system disorders. *Curr Opin Neurol*. 2019;32(3):313-319. doi:10.1097/WCO.0000000000000685

423. Rush C, MacLean H, Freedman M. Aggressive multiple sclerosis: proposed definition and treatment algorithm. *Nat Rev Neurol*. 2015;11(7):379-389. doi:10.1038/NRNEUROL.2015.85

424. Kıylıoğlu N. Prognostic-disability Biomarkers in Multiple Sclerosis: Review of the Literature from the Last Five Years Multipl Skleroz Olgularında Prognoz-Özürlülük Biyoişaretçileri: Son Beş Yıla Ait Literatürün Gözden Geçirilmesi. *Turk J Neurol*. 2018;24:203-215. doi:10.4274/tnd.79836

425. Pike AR, James GA, Drew PD, Archer RL. Neuroimaging predictors of longitudinal disability and cognition outcomes in multiple sclerosis patients: A systematic review and meta-analysis. 2022;57:103452. doi:10.1016/J.MSARD.2021.103452

426. Filippi M, Yousry T, Baratti C, et al. Quantitative assessment of MRI lesion load in multiple sclerosis - A comparison of conventional spin-echo with fast fluid-attenuated inversion recovery. *BRAIN*. 1996;119(4):1349-1355. doi:10.1093/brain/119.4.1349

427. Giovannoni G. Any evident MRI T2-lesion activity should guide change of therapy in multiple sclerosis--yes. *Mult Scler*. 2015;21(2):134-136. doi:10.1177/1352458514566261

428. Cappelle S, Pareto D, Tintoré M, et al. A validation study of manual atrophy measures in patients with Multiple Sclerosis. *Neuroradiology*. 2020;62(8):955-964. doi:10.1007/s00234-020-02401-3

429. Baber W, Tallantyre E. Manual magnetic resonance imaging measurements in multiple sclerosis: a study on reproducibility and disability. *Clin Med (Northfield Il)*. 2019;19(Suppl

2):116-116. doi:10.7861/CLINMEDICINE.19-2-S116

430. Fedorov A, Beichel R, Kalpathy-Cramer J, et al. 3D Slicer as an image computing platform for the Quantitative Imaging Network. *Magn Reson Imaging*. 2012;30(9):1323-1341. doi:10.1016/j.mri.2012.05.001

431. Zivadinov R, Horakova D, Bergsland N, et al. A Serial 10-Year Follow-Up Study of Atrophied Brain Lesion Volume and Disability Progression in Patients with Relapsing-Remitting MS. *Am J Neuroradiol*. 2019;40(3):446. doi:10.3174/ajnr.A5987

432. Mesaros S, Rocca MA, Sormani MP, Charil A, Comi G, Filippi M. Clinical and conventional MRI predictors of disability and brain atrophy accumulation in RRMS. A large scale, short-term follow-up study. *J Neurol*. 2008;255(9):1378-1383. doi:10.1007/S00415-008-0924-5

433. Gauthier SA, Mandel M, Guttmann CRG, et al. Predicting short-term disability in multiple sclerosis. *Neurology*. 2007;68(24):2059-2065. doi:10.1212/01.wnl.0000264890.97479.b1

434. Rahn AC, Köpke S, Stellmann J-PP, et al. Magnetic resonance imaging as a prognostic disability marker in clinically isolated syndrome: A systematic review. *Acta Neurol Scand*. 2019;139(1):18-32. doi:10.1111/ane.13010

435. Bernitsas E, Bao F, Seraji-Bozorgzad N, et al. Spinal cord atrophy in multiple sclerosis and relationship with disability across clinical phenotypes. *Mult Scler Relat Disord*. 2015;4(1):47-51. doi:10.1016/J.MSARD.2014.11.002

436. Clarke MA, Lakhani DA, Wen S, et al. Perilesional neurodegenerative injury in multiple sclerosis: Relation to focal lesions and impact on disability. *Mult Scler Relat Disord*. 2021;49:102738. doi:10.1016/j.msard.2021.102738

437. Comabella M, Sastre-Garriga J, Borras E, et al. CSF Chitinase 3–Like 2 Is Associated With Long-term Disability Progression in Patients With Progressive Multiple Sclerosis. *Neurol - Neuroimmunol Neuroinflammation*. 2021;8(6). doi:10.1212/NXI.0000000000001082

438. Uher T, Vaneckova M, Sobisek L, et al. Combining clinical and magnetic resonance imaging markers enhances prediction of 12-year disability in multiple sclerosis. *Mult Scler*. 2017;23(1):51-61. doi:10.1177/1352458516642314

439. Morris ZS, Wooding S, Grant J. The answer is 17 years, what is the question: understanding time lags in translational research. *J R Soc Med*. 2011;104(12):510. doi:10.1258/JRSM.2011.110180

440. Green LW, Ottoson JM, García C, Hiatt RA. Diffusion theory and knowledge dissemination, utilization, and integration in public health. *Annu Rev Public Health*. 2009;30:151-174. doi:10.1146/ANNUREV.PUBLHEALTH.031308.100049

441. Westfall JM, Mold J, Fagnan L. Practice-based research--"Blue Highways" on the NIH roadmap. *JAMA*. 2007;297(4):403-406. doi:10.1001/JAMA.297.4.403

442. Eisele P, Fischer K, Szabo K, et al. Characterization of Contrast-Enhancing and Non-contrast-enhancing Multiple Sclerosis Lesions Using Susceptibility-Weighted Imaging. *Front Neurol*. 2019;10(OCT):1082. doi:10.3389/fneur.2019.01082

443. Treaba CA, De Santis S, Granberg T, et al. Characterization of white matter lesions in early multiple sclerosis by combined magnitude and phase contrast at 7 Tesla and multi-shell diffusion imaging. *Mult Scler J*. 2018;24(2 Supplement):412-413. doi:10.1177/1352458518798590

444. Walsh AJ, Lebel RM, Eissa A, et al. Multiple sclerosis: Validation of MR imaging for quantification and detection of iron. *Radiology*. 2013;267(2):531-542. doi:10.1148/radiol.12120863

445. Absinta M, Sati P, Gaitan M, Maggi P, Cortese I, Filippi I. Architectural development of acute ms lesions at 7T phase contrast. *Neurology*. 2013;80.

446. Hagemeier J, Yeh EA, Heininen-Brown, M Bergsland N, Dwyer M, Carl E, Weinstock-Guttman B. Iron deposition in the subcortical deep-gray matter of pediatric multiple sclerosis patients. *Neurology*. 2012;78(1 Meeting Abstract). doi:10.1212/WNL.78.1

447. Sinnecker T, Schumacher S, Mueller K, et al. MRI phase changes in multiple sclerosis vs neuromyelitis optica lesions at 7T. *Neurol - Neuroimmunol Neuroinflammation*. 2016;3(4):e259. doi:10.1212/NXI.0000000000000259

448. Granberg T, Bergendal G, Shams S, et al. MRI-Defined Corpus Callosal Atrophy in Multiple Sclerosis: A Comparison of Volumetric Measurements, Corpus Callosum Area and Index. *J NEUROIMAGING*. 2015;25(6):996-1001. doi:10.1111/jon.12237

449. Raz E, Loh JP, Saba L, et al. Periventricular lesions help differentiate neuromyelitis optica spectrum disorders from multiple sclerosis. *Mult Scler Int*. 2014;2014:1-5. doi:10.1155/2014/986923